A multidisciplinary approach to provide improved methods for detecting bacteria in food and clinical samples

A thesis submitted to the University of Reading in fulfilment of the requirements for the degree of Doctor of Philosophy

School of Pharmacy

by

Esmie Lynn Agustin Wescott

April 2019

Declaration

The work described in this thesis was conducted at the School of Pharmacy, University of Reading and Thermo Fisher Scientific Oxoid Ltd. (Basingstoke, UK) between April 2015 and March 2019.

I confirm that this is my own work and the use of all material from other sources has been properly and fully acknowledged.

Esmie Lynn Agustin Wescott

Acknowledgements

First and foremost, I am very grateful to my supervisors Professor Helen Osborn, Dr. Richard Bovill and Dr. John Brazier for giving me the opportunity to conduct this research project. The PhD project would have been impossible to complete without your constant encouragement, guidance, patience and support. I would like to thank the BBSRC and Thermo Fisher Scientific for funding my research project.

I would like to thank the technical staff at the University of Reading, namely Dr. Radek Kowalczyk (NMR)Scientific, Nicholas Michael and Martin Reeves (Mass Spectrometry), Gez Griffin, Philip Mason and Ross Green (Stores) and Mark Clemont (Glassblowing). I am very grateful for the technical assistance of Mark Hutchins and the people who work at the chemistry, R&D and clinical sections at Thermo Fisher Scientific Oxoid (Basingstoke UK) for their knowledge and support on my chemistry and microbiological analysis. A big thank you to all of my former and current colleagues in Lab 228 and Office G9: Mai, Az, Jack, Ibrahim S., Sarah N., Ily, Adam, Charlotte, Cidalia, Rebecca, Irene, Divya, Ibrahim C., Laura, Rossana and Daniel.

I am very grateful for the continuous support, love and encouragement by the Wescott family: Denise, Andrew, Robert and Emma. I would like to thank my families from the Philippines and Canada. I would also like to thank my friends from high school (C2, the Cruz sisters and Ella Lama). To my mum, your unwavering love, patience and support – I cannot thank you enough.

And, to my significant other Thomas Wescott – you have been a caring, patient and supportive husband since embarking on this research project. You have been my source of motivation and encouragement, particularly during the tough times of my PhD. Maraming Salamat!

Abstract

The increasing level of threat of antimicrobial resistance due to less effective treatment of, and prevention against, bacterial infections is of growing concern. The Review on Antimicrobial Resistance predicts an estimated death toll of 10 million people a year by 2050, which is higher than the estimated mortality rate for cancer and diabetes combined. For decades, only a few classes of antibiotics have been developed by pharmaceutical companies. The lack of new antibiotics has led to the emergence of resistance for older drugs. Inappropriate and overconsumption of antibiotics are still common in healthcare and agricultural settings. To preserve the efficacy of existing antibiotics and to circumvent the urgency for discovering new drug treatments, one of the most effective ways to manage antimicrobial resistance is through developing rapid, point-of-care diagnostic tests.

One of the most common and well-established protocols to identify bacteria is the incorporation of synthetic enzyme substrates in solid culture media. Indoxyl glycosides have been widely and successfully used as chromogenic substrates for the detection and presumptive identification of bacterial pathogens. Based on the presence of glycosidase enzymes in the bacteria, the overall aim of this work was therefore to synthesise and analyse two previously synthesised fluorinated indoxyl β-galactosides, and four novel fluorinated indoxyl β-galactoside and β-glucosides to complement the existing range of commercially available substrates.

Preparation of indoxyl glycosides is recognised to be challenging. Therefore, in this project, one of the main objectives was to develop an efficient synthesis of the substrates by following the method by Böttcher and co-workers. Glycosidation via phase-transfer catalysis proved to be effective and this was successfully achieved for 1,2-*trans* glycosides. The per-*O*-acetyl fluorinated indoxylic acid allyl ester β-galactosides and β-glucosides were isolated with yields of 85-95% and 78-90%, respectively. The acetylated substrates were

deprotected via decarboxylation using silver-mediated reaction, followed by Zemplén de-*O*-acetylation to furnish the final fluorinated indoxyl β-galactosides and β-glucosides with varying yields from 19-31% and 48-90%, respectively. The overall yield for the glycosylation route for β-galactosides and β-glucosides varied from 7-21% and 21-58%, respectively. Attempts to synthesise unsubstituted indoxyl rhamnoside via phase-transfer catalysis and using trimethylsilyl trifluoromethanesulfonate as a promoter were unsuccessful.

The chromogenic properties of the fluorinated indoxyl β-glycosides were evaluated against several microorganisms in Nutrient Agar and Tryptone Soya Agar. Hydrolysis of the six fluorinated derivatives normally produced dark olive green and midnight blue colours that were highly restricted within microbial colonies. The new substrates colours are different from conventional substrates. Interestingly, the β-galactosides and β-glucosides were more highly sensitive for the detection of *Escherichia* and *Staphylococcus* species compared to commercially well-known chromogenic substrates 5-bromo-4-chloro-3-indolyl β-D-glucoside and 5-bromo-4-chloro-3-indolyl β-D-galactoside in Tryptone Soya Agar. Therefore, the colours and identification profiles of the derivatives complement the existing chromogenic substrates. Furthermore, the hydrolysis of two substrates 5-bromo-4-chloro-3-indolyl β-D-glucoside and 6-trifluormethyl-3-indolyl β-D-glucoside were analysed using quantitative HPLC analysis. The study revealed that 5-bromo-4-chloro-3-indolyl β-D-glucoside (X-β-D-gluc) formed a stronger affinity to the β-glycosidase enzyme than 6-(trifluormethyl)-3-indolyl β-D-glucoside (CF_3-β-D-gluc), suggesting that X-β-D-gluc reached saturation quicker than CF_3-β-D-gluc.

Therefore, the research work detailed in this project provided new and further insights on the applications of chromogenic substrates in culture media.

Table of Contents

Chapter 1 Introduction 1

1.1 The spread of antimicrobial resistance in modern society 2

1.1.1 Antibiotic-resistant infections in healthcare settings 3

1.1.2 The dwindling supply of new antibiotics 5

1.1.3 Prescribed antibiotics in healthcare settings in the UK and abroad 7

1.1.4 Unregulated supply of sub-standard and counterfeit antibiotic drugs 11

1.1.5 Excessive and inappropriate use of antibiotics in animal farming 12

1.2 Point-of-care diagnostic tools for rapid and early bacterial detection and identification 14

1.3 An overview of bacterial cell structure 15

1.4 Uptake of synthetic enzymatic substrates 18

1.5 Conventional approach for the detection and identification of bacterial pathogens 21

1.6 An overview of synthetic enzyme substrates in culture media 27

1.6.1 Chromogenic substrates in culture media 29

1.6.2 Fluorogenic substrates in culture media 31

1.7 Indoxyl substrates in culture media 32

1.8 Synthetic methodologies for preparing indoxyl glycosides 39

1.9 Comparison of the hydrolysis of different chromogenic substrates 43

1.10 Research aims and objectives 46

Chapter 2 Synthesis of indoxylic acid allyl esters and their fluorinated derivatives 48

2.1 Aims and Objectives 49

2.2 Introduction 50

2.2.1 Formation of indigo: enzyme hydrolysis of indoxyl glycoside 50

2.2.2 Features of indigo dye: colour and solubility 51

2.2.3 Traditional *vs* new methods: synthesis of indoxyl 53

2.3 Results and Discussion 58

2.3.1 Synthesis of indoxylic acid allyl esters and its fluorinated analogues 58

2.3.2 Formation of isatoic anhydrides using triphosgene and pyridine 58

2.3.3 The effect of fluorine substituents on the aromatic ring 60

2.3.4 *N*-Alkylation of isatoic anhydrides using NaH 64

2.3.5 Ring opening of *N*-alkylated isatoic anhydrides using NaH 67

2.3.6 Dieckmann condensation of the di-esters 68

2.4 Conclusions and Future Work 72

Chapter 3 Synthesis of indoxyl glycosides and their fluorinated derivatives 73

3.1 Aims and Objectives 74

3.2 Introduction 75

3.2.1 Introduction: general background on carbohydrates 75

3.2.2 General mechanism for glycosylation 76

3.2.3 Protecting group strategies in carbohydrate synthesis 79

3.2.4 Traditional *O*-glycosidation method towards indoxyl glycosides 80

3.2.5 Improved *O*-glycosidation route towards indoxyl glycoside 82

3.3 Results and Discussion 86

3.3.1 Chemical *O*-Glycosidation using PTC 87

3.3.2 Allyl ester deprotection and decarboxylation of fluorinated per-*O*-acetyl indoxyl ester β-glycosides..... 93

3.3.3 Zemplén de-*O*-acetylation of per-*O*-acetyl indoxyl glycosides..... 97

3.3.4 Purity analyses of fluorinated indolyl β-glycosides..... 103

3.3.5 Synthesis of indoxyl rhamnoside 103

3.4 Conclusions and Future Works..... 107

Chapter 4 Microbiological evaluation of the fluorinated indoxyl β-glycosides in culture media.....109

4.1 Indoxyl glycosides for bacterial testing 110

4.2 Overall aims and objectives..... 111

4.3 Target bacterial strains and preparation of chromogenic media 112

4.4 Results and Discussion 117

4.4.1 Colour observation of dimerised chromophores in agar media 117

4.4.2 General observations of indoxyl β-glycosides in agar media 117

4.4.3 The effect of prolong incubation of the chromogenic media 134

4.4.4 Differences in selectivities of indoxyl β-glycosides in agar media 135

4.4.5 Differences on the colour of the dimersied fluorinated chromophore 143

4.4.6 Evaluation of the bacterial hydrolysis of indoxyl glycosides 144

4.4.7 Determination of the rate of hydrolysis of indoxyl β-glycosides 146

4.5 Conclusion and Future Work..... 151

Chapter 5 Conclusions and Future Works 153

5.1 Conclusions 154

5.1.1 Summary 154

5.1.2 Synthesis of indoxylic acid allyl ester and its fluorinated erivatives 157

5.1.3 Synthesis of fluorinated indoxyl β-glycosides 158

5.1.4 Synthesis of indoxyl rhamnoside 160

5.1.5 Chromogenic evaluation of the fluorinated indoxyl β-glycosides 161

5.2 Future Work 162

5.2.1 Derivatisation of indoxyl-based substrates 162

5.2.2 Synthesis of indoxyl α-glycosides 165

5.2.3 Combination of MALDI-TOF MS and chromogenic media for bacterial detection and identification 168

Chapter 6 Experimental 170

6.1 Equipments and materials 171

6.1.1 Chemical and reagents 171

6.1.2 Thin layer chromatography 171

6.1.3 Flash column chromatography 171

6.1.4 Melting range 172

6.2 Analytical Instrumentations 172

6.2.1 Nuclear Magnetic Resonance (NMR) 172

6.2.2 Infrared (IR) 172

6.2.3 Mass Spectrometry (MS) 173

6.2.4 High-Performance Liquid Chromatography (HPLC) 173

6.3 Microbiology 174

6.3.1 Microorganism Strain List 174

6.4 Experimental methods and results of the precursor compounds prior to glycosidation 176

6.4.1 Synthesis of 1,2,3,4-tetra-O-acetyl-α,β-L-rhamnopyranose (33) 176

6.4.2 2,3,4-tri-O-acetyl-α-rhamnopyranosyl bromide (34) 177

6.4.3 Synthesis of allyl bromoacetate (19) 178

6.4.4 General procedure: Formation of isatoic anhydride using pyridine and triphosgene 179

6.4.4.1 Synthesis of 3,1-benzoxazine-2,4(1*H*)-dione (18a) 180

6.4.4.2 Synthesis of 6-fluoro-2*H*-3,1-benzoxazine-2,4(1*H*)-dione (18b) 181

6.4.4.3 Synthesis of 6,7-difluoro-2*H*-3,1-benzoxazine-2,4(1*H*)-dione (18c)..... 182

6.4.4.4 Synthesis of 7-(trifluoromethyl)-2*H*-3,1-benzoxazine-2,4(1*H*)-dione (18d).....183

6.4.5 General procedure: *N*-alkylation of isatoic anhydride using sodium hydride.....184

6.4.5.1 Synthesis of allyl 2-(2,4-dioxo-2*H*-benzo[*d*][1,3]oxazin-1(4*H*)-yl)acetate (20a) 185

6.4.5.2 Synthesis of allyl 2-(6-fluoro-2,4-dioxo-2*H*-benzo[*d*][1,3]oxazin-1(4*H*)-yl)acetate (20b)..... 186

6.4.5.3 Synthesis of allyl 2-(6,7-difluoro-2,4-dioxo-2*H*-benzo[*d*][1,3]oxazin-1(4*H*)-yl)acetate (20c) 187

6.4.5.4 Synthesis of allyl 2-(2,4-dioxo-7-(trifluoromethyl)-2*H*-benzo[*d*][1,3]oxazin-1(4*H*)-yl)acetate (20d) 188

6.4.6 General procedure: Formation of allyl *N*-[allyloxycarbonyl)methyl] anthranilate using sodium hydride 189

6.4.6.1 Synthesis of allyl *N*-[allyloxycarbonyl)methyl]anthranilate (21a) .. 190

6.4.6.2 Synthesis of allyl 5-fluoro-*N*-[allyloxycarbonyl)methyl]anthranilate (21b) 191

6.4.6.3 Synthesis of allyl 4,5-di-fluoro-*N*-[allyloxycarbonyl)methyl]anthranilate (20c) 192

6.4.6.4 Synthesis of 4-(trifluormethyl)-*N*-[allyloxycarbonyl)methyl] anthranilate (16d) 193

6.4.7 General procedure: Formation of indoxylic acid allyl ester via Dieckmann condensation 194

6.4.7.1 Synthesis of allyl 3-hydroxy-5-methyl-1*H*-indole-2-carboxylate (5a) 195

6.4.7.2 Synthesis of 5-fluoro-allyl 3-hydroxy-1*H*-indole-2-carboxylate (5a) 196

6.4.7.3 Synthesis of allyl 3-hydroxy-5,6-dimethyl-1H-indole-2-carboxylate (5c) 197

6.4.7.4 Synthesis of allyl 3-hydroxy-6-(trifluoromethyl)-1*H*-indole-2-carboxylate (5d) 198

6.5 Experimental methods and results of the glycosidated and deprotected compounds 199

6.5.1 General Procedure: Phase-transfer catalysis *O*-glycosylation 199

6.5.1.1 Synthesis of (5-fluoro-indox-3-ylic acid allyl ester)-2,3,4,6-tetra-*O*-acetyl-β-D-galactopyranoside (27a) 200

6.5.1.2 Synthesis of (5-fluoro-indox-3-ylic acid allyl ester)-2,3,4,6-tetra-*O*-acetyl-β-D-glucopyranoside 28a 201

6.5.1.3 Synthesis of (5,6-difluoro-indox-3-ylic acid allyl ester)-2,3,4,6-tetra-*O*-acetyl-β-D-galactopyranoside (27b) 202

6.5.1.4 Synthesis of (5,6-difluoro-indox-3-ylic acid allyl ester)-2,3,4,6-tetra-*O*-acetyl-β-D-glucopyranoside (28b) 203

6.5.1.5 Synthesis of [6-(trifluoromethyl)-indox-3-ylic acid allyl ester]-2,3,4,6-tetra-*O*-acetyl-β-D-galactopyranoside (27c) 204

6.5.1.6 Synthesis of [6-(trifluoromethyl)-indox-3-ylic acid allyl ester]-2,3,4,6-tetra-*O*-acetyl-β-D-glucopyranoside (28c) 205

6.5.2 General Procedure: De-*O*-allylation and decarb-*O*-oxylation of allyl ester207

6.5.2.1 Synthesis of *N*-acetyl-5-fluoro-3-indolyl-2,3,4,6-tetra-*O*-acetyl-β-D-galactopyranoside (31a) 208

6.5.2.2 Synthesis of *N*-acetyl-5-fluoro-3-indolyl-2,3,4,6-tetra-*O*-acetyl-β-D-glucopyranoside (32a) 209

6.5.2.3 Synthesis of *N*-acetyl-5,6-difluoro-3-indolyl-2,3,4,6-tetra-*O*-acetyl-β-D-galactopyranoside (31b)..... 210

6.5.2.4 Synthesis of *N*-acetyl-5,6-difluoro-3-indolyl-2,3,4,6-tetra-*O*-acetyl-β-D-glucopyranoside (32b)..... 211

6.5.2.5 Synthesis of *N*-acetyl-6-(trifluoromethyl)-3-indolyl-2,3,4,6-tetra-*O*-acetyl-β-D-galactopyranoside (31c) 212

6.5.2.6 Synthesis of *N*-acetyl-6-(trifluoromethyl)-3-indolyl-2,3,4,6-tetra-*O*-acetyl-β-D-glucopyranoside (32c) 213

6.5.3 General Procedure: Zemplén de-*O*-acetylation of per-*O*-acetyl indoxyl glycosides 215

6.5.3.1 Synthesis of 5-fluoro-3-indolyl β-D-galactopyranoside 3a 216

6.5.3.2 Synthesis of 5-fluoro-3-indolyl β-D-glucopyranoside (4a) 217

6.5.3.3 Synthesis of 5,6-difluoro-3-indolyl β-D-galactopyranoside (3b) 218

6.5.3.4 Synthesis of 5,6-difluoro-3-indolyl β-D-glucoside (4b) 219

6.5.3.5 Synthesis of 6-(trifluoromethyl)-3-indolyl β-D-galactopyranoside (3c).....220

6.5.3.6 Synthesis of 6-(trifluoromethyl)-3-indolyl β-D-glucopyranoside (4c).....221

6.5.4 General Prodedure: Preparation of chromogenic media..... 222

6.5.4.1 Inoculator well template with references to the bacteria utilised in this project. 223

6.5.4.2 Bacterial testing on solid culture media 224

6.5.5 General Procedure: Enzyme kinetics assay..... 242

Chapter 7 References 244

Abbreviations

β-Gal	β-Galactoside
β-Gluc	β-Glucoside
4-MU	4-Methylumbelliferone
5-F-β-D-gal	5-Fluoro-3-indolyl β-D-galactoside
5-F-β-D-gluc	5-Fluoro-3-indolyl β-D-galactoside
5,6-β-D-gal	5,6-Difluoro-3-indolyl β-D-galactoside
5,6-β-D-gal	5,6-Difluoro-3-indolyl β-D-glucoside
5-Br-4-Cl-β-D-gal	5-Bromo-4-chloro-3-indolyl β-D-galactoside
5-Br-4-Cl-β-D-gluc	5-Bromo-4-chloro-3-indolyl β-D-galactoside
6-CF_3-β-D-gal	6-(Trifluoromethyl)-3-indolyl β-D-galactoside
6-CF_3-β-D-gluc	6-(Trifluoromethyl)-3-indolyl β-D-glucoside
6-F-β-D-gal	6-Fluoro-3-indolyl β-D-galactoside
7-AMC	7-Amino-4-methylcoumarin
8HQ	8-Hydroxyquinoline
ABC	ATP binding cassette
AMR	Antimicrobial resistance
ATCC	American Type Culture Collection
b	Bending (Infrared)
BAP	7-{4-(β-alanylamino)}benzyloxy-3-ethoxycarbonylcoumarin triflouroacetate
br.	Broad (NMR)
br. s	Broad singlet (Infrared)
BTEAC	Benzyltriethylammonium chloride
cat.	Catalytic
CFU	Colony forming unit
CHE	3,4-Cyclohexenoesculetin

COSY	Correlation Spectroscopy
d	Out-of-plane deformation (Infrared)
DBU	1,8-Diazabicyclo(5.4.0)undec-7-ene
DCM	Dichloromethane
dd	Doublet of doublet (NMR)
ddd	Doublet of doublet of doublet (NMR)
DDDs	Defined Daily Doses
DDE	Diketo-diamino-ethylene
DEFT	Direct Epifluorescent Filter Microscopy
DIPEA	Diisopropylethylamine
DMF	Dimethylformamide
DMSO	Dimethyl sulfoxide
DNP	2,4-dinitrophenylhydrazine
dt	Doublet of triplet (NMR)
E. coli	*Escherichia coli*
EHC	Ethyl-7-hydroxycoumarin-3-carboxylate
ELSD	Evaporative Light Scattering Detector
ESBL	Extended-spectrum β-lactamases
ESI	Electrospray Ionisation
ESKAPE	*Enterococcus faecium*, *Staphylococcus aureus*, *Klebsiella pneumoniae*, *Acinetobacter baumannii*, *Pseudomonas aeruginosa* and *Enterobacter* species
FC	Flow Cytometry
FDA	Federal Drug Administration
FISH	Fluorescent *In Situ* Hybridisation
FT	Fourier Transform
h	Hour(s)

HICs	High Income Countries
HIV	Human Immunodeficiency Virus
HMBC	Heteronuclear Multiple Bond Correlation
HPLC	High Performance Liquid Chromatography
HSQC	Heteronuclear Single Quantum Coherence
Hz	Hertz
IR	Infrared
KESC	*Klebsiella*, *Enterobacter*, *Serratia*, *Citrobacter*
LMICs	Low- and Middle- Income Countries
LPS	Lipopolysaccharides
m	Medium (Infrared)
m	Multiplet (NMR)
Magenta-β-D-gluc	5-Bromo-6-chloro-3-indolyl β-D-glucoside
MALDI-TOF MS	Matrix-assisted Laser Desorption Ionisation Time-of-Fight Mass Spectrometer
min	Minutes(s)
MO	Molecular orbital
mol. equiv.	Molar equivalent
MRSA	Methicillin-resistant *Staphylococcus aureus*
MS	Mass Spectrometry
NA	Nutrient Agar
NCIMB	National Collection of Industrial Food and Marine Bacteria
NCTC	National Collection of Type Cultures
NGP	Neighbouring group participation
NIH	National Institute for Health
NMR	Nuclear Magnetic Resonance
OCC	Oxoid Culture Collection

ONPG	*o*-Nitrophenyl β-D-galactopyranoside
PBS	Phosphate-buffered saline
PCR	Polymerase chain reaction
PE	Petroleum ether 40-60
PEP	Phosphotranspyruvate
POC	Point-of-care
PTC	Phase-transfer catalysis
PTS	Phosphotransferase
q	Quartet (NMR)
R&D	Research and development
Ref.	References
R_f	Retention factor
Rouge-β-D-gal	6-Fluoro-3-indolyl β-D-galactoside
rt	Room temperature
s	Singlet (NMR)
s	Stretching (Infrared)
sat.	Saturated
S. auerus	*Staphylococcus aureus*
S. auerus v oxford	*Staphylococcus aureus v oxford*
S. epidermis	*Staphylococcus epidermis*
S. haemolyticus	*Staphylococcus haemolyticus*
S. pneumonia	*Staphylococcus pneumonia*
S. saprophyticus	*Staphylococcus saprophyticus*
spp.	Species
t	triplet (NMR)
TBAHS	Tetrabutylammonium hydrogensulfate
td	Triplet of doublet (NMR)

THF	Tetrahydrofuran
TLC	Thin layer chromatography
TMSOTf	trimethylsilyl trifluoromethanesulfonate
TSA	Tryptone Soya Agar
UV	Ultraviolet
UV/Vis	Ultraviolet-visible
VMD	Veterinary Medicines Directorate
VRE	Vancomycin-resistant *Enterococci*
w	Weak (Infrared)
X-β-D-gal	5-Bromo-4-chloro-3-indolyl β-D-galactoside
X-β-D-gluc	5-Bromo-4-chloro-3-indolyl β-D-glucoside
XLD	Xylose-lysine-deoxycholate

Aim to know more about the world than you did yesterday.

-Anonymous

Chapter 1 Introduction

1.1 The spread of antimicrobial resistance in modern society

In recent years, the discovery of new antibiotics has led to the treatment of many bacterial infectious diseases, and this has in turn contributed to a drop in mortality rate and increase in life expectancy. Antibiotics, also known as antibacterial agents, are medicines or drugs that are used to either destroy or inihibit the growth of microorganisms, including bacteria. Indeed, antibiotics are not only successfully responsible for saving countless lives, but have also contributed to the advancement of medical technology[1-3] such as the development of rapid assays and artificial intelligence to rapidly diagnose for antimicrobial resistance (AMR) and intrepret tests results;[4-7] medical devices and biomaterials that provides controlled release of antimicrobial agents that are used to treat infected wouds, and are utilised in dental or medical surgeries;[8-11] and, advanced 3D printing materials and systems that enables implants coated with antimicrobial properties preventing the spread of bacterial infections at the implant site.[12, 13] In fact, utilisation of antibiotics has also benifited the agriculture sector. Antibiotics are used to treat infections and diseases in farm animals. Moreover, it stops the the spread of infectious diseases to other group of animals that are healthy.[14]

However, despite these successes, the emergence and spread of antimicrobial resistance has jeopardised the achievements of antibiotics. AMR has been a challenge for clinicians and researchers.[15] According to the 2014 review on AMR, it has been estimated that up to 10 million deaths a year globally could be attributed to AMR by 2050, if antimicrobial resistance is allowed to increase.[16] Therefore, AMR caused by pathogens has been considered a global pandemic.[15, 17]

There are several interconnected factors for the emergence and spread of AMR in contemporary society as outlined below:

- Antibiotic-resistant infections in healthcare settings
- The dwindling supply of antibiotics
- Prescribed antibiotics in primary care settings in the UK and abroad
- Unregulated supply of sub-standard and counterfeit antibiotic drugs
- Excessive and inappropriate use of antibiotics in animal farming

These are one of the main contributing factors that accelerate the spread of AMR in all parts of the world, and at the same time, making antibiotics less effective to fight against the most dangerous forms of antibiotic-resistant bacteria.

1.1.1 Antibiotic-resistant infections in healthcare settings

Infections caused by antibiotic-resistant bacteria that fail to respond to treatments result in financial burden for hospitals, healthcare systems and societies due to prolonged illness, longer hospital stays for medical treatment, frequent hospitalisation visits and inevitable patient morbidity and mortality rates.[15, 18] According to the 2014 report, at least 700 000 people die every year worldwide due to drug-resistant infections.[16, 19] In Europe, about 25 000 patients die each year due to infections caused by multi-drug resistant bacteria with an associated cost of at least €1.5 billion in 2009.[20, 21] In the US, more than 99 000 deaths per year were implicated due to nosocomial (healthcare-associated) infections.[6, 22] The majority of the healthcare-associated infections that are found in healthcare settings are caused by the ESKAPE (***E****nterococcus faecium*, ***S****taphylococcus aureus*, ***K****lebsiella pneumoniae*, ***A****cinetobacter baumannii*, ***P****seudomonas aeruginosa* and ***E****nterobacter* species) organisms.

These organisms are particularly concentrated in healthcare settings, posing a risk to individuals who have an infection or are at risk of acquiring an infection because of their underlying conditions.[18, 23] Most of these organisms exhibit multiple-drug resistance,[24-27] making treatment very difficult. In England, bloodstream infections caused by antibiotic-resistant pathogens has increased by 35% between 2013 and 2017, as shown in **Figure 1**. Based on this data, *Enterobacteriaceae* spp. causes the highest number of blood stream infections, particularly *E. coli*, as these species are associated with the highest occurrence of infections, compromising 84% of the total.[28-30] Therefore, the World Health Organisation (WHO) listed ESKAPE bacteria as 'priority pathogens' that urgently need new antibiotics.[31]

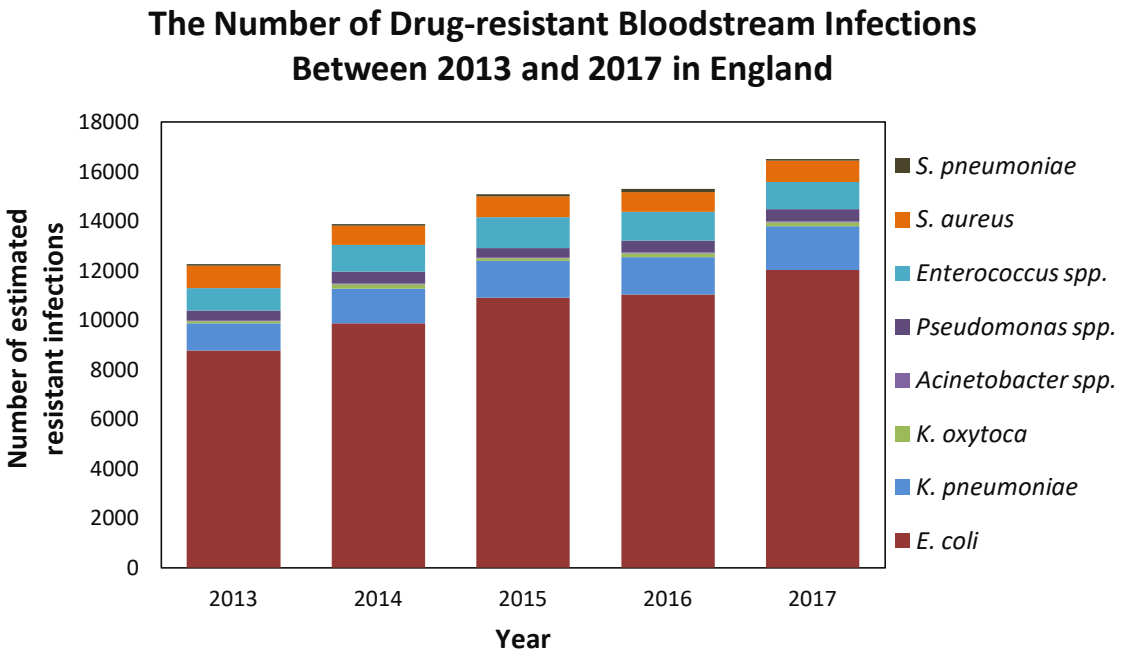

Figure 1. The number of bloodstream infections that are caused by antibiotic-resistant pathogens between 2013 and 2017.[30]

1.1.2 The dwindling supply of new antibiotics

Since the 1970s, there has been a decline in the discovery of new antibiotics.[15] **Figure 2** illustrates the decrease in the number of antibiotic drugs approved by the US Federal Drug Administration (FDA).[32-34] The estimated cost of pharmaceutical research and development (R&D) is about $800-900 million and 10 to 15 years for one approved drug.[15] This is combined with strict requirements and approval from regulatory bodies. Hence, this creates a barrier for the development of new antibiotics. The antimicrobial R&D efforts have become less economically attractive as there are fewer revenues to be made by pharmaceutical companies.[15] Out of $38 billion total venture capital investment, only $1.8 billion (or only less than 5%) was invested in antimicrobial development by private sectors between 2003 and 2013.[19, 35] Therefore, many large pharmaceutical companies such as Allergan, AstraZeneca, Bristol-Myers Squibb, Novartis and Sanofi withdrew from antimicrobial research programmes due to the undesirable and revenue setbacks of antibiotic business models.[36]

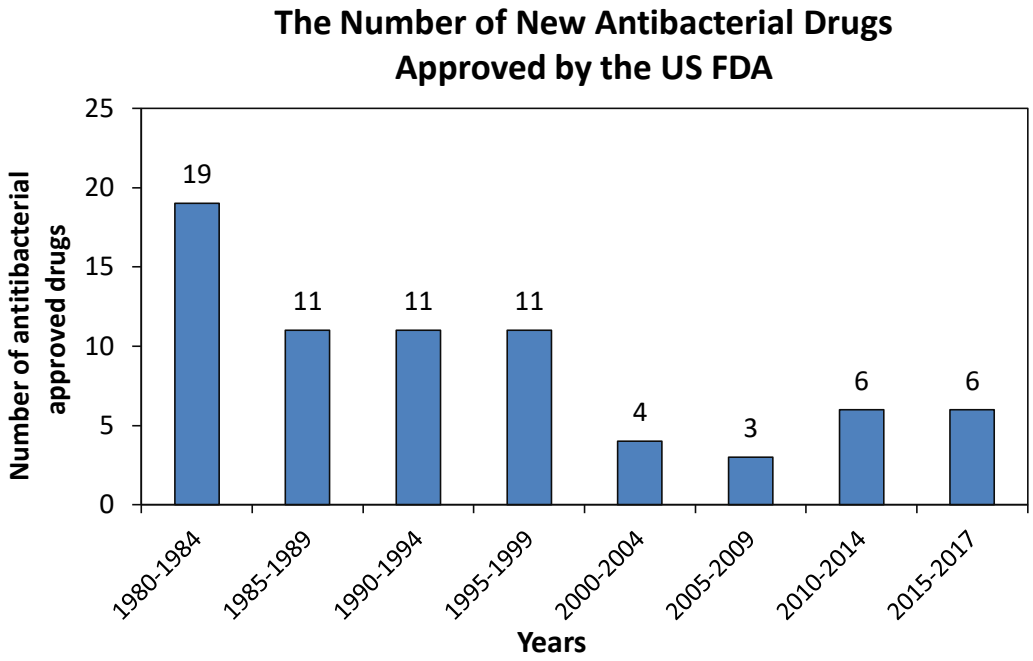

Figure 2. The drying pipeline of antibiotics approved by the US FDA from 1980 to 2017 to combat antibiotic resistance.[32-34]

Furthermore, the funding provided by the government and private investors for antimicrobial development was dwarfed by spending more money on cancer, diabetes and human immunodeficiency virus (HIV) research, which attract significant return investments. As illustrated in **Figure 3**, the US National Institute of Health (NIH), which is the world's largest single funder of health and biomedical R&D, revealed that the budget for AMR research was approximately $1.7 billion out of the total budget of $142.5 billion over the five-year spending period (2010-2014). The AMR research budget only represents approximately 1% of the NIH funding, in contrast to the research budget allocated to cancer, which was $26.5 billion, $14.5 billion for HIV and $5 billion for diabetes.[37, 38] The funding were used to cover studying various (infectious) diseases, drug and vaccination development programmes and enhancing public helalth awareness. Lastly, even if pharmaceutical industries, university researchers and the public were to step-up and make efforts to

develop new drugs immediately, there will be no effective treatments for some diseases within the next ten years.[15]

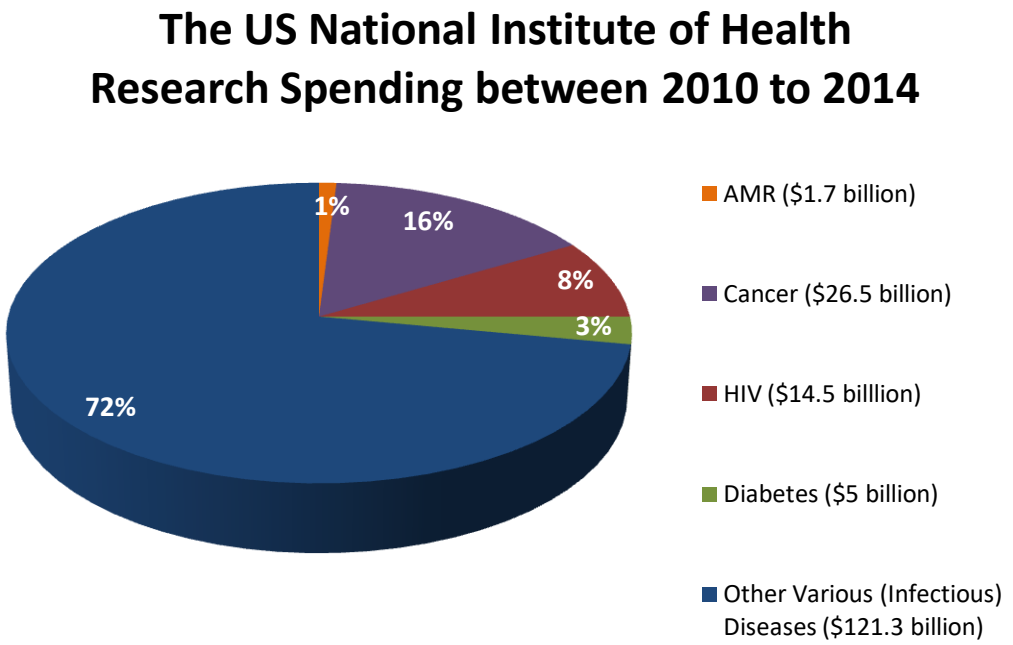

Figure 3. The US NIH research data over the five-year spending period (2010-2014) on various (infectious) diseases with the least funding allocated to AMR compared to cancer, HIV and diabetes research.[37, 38]

1.1.3 Prescribed antibiotics in healthcare settings in the UK and abroad

In Europe, over 90% of antibiotics are prescribed in primary care, [38, 39] where compliance of antibiotic use is based on a set of national treatment guidelines, particularly in the UK.[40] Over the last five years between 2012 and 2016, antibiotic consumption has declined by approximately 5% in the UK. As shown in **Figure 4**, Public Health England (PHE) published an annual report on tha national data on antibiotic prescribing and resistance in 2017. The report revealed that the highest level of antibiotics prescribed in England was in general practice followed by secondary care**.** In England, the most frequently prescribe antiobitics

agents are broad-spectrum antibiotics. Broad-spectrum antibiotics are antibacterial agents that either inhibit or kill a wide range of bacteria compared to narrow-spectrum antibiotics, which targets very specific bacteria. When a causative microorganism is unknown, the first line of treatment is to prescribe broad-spectrum antibiotics in order to avoid worsening the infection or spread of bacteria in other parts of the human body. Based from the published report, the three different classes of broad spectrum antibiotics that are frequently prescribed were penicillins followed by tetracyclines and macrolides.[28]

Whilst prescribing antibiotics differs profoundly from one country to another, prevalence of antibacterial infections is still prevalent. During the period between 2000 and 2015, antibiotic consumption, expressed in defined daily dose (DDD) increased by 65% from 21.1 to 34.8 billion DDDs over the 15-year period study and the rate of antibiotic consumption increased by 39% from 11.3 to 15.7 DDDs per 1 000 inhabitants per day. The research involved by estimating the total volume sales for each type of antibiotics for 76 countries over the study period. For each country, monthly and quarterly antibiotic consumption were reported for the hospital and prescribing sectors.[41]

A

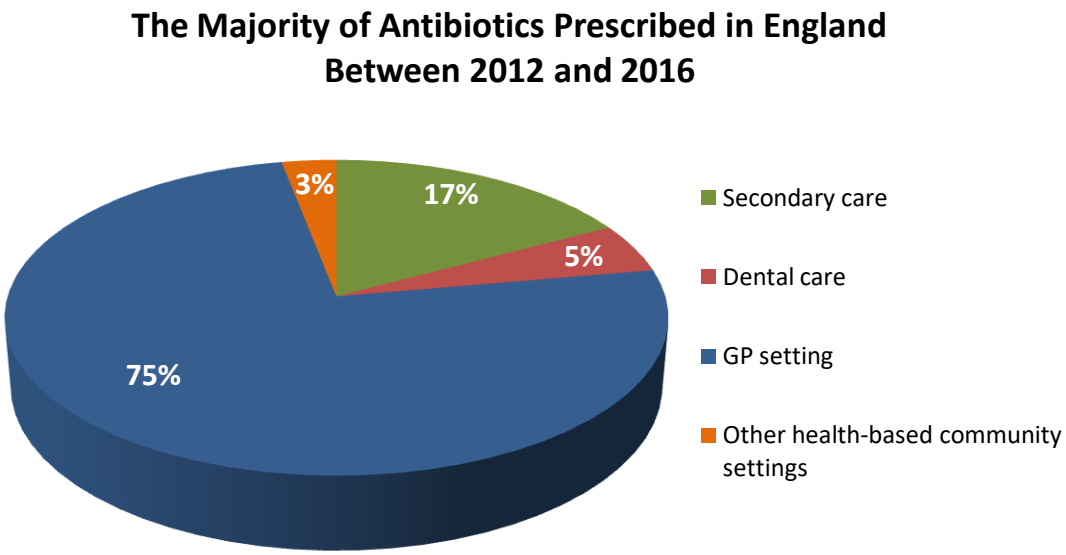

B

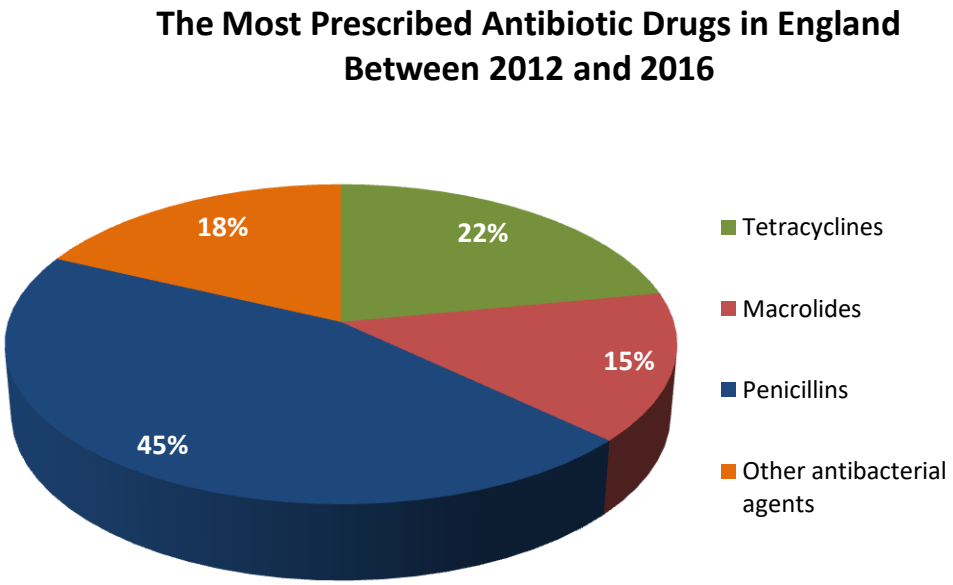

Figure 4. Between 2012 and 2016, **(A)** the majority of antibiotics prescribed in healthcare settings; and, **(B)** the most prescribed antibiotics reported in England.[28]

The consumption of antibiotics was mainly driven by low- and middle-income class (LMIC) compared to high-income class (HIC). In 2015, the highest antibiotic consumers were HICs, which were led by France, Italy and the USA; whilst, in 2015, the highest antibiotic consumers were LMICS, led by India, China and Pakistan. In HICS, the total antibiotic consumption increased by 6% from 9.7 to 10.3 billion DDDs; however, the antibiotic consumption rate decreased by 4% from 26.8 to 25.7 DDDs per 1 000 inhabitants per day. LMICs accounted for the greatest share in antibiotic consumption, which increased by 114% from 11.4 to 24.5 billion DDDs, and the the antibiotic consumption rate increased by 77% from 7.6 to 13.5 DDDs per 1 000 inhabitants per day. One of the primary drivers for the increased usage of antibiotics, especially for LMICs, was due to the increased economic development, providing access to goods and services that included antibiotics. In HICs, there was no correlation can be identified between antibiotic consumption and economic growth. Moreover, there has been a concern on the rapid increase of using 'last-resort' antibiotics such as colistin, glycylcyclines, oxazolidinones, carbapenems and polymyxins, both in HICs and LMICs.[41]

Assuming that there are no policies or regulations to reduce antibiotic consumption across all countries by 2030, the research study projected that antibiotic consumption will increase by up to 200% to 128 billion DDDs, which is higher than the estimated 42 billion DDDs in 2015. Also, antibiotic consumption rate would increase by 161% to 41.1 DDDs per 1 000 inhabitants per day. Lastly, if all countries converge in the 2015 total global consumption median of 17.8 DDDs per 1 0000 inhabitants per day by 2020, the projected global antibiotic consumption would increase by 32% to 55.6 billion DDDs by 2030.[41]

1.1.4 Unregulated supply of sub-standard and counterfeit antibiotic drugs

Injudicious antibiotic consumption is also fuelled by an unregulated supply chain, and distribution of counterfeit and poor quality antibiotics. As shown in **Figure 5**, there are several counterfeit or low-quality antibiotics that were detected in the world. Beta-lactam drugs classes were the most commonly reported counterfeit or sub-standard antibiotics.

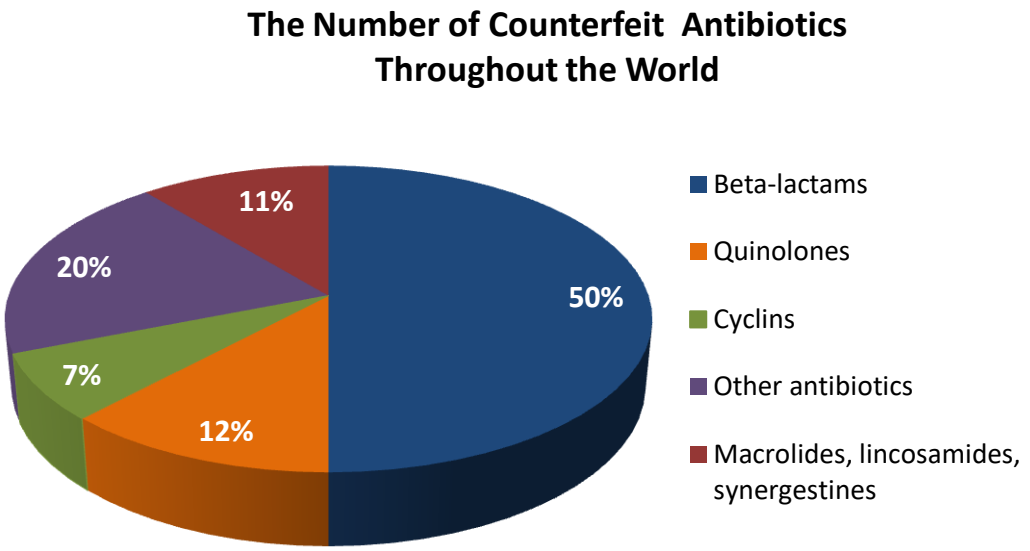

Figure 5. Distribution of 163 counterfeit antibiotic drugs detected in the world in 2009.[42-43]

These drugs are usually dispensed in the streets by unqualified drug vendors. Even retail pharmacies can provide antibiotics without prescription which easily accommodates the patient's financial ability to pay.[44] As an example, in some parts of India, 213 licenses of pharmacy retailers were cancelled by the FDA, due to non-compliance of dispensing medications without prescription and not providing bills.[45, 46] In addition, the FDA filed a court case against seven manufacturers distributing poor quality medicines, including antibiotics. The crackdown by the FDA against unregulated pharmacy and manufacturers is in line with the reported 64% of unapproved antibiotics sold in India.[47] Hence, there is a

need to address these issues to minimise, or to an extent eliminate, the irrational use of antibiotics through effective control policies and regulations.

1.1.5 Excessive and inappropriate use of antibiotics in animal farming

In animal agriculture, it was revealed that the annual global antimicrobial consumption ranges from approximately 63 000 tonnes[48] to over 240 000 tonnes.[49] This was projected to increase by 67% between 2010 and 2030. In the US, more than 70% of antibiotics were given to agriculture animals.[50] This can be linked to the controversial use of antibiotics as growth promoters rather than to treat infected farm animals. Antibiotics given to healthy animals rapidly enhanced their growth in order to reach full market weight very quickly. However, this practice results in the development of resistance to antibacterial drugs. In 2006, the EU initiated the ban of antibiotics as growth promoters, whilst in the US, antibiotics were re-labelled voluntarily to reduce the practice of using antibiotics as growth promoters.[51] Another high-profile example was the inappropriate use of colistin as an additive feed to farm animals in China. Colistin is considered as one of the last-resort antibiotic drugs against multi-drug resistant Gram-negative bacteria. In a Chinese study,[52, 53] the emergence of the colistin resistant bacterial gene, also known as MCR-1, rapidly increased in the provincial farming areas in China. The study reported that 15% of raw meat and 21% of the animals tested were positive to MCR-1 between 2011 and 2014, and 1% of the people were infected in 2014. Although currently confined to China, the gene is particularly worrying as the bacteria can transfer rapidly from animals to humans.[51]

In 2018, the UK government published a report on the estimated use of antibiotics in agriculture animals through annual collation of antbiotic sales data submitted by veterinary pharmaceutical companies to Veterinary Medicines Doctorate, which is an Executive Agency of the Department for Environment, Food and Rural Affairs (DEFRA). The VMD worked

alongside key food-producing animal sectors to develop, facilitate and coordinate antibiotic usage data collection systems. As shown in **Figure 6,** the data highlights the reduction of antibiotics for the past three consecutive years.[54]

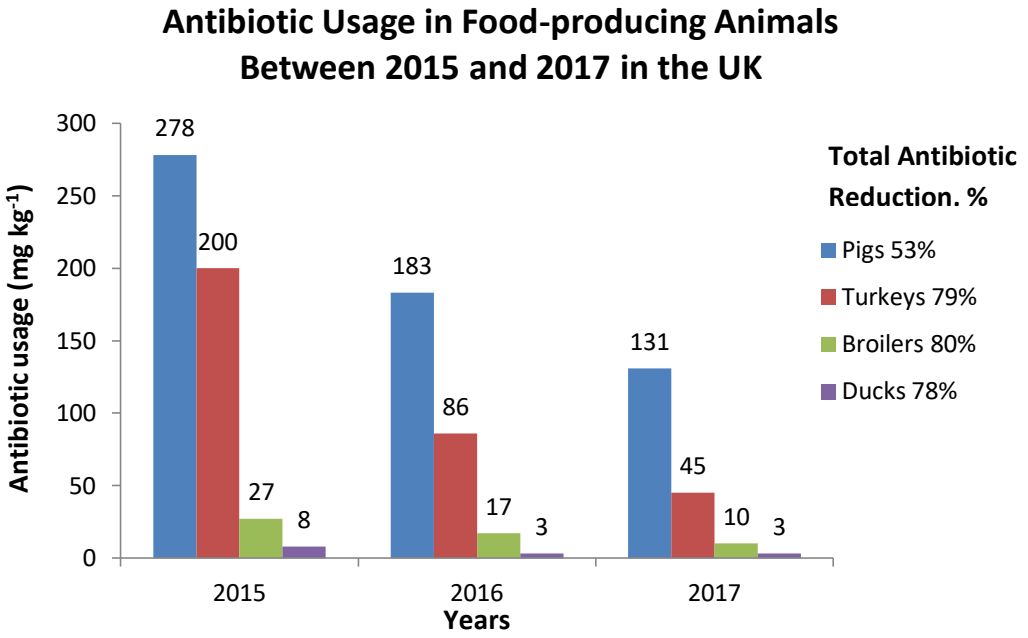

Figure 6. Reduction on antibiotic usage in pigs and meat poultry between 2015 and 2017.[54] The data highlighted the sharp reduction of antibiotic use in the agriculture industry through ongoing surveillance of antibiotic usage in animal livestocks and promoting awareness on excessive use of antibacterial agents in agricultural sector.

To monitor antibiotic resistance, VMD collated data from government laboratory obtained from food-producing animals by following two surveillance programmes. The European Union Harmonised Monitoring focussed on antibiotic resistance in zoonotic and commensal bacteria, for example, *Salmonella*, *Camphylobacter* and *E. coli* are commonly known microorganisms, which cause food poisoning.[55] Conversely, the clinical surveillance programme involved in the collection of samples from sick animals have been submitted to

goverment laboratories by farmers or veterinary surgeons for antibiotic susceptibility testing. The data findings from both frameworks were reported to VMD. Therefore, surveillance programmes monitor the changes and trends to predict shifting antibiotic resistance patterns.[54]

1.2 Point-of-care diagnostic tools for rapid and early bacterial detection and identification

Due to the increasing prevalence of antibiotic resistance to older antibiotics and the dwindling supply of new antibacterial agents, it is unlikely that resistance to antimicrobials will be eradicated in the coming decades. Nevertheless, one of the most effective solutions to this problem is to invest in rapid, point-of-care (POC) diagnostic tools to prevent unnecessary antibiotic use.[15, 38] Rapid diagnostic tools minimise and manage the demand for antibiotic drugs through correct usage and choice in community or hospital-based settings, agriculture and food production. POC diagnostics can be produced at relatively low cost and this could potentially reduce societal, hospital, agriculture, and R&D trial costs.[56-58]

Investment on rapid POC diagnostic tools would allow early identification of causative microorganisms whether the infection is viral or bacterial in a matter minutes or a few hours. If the identified microorganism is bacterial, this would allow a sick patient or an animal to receive more precise and targeted prescription of antibiotics and minimises the reliance on broad-spectrum antibiotics. In turn, diagnostic tools would revolutionise the diagnosis and treatment of infection and help slow down antibiotic resistance.[56-58]

1.3 An overview of bacterial cell structure

Bacteria are microorganisms that lack nucleus-enclosed membranes and organelles (such as mitochondria, Golgi apparatus, endoplasmic reticulum).[23, 59] A generalised cell component consists of a cell wall and membrane, and cytoplasm membrane containing many nucleoids and ribosomes.[18, 23, 38, 60]

The diversity of bacterial cells can be detected using microscopes to study cell morphology. One of the most important characteristics for identifying certain microbes is the shape of a cell. Two of the most common shapes are cocci and rods. Cocci are roughly spherical cells like *Staphylococcus aureus*, whilst *Bacillus megaterium* is an example of a rod-shaped bacterium. However, cells with the same shape are not necessary related.[18, 23, 38, 60]

Bacteria can be divided into two major groups: Gram-positive and Gram-negative bacteria. Both of these bacteria possess a cell wall, which is a strong, rigid layer outside the cell membrane. As shown in **Figure 7**, this rigid layer, known as peptidoglycan, is composed of two alternating polysaccharide derivatives, *N*-acetylglucosamine (NAG) and *N*-acetylmuramic (NAM) acids, and a few amino acids such L-alanine, D-glutamine, L-lysine and D-alanine.[18, 23, 38, 60]

In Gram-positive bacteria, 90% of the peptidoglycan predominantly makes up the cell wall. Embedded in the cell wall are teichoic and lipoteichoic acids, which contribute to the overall rigidity of the cell wall, as shown in **Figure 8A**.[23, 59, 60]

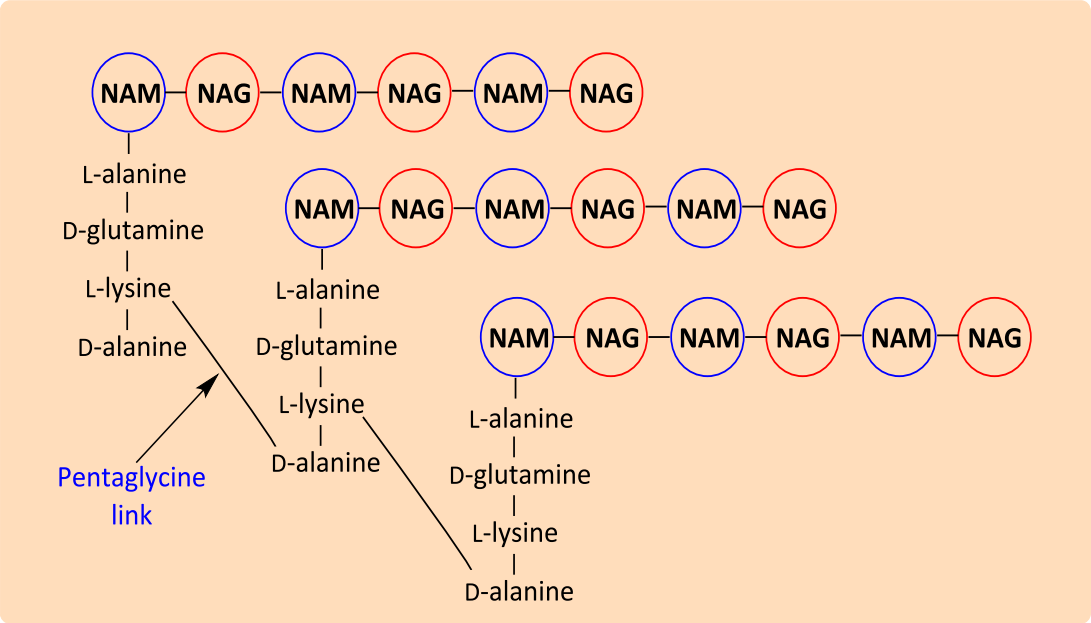

Figure 7. Structure of the repeating unit of peptidoglycan in bacterial cell. (Adapted from [61])

The cell wall of Gram-negative bacteria is more complex than for Gram-positive bacteria. Only 5-10% of the peptidoglycan makes up the overall cell wall, which consists mainly of an outer membrane located outside the cell wall. As shown in **Figure 8B**, the outer layer, also known as lipopolysaccharides (LPS), consists of *O*-polysaccharides, core polysaccharides and lipids.[23, 38, 59] LPS help to maintain the structure of the outer membrane and contribute to the negative charge on the bacterial surface and creates a permeability barrier. As the latter suggests, LPS is notably known to play a role in antibiotic resistance as it restricts the entry of the antibiotic when necessary; therefore, protecting the pathogenic bacteria against the host immune defences.[60]

Structural differences between the cell wall of Gram-positive and Gram-negative bacteria can be identified by Gram staining techniques. This involves the application of a violet iodine dye to stain the bacteria. Bacteria with a thick wall (20-40 nm), defined as Gram-positive, absorb the dye and are stained purple, whilst bacteria with a thin wall (2-4 nm), known as Gram-negative, will stain pink.[23, 38, 59-61]

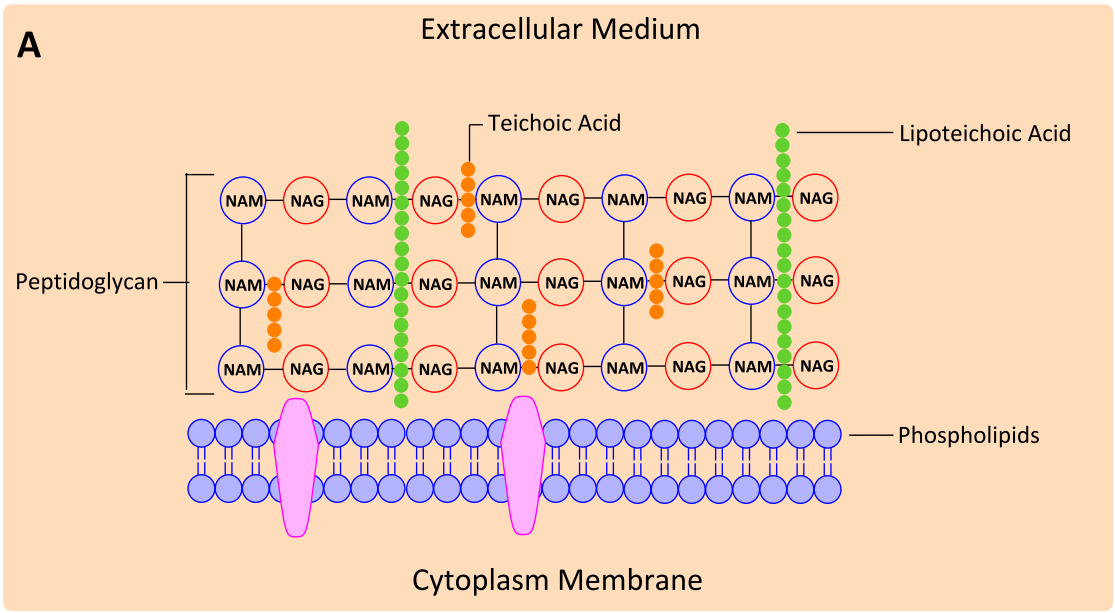

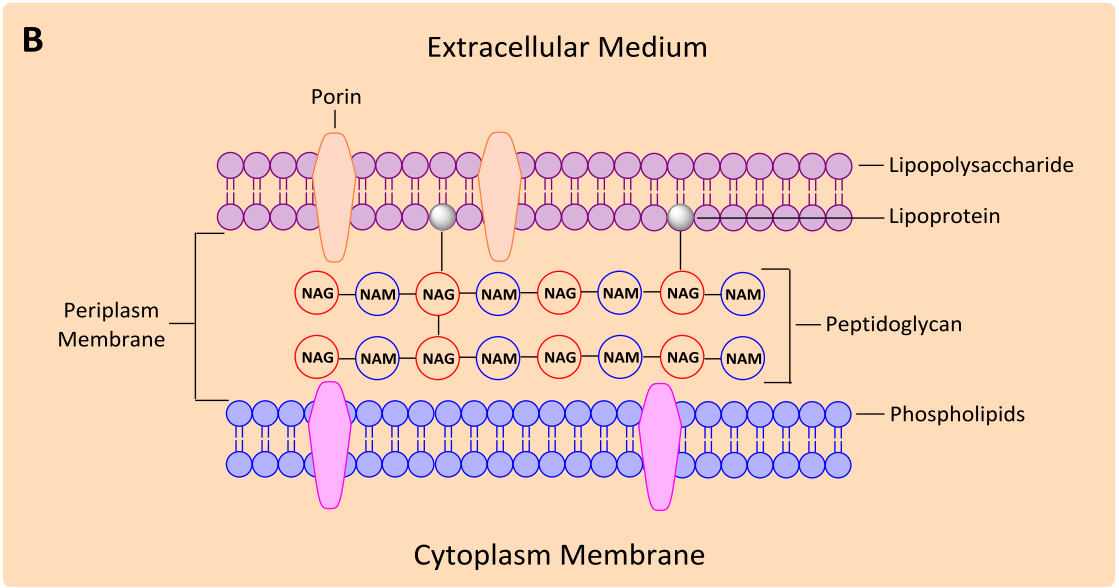

Figure 8. The cell wall structure of **(A)** Gram-positive and **(B)** Gram-negative bacteria. (Adapted from [59])

1.4 Uptake of synthetic enzymatic substrates

Although lipophilic substrates such as esters can enter the outer Gram-positive cell wall by passive diffusion, this is not possible in Gram-negative organisms, which are coated with a layer of LPS. The outer membrane of the Gram-negative contains porin channels that allow specific uptake of adequate nutrients to the cytoplasm membrane via passive diffusion. This process allows molecules to move from an external membrane with higher nutrient concentration to internal membranes with lower concentration.[23, 60, 62] As depicted in **Figure 9**, small molecules such solutes and ions up to large molecules such as dissacharides like sucrose and maltose could be facilitated via these three major transport porins.

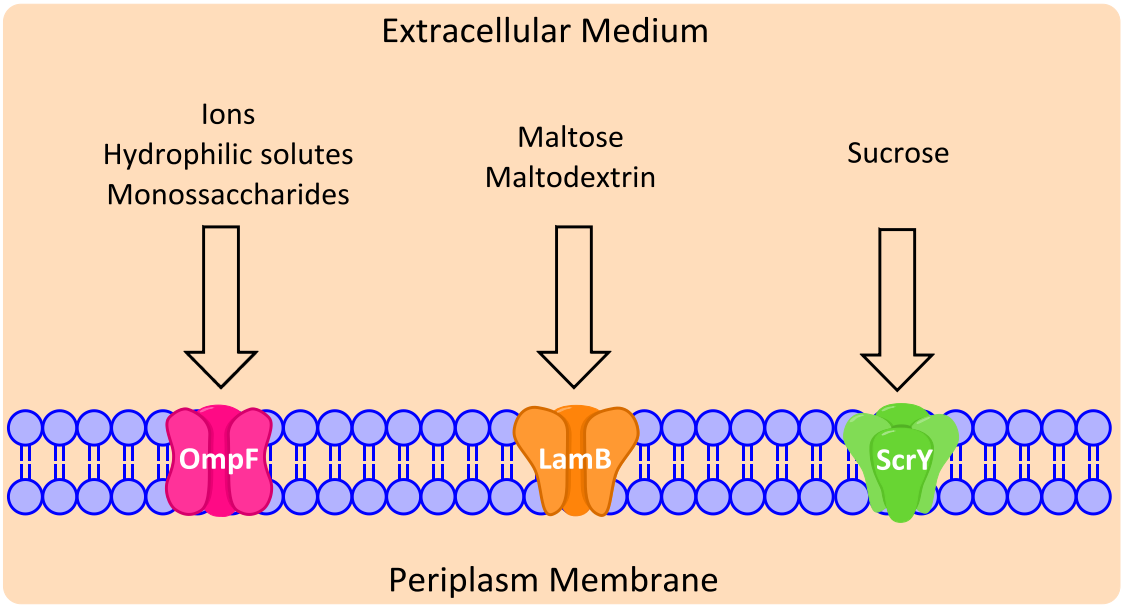

Figure 9. Glycosidic uptake through the periplasm membrane for Gram-negative bacteria. (Adapted from [63])

Many porins can be non-specific and allow entry of ions and small molecules. The first identified non-specific porin is OmpF in *E. coli*.[64] It transports ions, hydrophilic solutes and small molecules like monosaccharides and shows no particular specificity towards a molecule.[65] Hence, a small molecule like 5-bromo-4-chloro-3-indolyl β-D-galactoside with a molecular weight of 408.63 g mol^{-1} could enter via this transport system.

For fairly large molecules like disaccharides and oligosaccharides, specific porin channels are needed to transport the influx of these molecules. The best studied examples of sugar-specific porins are LamB and ScrY in Gram-negative bacteria *E. coli* and *Salmonella* spp.[64]

LamB (or maltoporin) porins facilitate the diffusion of maltose and other maltodextrins (up to maltoheptose) across the outer membrane. The *lamB* gene, which is part of *mal* regulon, is expressed to allow the permeation of maltose and maltodextrins with discrimination against the uptake of sucrose.[65] Furthermore, the porins allow the influx of monosaccharides such as glucose, lactose and arabinose.[64]

In contrast, ScrY (or sucrose channel porins) transport the disaccharide sucrose from the outer membrane in *E. coli* and *Salmonella* typhimurium. The sucrose uptake is regulated by sucrose regulon that consists of the scrKYABR genes.[65] In addition to sucrose, a large variety of sugars such as glucose, fructose, arabinose, maltose, lactose, raffinose and maltodextrins also rapidly diffuse through the porin.[64]

Within the outer cell wall, the cytoplasmic membrane of bacteria is a barrier that helps retain essential components inside the cell but allows transport of nutrients through three different mechanisms, as depicted in **Figure 10**.

Simple transport is exemplified by lac permease, a type of symporter, where a lactose molecule is transported along with a proton via the symporter into the cytoplasm. The lactose is cleaved and used for adenosine triphosphate (ATP) synthesis.[23]

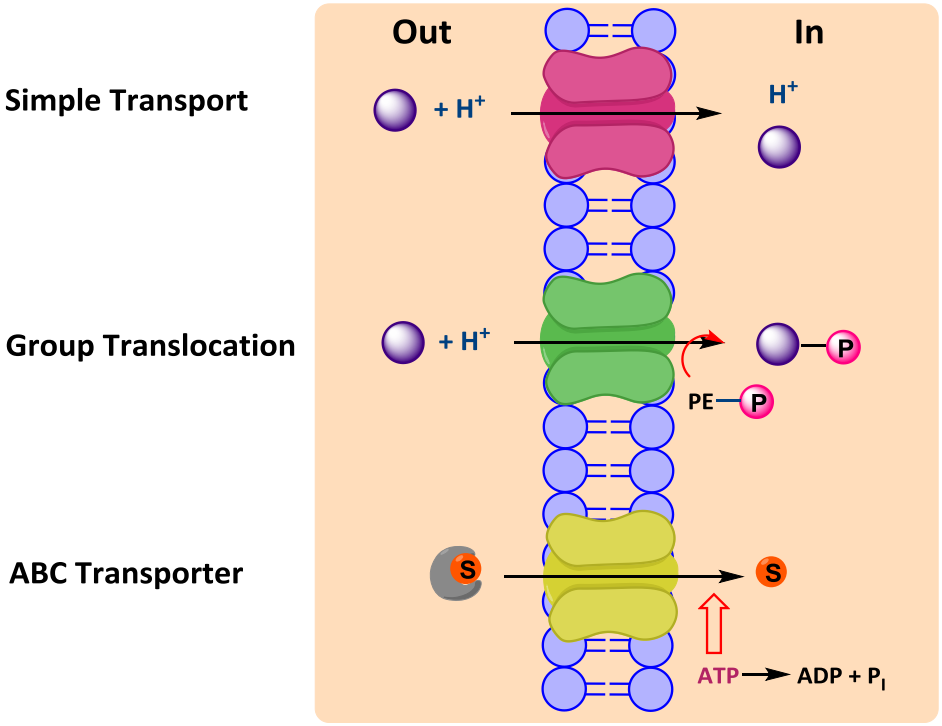

Figure 10. The three mechanisms of transport into cytoplasmic membrane.[23] Abbreviations: Substrate, S and phosphotranspyruvate, PEP.

In group translocation, the substrate is changed chemically during transport. Examples of this type of transportation are the translocation of sugars which are phosphorylated during transport by the phosphotransferase system. The system employs a series of transport proteins that catalyse the transport of sugar by phosphorylation driven by the energy provided by PEP through the cytoplasm membrane.[23]

Lastly, the ABC (ATP binding cassette) system employs high substrate-specific binding proteins. The periplasmic binding protein interacts to a membrane-spanning protein

contained within the cytoplasmic membrane that allows the transport of the substrate. Finally, the cytoplasmic ATP hydrolysing protein provides the energy required for the process.[23]

Chromogenic and fluorogenic substrates, such indoxyl glycosides and fluorescent coumarin heterocycles, are examples of synthetic enzyme substrates that are used to detect an enzymatic activity in bacteria. The substrates consist of two components: either a chromogen or fluorogen is linked to an ester, phosphate, peptide or glycoside. Hydrolysis of chromogenic and fluorogenic substrates by bacteria is dependent not only on the expression of hydrolase enzymes within the cell, but transportation of the substrate through the bacterial cell wall. When hydrolysed by an appropriate enzyme, the susbtrates will either produce a signal in a form of colour or fluorescence.

1.5 Conventional approach for the detection and identification of bacterial pathogens

It is often difficult to isolate pathogenic bacteria from food and clinical samples as they are often present in a very small number against the normal background flora. Direct inoculation of these samples results in an overgrowth of the organisms on an agar plate which are dominantly populated by the background flora making the detection impossible. Several antibiotics and inhibitory growth agents have been used to attempt selectively reduce the commensal bacteria without inhibiting the growth of bacterial pathogens.[66] These selective agents have been chosen based on empirical work and their concentrations are very crucial: Therefore, to reduce a small number of the targeted organisms, a suitable procedure must be found to reduce the number of background population.

Selective agents such as chemicals or antimicrobials are added to culture media to suppress the growth of unwanted organisms in a polymicrobial sample, allowing most of the desired microorganisms to grow. Finding suitable selective compounds are often difficult. Bacteria can be distinguished subjectively based on their clinical morphology, changes in pH of media and colouration of the microbial colony, due to their metabolism.[18] This requires a competent personnel with years of experience and, at this instance, automation and non-skilled processing are deemed to be inapplicable.

Pathogenic bacteria that are being recovered from food and environmental samples may result for some of the cells to be injured. Also, by transferring organisms directly to a broth that contains selective toxic agents, which decreases the growth of background flora, will eventually result in their death. Therefore, it is advisable to dilute the samples in non-selective or mildly selective broth. Otherwise, if the media is too nutritious, this will result in overgrowth of the targeted bacteria by the background flora. After suitable incubation periods, the samples are enriched and are inoculated into an agar plate containing selective agents filtering some of the bacteria that were not inhibited during the enrichment stage.[67, 68] To visualise the target bacteria, biochemical substrates may also be added into the agar medium to distinguish other organisms that were not inhibited. For example, MacConkey Agar containing sorbitol is a selective medium, which is effective at isolating *E. coli* O157. The medum contains sorbitol, which is fermented by most *E. coli*, producing pink colonies. In contrast, *E. coli* O157 does not ferment the sugar and, therefore, forming colourless colonies. To improve the selectivity of the medium, Chapman and co-workers[69] incorporated potassium tellurite into Sorbitol MacConkey Agar for the selection of verocytotoxin-producing (VT^+) *E. coli* O157 from cattle rectal swabs. The authors reported that potassium tellurite was used to isolate tellurite resistant VT^+ *E. coli* O157 from other *E. coli* serogoup and inhibited *Aeromonas* and *Providencia* species. The possible

mechnanisms of action of tellurite resistant- VT^+ *E. coli* O157 could be chromosomally or plasmid mediated,[70] phosphate transport pathway[71] or reduction of the substrate to metallic tellurium.[72] In addition, the authors also added cefixime to inhibit *Proteus* species.

From the isolation plate, further tests are performed to confirm the identity of typical colonies. The test can be done by using biochemical identification strips, latex agglutination or modern techniques. However, the procedure can be labour intensive and expensive, and thereby only applicable for food samples.[73-75] **Figure 11** shows the stages of the traditional approach of bacterial detection and identification.

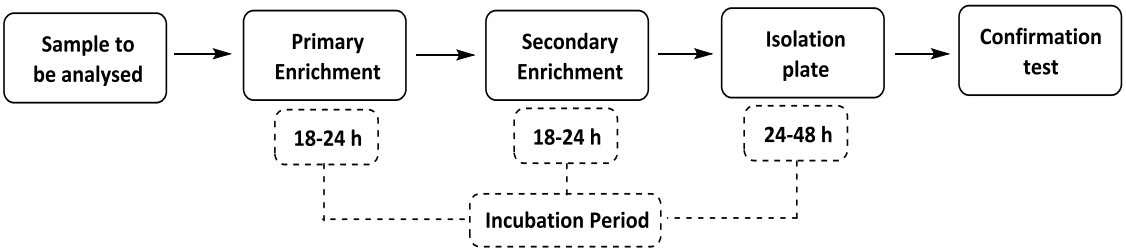

Figure 11. Conventional approach for the detection and identification of bacteria.[76] The time is in hours (or h).

In order to reduce the time to isolation and identification of any pathogens present in samples a variety of techniques have been investigated, as summarised in **Table 1**. It is tempting to anticipate the systematic replacements of culture methods over laboratory automations when looking into the future. In recent years, PCR and MALDI-TOF MS methods are making major contributions in diagnostic microbiology,[77-80] where exact identification may be obtained in a relatively short time. However, some selective isolation and enrichment, particularly from food samples, is still required.

Table 1. Summary of rapid diagnostic methods for the detection of food-borne and clinical bacteria.

Diagnostics Methods	Sensitivity CFU mL^{-1}	Time Before Results	Advantages	Disadvantages	Ref.
Adenosine-5'-triphosphate (ATP) Bioluminescence	10^4	0.5 h	Rapid analysis. Used in hygiene monitoring in food and hospital settings.	Unable to identify bacteria. Difficult to separate eukaryotic ATP. Factors such as pH, temperature and luciferase inhibitors may influence reaction. Merely a marker for viable cells and, therefore used mostly for effective disinfection	81, 82
Direct Epifluorescent Filter Microscopy (DEFT)	10^3 - 10^4	0.5 - 1 h	Able to distinguish between viable and dead cells. Enumaration of viable cells	Labour intensive. Sample pre-treatment prior to analysis. Unable to identify bacteria	75, 81, 83
Flow Cytometry (FC)	10^2 - 10^3	5 - 30 min	High-throughput screening (at least 1000 of cell per second).	Unable to distinguish between viable and dead cells. Must be a clean sample (no large particles or food sample matrix). Difficulties with the small size of bacteria. Unable to viable bacteria unless immunofluorescent labelling is used.	75, 81, 84

Table 1 (continued). Summary of rapid diagnostic methods for the detection of food-borne and clinical bacteria.

Diagnostics Methods	Sensitivity CFU mL^{-1}	Time Before Results	Advantages	Disadvantages	Ref.
Fluorescent *In Situ* Hybridisation (FISH)	10^4	3 h	Culture method is not required. Rapid, time of results within.	Pre-enrichment steps and selective isolation is required. Highly labour intensive. Unable to distinguish between viable and dead cells. Requires specific antigen for detection.	75, 85, 86
Immunological Methods	10^4 - 10^5	1 - 2 h	Rapid analysis. Can be performed in minimally equipped laboratories. Low cost.	Enrichments and isolation of target cells required. Non-specific binding of the antigen and/or antibody that can lead to false-positives. Mainly used for serotyping.	75, 87, 88
Impedance	1	6 - 24 h	High throughput screening (at least 100 samples simultaneously). High sensitivity if selective media used.	Food matrix may influence the analysis. Unable to identify bacteria and identify mixed cultures.	81, 89, 90

Table 1 (continued). Summary of rapid diagnostic methods for the detection of food-borne and clinical bacteria.

Diagnostics Methods	Sensitivity	Time Before Results	Advantages	Disadvantages	Ref.
Lab-on-a-chip	10^1 CFU μl^{-1}	2 - 5 h	Portable and flexible. Cost effective. Can be used in minimally equipped laboratory.	Enrichments and isolation of target cells required prior to electrochemical detection. Direct detection of bacterial pathogens.	91, 92
Matrix-assisted Laser Desorption Ionisation Time-of-Flight Mass Spectrometry (MALDI-TOF MS)	10^5 CFU mL^{-1}	1-2.5 h	Rapid analysis.	Enrichments and isolation of target cells required. Large cost initially for purchase of equipment.	93, 94
Polymerase Chain Reaction (PCR)	10^4 CFU mL^{-1}	3 - 5 h	May be rapid if enough bacteria. Many samples can be run at the same time. May be very specific.	Enrichment steps are required. Requires specific probe sequence for known organisms (Sequencing and primers required).	75, 95-97

1.6 An overview of synthetic enzyme substrates in culture media

To reduce the time taken for the selective isolation and enrichment steps, major improvements have been made by commercial manufacturers with the isolation plate. For the presumptive identification of targeted organisms, a more targeted inhibition for the commensal flora and the addition of markers has been utilised. Markers are originally reagents that have been used to detect the product's biochemical pathways such as the fermentation process of sugar or the production of ammonia from the deamination of amino acids. Other markers include ferric salts to detect hydrogen sulphide as a black precipitate,[98, 99] indole production from tryptophan[100, 101] and PYRase production.[102, 103] The markers can be used to selectively target pathogens and can be easily differentiated from commensal flora. For example, Hektoen Enteric Agar is a differential, selective culture medium for the isolation of *Shigella* and *Salmonella* enteric pathogenic specimens. The agar consists of thiosulfate and ammonium ferric citrate to differentiate hydrogen sulfide producing *Salmonella* from *Shigella*. With the inclusion of bromothymol blue as an indicator, the former produces blue-green coloured colonies with black colours in centre, which is due to the production of hydrogen sulfide. The agar also contains various carbohydrates such as lactose, salicin and sucrose, where these sugars were non-fermented by neither *Salmonella* nor *Shigellae*. Thus, the sugars are fermented by coliforms, which are also inhibited with the inclusion of bile salts.[104-106]

The introduction of chromogenic or fluorogenic substrates has been utilised to differentiate the targeted bacteria from a mixture of closely related organisms. The substrates consist of a coloured or fluorescent molecule (chromogen or fluorogen) linked to a substrate moiety (glycoside, peptide, phosphate or ester). When linked, the molecule loses its colour or fluorescence, and this return only on hydrolysis by the appropriate enzyme such as glycosidase, as shown in **Figure 12**. Ideally, the released coloured or fluorescent product

should be highly restricted within the targeted bacterial colonies as this allows clear differentiation amongst other flora that do not exhibit similar enzyme activity, especially when working with a polymicrobial culture. The substrates should not inhibit the bacterial growth.[18, 107, 108]

The synthetic enzyme substrates have been designed to detect hydrolase enzymes such as esterases, phosphatases, peptidases and glycosidases.[109] Glycosidase enzymes exhibit a high degree of specificity and are dependent on the sugar type, steric conformation and configuration of the anomeric linkage between the substrate and sugar.[110-111]

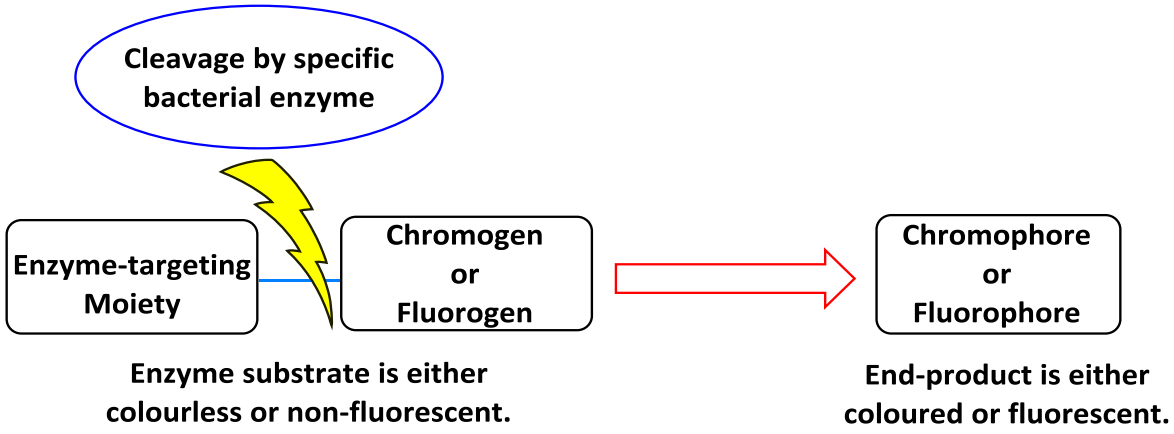

Figure 12. Hydrolysis of synthetic enzyme substrate by hydrolase enzymes from bacteria.

1.6.1 Chromogenic substrates in culture media

In biochemistry and clinical microbiology, one of the earliest and most well-known synthetic chromogenic substrates was *o*-nitrophenyl β-D-galactopyranoside (ONPG). Lederberg used ONPG to detect β-galactosidase in *Escherichia coli* in broth cultures. Upon hydrolysis, free *o*-nitrophenol is released and develops into the *o*-nitrophenoxide ion as a bright yellow coloured product in an alkaline solution, as shown in **Scheme 1**.[112]

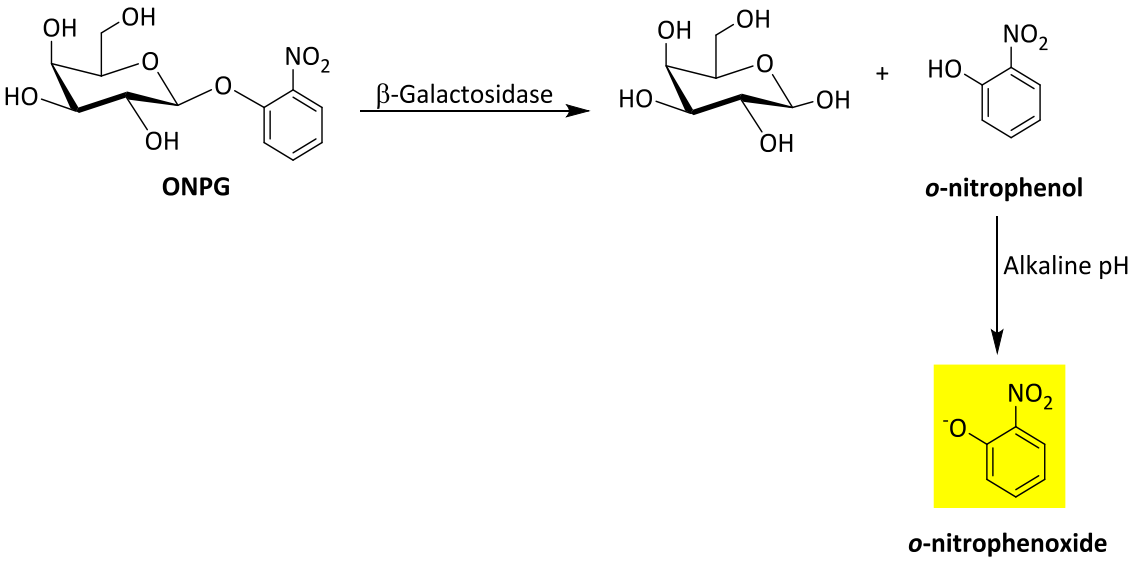

Scheme 1. Hydrolysis of ONPG to produce bright yellow coloured *o*-nitrophenoxide.[112]

Other chromogenic substrates like phenolphthalein have been used to detect phosphatase and β-galactosidase enzymes. For example, the substrate has been used to detect phosphatase within staphylococci, to produce a purple colour in alkaline solution.[113] Due to solubility of the coloured products,[109] these compounds are more applicable for use in commercial kits to identify bacteria based on their biochemical profiles, for example API®ID strips (Biomerieux) and the Oxoid Microbact system (Thermo Fisher Scientific, Basingstoke, UK). Sensitivity can be enhanced by derivatising the products with diazonium salts. For example, Oxoid OBIS kit is used for detection of PYRase in *Streptococci* and *Citrobacter*

species. The kit system only requires five minutes incubation and produces intensely coloured products.[114]

To decrease solubility and localise colouration for use in agar plates, esculin-β-D-glucoside has been used. Free esculetin released by β-glucosidase chelates with ferric ions in solution to produce a black precipitate around colonies, as depicted in **Scheme 2**.[115]

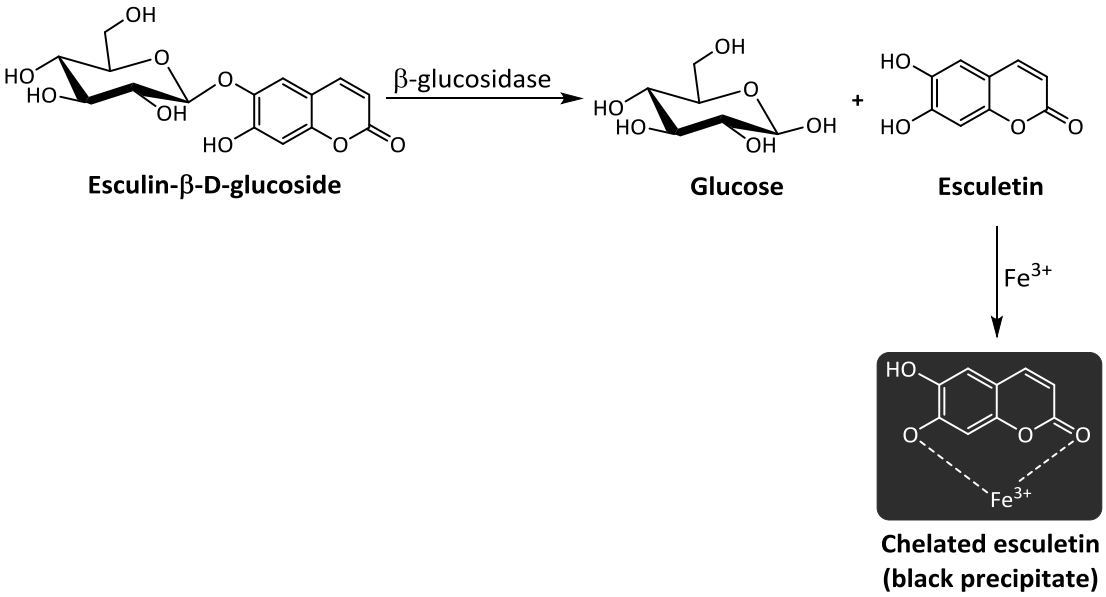

Scheme 2. Hydrolysis of esculine β-glucoside generating a black precipitate.[115]

As the complex may diffuse on agar plates with prolonged incubation, esculetin was modified to form 3,4-cyclohexenoesculetin.[116] Another chelating compound is 8-hydroxyquinoline, which also gives highly insoluble compounds with ferric salts,[117] as shown in **Figure 13**.

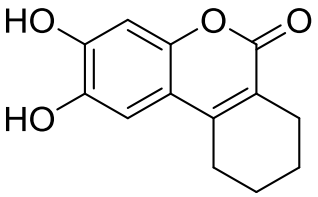

3,4-Cyclohexenoesculetin (CHE)

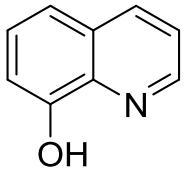

8-Hydroxyquinoline (8HQ)

Figure 13. Structures of 3,4-cyclohexenoesculetin (CHE) and 8-hydroxyquinoline (8HQ).

1.6.2 Fluorogenic substrates in culture media

Fluorogenic substrates can provide much more sensitive detection of enzymes than their chromogenic counterparts and this can be further amplified by the use of a fluorimeter. The most used fluorogens for bacterial identification are 4-methylumbelliferone (4-MU) and 7-amino-4-methylcoumarin (7-AMC). The substrates emit a blue fluorescence which is quenched when the enzyme substrate is formed.[118, 119]

To improve the detection properties of 4-MU, Chilvers and co-workers synthesised a derivative, ethyl-7-hydroxycoumarin-3-carboxylate (EHC). This enhanced fluorescence at physiological pH, and reduced bacterial growth inhibition and toxicity against several strains of β-galactosidase coliform strains in water analysis.[120] For the detection of β-alanyl aminopeptidase in *Pseudomonas Aeruginosa*, Viradi *et al.*[121] synthesised an amino peptide substrate, 7-{4-(β-alanylamino)}benzyloxy-3-ethoxycarbonylcoumarin triflouroacetate, as shown in **Figure 14.** The fluorogen exhibited higher sensitivity and stronger fluorescent intensity than 7-AMC.

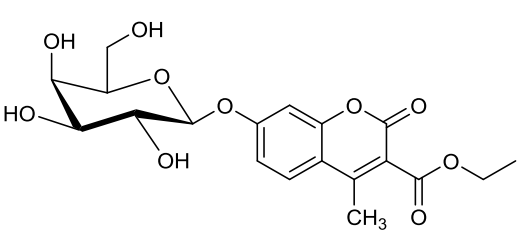

Ethyl-7-hydroxycoumarin-3-carboxylate (EHC)

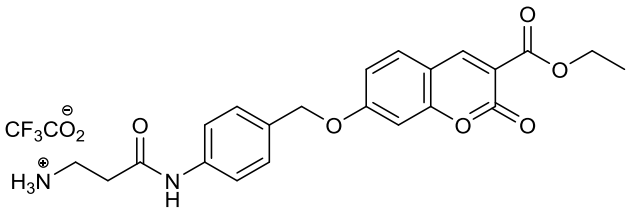

7-{4-(b-alanylamino)}benzyloxy-3-ethoxycarbonylcoumarin trifluoroacetate

Figure 14. Structures of the the optimised coumarin substrates EHC and β-alanyl aminopeptide as fluorogens.

Other well-known fluorogens are fluorescein and resorufin, which are again more fluorescent than 4-MU. Plovins and co-workers utilised fluorescein di-galactoside for the detection of β-galactosidase by flow cytometry in live *E. coli* cells.[122]

Despite their sensitivity, the use of fluorogens in bacterial identification has been limited due to the high aqueous solubility of fluorogenic substrates, and hence the inability for them to be used in agar media. They also require a UV lamp or fluorimeter for detection.

1.7 Indoxyl substrates in culture media

Although, the compounds described above have their advantages and drawbacks, the most commonly used chromogenic substrates, by far for bacterial identification, are those based on indoxyl. Coupling indoxyl to sugars stabilises the molecules producing a colourless substrate. When an appropriate enzyme cleaves the linkage, the free indoxyl is released and the coloured indigo is precipitated. Indoxyl-based substrates are considered powerful chromogenic substrates that are used extensively in histochemistry, biochemistry and bacteriology.[110-111]

In microbiology, one of the most well-known and widely used chromogenic substrates is 5-bromo-4-chloro-3-indolyl β-D-galactopyranoside (**1a**, 5-Br-4-Cl-β-D-gal or X-β-D-gal). James *et al*. described the X-β-D-gal as the 'gold standard' for bacterial detection.[123] As shown in **Scheme 3**, substrate **1a** is a colourless substrate; however, when incorporated in an agar medium in the presence of bacteria, the substrate is hydrolysed, releasing halogenated free indoxyl which dimerises to afford 5,5'-dibromo-4,4'-dichloroindigo when oxidised, producing a blue-green coloured-end product.

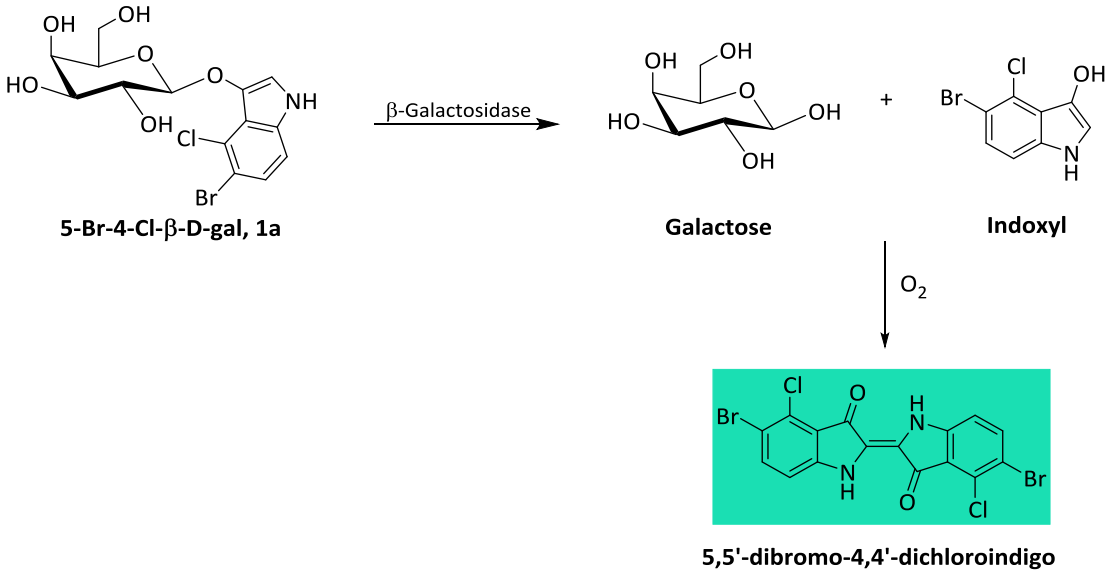

5-Br-4-Cl-β-D-gal, 1a **Galactose** **Indoxyl**

5,5'-dibromo-4,4'-dichloroindigo

Scheme 3. Hydrolysis of X-β-D-gal **1a** by β-galactosidase enzyme to release free 5-bromo-4-chloro-3-indoxyl that dimerises into blue-green coloured indigo product.

Apart from the high sensitivity, another advantage of indoxyl-based substrates is the intense colouration and insolubility of the dye, which therefore does not spread far from the site of enzyme action. This allows clear differentiation of microbial colonies growing on an agar medium that exhibit enzyme activity from those that do not. For example, *Salmonellae* may be differentiated from other members of the *Enterobacteriaceae* using Brilliance™

Salmonella agar, which consist of magenta caprylate (5-bromo-6-chloro-3-indolyloctanoate). A secondary chromogen, 5-bromo-4-chloro-3-indolyl β-D-glucopyranoside is incorporated in the medium to isolate other organisms such as *Klebsiella* and *Enterobacter* that produce β-glucosidase. Compared to conventional media like Xylose-Lysine-Deoxycholate (XLD), Oxoid Brilliance™ *Salmonella* agar offers a higher level of discrimination between the target organism *Salmonella* and other coliforms, as shown in **Figure 15**.

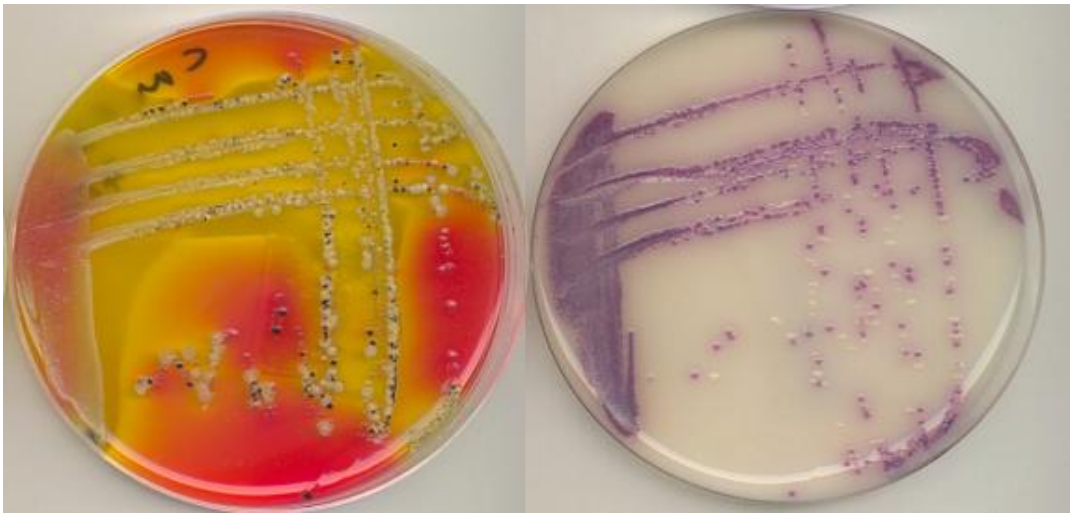

Figure 15. Comparison of two culture media. Commonly used XLD differential medium (left) Oxoid Brilliance™ *Salmonella* medium. Note that all purple colonies are *Salmonella* Typhimurium ATCC 14028 but they cannot easily be differentiated on XLD. Image courtesy of Thermo Fisher Scientific.

Different colours of the indigo product are produced by incorporating halides into the benzene ring. Examples of commercially available products are shown in **Table 2**.[110]

Table 2. Structures and colours produced from various commercially available indoxyl compounds.

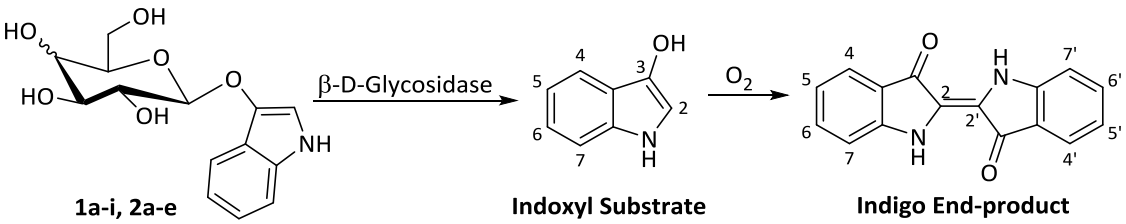

Indoxyl substrates	β-D-Gal	β-D-Gluc	Synonyms	λ_{max} [110]	Indigo Products	End-colour Product
5-Bromo-4-chloro-indoxyl	**1a**	**2a**	X	620	5,5'-Dibromo-4,4'-dichloroindigo	Blue-green
5-Bromo-indoxyl	**1b**	**2b**	Lapis	620	5,5'-Dibromoindigo	Lapis blue
5-Bromo-6-chloro-indoxyl	**1c**	**2c**	Magenta	565	5,5'-Dibromo-6,6'-dichloroindigo	Magenta
6-Chloro-indoxyl	**1d**	**2d**	Rose, Salmon	590	6,6'-Dichloroindigo	Red
Indoxyl (without substituents)	**1e**	**2e**	N/A	605	Indigo	Indigo
6-Fluoro-indoxyl	**1f**	**N/A**	Rouge	570	7,7'-Difluoroindigo	Rouge
5-Iodo-indoxyl	**1g**	**N/A**	N/A	610	5,5'-Diiodoindigo	Purple
3-Thio-indoxyl	**1h**	**N/A**	N/A	620	3,3'-Thioindigo	Purple
N-Methyl-indoxyl	**1i**	**N/A**	N/A	665	*N,N'*-Dimethylindigo	Green

Abbreviations: β-Galactoside, β-Gal; β-Glucoside, β-Gluc; and, N/A, not applicable as the material is not commercially available. (Table adapted from [110])

This difference in colouration makes it possible to detect two or more enzymes in one agar plate, and thus distinguish several organisms at the same time or aid in the identification of one organism that is biochemically closely related to others. For example, Oxoid Brilliance™ *Candida* Agar (**Figure 16**) is a selective differential chromogenic medium for the isolation and differentiation of species of the yeast *Candida*. The agar incorporates two chromogenic substrates, 5-bromo-4-chloro-3-indolyl β-D-*N*-acetylglucosamine and 5-bromo-6-chloro-3-indolyl phosphate, for the detection of glycosidase and alkaline phosphatase activities, respectively. Hydrolysis of the substrates generates colours ranging from beige to blue.[124]

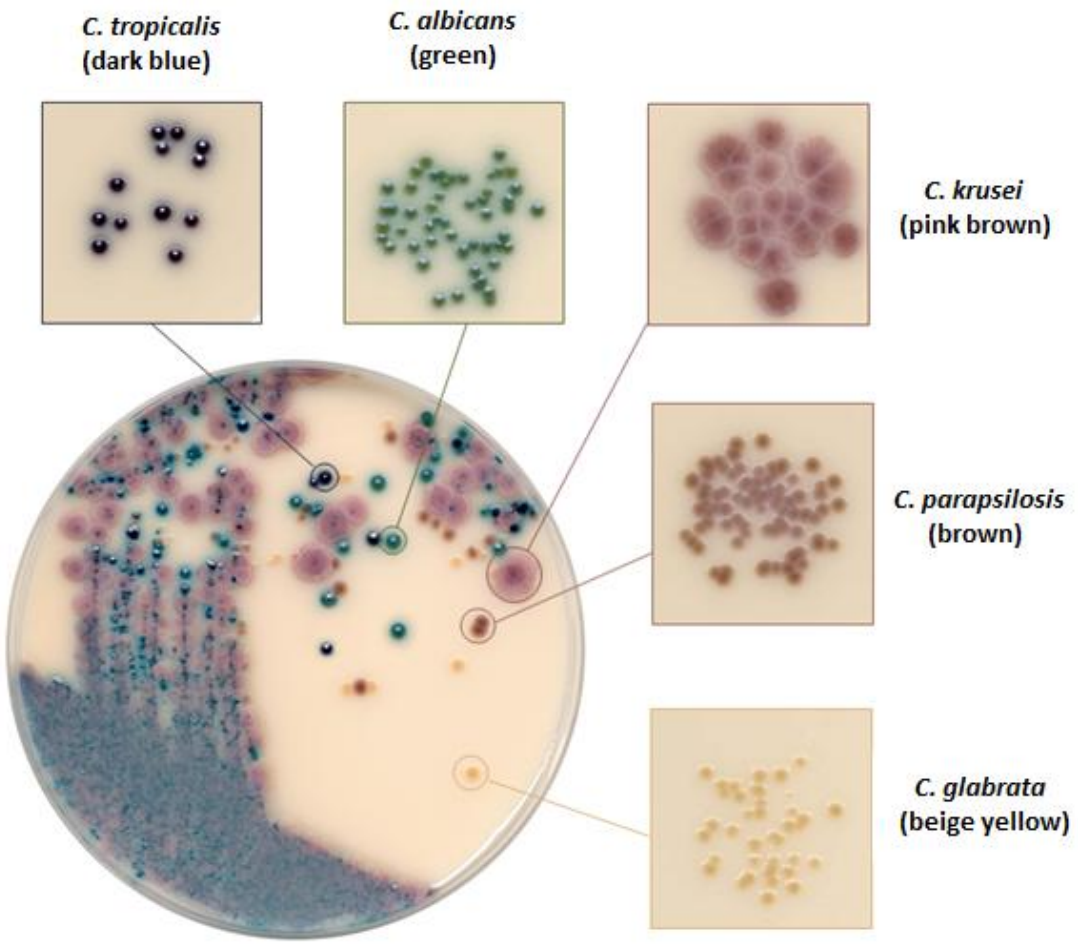

Figure 16. Oxoid Brilliance™ *Candida*. Different colours represent different species of the yeast Candida.[124] Image courtesy of Thermo Fisher Scientific.

Another example is Oxoid Brilliance *E.coli*/coliform selective agar. 5-Bromo-4-chloro-3-indolyl β-D-glucuronide is used to detect β-glucuronidase activity in *E.coli*, which generates distinctive purple colonies. Other coliforms (*Klebsiella*, *Enterobacter* and *Citrobacter*) hydrolyse 6-chloro-3-indolyl β-D-galactoside to produce pink colonies (**Figure 17**). Further examples of enzyme substrates and their applications are given in **Table 3**.

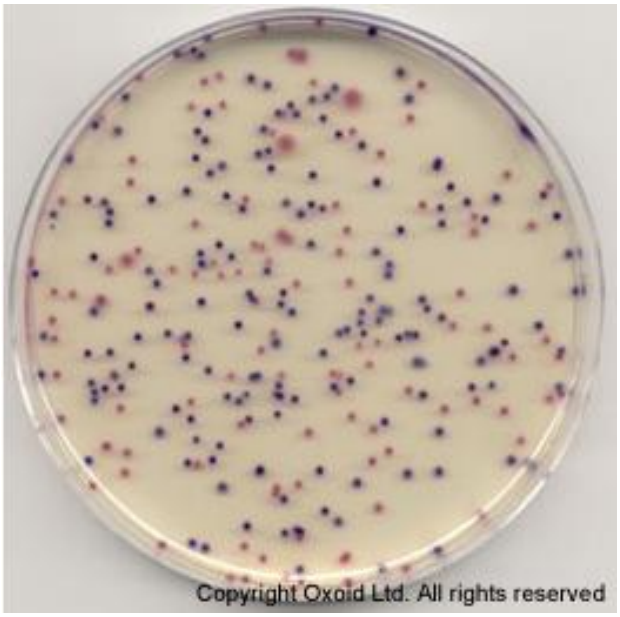

Figure 17. Oxoid Brilliance™ *E. coli*/coliform Selective Agar is a selective differential media use to discriminate *E. coli* against coliforms from food and water samples.[125] Reproduced with permission from Thermo Fisher Scientific.

Table 3. A summary of synthetic enzyme substrates that targets glycosidase enzymes produced by pathogens.

Glycosidase Enzyme	Microorganisms	Substrates	Samples
α-Galactosidase	*Salmonella*	Indoxyl	C and F
	E. coli O157:H7	Indoxyl	C and F
β-Galactosidase	*E. coli*	Indoxyl and FDG	C
	E. coli O157:H7	Indoxyl	C and F
	VRE	Alizarin	C
α-Glucosidase	*Cronobacter sakazakii*	Indoxyl	F
	Staphylococcus aureus	Indoxyl	C and F
	MRSA	Indoxyl	C
	VRE	Indoxyl	C
β-Glucosidase	KESC	Indoxyl	C
	ESBL producing enterobacteria	Indoxyl	C
	Vibrio	Indoxyl	C and F
	Enterococci	Indoxyl	C and W
	VRE	Indoxyl	C
	Listeria spp.	Indoxyl	F
Cellobiosidase	*C. sazakii*	Indoxyl	F
β-Glucuronidase	*E. coli*	4-MUG and Indoxyl	C, F and W
	ESBL producing *E. coli*	Indoxyl	C
β-ribofuranosidase	*Yersinia enterocolitica*	Indoxyl and 3',4'-Dihydroxyflavone	C
Hexosaminidase	*C. albicans*, *C. dubliniensis and C. tropicalis*	Indoxyl	C

Abbreviations: Clinical, C; Food, F; Water, W. Extended-Spectrum β-Lactamases, ESBL; *Klebsiella*, *Enterobacter*, *Serratia*, *Citrobacter*, KESC; Methicillin-resistant *Staphylococcus aureus*, MRSA; and, Vancomycin-resistant *Enterococci*, VRE. (Results adapted from [109])

1.8 Synthetic methodologies for preparing indoxyl glycosides

One of the major limitations of indoxyl glycosides is their synthesis, particularly the glycosidation step. Traditional glycosidation via the Michael reaction is usually performed in acetone by addition of 1M NaOH, followed by de-*O*-acetylation. The usual key precursor, a 1-acetyl-3-indolinone (also known as *N*-acetyl indoxyl) is coupled with a glycosyl halide, followed by deprotection using a base to produce indolyl β-D-galactoside as the final product (**Scheme 4**). The route usually provides products in very low yields.[126, 127]

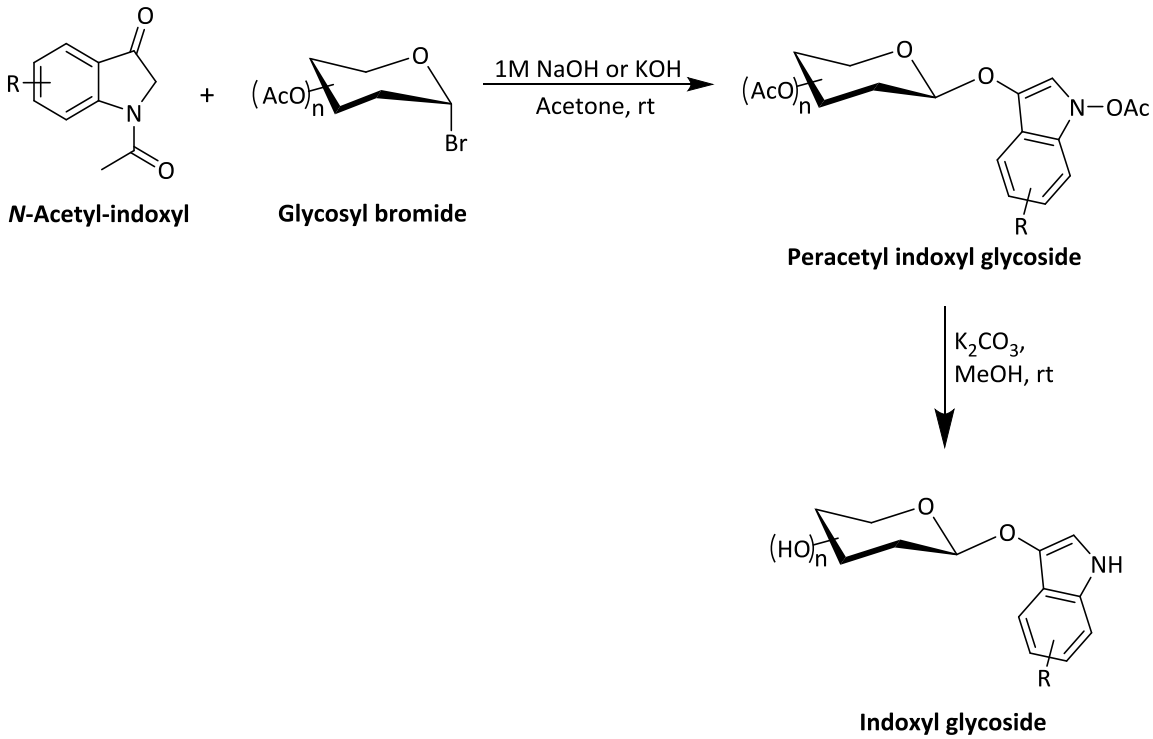

***N*-Acetyl-indoxyl** **Glycosyl bromide** **Peracetyl indoxyl glycoside** **Indoxyl glycoside**

Scheme 4. *O*-Glycosidation via the Michael reaction pathway to produce indoxyl glycosides using *N*-acetyl indoxyl as a key precursor.[127] Abbreviation: Room temperature, rt.

Improvement in the synthetic route of indoxyl glycosides is very crucial to produce products in high yields. Böttcher and co-workers[128] optimised the synthetic route using phase-transfer catalysis (PTC) glycosylation using tetrabutylammonium hydrogen sulfate (TBAHS). Indoxylic acid allyl ester is coupled with the glycosyl bromide, followed by two deprotection steps (**Scheme 5**). The improved route provides high-yielding per-*O*-acetyl indoxylic acid allyl ester glycosides saving chemists time and effort to produce the desired chromogenic substrates prior to microbiological analysis.

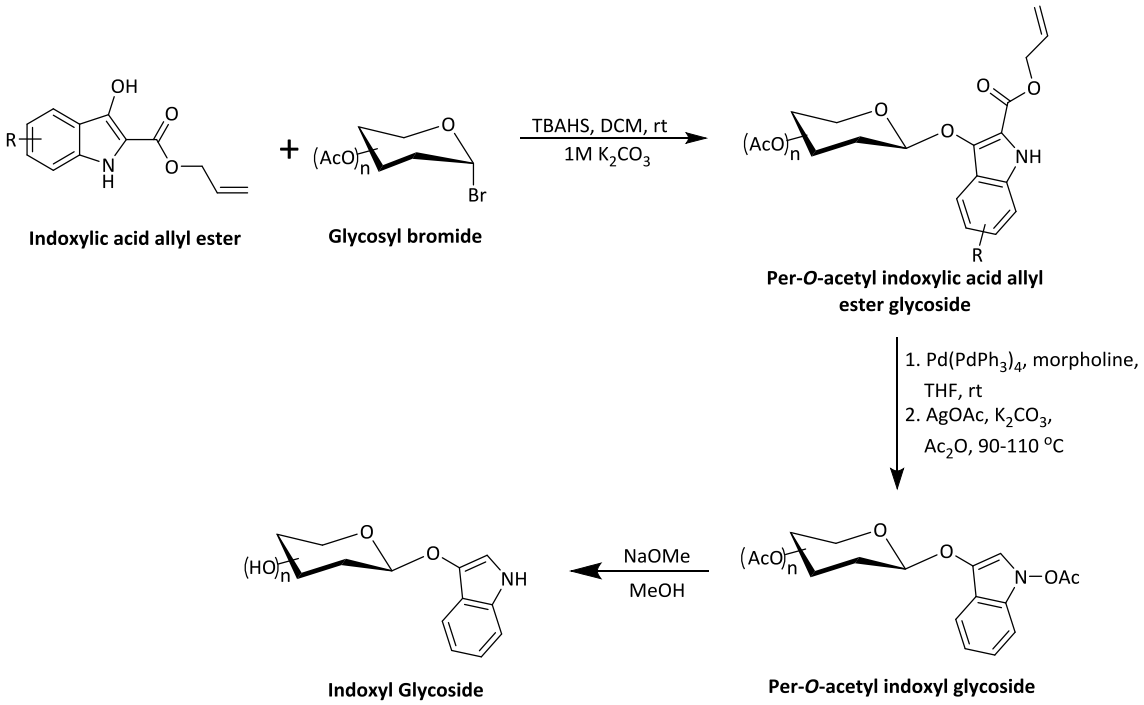

Scheme 5. Optimised *O*-glycosidation pathway developed by Böttcher and co-workers.[128]

The developed route could potentially allow glycosidation of indoxyls with less known sugars like L-(+)-rhamnose. The glycoside is currently not commercially available; although, the chemically related sugar structure L-fucose coupled to an indoxyl is sold by chemical vendors.[129] Therefore, the former is of interest to investigate its application in diagnostic microbiology.

As shown in **Scheme 6**, L-(-)-fucose and L-(+)-rhamnose are metabolised by *E. coli* through parallel phosphorylated pathways mediated by different enzymes that include a permease, an isomerase, a kinase and an aldolase. When the L-(-)-fucose or L-(+)-rhamnose enter the permease, the sugars are isomerised to L-fuculose or L-rhamnulose, followed by phosphorylation to produce L-fucose-1-phosphate or L-rhamnulose-1-phosphate by their respective kinases. The stereochemical differences of both the sugars disappear when the phosphorylated sugars are cleaved by their corresponding aldoses to yield dihydrooxyacetone phosphate and L-lactaldehyde. In the case of *E. coli*, there are two homologous sets of inducible proteins that are specific for the metabolism of their corresponding sugars and are coded by two different clusters of operon genes: fuc A and rha D for fucose and rhamnose sugars, respectively.[130, 131]

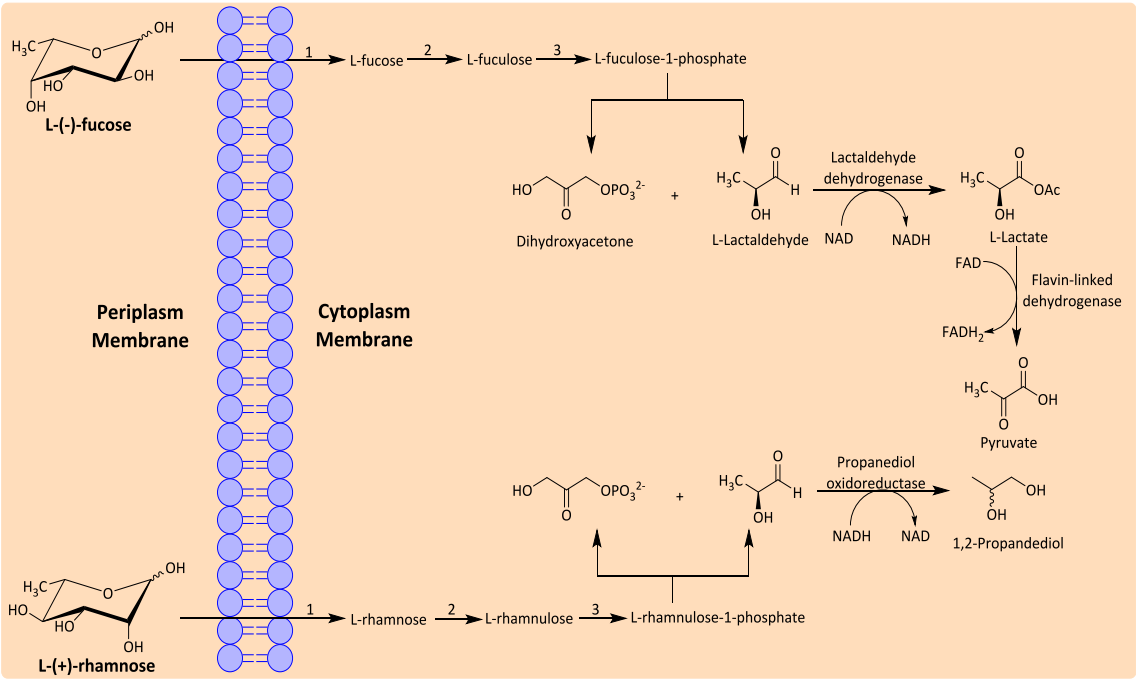

Scheme 6. The phosphorylated pathway of L-(-)-fucose and L-(+)-rhamnose sugars in *E. coli*.[130-131]

Subsequently, L-lactaldehyde follows two different metabolism pathways. Under aerobic conditions, the aldehyde is oxidised to L-lactate by the catalysis of nicotinamide adenine nucleotide[132] dependent lactaldehyde dehydrogenase, followed by further oxidation by flavin-linked dehydrogenase to produce pyruvate. Under anaerobic conditions, L-lactaldehyde is reduced to 1,2-propanediol by an nicotinamide adenine dinucleotide-linked propanediol oxidoreductase. Thus, the pathways allow for the fermentation process of these sugars.

L-(+)-rhamnose carbohydrate can also be catabolise in microorganisms like fungi without going through the phosporylated pathway. As shown in **Scheme 7**, the diagram describes the enzyme activities when the sugar enters the cytoplasm membrane.

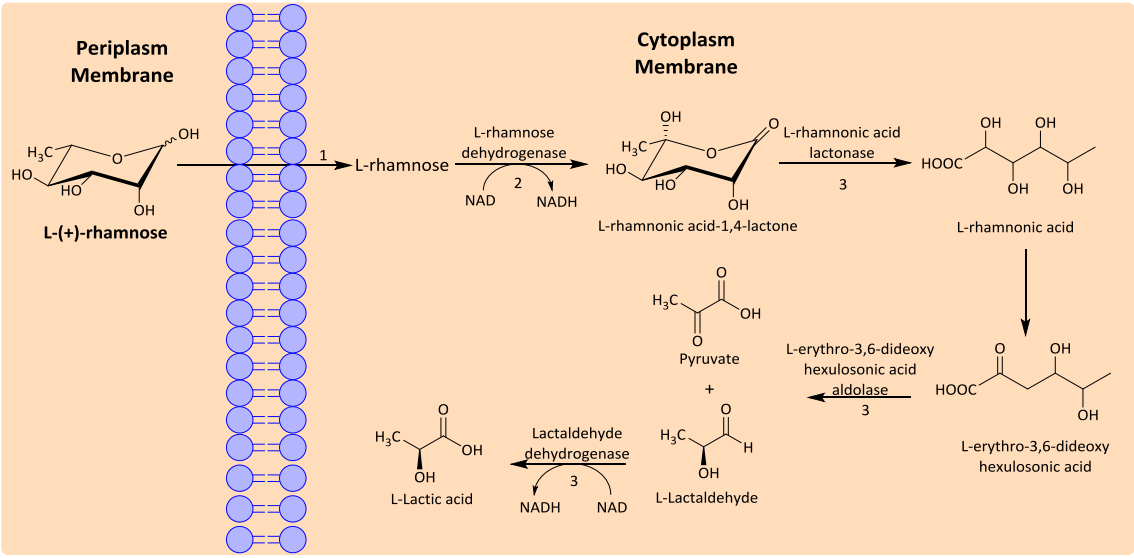

Scheme 7. The non-phosphorylated pathway of L-(+)-rhamnose sugars in fungi.[133]

L-(+)-rhamnose is catabolise by a series of enzymes utilising nicotinamide adenine dinucleotide (NAD): L-rhamnose-1-dehydrogenase, L-rhamnonic acid lactonase, L-rhamnonic acid dehydratase and L-erythro-3,6-dideoxyhexulosonate aldolase. The corresponding intermediates are: L-rhamnonic acid-1,4 lactone, L-rhamnonic acid, L-erythro-3,6-dideoxyhexulosonic acid, pyruvate and L-lactaldehyde. The L-lactaldehyde is then oxidised L-lactaldehyde dehydrogenase in NAD-induced oxidation to produce L-lactate.[133]

1.9 Comparison of the hydrolysis of different chromogenic substrates

It may be anticipated that differences in the substituents of the indoxyl chromogens would have little effect on hydrolysis of the substrate and that the enzyme would only be specific for the non-chromogen structure and its bonding to the chromogen. However, this is not the case. Perry *et al*.[134] conducted a study on various different indolyl β-D-glucosides and found that the number of strains of *Citrobacter freundii* and *Shigella sonnei* that could hydrolyse the substrates differed, as provided in **Table 4**.

Table 4. Differences in the number of strains that hydrolysed different indoxyl β-D-glucosides.[134]

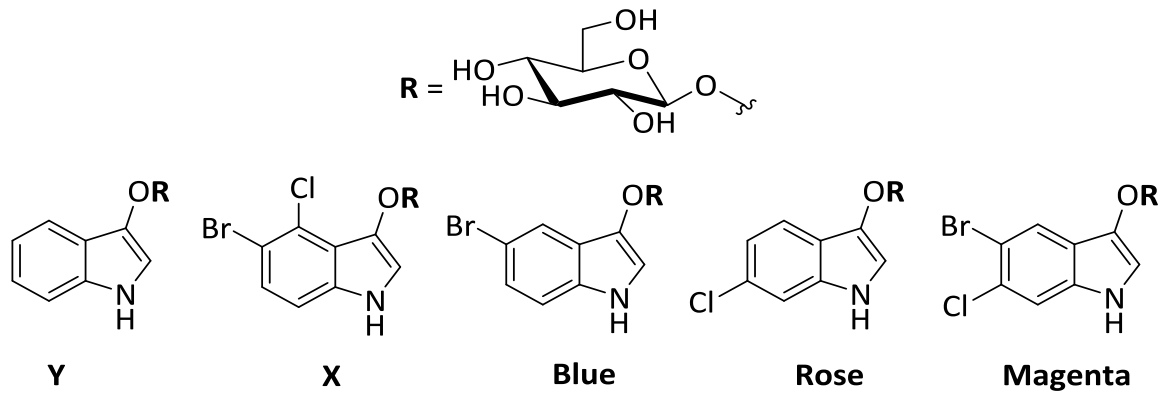

Organisms	No. of strains	Y	X	Blue	Rose	Magenta
Citrobacter freundii	10	0	1	7	7	3
Shigella sonnei	5	2	0	2	0	0

Note: The results indicated the number of strains that exhibited β-glucosidase activity with each substrate.

Aside from indoxyl substrates, the authors also observed even greater differences on the hydrolysis of other chromogens (**Table 5**).

Table 5. Differences in the number of strains that hydrolyses different chromogenic substrates.[134]

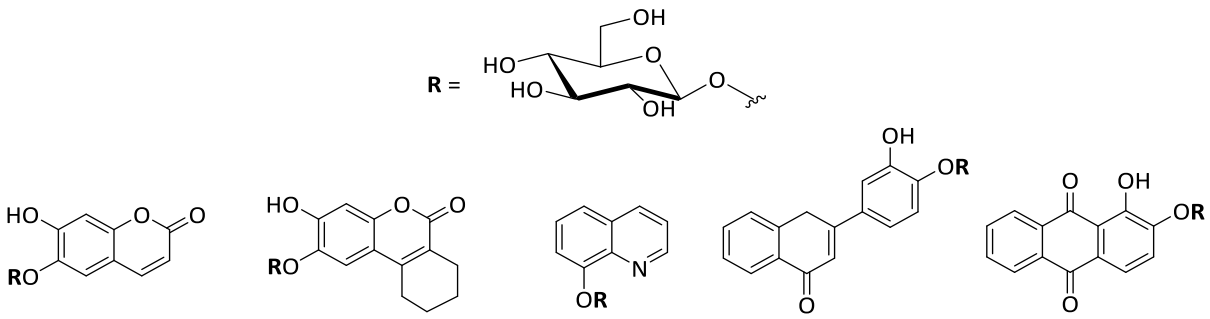

Organisms	No. of strains	Esculin	CHE	8HQ	DHF	Alizarin
Citrobacter freundii	10	0	2	0	0	10
Escherichia coli	10	0	0	0	0	10
Klebsiella pneumonia	10	10	10	8	10	10
Salmonella spp.	10	0	0	0	0	0
Shigella sonnei	5	0	0	2	0	5
Yersinia enterocoltica	5	0	0	0	0	0
Enterococcus faecalis	20	20	20	0	20	20
Listeria spp.	20	20	20	0	20	20

The authors hypothesised that different activities exhibited by the indoxyl chromogenic glycosides may either be due to the rate of substrate uptake through the cell envelope, or differences in substrate hydrolysis within different species.[134] Since indoxyl-based substrates are the most commonly used chromogenic substrates, it would be interesting to investigate the molecular structure of the indoxyl and how it affects the rate of hydrolysis.

1.10 Research aims and objectives

Indoxyl substrates are the most commonly used chromogenic substrates in diagnostic microbiology because of their very unique and distinctive features. One of the major advantages of indoxyl glycosides is that indoxyl can be derivatised to provide a wide range of colours that can be utilised for better discrimination of different microorganisms in culture media. Therefore, the aim of this project is to produce a series of fluorinated indoxyl glycosides (**Figure 18**): two previously synthesised substrates **3a** and **3b**, which were furnished in low yields,[127] and four novel substrates **3c** and **4a-c** to increase the range of colours that are currently available. In particular, fluorinated indoxyl substrates were selected to complement the currently available range of halogenated indoxyl derivatives.

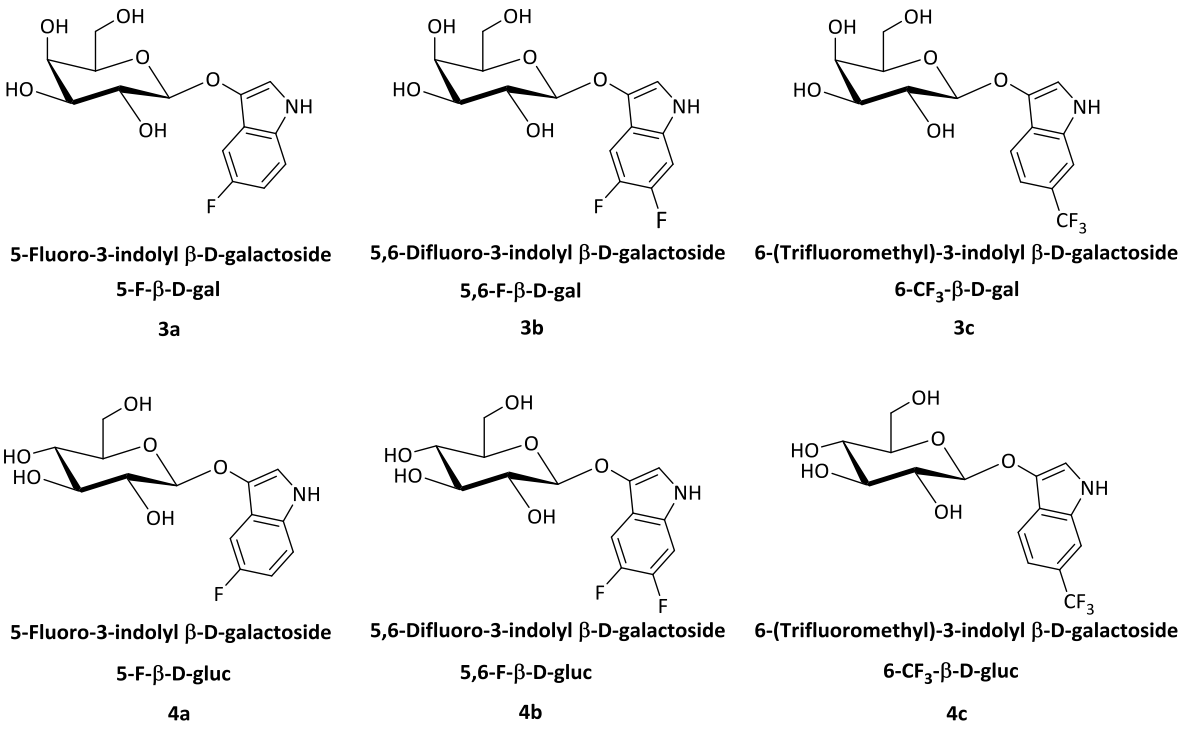

Figure 18. The structures of the six fluorinated indoxyl glycosides of interest.

One of the main objectives of this research was therefore to develop an efficient synthetic route to the fluorinated indoxyl glycosides. This was deemed necessary as current synthetic methods for entry to complementary indoxyl glycosides produce very low yields that limits their applicability and renders the substrates expensive.

A further objective was to assess the chromogenic properties of the fluorinated indoxyl glycosides using a range of microorganisms of relevance for food and clinical health in non-selective culture media. This would ascertain whether the colours generated by these new substrates would complementary to those of existing chromogenic substrates. In order to gain a better understanding of structural details that affect the rate of hydrolysis of the indoxyl substrates, kinetic studies were also designed and conducted.

Chapter 2 Synthesis of indoxylic acid allyl esters and their fluorinated derivatives

2.1 Aims and Objectives

Indoxyl glycosides such as 5-bromo-4-chloro-3-indolyl β-D-galactopyranoside **1a** are the most commonly used chromogenic substrates in agar plates for the detection and presumptive identification of bacteria. Expanding the number of colours produced by the substrates would allow more substrates to be used in one agar plate producing better discrimination of different species of bacteria. One way in which the range of colours could be expanded is to introduce a wider range of halogen in the aromatic ring of the indoxyl.[107, 111]

The aim of this chapter was therefore to develop an efficient route for the synthesis of four novel indoxylic acid allyl ester **5a-d** (**Figure 19**) as key intermediates for the synthesis of indoxyl glycosides.

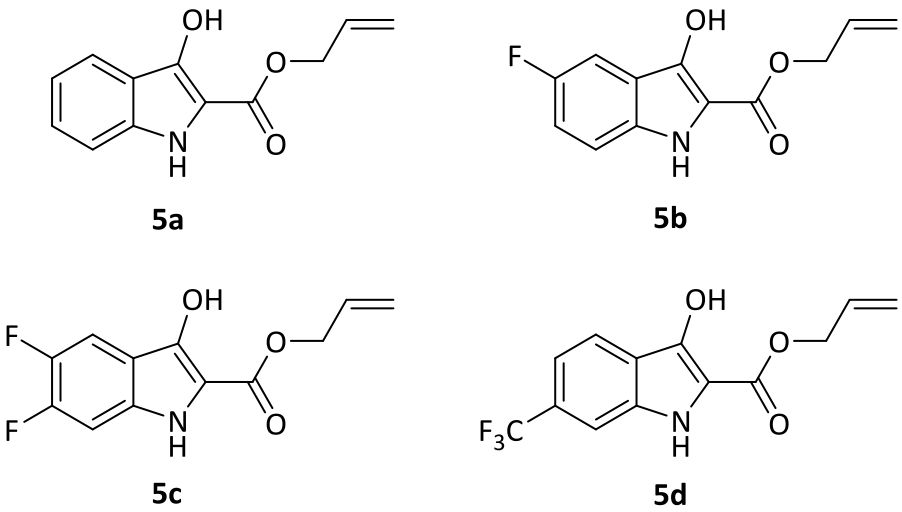

Figure 19. Indoxylic allyl acid ester and its fluorinated derivatives.

2.2 Introduction

2.2.1 Formation of indigo: enzyme hydrolysis of indoxyl glycoside

Indoxyl glycosides and their derivatives are the most commonly used chromogenic substrates in a solid culture media that can be utilised for the detection of bacteria based on the profile of glycosidase enzymes.[110] **Scheme 8** illustrates that upon hydrolysis of an indoxyl glycoside, the colourless, underivatised free indoxyl **6a** is released. This will then equilibrate to 3-indolinone **6b**, and under basic and UV conditions, will form a radical **6d**. The radical **6d** will react with another of the same type, and will dimerise to form a white indigo **6e**. Finally, when exposed to air, the dimerised compound is oxidised to form a coloured and insoluble indigo **6f**.[126, 127]

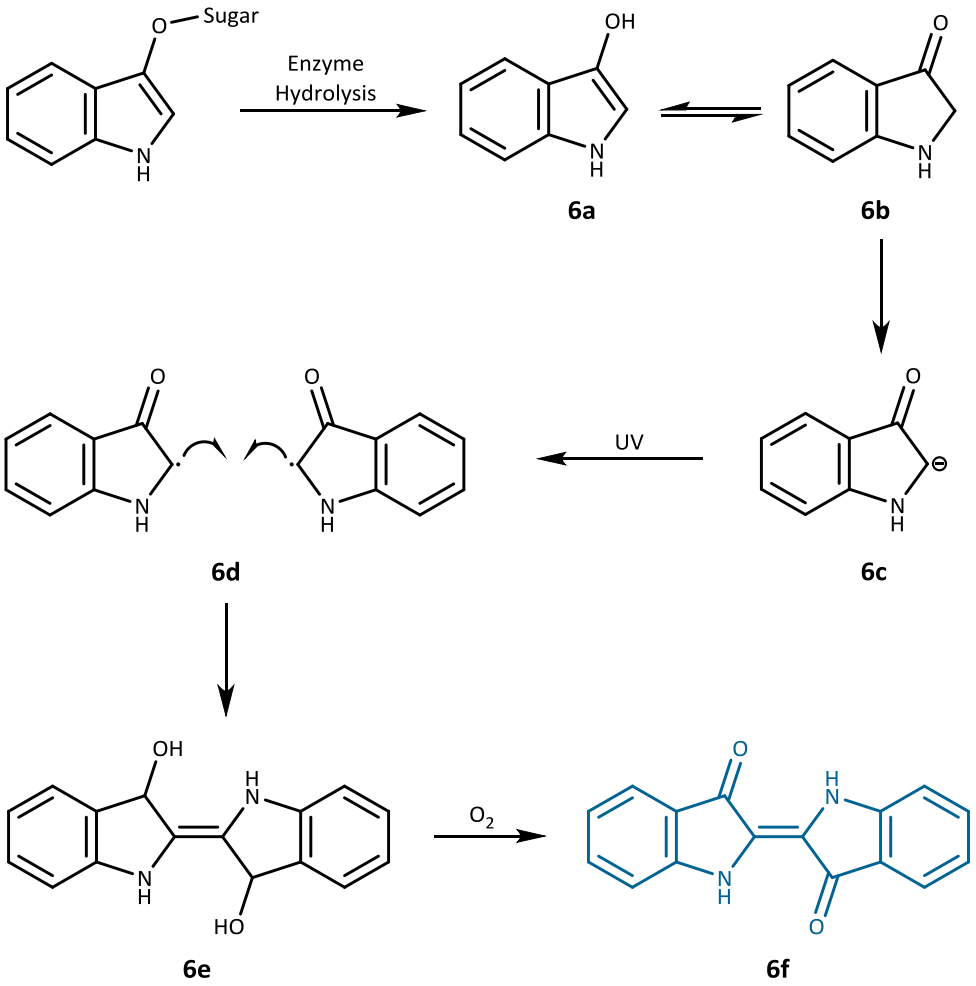

Scheme 8. Reaction scheme for the formation of indigo **6f** from indoxyl **6a** via enzyme hydrolysis.[127]

2.2.2 Features of indigo dye: colour and solubility

The structural unit responsible for the blue colour of indigo dye is the diketo-diamino-ethylene (or DDE), as shown in **Figure 20**. The electronic arrangement of the molecular centre DDE is highly polarisable. This was illustrated by Klessinger and Lutke,[135, 136] where the primary chromphore unit of indigo is a crossed-conjugated *H*-chromophore system. The proposed system consists of two nitrogen atoms as electron donor groups and two carbonyl groups as acceptors that have been crossed together via the ethylenic bridge resulting in the absorption at longer wavelength of light.[135-137] This gives a bathochromic or 'red' shift making the colour of the molecule indigo blue. Also, the unshared (*n*) electrons of the auxochrome (NH and OH) interact with π electrons of the chromophore (C=C) to either enhance the absorption and/or shift the absorption to a longer wavelength of the chromogen (a molecule containing a chromophore).[138, 139] In both solid state and in solution, the structure of indigo adapts the *trans*-isomer instead of the *cis*-isomer, since the former is stabilised by intramolecular hydrogen C=O···H–N bonds.[140-142]

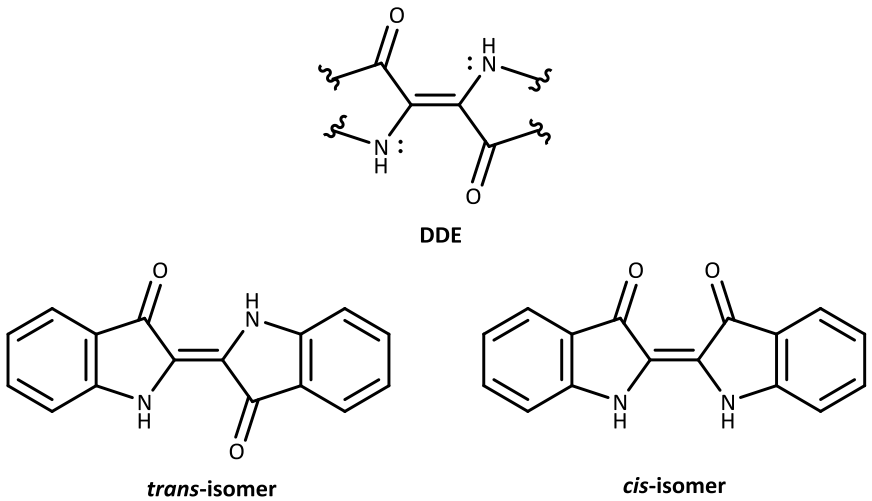

Figure 20. Core unit of indigo dye DDE adapts the crossed-conjugated *H*-chromophore system. Indigo exists as the *trans*-isomer instead of the *cis*-isomer.[135]

Due to the polymeric and highly polar nature of indigo dye, the compound is insoluble in water and most common organic solvents. Therefore, incorporation of the chromogen coupled to a sugar in an agar medium in the presence of specific bacteria will allow hydrolysis of the substrate. The dye will then precipitate and is highly restricted within microbial colonies, making clear differentiation between species that demonstrate enzyme activities from those that do not.[135]

The aromaticity of the indigo dye only plays a secondary role in the UV-Vis absorption of indigo.[143] Although, decorating the ring of the dye with halogens shifts the wavelength of the absorption in the visible spectrum producing different coloured indigo derivatives. The bathochromicity shift of the indigo can be explained by the valence-bond approach, as shown in **Scheme 9**. The resonance structures of **7a-e** contributed to the primary chromogen unit of the dye. Furthermore, **7a** and **7c** are more stable than **7b** and **7d**, due to the retention of aromaticity within the benzene region. Resonance **7e** has a negative charge on both oxygen atoms and a positive charge on both nitrogen atoms. Using this approach may explain the effect of substituents on the benzene ring.[136, 144]

Therefore, this allows better discrimination of the bacterial colonies when incorporated in an agar medium. For such a small molecule with absorptions at a very long wavelength that could be shifted in the visible spectrum, the outlined features make indoxyl an excellent candidate as a chromogenic substrate.

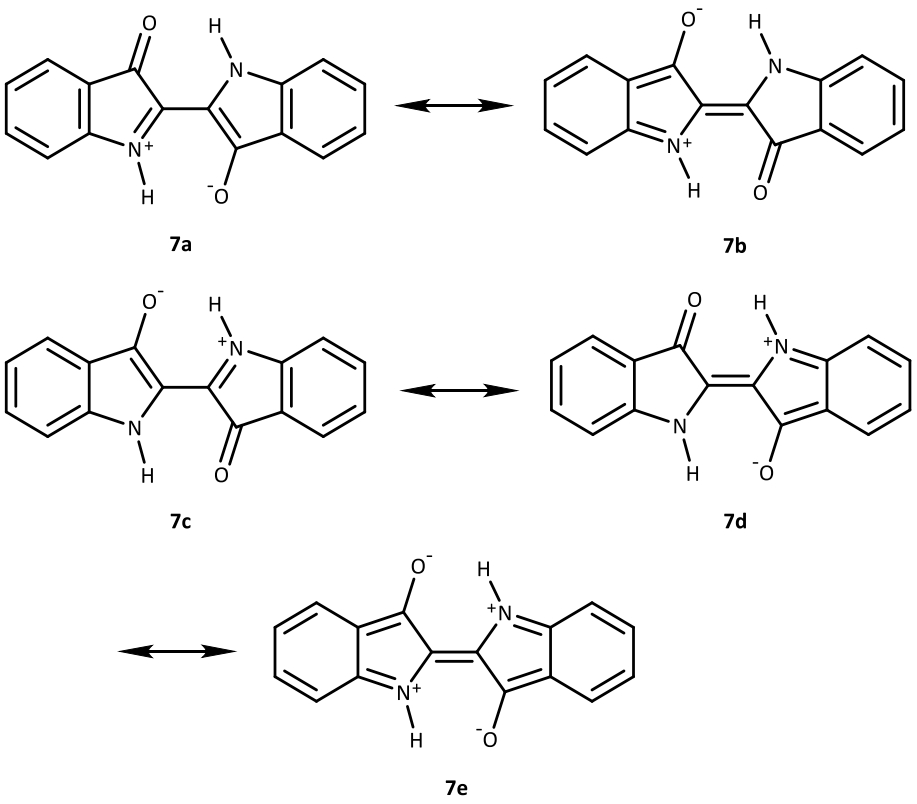

Scheme 9. The resonance structures of indigo **7a-e**.[136]

2.2.3 Traditional versus new methods: synthesis of indoxyl

Indoles are one of the most versatile and important heterocyclic compounds and exhibit a wide range of biological and pharmaceutical activities such as anti-cancer, anti-depressant, anti-viral and antimicrobial.[145] The development of routes to their derivatives has been a significant theme in organic synthesis. They are historically prepared via 1-acetyl-3-indolinone **8** as a key precursor. There have been many reports on the synthesis of this key precursor.[146-154] Most of the synthetic routes involve alkylation and cyclisation steps, as shown in **Scheme 10**. Within our laboratory, this traditional route has been utilised to produce 1-acetyl-3-indolinone and its halogenated analogues, which were successfully prepared prior to glycosidation. However, when *N*-acetyl-3-indolinone reacts with acetylated glycosyl bromide by dissolving the compounds in acetone with either NaOH or KOH, the route produced low-yielding acetylated indoxyl glycosides owing to early dye

formation and sugar hydrolysis. This especially happens for indoxyl derivatives, and for more complex and rare sugar structures.[128, 155]

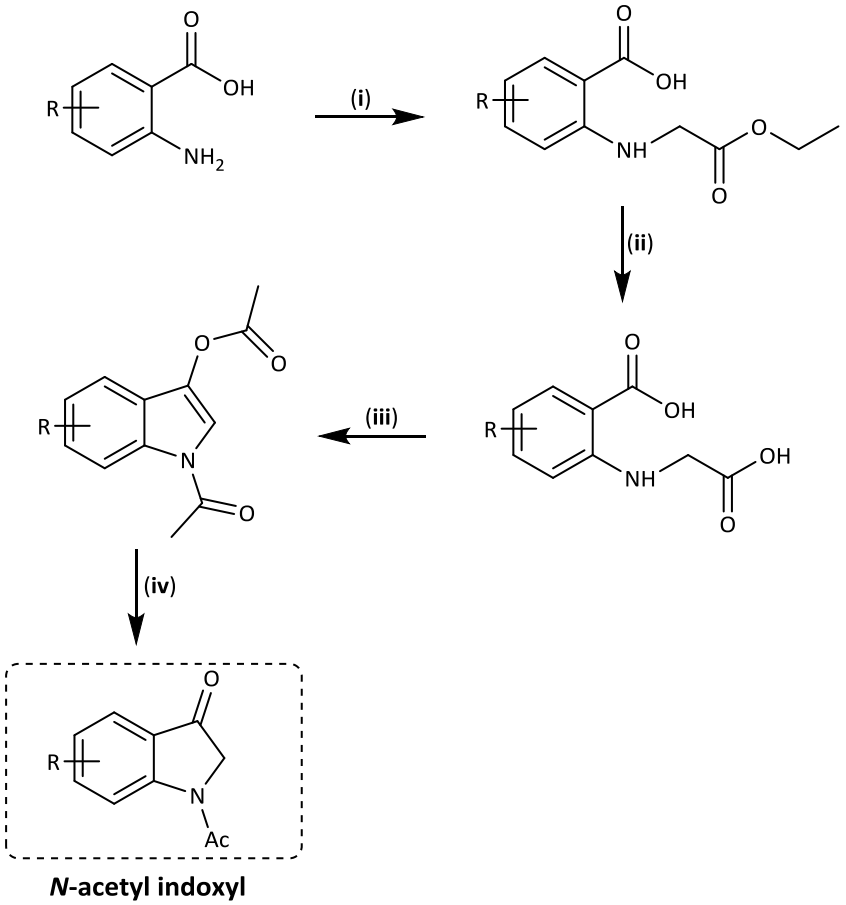

Scheme 10. An example of the conventional route towards indoxyl glycoside via *N*-acetyl indoxyl, which was developed by Parshotam and co-workers.[127] **(i)** Ethyl glyoxylate, MeOH, AcOH, 2.25 hrs, $NaBH_4$, 1.75 hrs; **(ii)** 1M NaOH, 3 hrs, rt (52-89%); **(iii)** Ac_2O, Et_3N, µv, 1 min, 80 °C, 300 W (49-71%); **(iv)** 90% H_2SO_4, 1.25 hrs (38-92%).

N-Acety indoxyl is traditionally coupled to acetylated sugar donors using a strong base like 1M KOH or 1M NaOH, as illustrated in **Scheme 11**. Under basic condition, the equilibrium tends to favour the keto, rather than the enol, form. This is because the C=O bond of the ketone is more stable than the C=C bond of an enol.[156, 157] Therefore, only a small proportion of enol in solution would readily react with an acetylated glycosyl bromide.

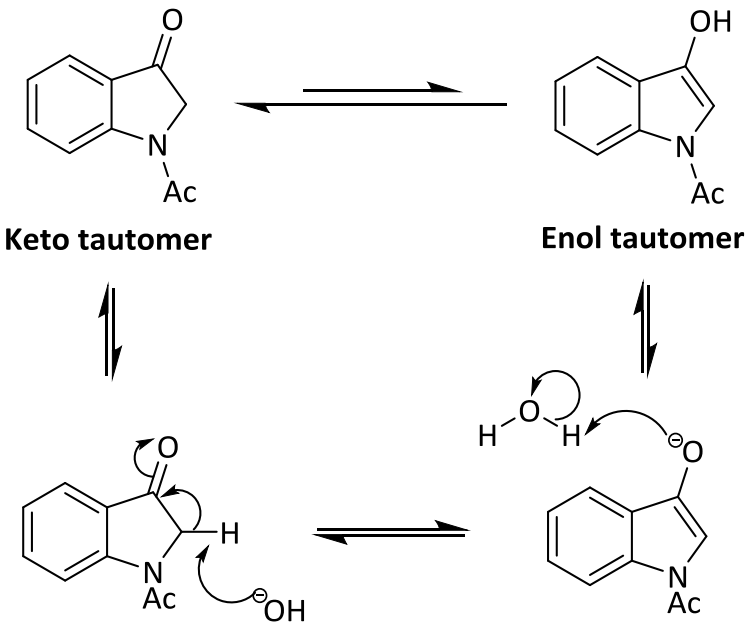

Scheme 11. Keto-enol tautomerism of *N*-acetyl indoxyl using 1M KOH or NaOH.[157]

To overcome these challenges, *N*-acetyl indoxyl can be modified by protecting the C-2 position of the indoxyl using an allyl ester group and having a hydroxyl, rather than a ketone, group at the C-3 position, as shown in **Figure 21**. This simple modification makes the indoxyl more accessible for coupling with an acetylated halide sugar.

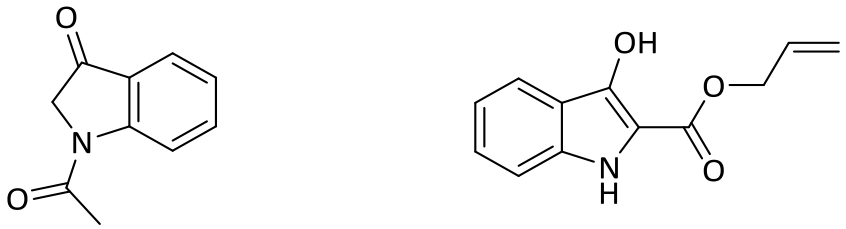

***N*-Acetyl indoxyl**
8

Indoxyl acid allyl ester
5

Figure 21. The key precursors **8** and **5**. Indoxylic acid allyl ester synthetic route was chosen in this project prior to glycosidation with a sugar.

Therefore, the new and unconventional approach towards the synthesis of indoxyl glycoside via indoxylic acid allyl ester, which was developed by Böttcher and co-workers, has been utilised for this project. As shown in **Scheme 12**, the synthetic pathway for the preparation of derivatised indoxylic acid allyl esters was achieved by Böttcher *et al*. achieved in seven steps. The first step involved was *N*-acetylation of the starting material i.e. the halogenated methyl anilines **9a-c** using Ac_2O. Then, the resultant compounds **10a**-**c** were oxidised using $KMnO_4$, followed by de-*N*-acetylation using sodium hydroxide solution to give anthranilic acids **12a-c**. The compounds were treated with pyridine and triphosgene to produce isatoic anhydrides **13a**-**c**. The next step was the *N*-alkylation of **14a-c** using sodium hydride and allyl bromoacetate, followed by opening the ring of the *N*-alkylated anhydrides **14a**-**c** using sodium hydride in allyl alcohol to afford **15a-c**. Finally, indoxylic acid allyl esters **16a**-**c** were obtained by Dieckmann condensation. By blocking the reactive C-2 position of the intermediate, the side formation of the indigo dye was suppressed.[128, 158]

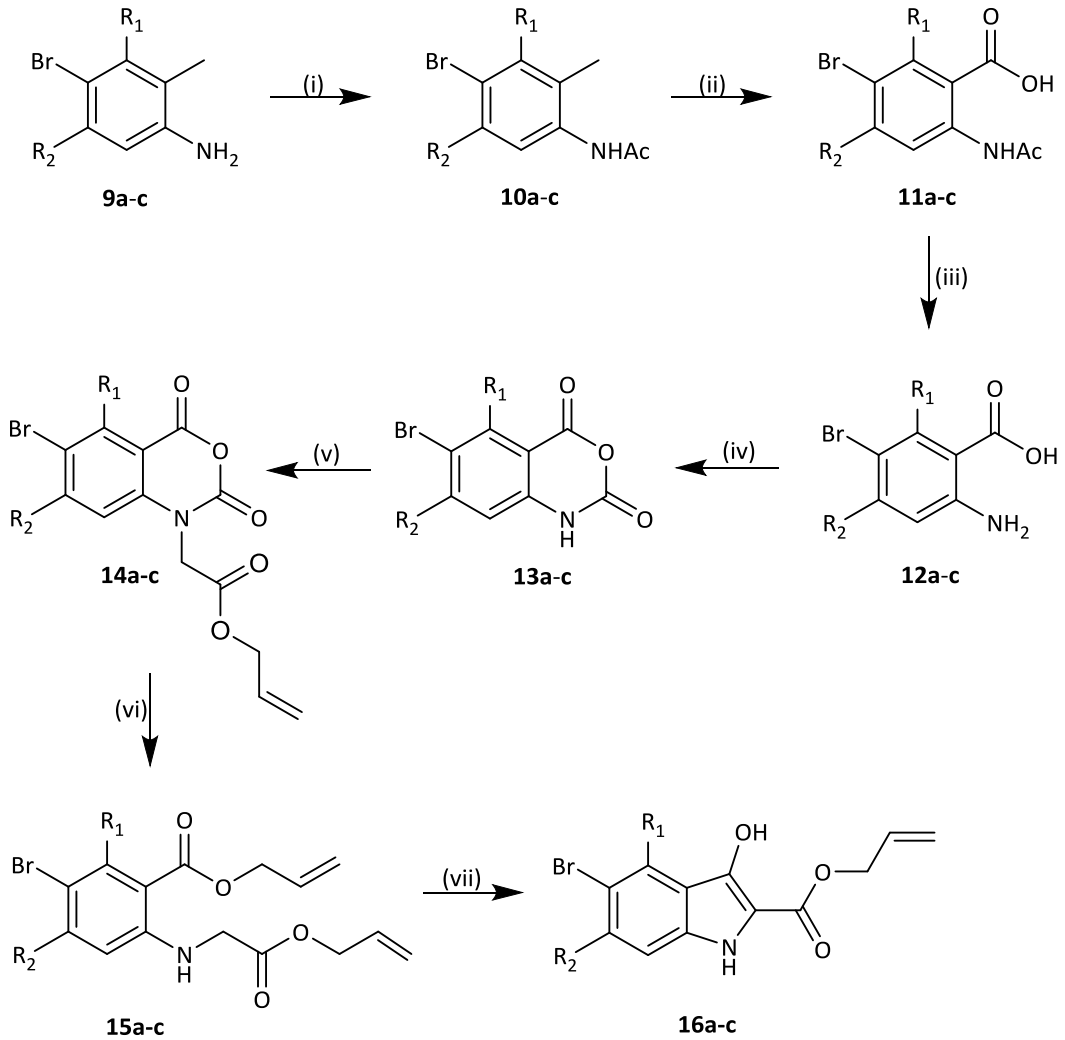

9a-c **10a-c** **11a-c** **12a-c** **13a-c** **14a-c** **15a-c** **16a-c**

R_1	R_2	(i)	(ii)	(iii)	(iv)	(v)	(vi)	(viii)
Cl	H	**10a** 97%	**11a** 70%	**12a** 88%	**13a** 80%	**14a** 93%	**15a** 80%	**16a** 84%
H	H	**10b** 85%	**11b** 66%	**12b** 93%	**13b** 94%	**14b** 99%	**15b** 75%	**16b** 80%
H	Cl	**10c** 96%	**11c** 63%	**12c** 94%	**13c** 82%	**14c** 84%	**15c** 84%	**16c** 76%

Scheme 12. Synthesis of indoxylic acid allyl ester derivatives developed by Bottcher *et al*.[158]

(**i**) Ac_2O, DCM, 0 °C - rt, 5-16 h (85 – 97%); **(ii)** $MgSO_4$, $KMnO_4$, reflux , 6 h (88-94%); **(iii)** NaOH, reflux (63-76%); **(iv)** MeCN, triphosgene, pyridine, DCM, 50 °C, 4 h (80-94%); (**v**) DMF, sodium hydride, allyl bromoacetate rt, overnight (84-99%); (**vi**) allyl alcohol, NaH, rt, 6.5 h (75-84%); **(vii)** Et_2O, KO^tBu, reflux, 2 h (76-84%).

2.3 Results and Discussion

2.3.1 Synthesis of indoxylic acid allyl esters and its fluorinated analogues

The synthetic route developed by Bottcher and co-workers was utilised to prepare the indoxylic acid allyl esters in four steps prior to glycosidation. The reactions were performed under inert conditions.

2.3.2 Formation of isatoic anhydrides using triphosgene and pyridine

In the first step, commercially available anthranilic acid and its fluorinated analogues were treated with pyridine and triphosgene to produce isatoic anhydrides. The triphosgene was dissolved in DCM and was added drop-wise together with pyridine into the anthranilic acid solution. The reaction was left stirring for approximately 3-5 hours at rt. Then, the reaction was quenched with water and DCM, and the precipitate was collected by vacuum filtration. The crude product was freeze-dried for a week, and was not purified as this may lead to degradation. As summarised in **Table 6**, the isatoic anhydride and its fluorinated derivatives **18a-d** were furnished with yields of 75-92%, which were very similar to the yields of compounds **13a-c** (**Scheme 12**).[158, 159]

Table 6. Yields of isatoic anhydrides and the fluorinated derivatives **18a-d**.

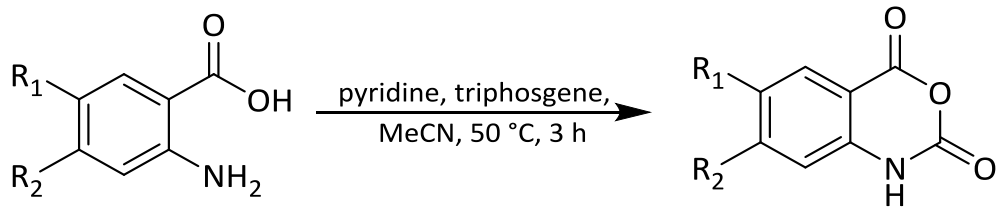

17a-d **18a-d**

R_1	R_2	Starting Materials	Resultant Compounds	Yields (%)
H	H	**17a**	**18a**	84
F	H	**17b**	**18b**	92
F	F	**17c**	**18c**	77
H	CF_3	**17d**	**18d**	75

The successful synthesis of isatoic anhydrides **18a-d** can be confirmed by different analytical techniques. The ^{1}H NMR spectrum of a representative isatoic anhydride, 5-fluoro isatoic anhydride **18b**, is shown in **Figure 22**. The spectrum revealed the disappearance of a broad singlet from the OH and NH_2 groups at approximately 8.61 ppm for the starting material 2-amino-5-fluorobenzoic acid **17b** (**Figure 22**, top). The transformation can be further confirmed by the presence of a single resonance of the secondary amide at 11.70 ppm proving that **18b** was furnished. Both the ^{13}C NMR and IR spectra revealed the presence of two carbonyl groups with characteristic signals at 159.14 and 146.74 ppm, and 1758 cm^{-1}, respectively. Moreover, the expected m/z calculated for $(M+H)^{+}$ was 180.0181 g mol^{-1}, and the result gave an accurate mass of 180.0102 g mol^{-1}.

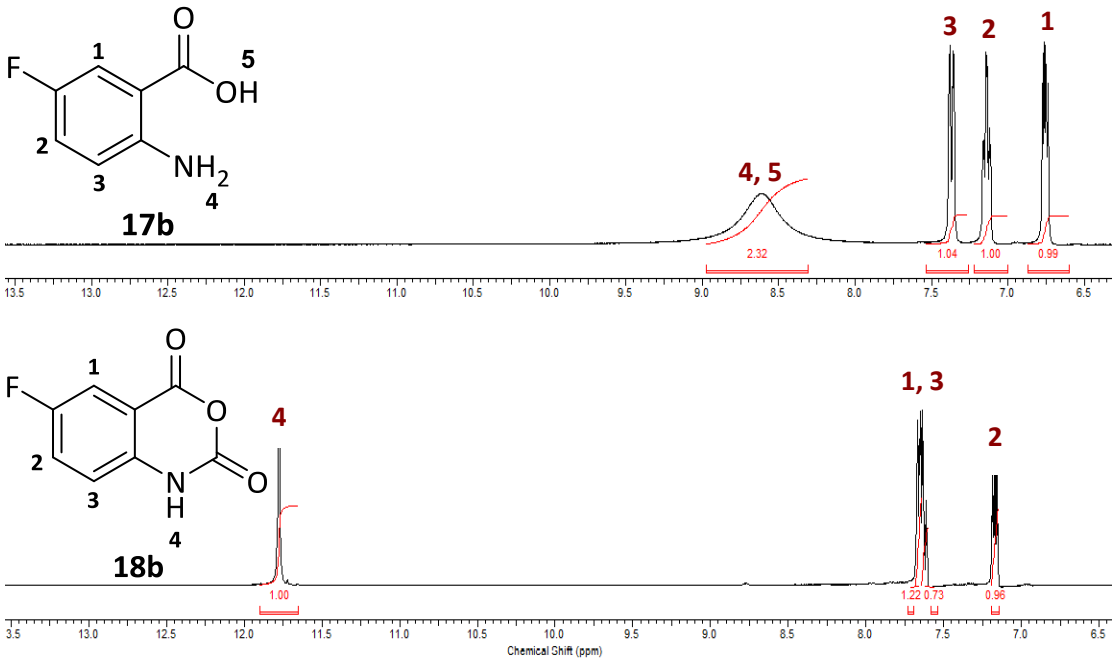

Figure 22. ^{1}H NMR spectroscopic analysis of the 2-amino-5-fluorobenzoic **17b** and 5-fluoro isatoic anhydride **18b** in DMSO-d_6.

2.3.3 The effect of fluorine substituents on the aromatic ring

The effect of fluorine substituents on the adjacent proton and carbon is manifested in the ^{1}H and ^{13}C spectroscopic analyses by the increased splitting patterns. Normally, the splitting pattern for the aromatic ring can be observed as doublets and triplets as manifested on the underivatised compound **18a**, which served as a control (**Figure 23**). The aromatic protons of compound **18b** with the nearby single fluorine atom can be observed as doublet of doublet. Correlation Spectroscopy (COSY) NMR was used to determine which neighbouring hydrogen atom couples with another hydrogen atom in the benzene ring.

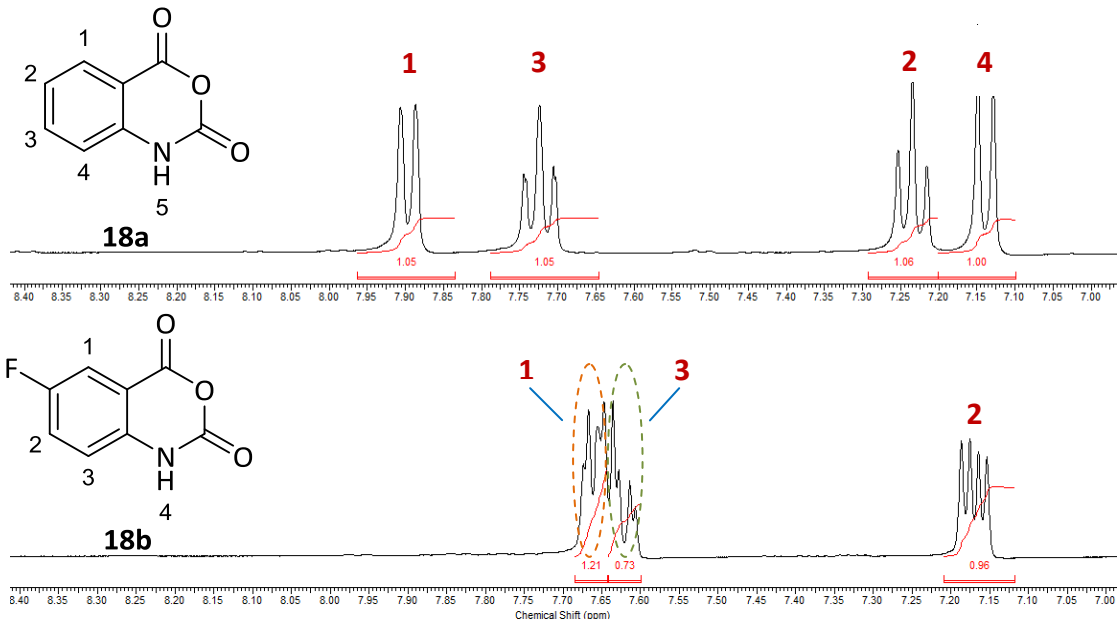

Compounds	Splitting Patterns			
	1	**2**	**3**	**4**
18a	d	t	t	d
18b	dd	dd	dd	N/A

Figure 23. The effect of fluorine on the aromatic ring by comparing the ^{1}H NMR spectra of compounds **18a** and **18b**. Both compounds were dissolved in DMSO-d_6. Splitting patterns: doublet, d; doublet of doublet, dd; and, triplet, t.

For carbon attached to a single fluorine substituent on the aromatic ring, a strong doublet was observed in the ^{13}C spectrum of **18b.** Without any fluorine substituents on the benzene ring, no splitting of carbons can be observed, as shown in **Figure 24**.

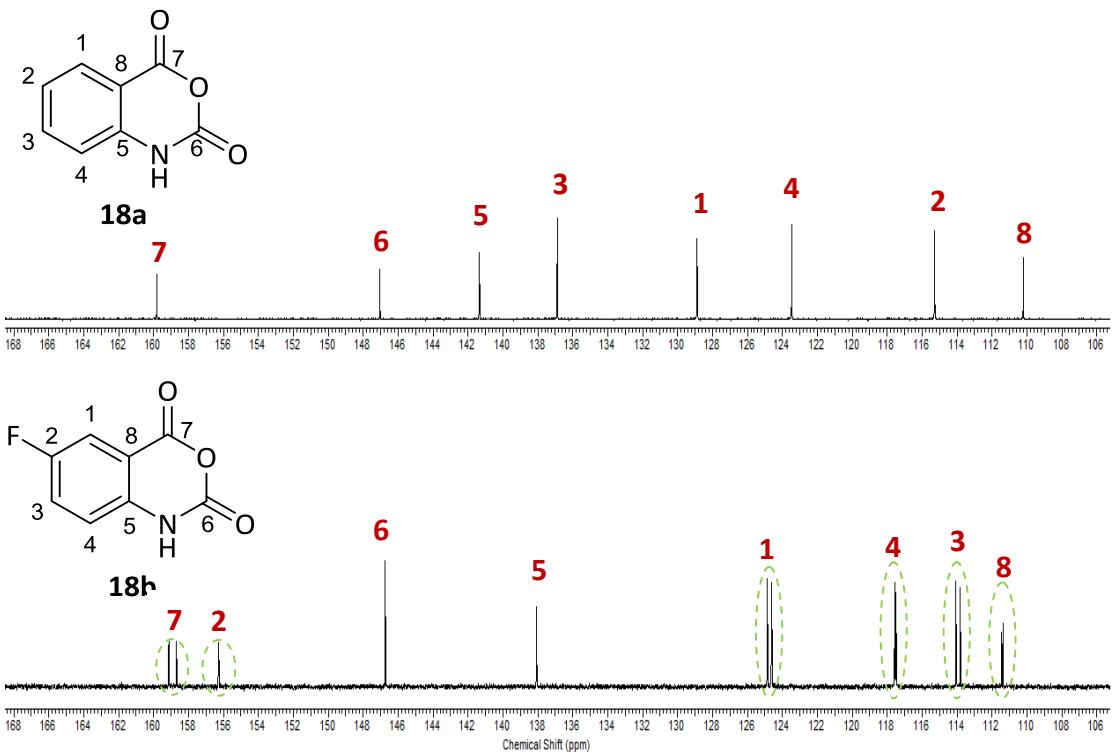

Figure 24. The effect of fluorine on the aromatic ring by comparing the ^{13}C NMR spectra of compounds **18a** and **18b**. Both compounds were dissolved in DMSO-d_6. Encircled in green means that the resonance split.

The spin-spin coupling of fluorine to its neighbouring hydrogen and carbon are highly variable in magnitude.[160] Fluorine is highly electronegative and its influence on protons and carbons is largely based on the inductive effects. For compound **18b (Figure 25**), $^{3}J_{H\text{-}F}$ and $^{4}J_{H\text{-}F}$ coupling constants of fluorine to its nearby protons were 8.5 Hz and 3.0 Hz, respectively. For carbon, $^{1}J_{C\text{-}F}$ and $^{2}J_{C\text{-}F}$ coupling constants were 242.0 and 24.0 Hz, respectively. Based from the literature, $^{3}J_{H\text{-}F}$ coupling constant was approximately 8 Hz and $^{4}J_{H\text{-}F}$ was between 1 and 3 Hz.[160] On the other hand, the fluorine coupling to the *ipso* carbon ($^{1}J_{C\text{-}F}$) varied considerably, depending on the fluorine substitution environment, but usually the coupling constant was 250 Hz or larger. Finally, $^{2}J_{C\text{-}F}$ coupling constant was between 20-26 Hz.[160]

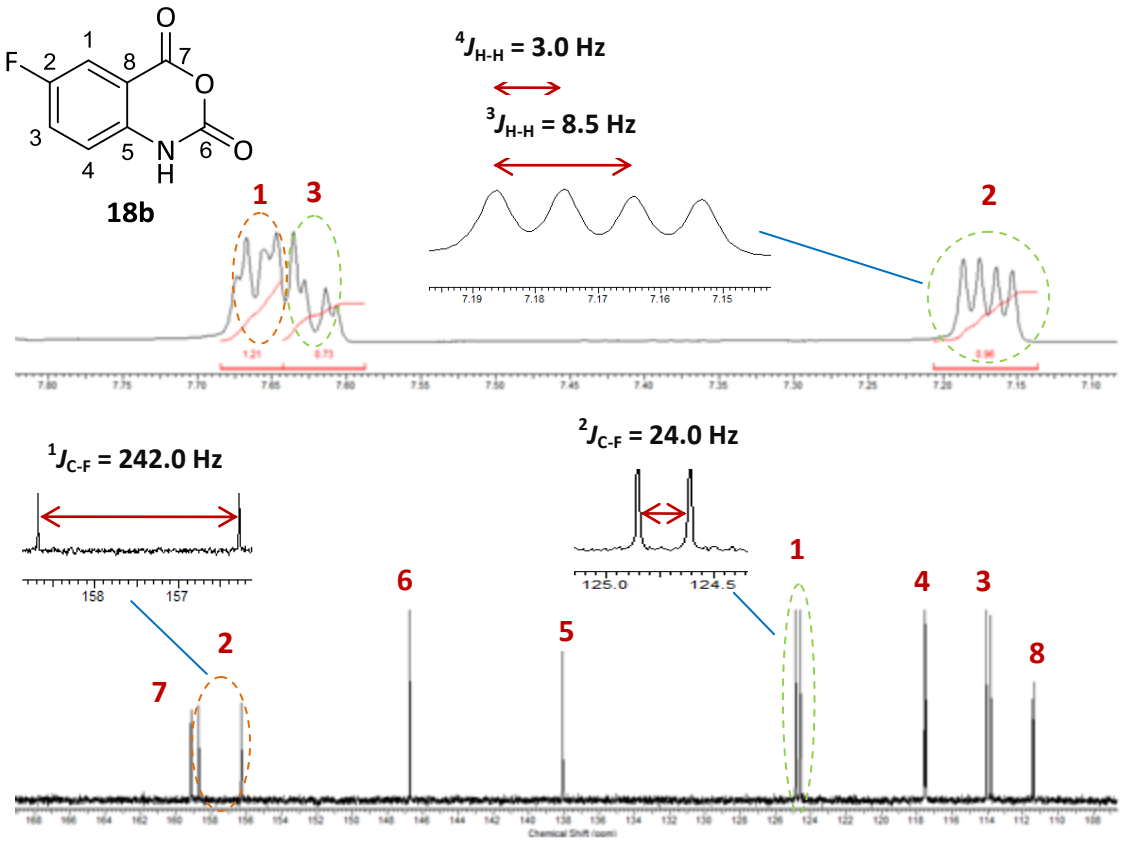

Figure 25. The spin-spin coupling of fluorine to its neighbouring hydrogen and carbon on the aromatic ring of 5-fluoro isatoic anhydride **18b** as illustrated on the ^{1}H NMR (top) and ^{13}C NMR (bottom) spectra. The compound was dissolved in DMSO-d_6.

It can be deduced that as fluorine substituent gets farther away from the protons or carbons, its influence drops-off dramatically. In addition, the noticeable inductive effect of fluorine to its neighbouring proton or carbon was consistent throughout the synthetic route. Lastly, another method to confirm the presence of fluorine on the aromatic ring was ^{19}F NMR spectroscopy. The spectrum for compound **18b** exhibited a single resonance for fluorine at -118.81 ppm when dissolved in DMSO-d_6. From the literature, the chemical shift of mono-substituted fluorobenzene was approximately -113 ppm when dissolved in benzene-d_6.[160]

2.3.4 *N*-Alkylation of isatoic anhydrides using NaH

The reagent allyl bromoacetate **19** must be first prepared prior to *N*-alkylation of istaoic anhydrides. The method used to synthesise the reagent was developed by Bolsønes *et al*.[161] as shown in **Scheme 13**. The reagent was prepared by bromination of the allyl alcohol using bromoacetyl bromide, and K_3PO_4 as a catalyst for the reaction. The reagent was produced in a very high yield (98%). As manifested in the ^{1}H NMR spectrum (**Figure 26**), the key reagent was furnished and was used for the *N*-alkylation of isatoic anhdyrides.

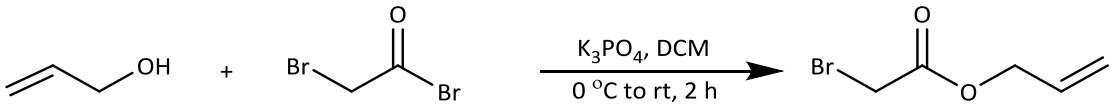

Allyl alcohol **Bromoacetyl bromide** **Allyl bromoacetate, 19**

Scheme 13. Synthesis of allyl bromoacetate **19** as a key reagent for the *N*-alkylation of isatoic anhydrides. Allyl alcohol, bromoacetyl bromide, K_3PO_4 0 °C to rt, 2 h (98%).

The ^{1}H NMR spectrum revealed the presence of the allyl ester group, which can be deduced as follows: one proton from methine group at 5.83 ppm; two protons from allyl group at 5.35 and 5.29 ppm, two protons from methylene group at 4.68 ppm; and, two protons from the methylene group adjacent to bromine at 3.87 ppm. Furthermore, both the ^{13}C NMR and IR spectra revealed the presence of one carbonyl group with characteristic signals at 166.90 ppm and 1732 cm^{-1}.

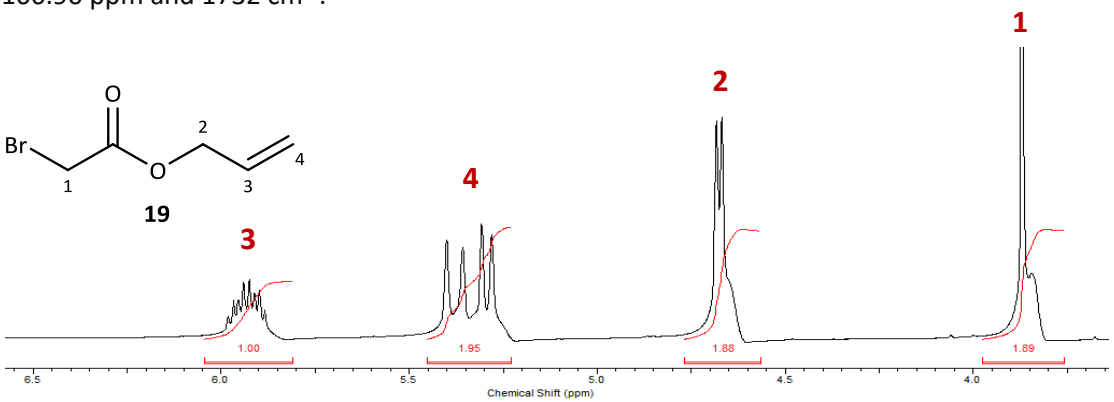

Figure 26. ^{1}H spectrum of allyl bromoacetate **19** in $CDCl_3$.

Subsequently, the isolated isatoic anhydride and its fluorinated analogues were *N*-alkylated using NaH (57-63% oil dispersion) and allyl bromoacetate.[162] The NaH was added portion-wise into the reaction mixture at 0 °C. The reaction was exothermic; hence, an ice-bath was needed to cool the reaction whilst adding the reagent. After 45 minutes, the ice-bath was removed, and the key reagent **19** was added dropwise into the mixture. The reaction was left stirring overnight. The next day the reaction was quenched with water and the product was collected by vacuum filtration. The crude products were freeze-dried for one week, and were not purified as they are prone to degradation. Hence, the products were left untreated and were used directly for the next step. The *N*-alkylated isatoic anhydride and its fluorinated derivatives **20a-d** were furnished with yields of 87-97%, as summarised in **Table 7**.

Table 7. Yields of *N*-alkylated isatoic anhydrides and its fluorinated derivatives **20a-d**.

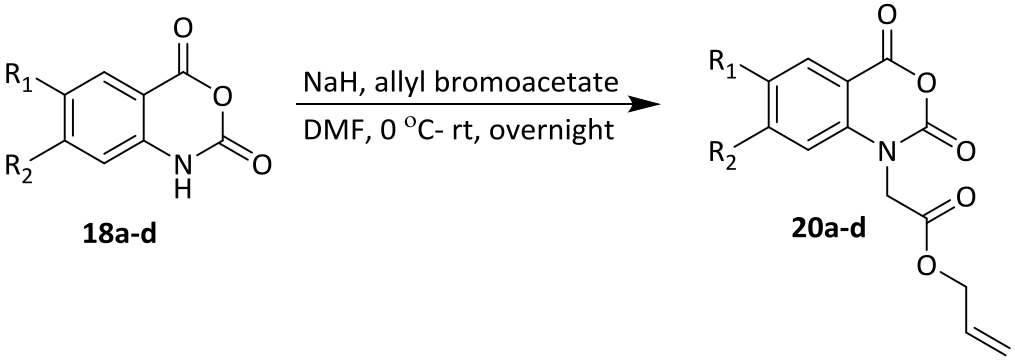

R_1	R_2	Starting Materials	Resultant Compounds	Yields (%)
H	H	**18a**	**20a**	97
F	H	**18b**	**20b**	94
F	F	**18c**	**20c**	87
H	CF_3	**18d**	**20d**	97

The ^{1}H NMR spectrum of a representative compound *N*-alkylated isatoic anhydride **20b** is shown in **Figure 27**. The proton resonance at 11.70 ppm of 5-fluoro isatoic anhydride **18b** disappeared when displaced by the allyl ester group. For the resultant compound **20b**, the presence of the allyl ester group can be observed on the ^{1}H NMR spectrum at regions between 4.5-6.0 ppm. The integrals of the allyl ester can be deduced as follows: one proton from the methine group at 5.92 ppm, two protons from the vinyl group at 5.34 and 5.24 ppm, two protons from methylene group at 4.97 ppm; and, two protons from the methylene group at 4.68 ppm. ^{13}C NMR spectroscopic analysis revealed the presence of the carbonyl group of the allyl ester at approximately 166-167 ppm.

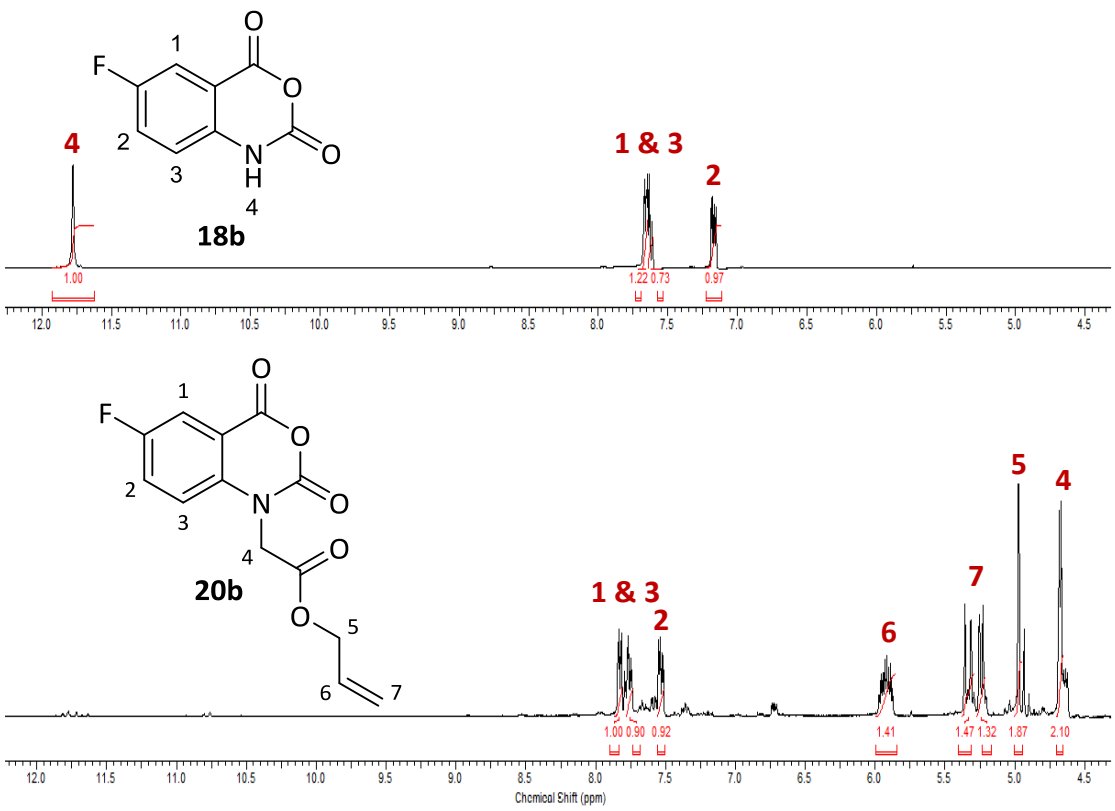

Figure 27.^{1}H NMR spectroscopic analysis of compounds **18b** and **20b**. Both compounds were dissolved in DMSO-d_6.

2.3.5 Ring opening of *N*-alkylated isatoic anhydrides using NaH

Opening the ring of the anhydrides was achieved using a catalytic amount of sodium hydride in allyl alcohol. The reaction was left to stir for an hour. After the reaction was completed as evidenced by thin layer chromatography (TLC) analysis, the solvent was evaporated to dryness. The crude products were purified using normal phase flash column chromatography with a mobile phase system of 2:1 petroleum ether (PE) 40-60: ethyl acetate (EtOAc). The yields (75-86%) for the the di-esters are as indicated in **Table 8**.

Table 8. Yields of the di-ester compounds **21a-d**.

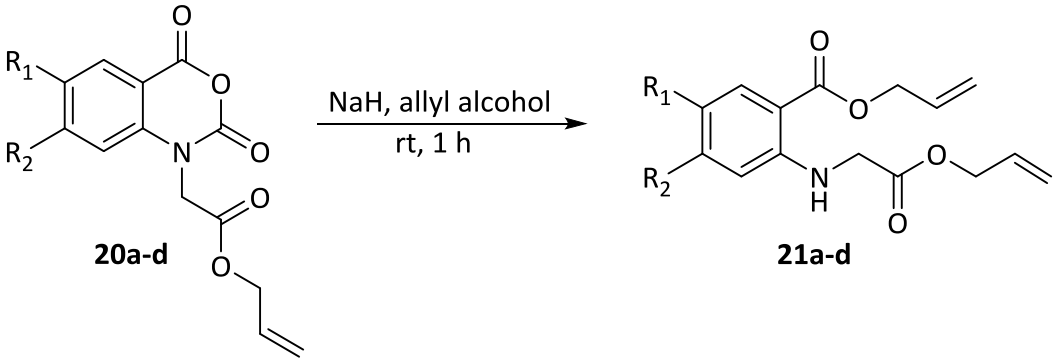

R_1	R_2	Starting Materials	Resultant Compounds	Yields (%)
H	H	**20a**	**21a**	75
F	H	**20b**	**21b**	49
F	F	**20c**	**21c**	79
H	CF_3	**20d**	**21d**	86

The ^{1}H NMR spectrum of a representative resultant compound **21b** is shown in **Figure 28**. The spectrum revealed the presence of another allyl ester group at 4-6 ppm. Also, the presence of the secondary amide is indicated by a singlet peak at 8 ppm. The integrals of the newly formed allyl ester group can be deduced as follows: one proton from the methine group at 6.03 ppm, two protons from the vinyl group at 5.40 and 5.35 ppm; and, two protons from the methylene group at 4.78 ppm. The mass spectrometry analysis gave an accurate mass, where $(M+H)^+$ was 294.1136 g mol^{-1} and 294.1147 g mol^{-1} was expected.

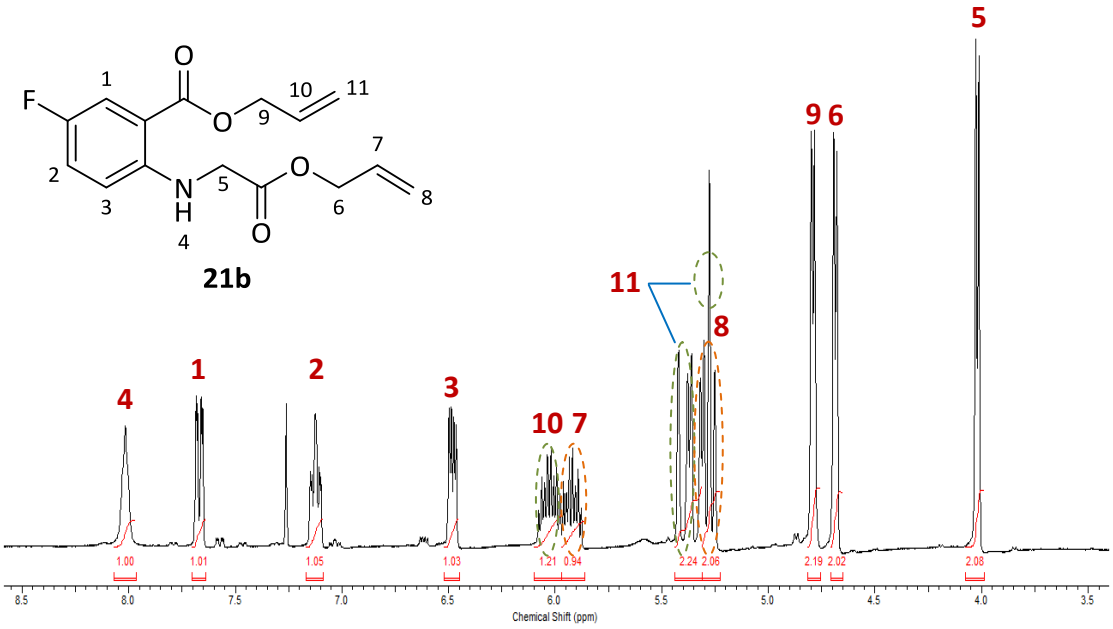

Figure 28. ^{1}H NMR spectroscopic analysis of compounds **18b**, which was dissolved in $CDCl_3$. Note that the peaks overlapped for positions 10 and 7 as well as 11 and 8.

2.3.6 Dieckmann condensation of the di-esters

Indoxylic acid allyl ester **5a** and its fluorinated derivatives **5b**-**d** were obtained by Dieckmann condensation.[163-164] By blocking the reactive C-2 position of the intermediate, the side formation of the indigo dye was suppressed. The reaction was conducted under reflux for 1 hour with diethyl ether and potassium *tert*-butoxide (KO^{t}Bu). After the reaction was completed, the product was precipitated using 1M HCl and was washed with 0.5 M HCl. The crude product was collected using vacuum filtration. The products were partially purified using normal phase flash column chromatography (3:1 PE 40-60: EtOAc) with yields of 31-49% (**Table 9**), which were lower compared to the yields of the key intermediates **16a-c** (**Scheme 11**) synthesised by Böttcher and co-workers (76-84%).[158]

Table 9. Yields of indoxylic acid allyl ester and its fluorinated derivatives. **3a-d**.

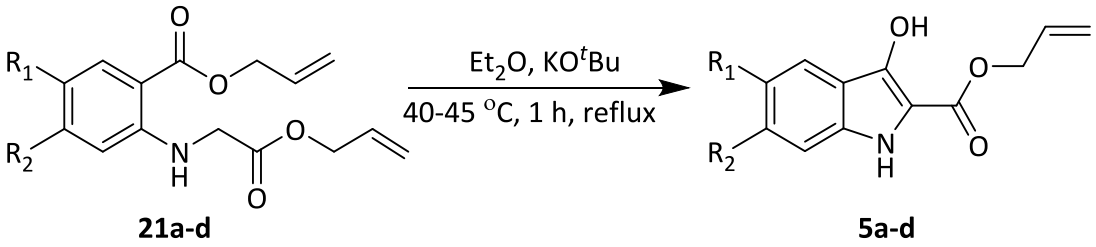

21a-d **5a-d**

R_1	R_2	Starting Materials	Key Precursors	Yields (%)
H	H	**21a**	**5a**	49
F	H	**21b**	**5b**	69
F	F	**21c**	**5c**	38
H	CF_3	**21d**	**5d**	49

As shown in **Scheme 14**, the most likely mechanism for this ring closure, starting from the di-ester **21b**, is a base-catalysed cyclisation and elimination process that produced the fluorinated indoxylic acid allyl ester **3b** as a key precursor.

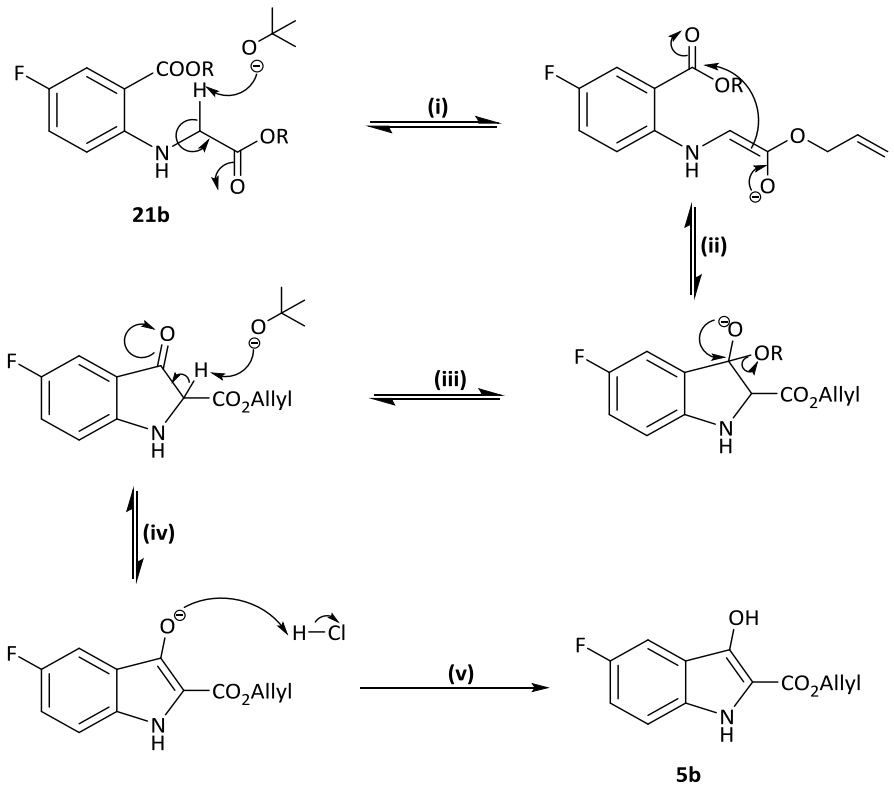

21b **5b**

Scheme 14. Cyclisation and elimination steps via Dieckmann condensation procedure.

The reaction mechanism of the intramolecular acylation of the di-ester used KO^{t}Bu as a base attacking the α-position of the di-ester. For nucleophilic substitution reactions like Dieckmann condensation, the bulky alkyl groups of KO^{t}Bu might have hindered its interaction with the steric di-ester. Hence, this may slow down the reaction and might take longer to react.

The ^{1}H NMR spectrum of a representative indoxylic acid allyl ester, 5-mono-fluoro indoxylic acid allyl ester **5b**, a novel compound, is illustrated in **Figure 29**. The spectrum revealed the presence of two singlet resonances of the OH and NH groups at approximately 10.94 ppm and 9.44 ppm, respectively. Another indication for the successful cyclisation was the presence of the allyl carboxylate group, which can be deduced as follows: one proton from the methine at 6.05 ppm; two protons from the allyl group at 5.44 and 5.26 ppm; and, two protons from the methylene group at 4.80 ppm. The aromatic protons were present at 7.0-7.5 ppm.

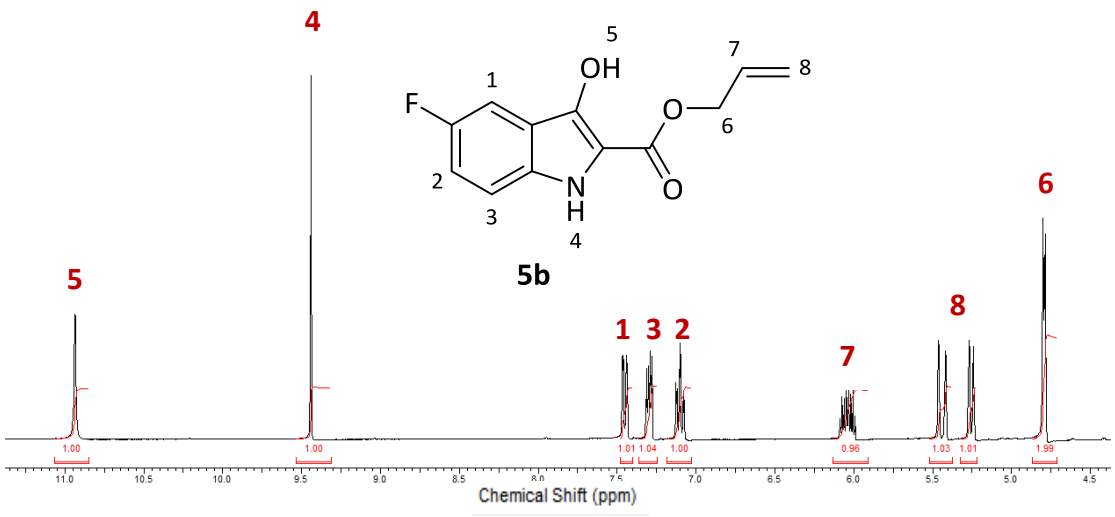

Figure 29. ^{1}H NMR spectrum of 5-mono-fluoro indoxylic acid allyl ester **5b**.

Finally, another indication of the successful synthesis of the key precursor was disclosed in ^{13}C NMR and IR spectroscopic analyses (**Figure 30**). The spectra revealed the presence of the carbonyl group at the C-2 of the key intermediate **5b** with characteristic signals at 160.95 ppm and 1738.83 cm^{-1}, respectively. Furthermore, the IR spectra revealed the presence of N-H and O-H broad peaks between 3500 and 3000 cm^{-1}. Finally, the mass spectrometry analysis gave the accurate masses, where $(M+Na)^+$ was 256.0380 g mol^{-1} and 257.0459 g mol^{-1}, and 256.0391 g mol^{-1} and 257.0470 g mol^{-1} was expected, respectively.

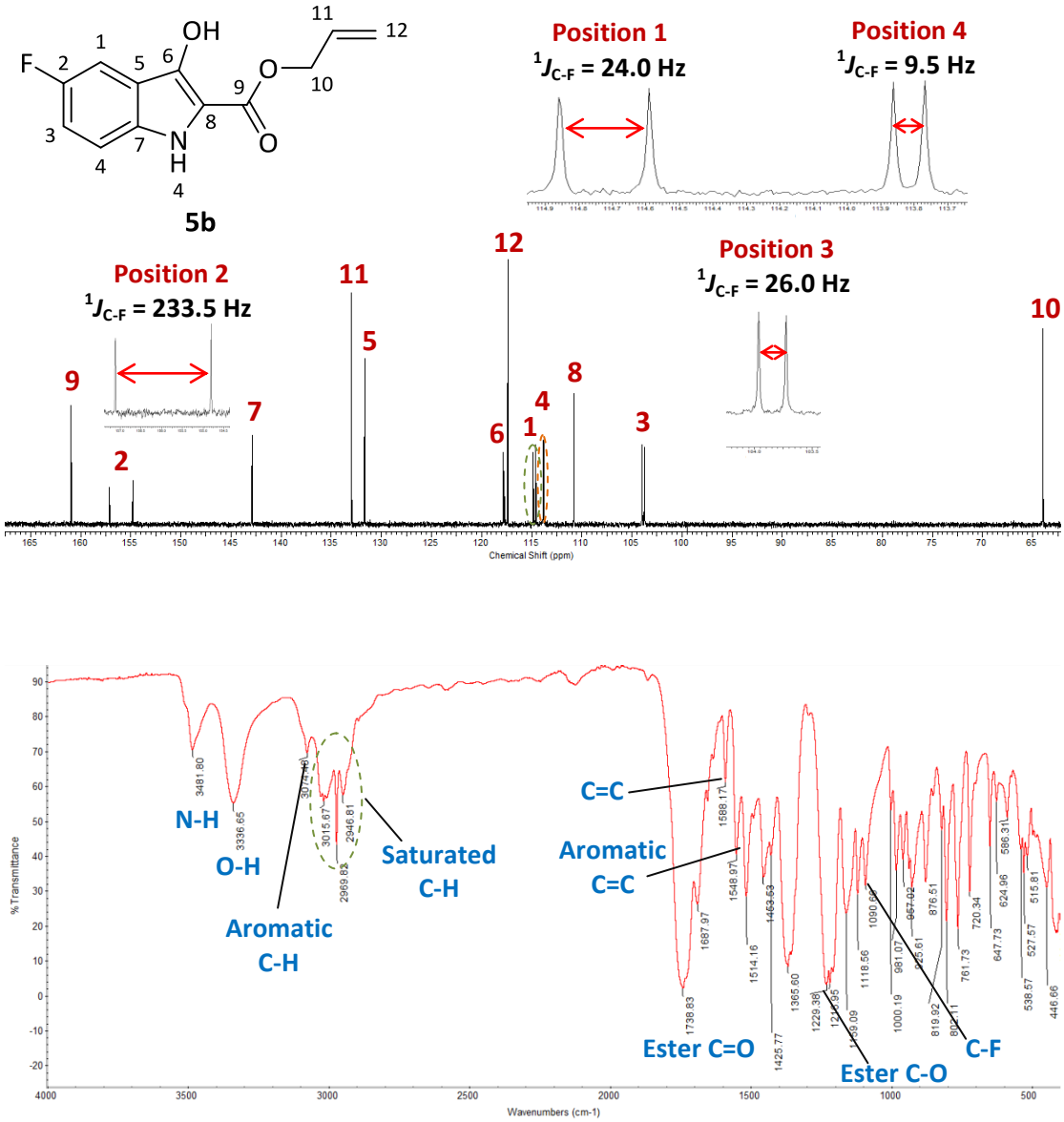

Figure 30. ^{13}C NMR (top) and IR (bottom) spectroscopic analyses of 5-fluoro indoxylic acid allyl ester **5b**. For the NMR analysis, compound **5b** was dissolved in DMSO-d_6.

2.4 Conclusions and Future Work

The improved synthetic method developed by Böttcher and co-workers was the most suitable method prior to glycosidation based on other literature reviews.[108, 165] The unconventional route pursued was more efficient and convenient than the traditional methods to produce the key intermediate. Compared to *N*-acetyl indoxyls, the indoxylic acid allyl esters were more robust and accessible for coupling with an acetylated glycosyl donor. In addition, the presence of the allyl ester group at the C-2 position of the indoxyl suppresses the unwanted dye formation. The improved method was found to be reproducible as the reactions can be repeated several times. The reactions were performed in scales up to approximately 7-25 g and gave reproducible overall yields of 20-30%

To improve the yields of the indoxylic acid allyl esters, the cyclisation reaction could be potentially optimised by using smaller alkoxides such as MeO^- and EtO^-. Moreover, the reaction might be accomplished by a simple microwave-assisted Dieckmann condensation method to improve the yields or speed-up the reaction within an hour.[166] Furthermore, it is advisable that the reactions must be performed in 10-30 g of starting materials to produce the key precursors in adequate yields prior to glycosidation.

Chapter 3 Synthesis of indoxyl glycosides and their fluorinated derivatives

3.1 Aims and Objectives

To expand the existing range of commercially indoxyl glycosides for bacterial analysis, the overall aims and objectives of this part of the programme were to generate the β-glycosides of the fluorinated derivatives of indoxyl in high yields, as shown in **Figure 31.** Traditionally, the glycosylation reaction between a halide sugar and *N*-acetyl indoxyl is usually conducted in acetone with 1M sodium hydroxide solution, followed by subsequent deprotection. This synthetic stage is very crucial to form indoxyl glycoside as a substrate, which will be used for microbiological analysis. Unfortunately, the synthesis of indoxyl glycosides, especially for its derivatives, is often very problematic and low-yielding.[158] To improve the yields, phase transfer catalysis (PTC) was utilised in this project followed by subsequent deprotection steps to furnish the fluorinated indoxyl β-glycosides. The project was also further extended to the glycosylation of underivatised indoxyl to a lesser known carbohydrate, L-(+)-rhamnose, to widen the existing portfolio of known indoxyl enzyme substrates.

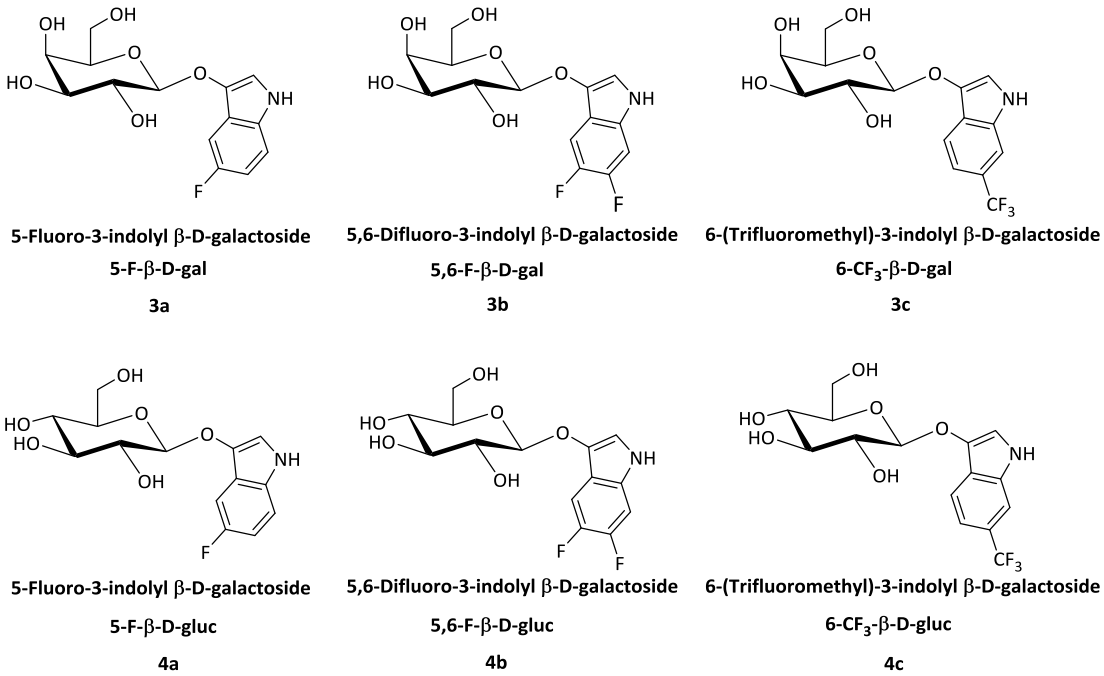

Figure 31. The synthesised fluorinated indoxyl-β-D-glycosides using PTC reaction prior to bacterial detection.

3.2 Introduction

3.2.1 Introduction: general background on carbohydrates

Carbohydrates are one of the most abundant groups of natural products and are essential for living. They are present in humans, animals, plants, yeast, fungi, viruses and bacteria. They have been involved in various important biological processes such as cell-cell recognition, proliferation of cells, the onset of bacterial and viral infections, hormone activities and, for therapeutic applications such as anti-cancer, anti-retroviral, diabetes and antibiotics.[167-179] To make long chains of sugars, the simplest carbohydrates, known as monosachharides, can be joined together by covalent bonds known as the glycosidic linkage to form multiple units of sugars like disaccharides, oligosaccharides and polysaccharides.[180]

Carbohydrates are important sources of energy in organisms, especially in bacterial cells.[181] In general, bacteria possess certain glycosidase enzymes that are capable of hydrolysing the relevant sugars based on sugar type, steric conformation and configuration of the glycosidic bond as illustrated in **Scheme 15**.[110, 111] In enzymatic bacteriology, the most commonly targeted enzymes are β-glucosidases and β-galactosidases. These can be targeted by using synthetic enzyme substrates, particularly indoxyl glycosides, to detect various microbial species in food, clinical and water samples, and allow presumptive identification of bacteria.

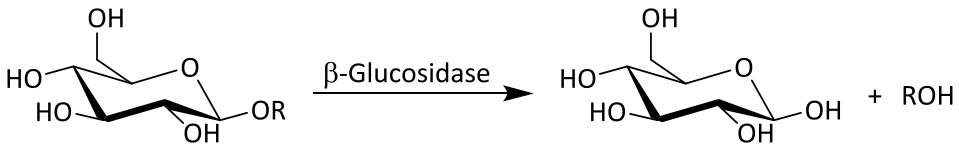

R = Aglycon

Scheme 15. Hydrolysis of β-glucoside by β-glucosidase enzyme.

3.2.2 General mechanism for glycosylation

Most glycosylation reactions involve nucelophilic displacement at the anomeric centre. As detailed in **Scheme 16**, the most common prototype of glycosylation mechanism is presented in two different synthetic pathways. The unimolecular S_N1 starts with a catalyst/promoter activating the anomeric leaving group resulting in its departure and formation of an oxocarbenium ion. Since the oxygen has lone pairs, the anomeric oxocarbonium is stabilised by resonance. A nucleophile bearing one free hydroxyl group attacks either the top or bottom face of the glycosyl cation leading to a mixture of α- and β-glycosides.[182]

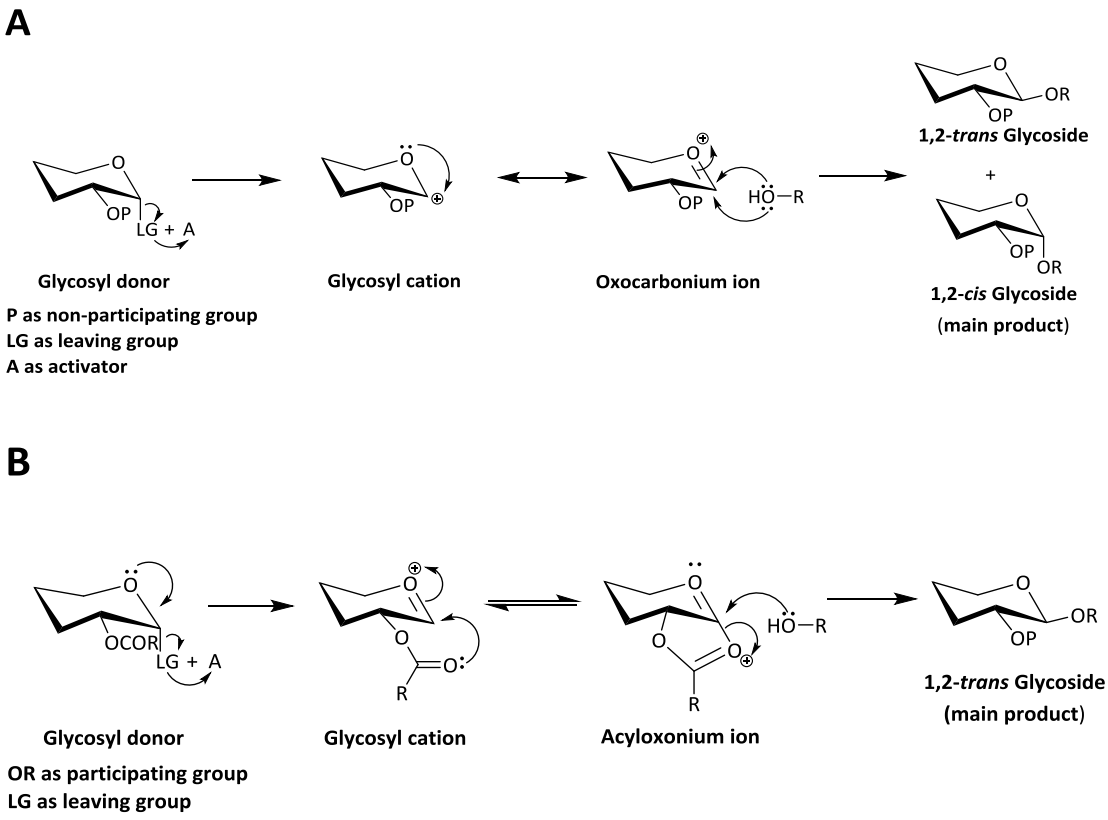

Scheme 16. General reaction mechanism of glycosylation. (**A**) S_N1 pathway without the neighbouring participating group affords α- and β-glycosidic mixture. (**B**) S_N2 pathway with anchimeric assistance to form 1,2-*trans* glycoside stereoselectively.[182]

After the loss of the anomeric leaving group, 1,2-*trans* glycosides can be stereoselectively formed by anchimeric assistance of a neighbouring group at the C-2 position by following the bimolecular S_N2 displacement. Generally, an ester moiety, such as an acetate or benzoate, is utilised to participate in the glycosylation reaction.

There are many factors that influence the outcome of the glycosylation. Careful consideration of the selection of sugar protecting groups, leaving groups, promoters, solvent, temperature and pressure are required to achieve the desired glycosides stereoselectively in adequate yields. Some of the most common sugars and activators utilised in glycosylation reactions are summarised in **Table 10**.

Table 10. Most common examples of sugar donors and activators used in glycosylation.

Glycosyl donors	Catalysts/ Promoters	Advantages	Disadvantages	Ref.
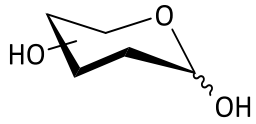	Lewis acid, ion-exchange resin, triflic acid	Protection group is unnecessary.	Produce a mixture of anomers.	183-184
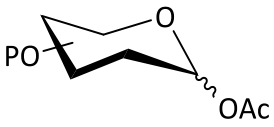	$BF_3{\cdot}OEt_2$, TMSOTf,	Glycosyl donor is easily prepared and very stable.	Produce a mixture of anomers.	185-186
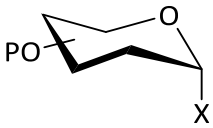 X as F, Cl and Br	K_2CO_3, KOH, NaOH, NaH, Ag salts, TMSOTf	Preserves the glycosyl ring. Uses protecting groups that can be easily removed in basic conditions. Produces *O*-β-glycoside via anchimeric assistance.	More applicable for aglycones. Prone to glycosyl hydrolysis and decomposition. Glycosyl halides are unstable to heat and moisture. Ag salts are sensitive to light. Use of activator in excess is often required.	187-190
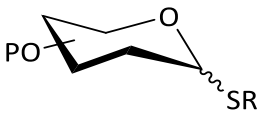 R = alkyl, Ph	$NBS/Sm(OTf)_3$ NIS/TMSOTf, AgOTf	Thiols are very stable leaving group. Thiosugars can be converted to other glycoside donors.	Resultant compound releases an unpleasant smell due to sulfur. Produce a mixture of anomers.	191-193
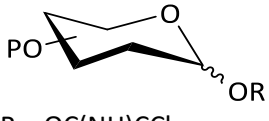 R = $OC(NH)CCl_3$	AgOTf, $BF_3{\cdot}OEt_2$, TMSOTf	Glycosyl donor is easily prepared. Depending on the type of base, α- or β-anomer can be obtained.	Reaction is air sensitive and immediate use is required. Side-product formation via Chapman rearrangement	194-196

P is a protecting group

3.2.3 Protecting group strategies in carbohydrate synthesis

It is a central theme in carbohydrate chemistry to protect the free hydroxyl groups if they are not required for a transformation. The most common starting point is to protect most, or even all, of the hydroxyl groups with the aim of removing each of the blocking groups at the very end of the reaction sequence. In some cases, selective protection of a particular hydroxyl group is important allowing chemoselective reactions, particularly at the anomeric centre (or C-1) of a glycosyl. The most commonly used protecting groups are summarised in **Table 11** for the preparation of glycosides. These protecting groups are chosen since they can be removed under mild conditions, preserving the glycosidic bond. Other protecting groups have been reviewed by Codée *et al*. and Guo and Ye.[197, 198]

Table 11. Summary of the common protecting groups utilised in glycoside synthesis.

Protecting groups	Type	Protection Conditions	Cleavage Condition	References
Acetyl (Ac) 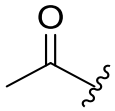	Ester	NaOAc, Ac_2O, approx. 100 °C	NaOMe, MeOH or THF, rt	199-200
		Pyridine, Ac_2O, rt	NaOMe or $NaHCO_3$, MeOH, rt	201-202
Benzoyl (Bz) 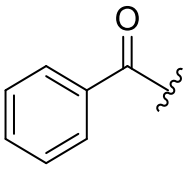	Ester	BnCl, pyridine, rt	$NaHCO_3$ MeOH, rt	203-204
Benzyl (Bn) 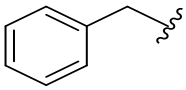	Ether	TMSOTf, PhCHO, Et_3SiH, toluene, -78 to -30 °C	Et_3SiH 10% Pd/C, CH_3OH, rt, 30-120 min	205-206

By varying the reaction conditions, different anomers may be formed stereoselectively. Esters, such as acetates and benzoates, at the C-2 position are responsible for the formation of 1,2-*trans* glycosides by anchimeric assistance. On the other hand, ether-type protecting groups, like benzyl, at the C-2 position are less reactive compared to ester-type protecting groups, like acetyl and benzoyl. As illustrated in F**igure 32**, this can be justified by the electron withdrawing effect of the carbonyl oxygen from esters, thereby, decreasing the electron density and nucleophilicity of the anomeric leaving group. Therefore, aside from unwanted side reactions, the inherent properties of the protecting groups themselves influence the stereochemical outcome of the glycosylation.[207]

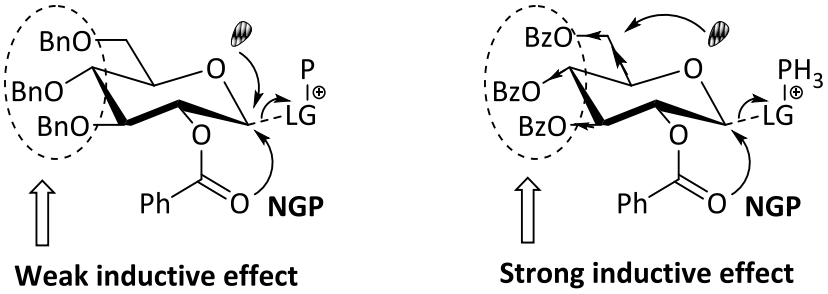

Figure 32.The effect of ether-type/ester-type protecting groups at C-3, C-4 and C-5 positions on the carbohydrate ring. Neighbouring group participation, NGP.[207]

3.2.4 Traditional *O*-glycosidation method towards indoxyl glycosides

O-Glycosidation between an indoxyl acceptor and glycosyl donor is the most crucial step towards the synthesis of indoxyl glycosides. As summarised in **Table 12**, the formation of the glycosides can be very challenging and low-yielding especially for glucose derivatives and more complex glycosides.

Table 12. Synthesis of indoxyl glycosides via Michael *O*-glycosidation.

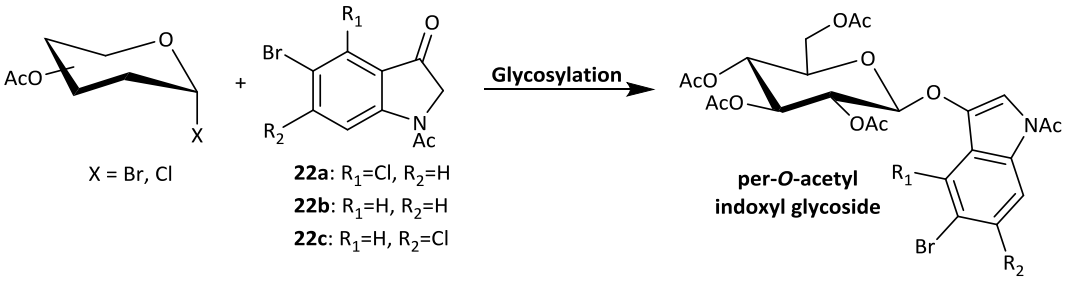

Glycosyl Donors	Indoxyl Acceptors	Glycosylation Conditions	Products & Yields (%)	Ref.
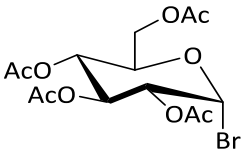	**22b**	NaOH, acetone, 0-5 °C, N_2	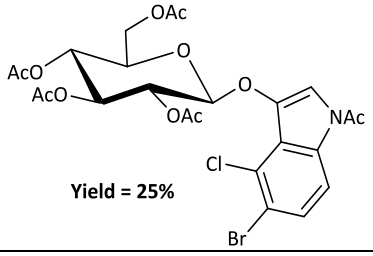 **Yield = 25%**	150
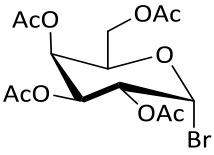	**22c**	NaOH, acetone, 0-5 °C, N_2	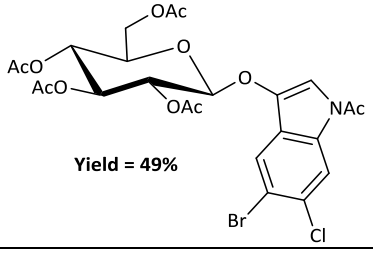 **Yield = 49%**	150
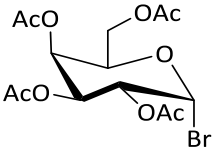	**22c**	NaOH, Acetone, 0-5 °C, N2	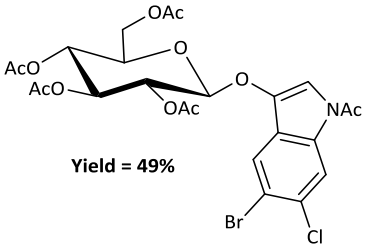 **Yield = 49%**	208
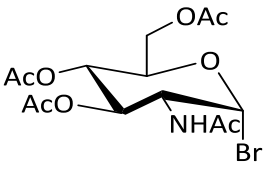	**22a**	NaOH, acetone, 0°C- rt	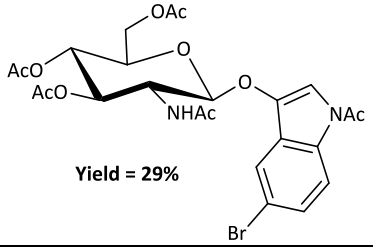 **Yield = 29%**	208
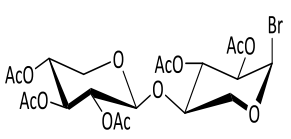	**22b**	NaOH, Acetone, 0 °C, N_2	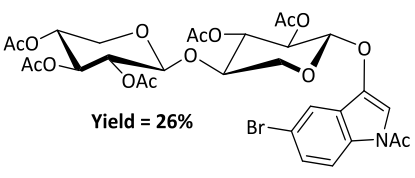 **Yield = 26%**	209

The conventional method uses acetone with a base such as 1M KOH or NaOH, followed by deprotection using base hydrolysis for the preparation of the *O*-glycosides. As shown in **Figure 33**, the *N*-acetyl indoxyl also co-exists in the enol form when a base is present. However, only a small proportion of enol in solution would readily react with an acetylated sugar bromide as glycosyl donor, since the keto form is more favoured, generating low yields of acetylated β-glycosides. Other problems associated with the methodology are sugar hydrolysis and early dye formation due to exposure to water causing unwanted side reactions.

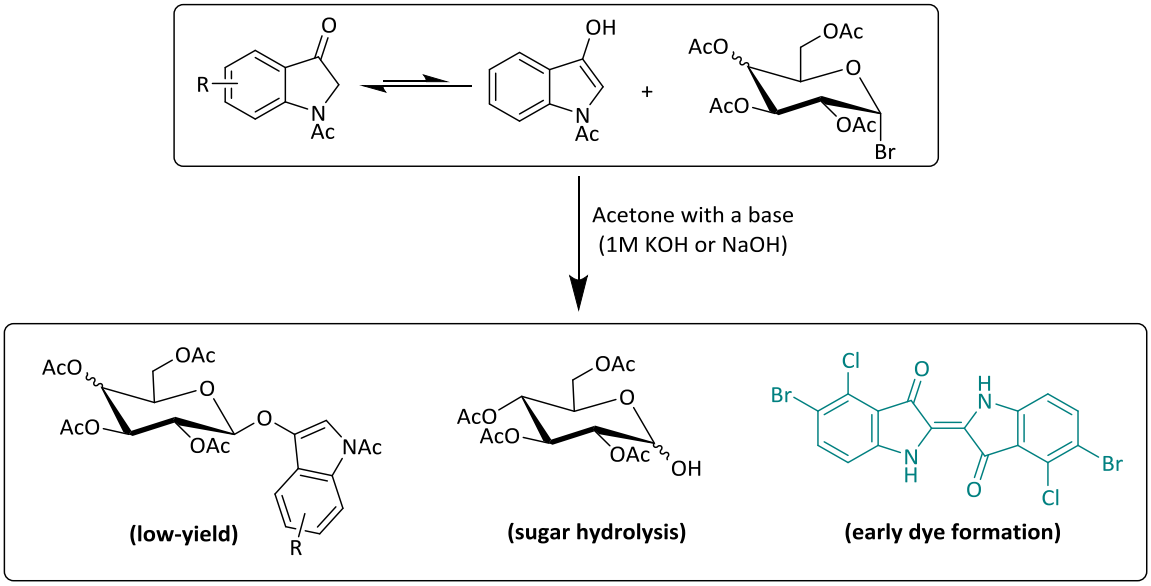

Figure 33. Glycosylation between *N*-acetyl indoxyl and glycosyl bromide producing peracetylated indoxyl glycoside in low yield and other side products.

3.2.5 Improved *O*-glycosidation route towards indoxyl glycoside

To address these challenges, Böttcher and co-workers developed a novel glycosidation pathway that produces high-yielding acetylated indoxyl glycosides, as summarised in **Scheme 17**. Phase-transfer glycosidation was carried out using TBAHS as a catalyst to couple the indoxyl with a glycosyl donor. For this reaction, a glycosyl bromide was chosen as a sugar donor because the bromide at the anomeric position is a good leaving group that has an

appropriate balance of stability and reactivity compared with its halogen counterparts. On the other hand, iodide is more useful for solely creating the α-anomer.[188] Hence, glycosyl bromides **23a-b** were more suitable for the biphasic reaction creating the β-*O*-glycosides by anchimeric assistance. At this stage, the purified products were protected by ester groups and the glycosides **24a-d** were produced in high yields.[158]

Subsequently, the allyl ester was cleaved from the indoxyl by selective treatment with $Pd(PPh_3)_4$ and morpholine in THF, followed by mild decarboxylation using silver acetate and K_2CO_3.[210] The concomitant problem with decarboxylation was the decomposition of the material at very high temperatures (160-170°C) for longer periods of time (16 h for copper/1,10-phenanthroline-complex as a catalyst).[211, 212] Therefore, a silver-based catalyst was used to effectively promote decarboxylation of the carboxylic acid at temperatures of 90-110 °C for 20-40 min or at moderate temperatures of 80-100 °C for 20 min. Finally, the per-*O*-acetyl indoxyl glycosides **25a**-**d** were deacetylated via Zemplén deprotection using a catalytic amount of sodium methoxide in methanol to give free brominated indoxyl glycosides **26a-d**.[128]

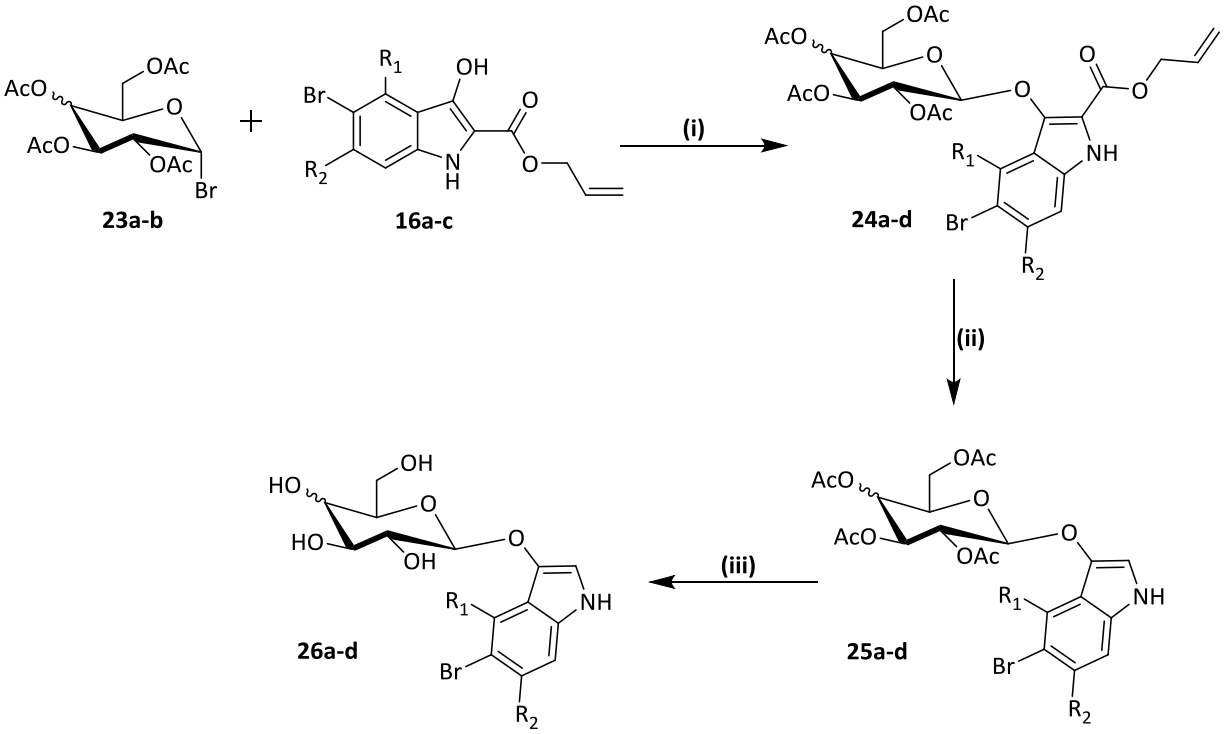

R_1	R_2	Indoxyl Acceptor	Glycosyl Donor	(i)	(ii)	(iii)
H	H	**16b**	**23a**	**24a**	**25a**	**26a**
		80%	Gal	80%	75%	80%
Cl	H	**16a**	**23b**	**24b**	**25b**	**26b**
		84%	Glu	77%	74%	75%
Cl	H	**16a**	**23a**	**24c**	**25c**	**26c**
		84%	Gal	86%	88%	80%
H	Cl	**16c**	**23a**	**24d**	**25d**	**26d**
		76%	Gal	70%	87%	99%

Scheme 17. Synthesis of brominated indoxyl glycosides by Böttcher and co-workers.[158] **(i)** TBAHS, 1M K_2CO_3, DCM, rt, 2 h. **(ii)** THF, morpholine, $Pd(PPh_3)_4$, rt, overnight; Ac_2O, AgOAc, K_2CO_3, 90-110 °C reflux, 20 min to 1 h. **(iii)** MeOH, cat. NaOMe, Amberlite H^+. Note: Glycosyl donors used for step **(i)** were acetobromogalactoside **23a** and acetobromoglucoside **23b**.

3.2.5. The anomeric affect

It was anticipated that PTC would generate the acetylated β-glycoside derivatives stereoselectively as a result of the neighbouring group participation. In the absence of stereochemical control, the α-glycoside is the dominant product, which is thermodynamically favoured by the anomeric effect.[213, 214] For sugars, an electronegative substituent at the anomeric position prefers to occupy the axial, rather than the equatorial, position due to a stereoelectronic effect from one of the lone pairs of oxygen. As shown in **Figure 34A**, a popular and widely used explanation for this is based on the molecular orbital (MO) interaction between lone pair of oxygen (non-bonding) in the ring and the C-1σ* (sigma anti-bonding) orbital of the α-anomer. Due to the hyperconjugation interaction, the β-anomer cannot be afforded due to poor orbital overlap.[215]

Another explanation for the stabilisation of α-glycosides considers the dipole-dipole interaction. As shown in **Figure 34B**, the dipole moments between the oxygen in the ring and bromide of the β-anomer are aligned together, thereby repelling each other. For the axial position, the dipoles of the heteroatoms are opposite of each other, hence stabilising the α-anomer by creating a lower energy barrier.[216]

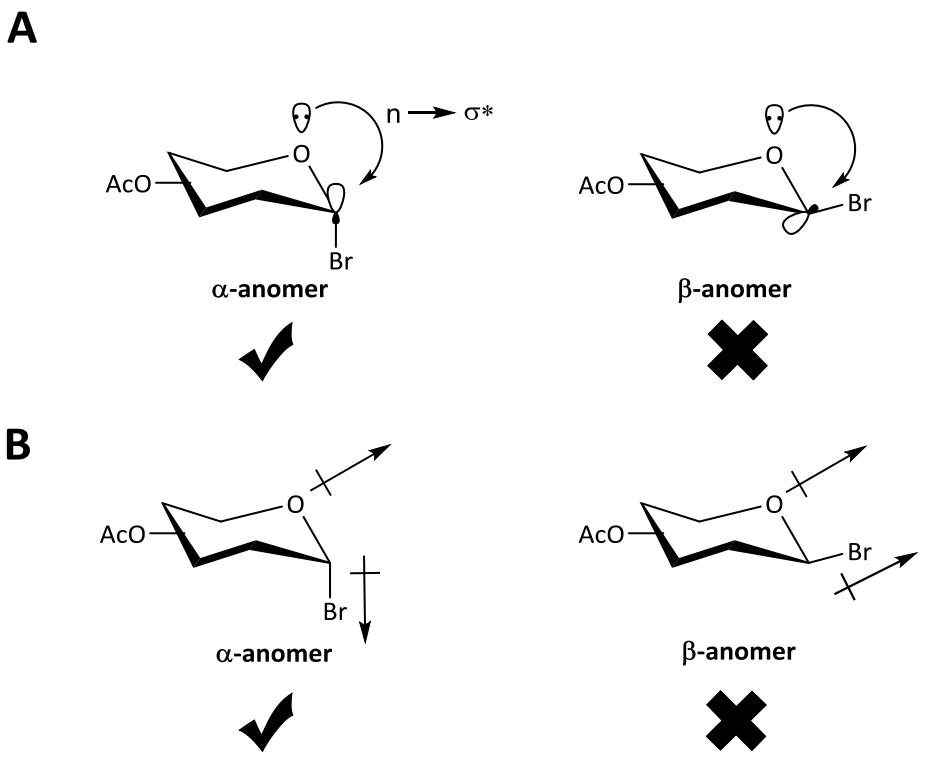

Figure 34. The anomeric effect on acetobromoglycosides. (**A**) n→ σ* interaction explanation based on the MO theory; (**B**) dipole-dipole interaction between the oxygen in the ring and anomeric bromide. (Adapted from [215, 216])

3.3 Results and Discussion

The synthetic route developed by Bottcher and co-workers was utilised to synthesise fluorinated indoxyl β-glycosides. Unlike the conventional glycosidation reaction, the indoxylic acid allyl ester is utilised as key intermediate. The key precursor reacts with with brominated sugar using biphasic system, followed by deprotection steps to produce β-D-glycosides. This work can be extended to less familiar sugar such as L-rhamnose as the authors has previously synthesised the key intermediate with less known or complex sugars such as fucose, sialic acid and 6'-sialyl lactose. Under inert conditions, the indoxyl glycosides were furnished in four steps prior to microbial testing.

3.3.1 Chemical *O*-Glycosidation using PTC

PTC was performed between an indoxylic acid allyl ester acceptor and acetyl glycosyl bromide donor, as shown in **Scheme 17**. The reaction was carried out using tetrabutylammonium hydrogensulfate (TBAHS) as a catalyst and a biphasic system uses water and DCM. The water layer contains K_2CO_3 to keep the reaction under alkaline conditions. The organic molecules are solubilised in DCM to avoid sugar hydrolysis or early dye formation. The tetraalkyl ammonium salt acted as a phase-transfer agent, allowing a low concentration of carbonate ions to pass to the organic phase.

In this reaction, PTC promotes an S_N2 displacement reaction, as depicted in the scheme below (**Scheme 18**). The deprotonated indoxyl attacked the top-face of the sugar donor producing 1,2 *trans*-glycoside stereoselectively.

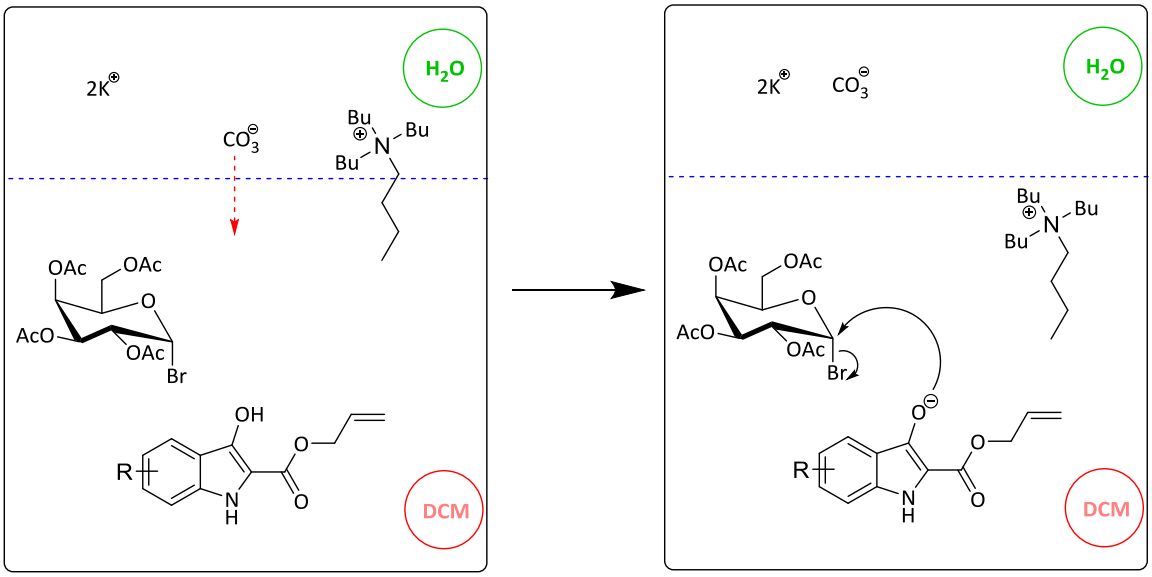

Scheme 18. Synthesis of indolyl-β-D-galactoside using PTC. (Adapted from [156])

As summarised in **Table 13**, the products **26a-c** and **27a-c** were purified using flash column chromatography (2:1 PE 40-60:EA) with yields of 75-95%, which were very consistent and slightly higher than the yields produced by Böttcher and co-workers of brominated glycoside derivatives **24a-d** (**Scheme 16**) with 70-86%.

Table 13. Synthesis of the acetylated fluorinated indoxyl β-*O*-glycosides **27a-c** and **28a-c** using PTC.

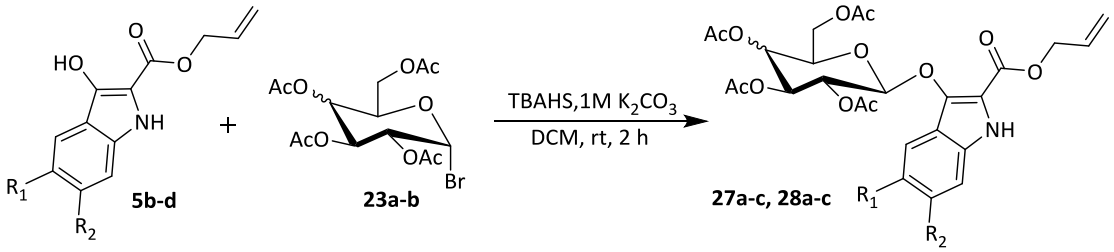

R_1	R_2	Indoxyl Acceptor	Glycosyl Donor	Resultant Compounds	Yields (%)
F	H	**5b**	**23a** Gal	**27a**	95
F	F	**5c**	**23a** Gal	**27b**	85
H	CF_3	**5d**	**23a** Gal	**27c**	89
F	H	**5b**	**23b** Gluc	**28a**	78
F	F	**5c**	**23b** Gluc	**28b**	86
H	CF_3	**5d**	**23b** Gluc	**28c**	90

In theory, the yields for the fluorinated indoxyl β-galactosides **27a-c** are supposedly higher than β-glucosides **28a-c**, which can be explained by the stereochemical differences between the two glycosides. The difference between the sugar galactose and glucose is the stereochemistry at the C-4 position on the carbohydrate ring. As shown in **Scheme 19**, for galactose, the axial C-4 oxygen interacts with electronegative oxygen stabilising the oxocarbenium ion. Hence, the rate of of galactoside formation was faster. In contrast, glucose contains an equatorial C-4 oxygen, and does not interact with the oxocarbenium ion, thus the glycosylation occurred at a slower rate.[217]

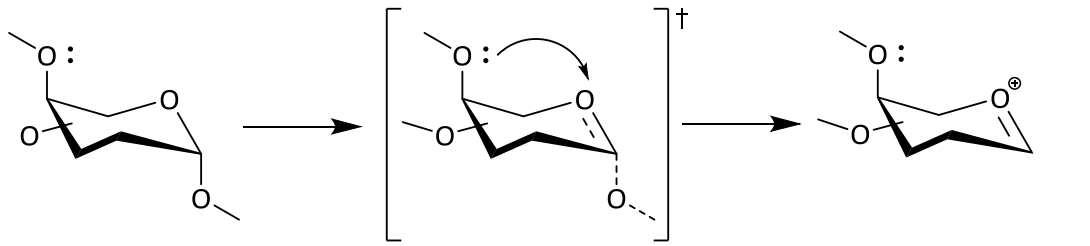

Scheme 19. Mechanism for the stabilisation of oxocarbenium ion galactoside via the axial C-4 electron donation during glycosylation.[217]

The successful synthesis and isolation of the indoxyl and their fluorinated ester glycosides can be confirmed by different analytical techniques. The ^{1}H NMR spectra of the representative compounds (5-mono-fluoro-indol-3-ylic acid allyl ester)-2,3,4,6-tetra-*O*-acetyl-β-D-galactopyranoside **27a** and (5-mono-fluoro-indol-3-ylic acid allyl ester)-2,3,4,6-tetra-*O*-acetyl-β-D-glucopyranoside **28a**, are shown in **Figure 35**.

The successful glycosylation was indicated by the upfield shift of of H-1 from approximately 6 ppm for the donor to 5 ppm in the product. For the β-galactoside, the proton spin-spin coupling for H-1 was 8.0 - 8.5 Hz of the carbohydrate ring, which confirms the formation of 1,2-*trans* glycosides. The large vicinal coupling indicated an equatorial orientation of the β-anomer, as described by the Karplus equation.[218, 219]

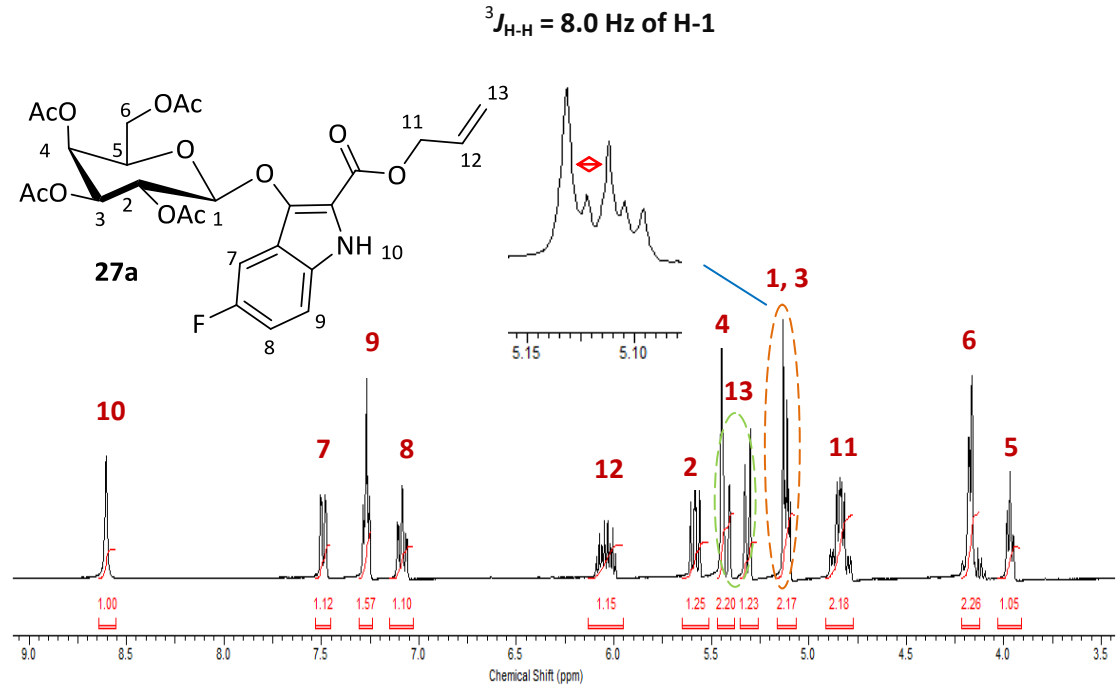

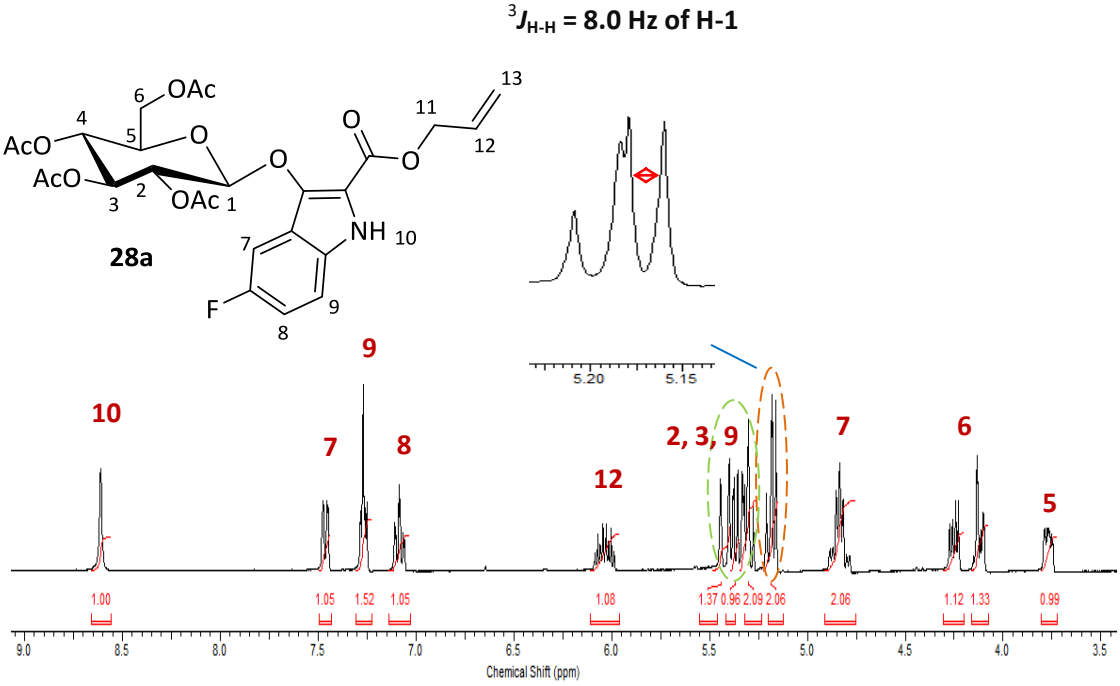

Figure 35. ^{1}H NMR spectroscopic analysis of compounds **27a** and **28a**. Note that the anomeric protons overlapped with their neighbouring protons on the carbohydrate ring. Both compounds were dissolved in $CDCl_3$.

The $^{3}J_{H\text{-}H}$ values together with the chemical shift for the H-1 proton of the glycosidated compounds are listed below in **Table 14**.

Table 14. The spin-spin coupling constants together with their chemical shifts of the glycosidated compounds **27a-c** and **28a-c**.

Compounds	Chemical Shift (ppm)	$^{3}J_{H\text{-}H}$ Values (Hz)
27a	5.12	8.0
27b	5.10	8.0
27c	5.13	8.5
28a	5.17	8.0
28b	5.15	8.0
28c	5.19	8.0

^{13}C Spectroscopic analysis (**Figure 36**) revealed the presence of C-1 of the carbohydrate ring at 102 ppm. Another indication of the successful glycosidation was the presence of only four, instead of five, acetyl protecting groups, which can be deduced as follows: four carbonyl groups at 169-170 ppm and four methyl groups at 20 ppm. For compounds **27a** and **28a**, the spin-spin coupling constant values of fluorine to the *ipso* carbon were 239.0 and 239.5 Hz, respectively.

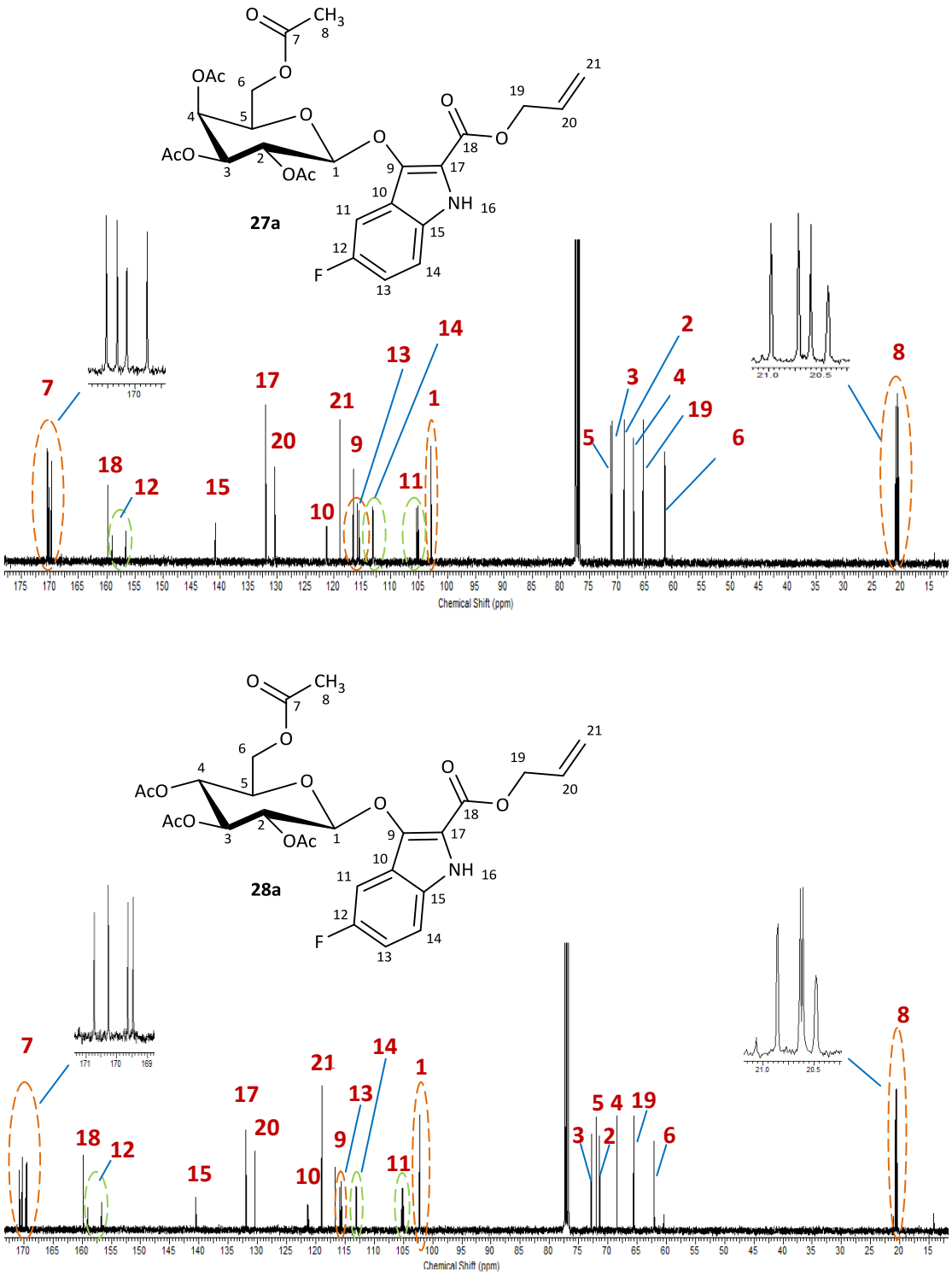

Figure 36. ^{13}C NMR spectroscopic analysis of compounds **27a** and **28a**. Both compounds were dissolved in $CDCl_3$.

3.3.2 Allyl ester deprotection and decarboxylation of fluorinated per-*O*-acetyl indoxyl ester β-glycosides

After the per-*O*-acetyl indoxyl ester glycosides **27a-c** and **28a-c** were purified by normal phase column chromatography on silica gel, the next stage was de-*O*-allylation by mild treatment with $Pd(PPh_3)_4$ and morpholine in THF, where the reaction was left overnight at rt under an argon atmosphere.[210, 220, 221] As shown in **Scheme 20**, the allylic nucleophile was activated by Pd(0) and morpholine, creating a carboxylated group at the C-2 position of the indoxyl. The process further activated the deprotonated morpholine to trap the π allyl palladium complex producing the allylated by-product and regenerating palladium.

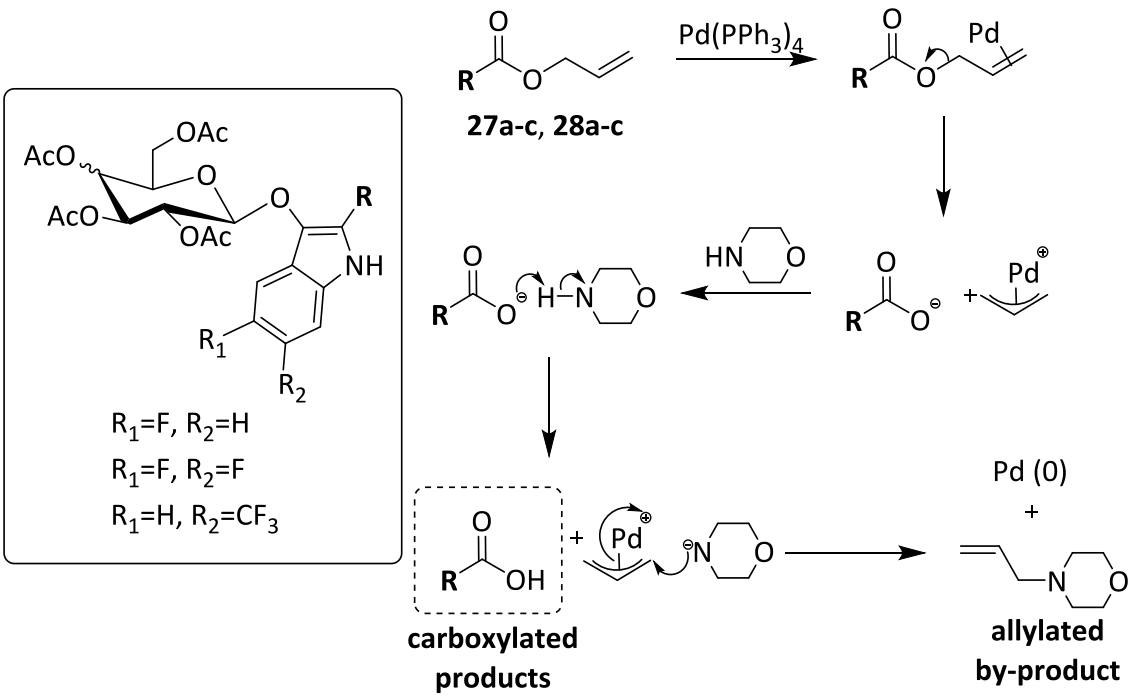

Scheme 20. De-*O*-allylation of indoxylic acid allyl esters β-glycosides **27a-c** and **28a-c**.

Subsequently, the carboxyl derivatives were decarboxylated using AgOAc and K_2CO_3 in acetic anhydride at temperatures of 90-110 °C from 20 to 60 minutes. Under these conditions, simultaneous protection of the *N*-position as an amide occurred, as shown in **Scheme 21**.

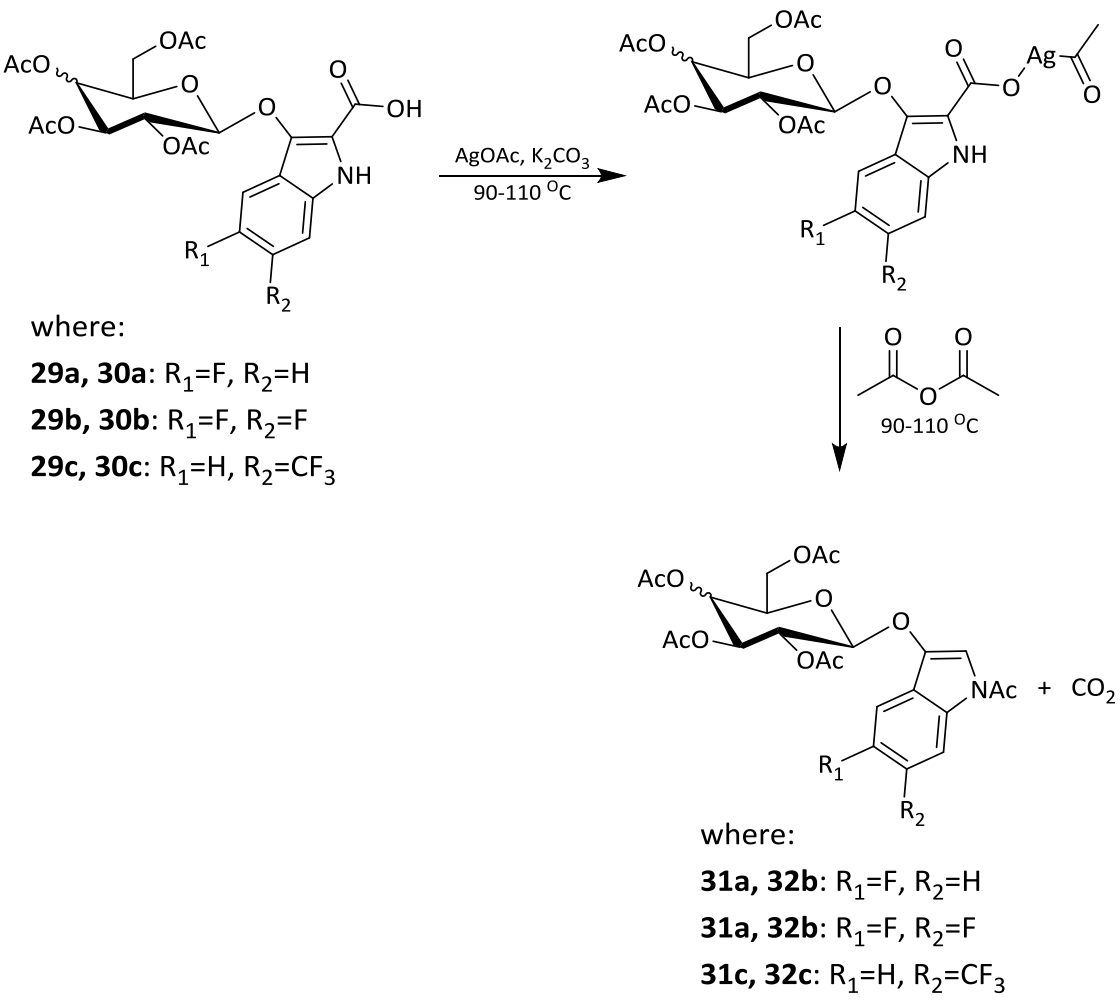

where:

29a, 30a: R_1=F, R_2=H

29b, 30b: R_1=F, R_2=F

29c, 30c: R_1=H, R_2=CF_3

where:

31a, 32b: R_1=F, R_2=H

31a, 32b: R_1=F, R_2=F

31c, 32c: R_1=H, R_2=CF_3

Scheme 21. Decarboxylation of the carboxylated products of fluorinated derivatives **29a-c** and **30a-c** to furnish **31a-c** and **31a-c.**

As summarised in **Table 15**, the per-*O*-acetyl fluorinated indoxyl glycosides **31a-c** and **32a-c** were successfully afforded after purification by flash column chromatography (1:1 PE 40-60:EA) on silica gel in moderate yields of 40-77%. The yields for the fluorinated analogues were lower compared to the results for the brominated derivatives **25a**-**d** with 74-88% (**Scheme 17**) reported by Böttcher et al.[158]

Table 15. Decarboxylated fluorinated indoxyl β-glycosides **31a-c** and **32a-c**.

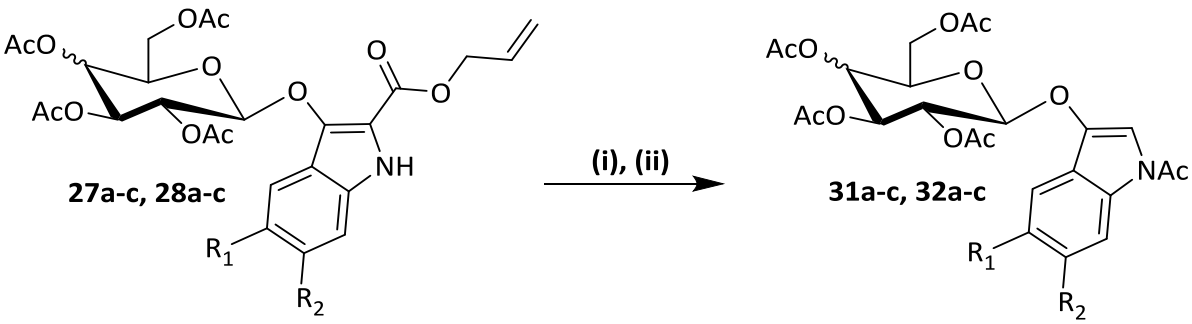

β-Glycosides	R_1	R_2	Starting Materials	Resultant Compounds	Yields (%)
β-Galactoside	F	H	**27a**	**31a**	40%
	F	F	**27b**	**31b**	61%
	H	CF_3	**27c**	**31c**	77%
β-Glucoside	F	H	**28a**	**32a**	57%
	F	F	**28b**	**32b**	42%
	H	CF_3	**28c**	**32c**	72%

(i): $Pd(PPh_3)_4$, morpholine, THF, rt, overnight; **(ii):** AgOAc, K_2CO_3, Ac_2O, 90-100 °C, 30-60 min.

The lower yield of fluorinated analogues could be due to some decomposition of the material at high temperatures (90-110 °C) at longer periods of time (20-60 min), following the early works by Böttcher and co-workers.[128] From a recent paper,[222] the authors optimised the decarboxylation method by decreasing the temperatures between 90 and 105 °C for 15 minutes. The improved method managed to cleave the carboxyl group producing the per-*O*-acetyl indoxyl glycosides with significant yields.

As shown in **Figure 37**, the ^{1}H NMR spectroscopic analysis of the representative compounds β-galactoside **31a** and β-glucoside **32a** revealed the disappearance of the allyl carboxylate group. The presence of a proton at position C-10 of the indoxyl ring was indicated by a peak at 8.35 ppm with a broad singlet resonance. This was also confirmed by ^{13}C NMR spectroscopic analysis, where the resonance for tertiary carbon of compounds **31a** and **32a** were found at 117.91 and 117.95 ppm, respectively. Furthermore, the nitrogen of the

indoxyl ring was acetylated using acetic anhydride to avoid early indigo formation, producing a single peak that was observed at 2.59 for both compounds. The *N*-acetylation was further confirmed by ^{13}C NMR spectroscopic analysis, where the chemical shift for the quaternary carbon of acetylated inodxyl glycosides **31a** and **32a** were present at 167.90 and 167.97 ppm, respectively.

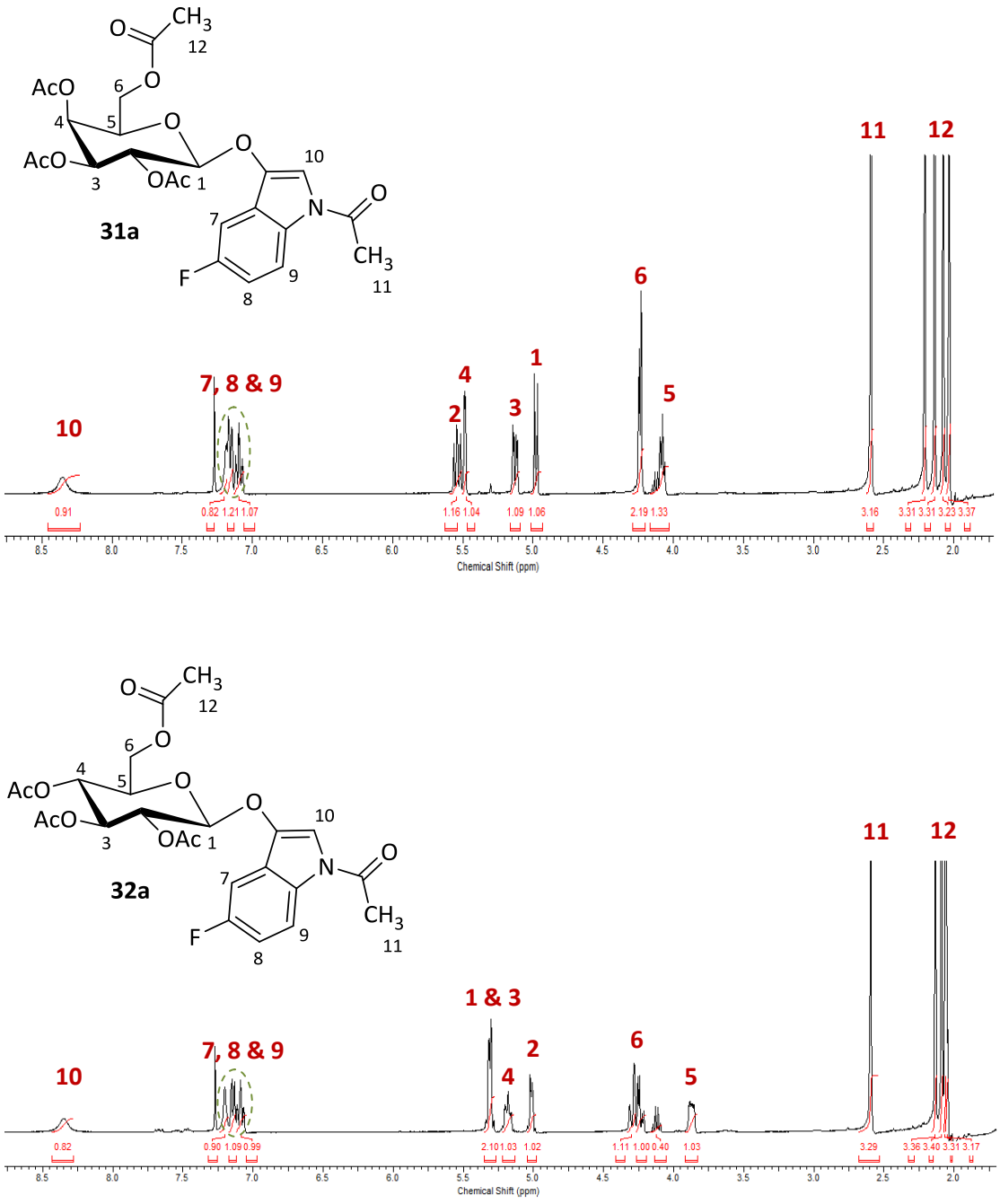

Figure 37. ^{1}H NMR spectroscopic analysis of compounds **31a** and **32a**. Both compounds were dissolved in $CDCl_3$.

3.3.3 Zemplén de-*O*-acetylation of per-*O*-acetyl indoxyl glycosides

Finally, the fluorinated per-*O*-acetyl β-glycosides **31a-c** and **32a-c** were deprotected via Zemplén de-*O*-acetylation using a catalytic amount of sodium methoxide in methanol to give free indoxyl glycosides **3a-c** and **4a-c**. As shown in **Scheme 22**, the hydrolysis of the ester group using sodium methoxide as a base produced the free fluorinated indoxyl glycosides. To remove the sodium ion in solution, Amberlite H^+ resin was added after the reaction was complete.

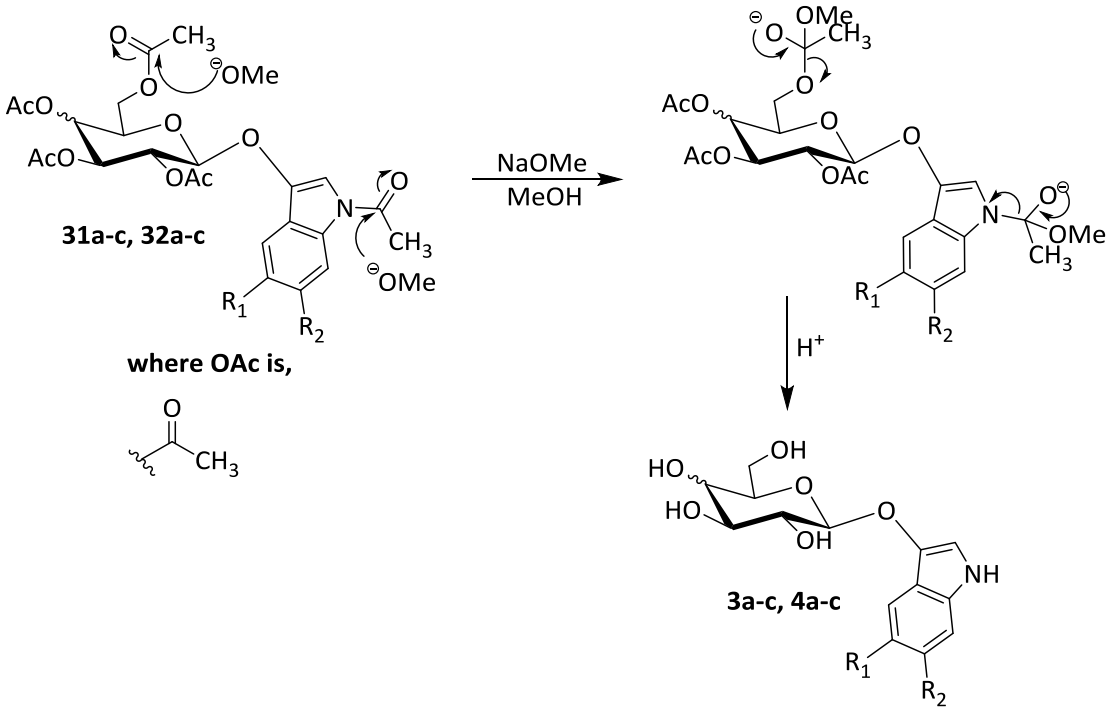

Scheme 22. De-*O*-acetylation of per-*O*-acetylated glycoside **31a-c** and **32a-c** using NaOMe as catalyst to produce the fluorinated indoxyl β-glycosides **3a-c** and **4a-c**.

Based on the works by Bottcher *et al*. the yields for the deprotected indoxyl glycosides **26a-d** were 75-90% (**Scheme 17**).[158] However, there was no reported purification methods employed for the derivatives after the de-*O*-acteylation process.

For this project, the crude fluorinated indoxyl glycosides were initially purified by flash column chromatography in normal phase with an eluent system of 9:1 DCM:MeOH However, the derivatives were difficult to recover as they were retained on the surface by the stationary phase for prolong periods of time (2-4 hours). Since the carbohydrate is hydrophilic, this implied the polar interaction between a glycosyl moiety of indoxyl and the hydroxyl group of the silica gel.[223, 224] There were also concerns on the pH of the normal phase silica having pH values of 0.3-3.5,[225] causing sugar hydrolysis.

Therefore, early dye formation was observed on the column when attempting to recover the purified derivatives. Furthermore, increasing the volume of MeOH, as a mobile phase solvent, to more than 10% is not recommended as the solvent can dissolve some of the silica gel and hence contaminating the purified products.

To avoid hydrolysis and early dimerisation, reversed-phase silica with eluent system of 70:30 0.1% formic acid in H_2O:MeCN was utilised for the purification. The reversed-phase method was effective when purifying the derivatives. The purified products were collected within 15-30 minutes without difficulties. **Figure 38** illustrates the difference between normal phase and reversed-phase silica.

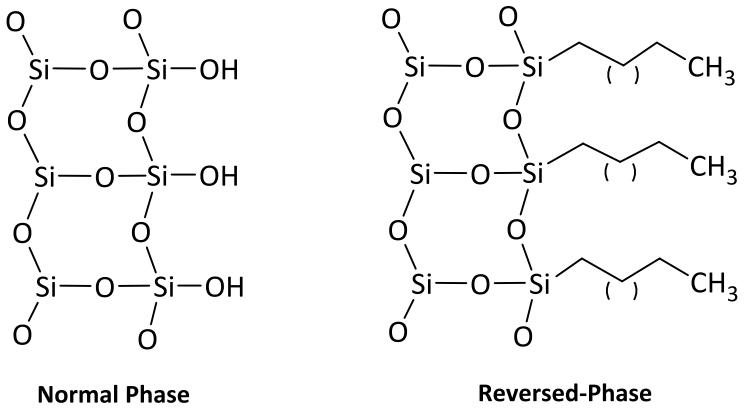

Figure 38. Structure of different stationary phases for purifying free indoxyl glycosides.

The process of finding the appropriate purification methodology affected the yields of the fluorinated indoxyl glycosides as summarised in **Table 16**.

Table 16. Yields of de-*O*-acetylated fluorinated indoxyl β-glycosides **3a-c** and **4a-c**.

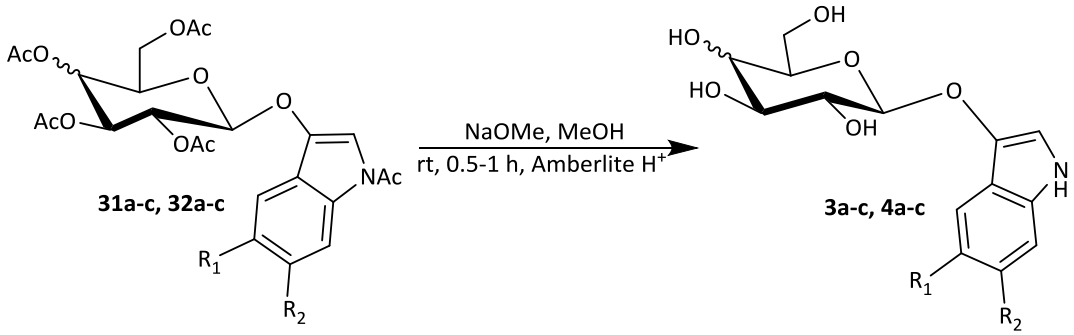

β-Glycosides	R_1	R_2	Starting Materials	Resultant Compounds	Yields (%)
β-Galactoside	F	H	**31a**	**3a**	19%
	F	F	**31b**	**3b**	66%*
	H	CF_3	**31c**	**3c**	31%*
β-Glucoside	F	H	**32a**	**4a**	48%
	F	F	**32b**	**4b**	45%
	H	CF_3	**32c**	**4c**	90%*

*Purified via normal-phase flash column chromatography (9:1 DCM:MeOH).

The successful deacetylation and purification of compounds was confirmed by ^{1}H NMR spectroscopic analysis of the representative derivatives 5-fluoro-3-indolyl β-D-galactopyranoside **3a** and 5-fluoro-3-indolyl β-D-glucopyranoside **4a**, as shown in **Figure 39**.

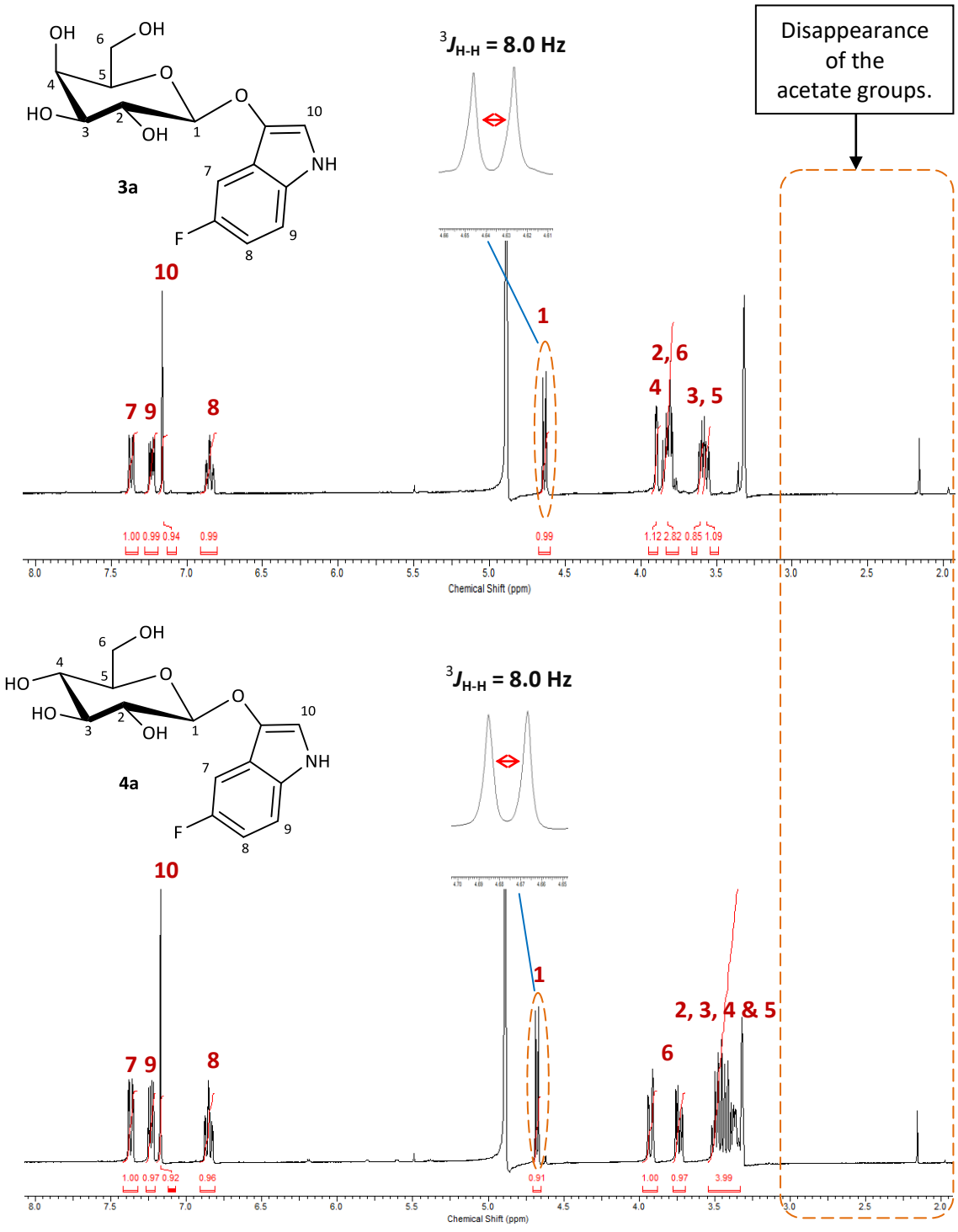

Figure 39. ^{1}H NMR spectroscopic analysis of 5-fluoro-3-indolyl β-D-galactopyranoside **3a** and 5-fluoro-3-indolyl β-D-glucopyranoside **4a**. The de-*O*-acetylated indoxyl glycosides were dissolved in MeOD.

The ^{1}H NMR spectra revealed the disappearance of the acetate groups at 2.00-2.30 ppm. The OH and NH groups of the sugar and indoxyl rings disappeared from the spectrum due to exchange with deuterium when dissolved in deuterated methanol for the NMR analysis. The H-1 of the glycosyl ring was present as a doublet at 4.64 ppm with a coupling constant of 8.0 Hz, hence confirming formation of the 1,2-*trans* glycosides.

When the derivatives were deprotected, the chemical shift of the anomeric proton slightly shifted upfield from approximately 5 to 4 ppm. The $^{3}J_{H\text{-}H}$ values together with the chemical shift for H-1 of the glycosidated compounds are listed below in **Table 17**.

Table 17. Comparison of the chemical shift together with the spin-spin coupling constants of the acetylated **27a-c** and **28a-c**, and deprotected **3a-c** and **4a-c** fluorinated derivatives.

Compounds	Chemical Shift (ppm)	$^{3}J_{H\text{-}H}$ Values (Hz)	Compounds	Chemical Shift (ppm)	$^{3}J_{H\text{-}H}$ Values (Hz)
27a	5.12	8.0	**3a**	4.64	8.0
27b	5.10	8.0	**3b**	4.51	8.0
27c	5.13	8.5	**3c**	4.89	8.0
28a	5.17	8.0	**4a**	4.68	8.0
28b	5.15	8.0	**4b**	4.66	7.5
28c	5.19	8.0	**4c**	4.73	7.5

As shown in **Figure 40**, the ^{13}C NMR spectroscopic analysis of the representative compound 5-fluoro-3-indolyl β-D-glucopyranoside **4a** revealed the disappearance of the acetate groups at 170 and 120 ppm for carbonyl and methyl groups, respectively. The IR spectroscopic analysis revealed the presence of the NH and OH groups at approximately 3460 and 3360 cm^{-1}. No sharp peak was observed at 1700 cm^{-1} for the carbonyl group, indicating successful de-*O*-acetylation. Finally, the mass spectrometry analysis of the final derivatives **3a** and **4a**, which both have the same accurate masses, where $(M+H)^{+}$ of 336.0854 g mol^{-1}, and 336.0854 g mol^{-1} were expected.

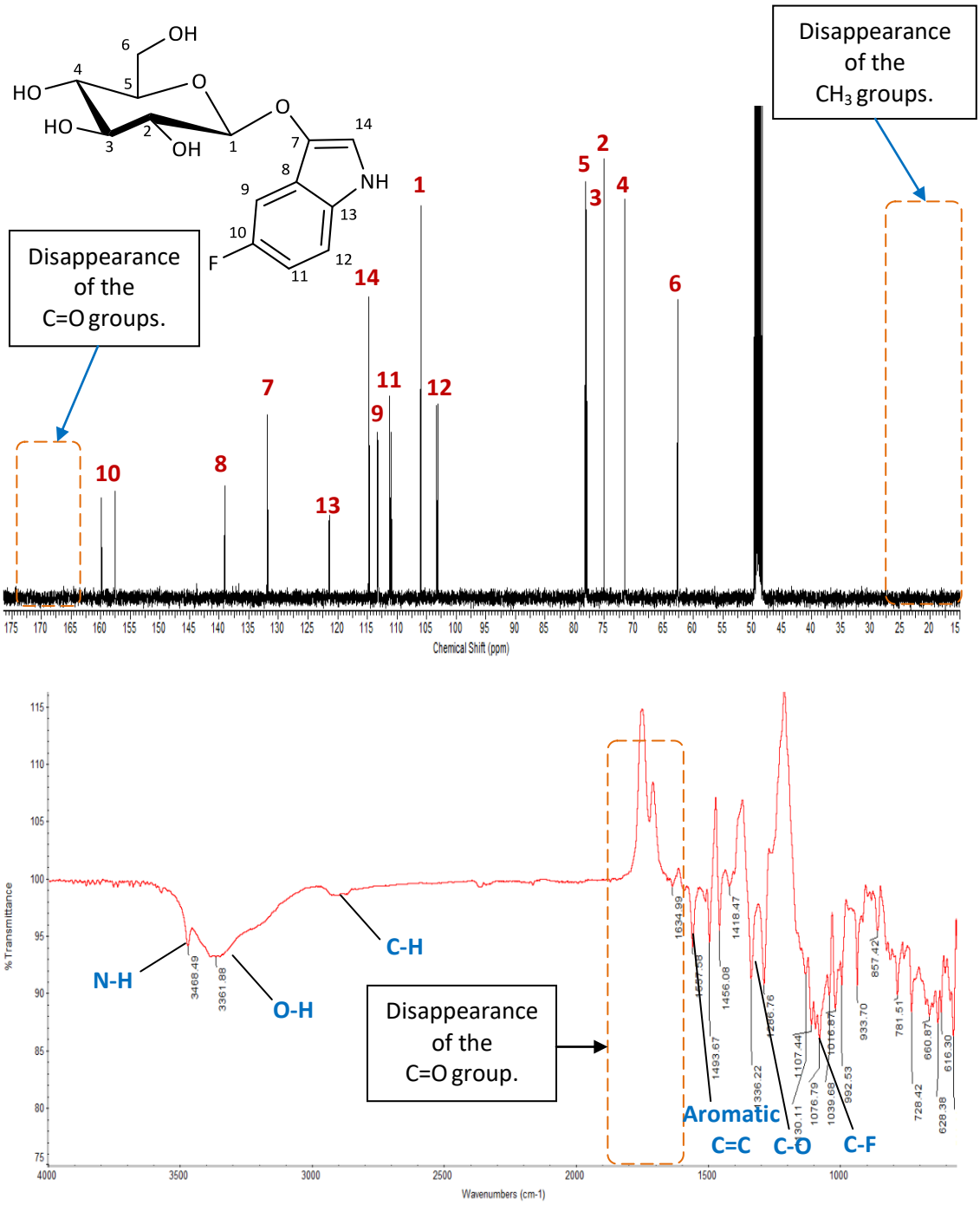

Figure 40. Successful de-*O*-acetylation as proven by ^{13}C NMR (top) and IR (bottom) spectroscopic analysis of 5-fluoro-3-indolyl β-D-glucopyranoside **4a**. For the NMR analysis, the compound was dissolved in MeOD.

3.3.4 Purity analyses of fluorinated indolyl β-glycosides

To confirm the purity of the synthesised fluorinated indoxyl β-galactosides **3a-c** and β-glucosides **4a-c**, high performance liquid chromatography (HPLC, Agilent 1100) was utilised. Prevail™ Carbohydrate ES HPLC column (Grace Davison Discovery Sciences), with dimensions of 53 mm x 7.0 mm, was used to primarily analyse the chromogenic substrates. The purities are listed on **Table 18**.

Table 18. Purity of the fluorinated indolyl β-galactosides **3a-c** and β-glucosides **4a-c**.

Compounds	Indolyl β-D-glycosides	Retention Time (min)	Maxima UV Absorption (λ_{max}, nm)	Purity (%)
3a	5-Fluoro-3-indolyl β-D-galactopyranoside	3.480	285	99
3b	5,6-Difluoro-3-indolyl β-D-galactopyranoside	4.237	285	99
3c	6-(Trifluoromethyl)-3-indolyl β-D-galactopyranoside	4.766	287	97
4a	5-Fluoro-3-indolyl β-D-glucopyranoside	3.843	287	98
4b	5,6-Difluoro-3-indolyl β-D-glucopyranoside	4.428	282	>99
4c	6-(Trifluoromethyl)-3-indolyl β-D-glucopyranoside	4.914	282	>99

3.3.5 Synthesis of indoxyl rhamnoside

Phase-transfer glycosidation has been an efficient and facile method to produce indoxyl glycosides. Therefore, the initial aim of this investigation was to employ the biphasic route with lesser known carbohydrates like L-(+)-rhamnose in order to broaden the portfolio of indoxyl glycosides for bacterial analysis. As shown in **Scheme 23**, L-rhamnose monohydrate was acetylated using pyridine and acetic anhydride to afford the acetylatated rhamnopyranose **33**, followed by bromination using HBr in acetic acid to furnish the 2,3,4-tri-*O*-acetyl-α-L-rhamnosyl bromide **34**. The PTC method using TBAHS in DCM was

investigated to couple rhamnosyl bromide with indoxylic acid allyl ester **5a**. However, the PTC method was unsuccessful to obtain the desired product **35**.

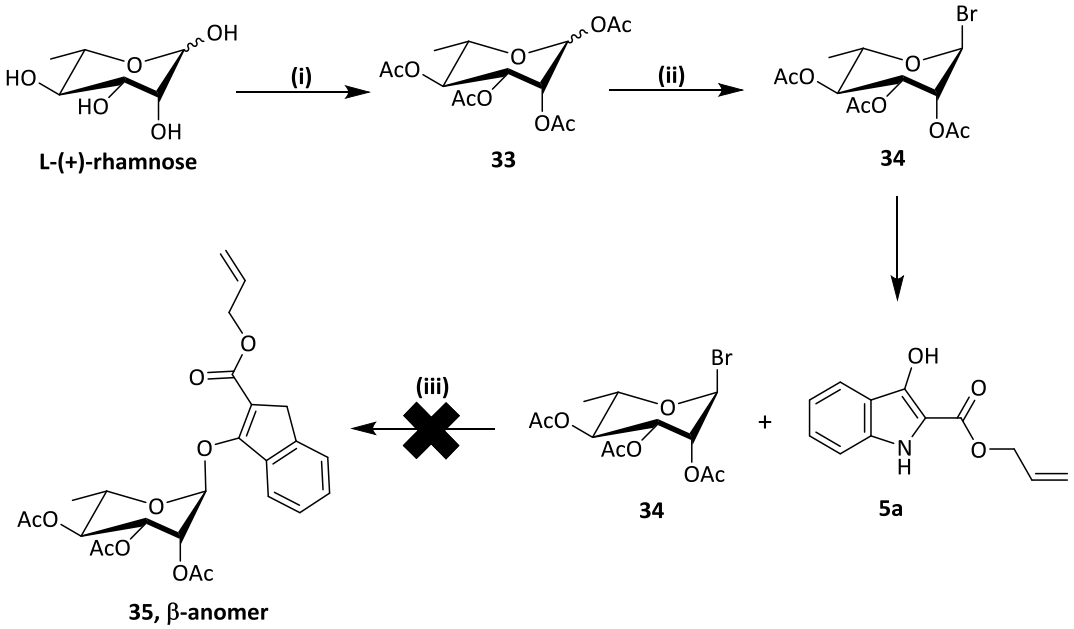

Scheme 23. Synthetic route towards per-*O*-acetyl indoxyl-α-rhamnoside. **(i)** pyridine, Ac_2O, rt, (95%); **(ii)**, HBr in acetic acid, DCM (87%); **(iii)** TBAHS, 1M K_2CO_3, DCM, rt, 2 h.

Thus, during the reaction, degradation of the glycosyl bromide was observed as the colour of the solution turned from yellow to black. Another indication of the failed glycosidation was manifested on the ^{1}H NMR spectrum (data not provided).

Although, the PTC method has been utilised by Demetzos *et al.*[226] to glycosidate the flavanoid quercetin with L-rhamnose bromide using 1.25 M KOH and benzyltriethylammonium chloride (BTEAC) in $CHCl_3$.[227] This did not prove effective with indoxyl acceptors and therefore an alternative method was sought.

Hutchins and co-workers successfully utilised trimethylsilyl trifluoromethanesulfonate (TMSOTf) as a promoter for the glycosidation nadifloxacin with lesser known sugars such as arabinofuranoside, mannoside, xylofuranoside in moderate yields (23-73%). In addition, the authors utilised the promoter to produce 1,2-*cis* glycosides.[63] Therefore, TMOSTf was used for the glycosidation of the acetylated α,β-rhamnoside **33** with either indoxylic acid allyl ester **35** or commercially available indoxyl acid methyl ester **36** to fursnish α,β-indoxyl rhamnoside, as shown in **Scheme 24**. Tetramethylurea was added as an acid scavenger. A summary of the different reaction conditions that were investigated in an attempt to prepare the indoxyl rhamnosides is provided in **Table 19**.

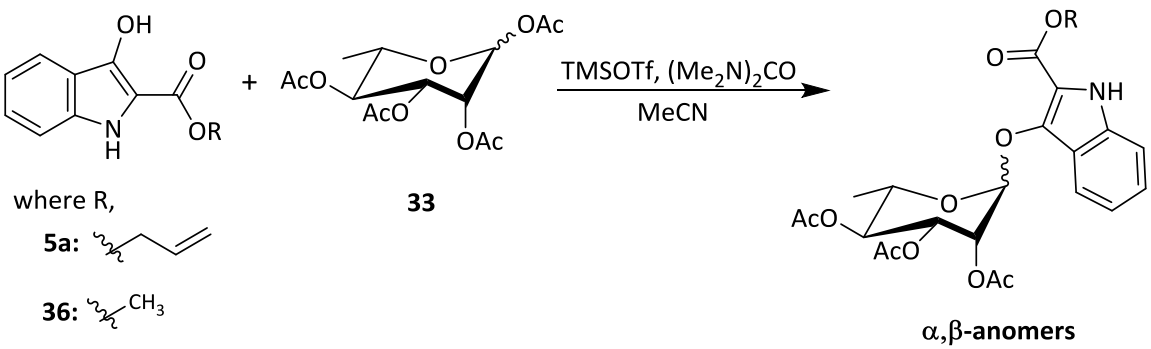

Scheme 24. *O*-Glycosidation reaction using TMSOTf as a promoter. Note that using two different indoxyl key precursors **5a** and **36** did not optimise the reaction.

Table 19. Comparisons of starting materials and reaction conditions for the glycosidation of indoxyl and L-(+)-rhamnose.

		Molar equivalence				
Entry	**Coupling Method**	**Indoxyl acceptors**	**Glycosyl donor**	**Promoters**	**Reaction Conditions**	**Comments**
1	PTC	**5a** 1.0	**34** 1.0	TBAHS = 1.5	DCM, rt for 30 min	Decomposition of product.
2	PTC	**5a** 1.0	**34** 1.0	TBAHS = 1.5	DCM, 0 °C for 4 hrs, and rt for 30 min	Decomposition of product.
3	TMSOTf	**36** 1.0	**33** 1.0	TMSOTf = 2.0	MeCN, rt for 5 hrs	Isolation of impure products.
4	TMSOTf	**5a** 1.0	**33** 2.0	TMSOTf = 10.0	MeCN, rt for 2 hrs	Isolation of impure products.

After the glycosidation, the crude product was purified by automated flash column chromatography using normal phase silica and an isocratic solvent of 1:1 PE 40-60:EA to isolate the product. However, separating the mixtures was proved be difficult.

At this stage, it was decided to continue with the decarboxylation of the product mixture **37** by following the method by Böttcher and co-workers of decarboxylation,[128] as shown in **Scheme 25**.

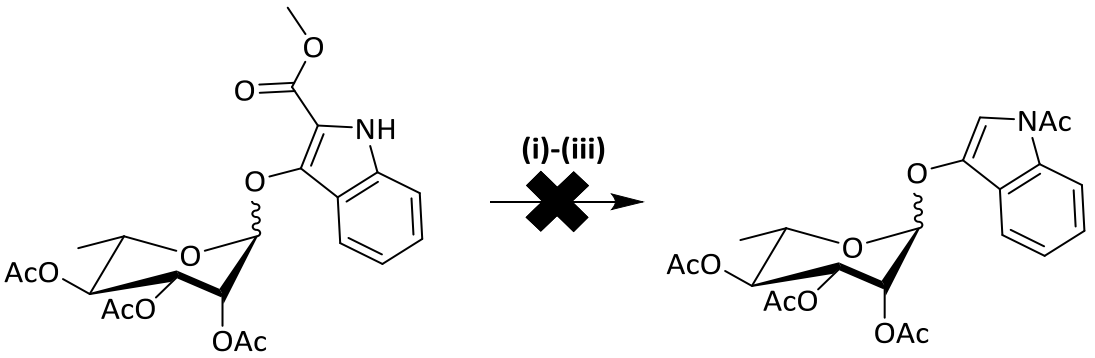

Scheme 25. Decarboxylation of compound **37** to produce the decarboxylated α,β-anomers, **38**. **(i)** NaOMe, MeOH, rt, 3 hr; (**ii**) 0.1 M NaOH, reflux, 1 h; (**iii**) AgOAc, K_2CO_3, AC_2O, 95-100 °C, 45 min.

Automated flash column chromatography using normal phase silica and a gradient solvent system of PE 40-60:EA was utilised in an attempt to purify the crude product. However, ^{1}H NMR spectroscopic analysis revealed that the desired product was not successfully isolated (data not provided).

3.4 Conclusions and Future Works

A range of fluorinated indoxyl glycosides have been synthesised and purified. Under an inert condition, the reactions were performed in scales up to approximately 0.5-3.5 g and gave reproducible overall yields of 7-21% and 16-58% for fluorinated indoxyl β-galactosides **3a-c** and β-glucosides **4a-c**, respectively.

The facile preparation of acetylated indoxylic acid allyl ester glycosides has been successfully achieved via phase-transfer catalysis using TBAHS as a phase-transfer agent. The coupling method followed the S_N2 style of reaction to form 1,2-*trans* glycosides. Based on the ^{1}H NMR spectroscopic analysis of each compound, the spin-spin coupling constant of the doublet for the anomeric centre was aprroximately 8 Hz. The yields for the purified acetylated indoxyl

glycosides **27a-c** and **28a-c** were 78-95% – higher than the yields provided by the Michael *O*-glycosidation **(Table 12)**.

The de-*O*-allylation and decarboxylation of the allyl ester of indoxyl provided the desired products **31a-c** and **32a-c** with moderate yields of 40-77%. Deprotection of the acetylated indoxyl glycosides was conducted via Zemplén de-*O*-acetylation using sodium methoxide as a catalyst. To purify the crude product, the purification was initially carried out using normal phase column chromatography procedure with an isocratic system of 9:1 DCM:MeOH. However, the purification method produced early dimerisation and sugar hydrolysis compromising the yields of the purified indoxyl glycoside products. Nevertheless, fluorinated indoxyl β-D-glycosides were successfully isolated using automated reverse-phase column chromatography. The yields the successfully isolated β-galactosides **3a-c** and β-glucosides **4a-c** were 19-31% and 48-90%, respectively.

Due to the successful glycosidation and isolation of fluorinated indoxyl β-glycosides, PTC was used to synthesise the underivatised indoxyl rhamnoside. However, the preparation of the compound was unsuccessful. Attempts to synthesise the compound via TMSOTf as a promoter was chosen to furnish α,β-anomers. To separate the mixture, automated column chromatography was utilised; however, the products were difficult to isolate. Therefore, the purified product was subjected to decarboxylation following the method by Böttcher and co-workers.[158] Based on ^{1}H NMR spectroscopic analysis, the desired product was not successfully isolated.

Chapter 4 Microbiological evaluation of the fluorinated indoxyl β-glycosides in culture media

4.1 Indoxyl glycosides for bacterial testing

The traditional approach for screening selectively enriched bacterial samples in order to detect pathogens in the presence of large numbers of commensal organisms can be very time consuming and costly. To simplify the procedure, it is often advantageous to incorporate chromogenic substrates in isolation plates. Only those organisms that contain the relevant enzyme will cleave the substrate and produce a colour around the target organism colonies. These colonies can be further tested to provide confirmed identification. Indoxyl glycosides are widely used substrates for this application as they are soluble in water and are often very specific. In addition, when the sugar portion of the glycoside is removed the free indoxyl readily dimerises and is oxidised by air to produce highly coloured insoluble indigo compounds that are deposited in and around microbial colonies on agar plates.

The colour of the indigo product is dependent on substituents on the phenyl ring and on the amino group. Thus, two or more different indoxyl substrates can be used to determine the presence of two or more different enzymes at the same time with an organism producing both enzymes giving a hybrid colour. As illustrated in **Figure 41**, the inclusion of two different chromogenic substrates, namely 5-bromo-4-chloro-indoly β-D-galactopyranoside (**1a** or X-β-D-gal) and 5-bromo-6-chloro-3-indolyl β-D-glucopyranoside (**2c** or Magenta-β-D-gluc), into a non-selective media are used for the detection of urinary tract pathogens. *E. coli* species appear to be blue/green since the organism expresses β-galactosidase enzyme, whereas *Enterococcus* species appeared as purple/red colour. When coliforms (*Klebsiella*, *Enterobacter*, *Serratia* groups) hydrolysed both glycosides, the substrates released a mixed colour.[111] Combining the two substrates increases the specificity and discriminatory ability of the medium; hence, reducing the reliance for further testing.[107] Therefore, this stage of the programme sought to investigate the chromogenic properties of the six synthesised fluorinated indoxyl glycosides.

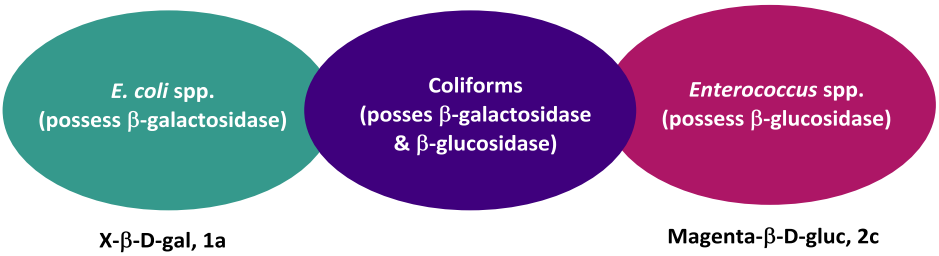

Figure 41. Combination of two different indoxyl glycosides (left and right) forming a hybrid colouration (middle) on the bacterial colonies.[111]

Furthermore, it is apparent that the effect of substituents, for instance replacing the bromine by chlorine, can alter the specificity of the substrates presumably by altering the rate of bacterial uptake and rate of hydrolysis of the substrate.[126]

4.2 Overall aims and objectives

This study was intended to evaluate the chromogenic properties of the synthesised fluorinated indoxyl glycosides for the bacterial detection of enzymes β-galactosidase and β-glucosidase when tested against several bacteria in Nutrient Agar (NA) and Tryptone Soya Agar (TSA). The fluorinated indoxyl compounds were compared for their specificity, and rate of uptake and hydrolysis with other commercially available indoxyl compounds (**Figure 42**) such as 5-bromo-4-chloro-3-indolyl β-D-galactopyranoside (**1a**, 5-Br-4-Cl-β-D-gal or X β-D-gal), 5-bromo-4-chloro-3-indolyl β-D-glucopyranoside (**2a**, 5-Br-4-Cl-β-D-gal or X-β-D-gluc) and 6-fluoro-3-indolyl β-D-galactopyranoside (**1f**, 6-F-β-D-gal or Rouge-β-D-gal).

A

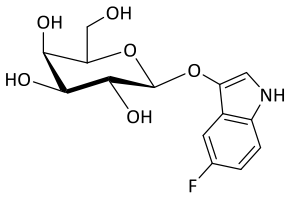

5-Fluoro-3-indolyl β-D-galactoside
5-F-β-D-gal
3a

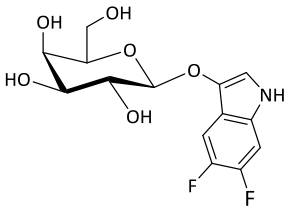

5, 6-Fluoro-3-indolyl β-D-galactoside
5, 6-F-β-D-gal
3b

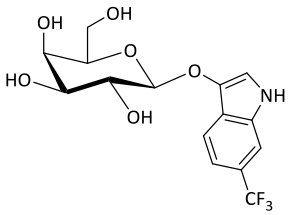

6-(Trifluoromethyl)-3-indolyl β-D-galactoside
6-CF_3-β-D-gal
3c

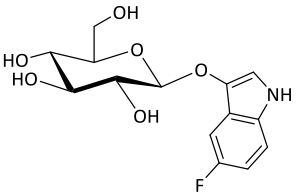

5-Fluoro-3-indolyl β-D-glucoside
5-F-β-D-gluc
4a

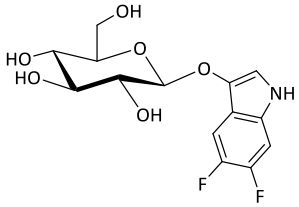

5, 6-Fluoro-3-indolyl β-D-glucoside
5, 6-F-β-D-gluc
4b

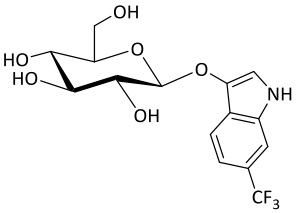

6-(Trifluoromethyl)-3-indolyl β-D-glucoside
6-CF_3-β-D-gluc
4c

B

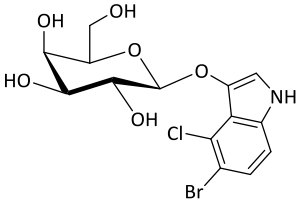

5-Bromo-4-chloro-3-indolyl β-D-galactoside
5-Br-4-Cl-β-D-gal or X-β-D-gal
1a

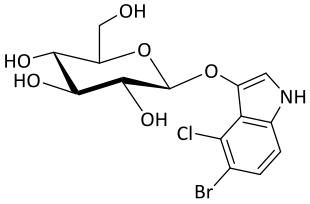

5-Bromo-4-chloro-3-indolyl β-D-glucoside
5-Br-4-Cl-β-D-gluc or X-β-D-gluc
2a

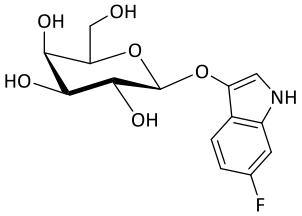

6-Fluoro-3-indolyl β-D-galactoside
6-F-β-D-gal or Rouge-β-D-gal
1f

Figure 42. (**A**) Fluorinated derivatives of indoxyl glycosides; and, (**B**) commercially available chromogens that have been utilised for the detection of bacteria.

4.3 Target bacterial strains and preparation of chromogenic media

Fluorinated indoxyl glycosides **3a**-**c** and 4**a**-**c** and commercially available chromogenic substrates **1a**, **2a** and **1f** were tested against a range of microorganisms found in clinical, food, and water samples. As summarised in **Tables 20** and **21**, a wide range of Gram-positive and Gram-negative were available.

Table 20. Summary of Gram-positive microorganisms along with their pathogenecity and presence (+) and absence (-) of the targeted enzymes utilised in this study.

Bacterial Species	Pathogenecities	Targeted Enzymes		Ref.
		β-Galactosidase	β-Glucosidase	
Bacillus cereus	Food poisoning, respiratory and urinary tract infections, non-gastrointestInal infections (systemic, wound, eyes and gum inflammation), anthrax like progressive pneumonia, bacteraemia, septicaemia, endocarditis, meningitis.	-	+	228, 229
Bacillus licheniformis	Food poisoning, infections of wounds, the ears, eyes, respiratory tract and urinary tract.	-	+	230, 231
Bacillus subtilis	Food poisoning, septicaemia, endocarditis, endocarditis, meningitis non-gastrointestinal (respiratory and eye infections).	-	+	232, 233
Enterococcus faecalis	Endocarditis, neonatal meningitis, nosocomial infections e.g. urinary tract infection, surgical wound infection and bloodstream infection.	+	+	234, 235,1 90
Enterococcus faecium	Endocarditis, neonatal meningitis, nosocomial infections e.g. Urinary tract infection, surgical wound infection and bloodstream infection.	+	+	234, 236, 190
Staphylococcus aureus	Abscesses, surgical wound infection, bacteremia, food poisoning	-	-	237, 238

Table 20 (continued). Summary of Gram-positive microorganisms along with their pathogenecity, and presence (+) and absence (-) of the targeted enzymes utilised in this study.

Bacterial Species	Pathogenecity	Targeted Enzymes		Ref.
		β-Galactosidase	β-Glucosidase	
Staphylococcus aureus v. oxford	Skin and soft tissue infections.	No data found.	No data found.	[239]
Staphylococcus epidermis	Pathogenic for immunocompromised patients and dwells in medical devices (catheters, pacemakers and implants).	-	+	[240, 241]
Staphylococcus haemolyticus	Urinary tract infection, septicaemia, peritonitis. Wound, bone, and joint infections.	+	+	[241, 242]
Staphylococcus saprophyticus	Urinary tract infection (especially in women during the reproductive years), acute cystitis.	-	+	[242, 241]
Streptococcus agalactiae GBS	Pathogenic for immunocompromised adults, neonatal septicaemia and pneumonia, meningitis.	-	-	[243, 244]
Streptococcus pneumoniae	Pneumonia, middle ear infections and meningitis	+	-	[245, 246]
Streptococcus pyogenes	Pharyngitis, scarlet fever, septicaemia, skin infections to invasion of soft tissues, induced toxic shock syndrome.	-	+	[126, 247, 244]
Streptococcus viridans	Pathogenic for immunocompromised patients, bacteraemia, endocarditis, upper respiratory tract infections.	-	+	[126, 248, 249]

Table 21. Summary of Gram-negative microorganisms along with their pathogenecity, and presence (+) and absence (-) of the targeted enzymes utilised in this study.

Bacterial Species	Pathogenicity	Targeted Enzymes		Ref.
		β-Galactosidase	β-Glucosidase	
Burkholderia cepacia	Respiratory infections associated with pneumonia and septicaemia.	+	+	250, 251, 252
Citrobacter freundii	Nosocomial infections e.g. urinary tract, respiratory tract and blood) gastroenteritis, neonatal meningitis, and septicaemia.	+	+	244, 123, 253
Cronobacter sakazakii	Necrotising enterocolitis, sepsis meningitis, bacteraemia in neonates and infants.	+	-	126, 254, 255
Enterobacter aerogenes	Pathogenic for immunosupressed patients and dwells in medical devices such as endotracheal tubes or urinary catheters.	+	+	244, 256, 240
Enterobacter cloacae	Nosocomial infections e.g. lower respiratory tract, skin to soft tissue, urinary tract, intra-abdominal and eye. Bacteraemia, endocarditis, septic arthritis, osteomyelitis.	+	+	244, 257, 240
Escherichia coli	Urinary tract infection, septicaemia, enteritis, neonatal meningitis	+	-	244, 240, 258
Escherichia hermanii	Pathogenic for immunocompromised patients and dwells in catheters and causes urinary tract infection (pyelonephritis),	+	-	244, 240, 259

Table 21 (continued). Summary of Gram-negative microorganisms along with their pathogenecity, and presence (+) and absence (-) of the targeted enzymes utilised in this study.

Bacterial Species	Pathogenicity	Targeted Enzymes		Ref.
		β-Galactosidase	β-Glucosidase	
Klebsiella pneumoniae	Nosocomial infections e.g. the urinary tract, respiratory tract, lung, wounds and blood.	+	+	244, 240, 260
Pseudomonas aeruginosa	Pathogenic for immunosupressed patients and causes noscomial infections e.g. bloodstream, urinary tract and pneumonia.	-	-	261, 190
Salmonella serotypes*	Gastroenteritis, bacteraemia and enteric fever.	-	-	244, 240, 262
Serratia marcescens	Nosocomial infections in the urinary tract and central nervous system. Other healthcare-related infections e.g. bacteraemia and pneumonia.	+	+	244, 240, 263

**Salmonella* serotypes are Abony, Dublin, Enteriditis, Typhimurium and Virchow.

The indoxyl glycosides were incorporated in non-selective culture media, Nutrient Agar and Tryptonse Soya Agar, at a concentration of 100 mg L^{-1}. Before the substrates were added, the agars were sterilised by autoclaving at 121 °C for 15 minutes. Thirty-seven different strains of bacteria were inoculated from the stock culture media into Nutrient Broth, and were grown overnight at 37 °C. The cultured bacteria were diluted in a saline solution to an approximate concentration of 1.5 x 10^7 CFU mL^{-1}. Subsquently, the bacteria were inoculated in chromogenic media and were incubated at 37 °C for up to 20 and 40 hours. Alongside with control plates without chromegenic substrates, the bacterial colonies formed colours.

4.4 Results and Discussion

4.4.1 Colour observation of dimerised chromophores in agar media

Tables 22a to **25d** provide the results that demonstrate the ability of the indoxyl glycosides to detect different bacterial strains and species. The six fluorinated derivatives and commercially available substrates normally produced colours of dark olive green for substrates **3a**, **3b**, **4a** and **4b**, midnight blue for substrates **3c** and **2c,** blue-geen for 5-Br-4-Cl-β-D-gal **1a** and 5-Br-4-Cl-β-D-gluc **2a** and rouge for 6-F-β-D-gal **1f**. The colour variation relative to their respective chromogen can be influenced by the colour of agar, the colour of bacterial colony or a reaction between the constituents of an agar and the hydrolysed indoxyl compounds.

4.4.2 General observations of indoxyl β-glycosides in agar media

When analysing the data in **Tables 22a-25d**, a focus was placed on identifying bacteria that could be better identified using the fluorinated indoxyl glycosides, compared with the current commercially available indoxyl glycosides. The number of Gram-negative bacteria that gave colouration was almost the same when the organisms were cultured in NA and TSA. However, the number of Gram-positive bacteria that hydrolysed the substrates was greater in TSA than NA (**Tables 22**-**25, a** and **b**). For example, most of *Staphylococcus* and *Enterococcus* species hydrolysed more substrates in TSA than NA. TSA mainly consists of pancreatic digest of casein, which is rich in amino acids and other nitrogenous substances (**Chapter 6**, **Table 32**). This constituent perhaps facilitated the hydrolysis of the substrates in TSA.

Table 22a. Evaluation of indoxyl β-galactosides in NA against several Gram-positive microorganisms for 20 hours at 37 °C

Microorganisms	References	Commercially Available Substrates		Synthesised Substrates		
Gram-positive	**OCC no.**	**5-Br, 4-Cl 1a**	**6-F 1f**	**5-F 3a**	**5,6-F 3b**	**6-CF_3 3c**
Bacillus cereus	754	-	-	-	-	-
Bacillus licheniformis	922	+ Blue green	-	-	± Olive green	++ Grey
Bacillus subtilis	214	-	-	-	-	-
Enterococcus faecalis	501	-	-	-	-	-
Enterococcus faecalis	640	± Blue green	-	-	-	-
Enterococcus faecium	220	± Blue green	-	-	Tr Olive green	Tr Midnight blue
Staphylococcus aureus	198	-	-	-	-	-
Staphylococcus aureus	638	-	-	-	-	-
Staphylococcus aureus v. oxford	100	-	-	-	-	-
Staphylococcus epidermis	919	-	-	-	-	-
Staphylococcus haemolyticus	2223f	-	-	-	-	-
Staphylococcus saprophyticus	2079	++ Blue green	± Pink	-	++ Olive green	+ Midnight Blue
Streptococcus agalactiae GBS	762	-	-	-	-	± Midnight Blue
Streptococcus pneumoniae	1548	-	-	-	-	-
Streptococcus pyogenes	624	-	-	-	-	-
Streptococcus viridans	1683	-	-	-	-	-

Amount of colouration by eye: Strong, ++; Moderate, +; Weak, ± ; Trace, Tr; and, No colouration, - .

Table 22b. Evaluation of indoxyl β-galactosides in NA against several Gram-positive microorganisms for 40 hours at 37 °C

Microorganisms	**References**	**Commercially Available Substrates**		**Synthesised Substrates**		
Gram-positive	**OCC no.**	**5-Br, 4-Cl 1a**	**6-F 1f**	**5-F 3a**	**5,6-F 3b**	**6-CF_3 3c**
Bacillus cereus	754	-	-	-	-	-
Bacillus licheniformis	922	++ Blue green	++ Rouge	+ Blue	++ Olive gree	++ Grey
Bacillus subtilis	214	-	-	-	-	-
Enterococcus faecalis	501	-	-	-	-	-
Enterococcus faecalis	640	+ Blue green	-	-	-	-
Enterococcus faecium	220	+ Blue green	-	-	± Olive green	± Midnight blue
Staphylococcus aureus	198	-	-	-	Tr Olive green	-
Staphylococcus aureus	638	-	-	-	-	-
Staphylococcus aureus v. oxford	100	-	-	-	-	-
Staphylococcus epidermis	919	-	-	-	-	-
Staphylococcus haemolyticus	2223f	-	-	-	Tr Olive green	-
Staphylococcus saprophyticus	2079	++ Blue green	+ Rouge	-	++ Olive green	++ Midnight blue
Streptococcus agalactiae GBS	762	-	-	-	-	+ Midnight blue
Streptococcus pneumoniae	1548	-	-	-	-	-
Streptococcus pyogenes	624	-	-	-	-	-
Streptococcus viridans	1683	-	-	-	-	-

Table 22c. Evaluation of indoxyl β-galactosides in NA against several Gram-negative microorganisms for 20 hours at 37 °C.

Microorganisms	References	Commercially Available Substrates		Synthesised Substrates		
Gram-negative	**OCC no.**	**5-Br, 4-Cl 1a**	**6-F 1f**	**5-F 3a**	**5,6-F 3b**	**6-CF_3 3c**
Burkholderia cepacia	770	-	-	-	-	-
Citrobacter freundii	370	+ Blue green	+ Rouge	+ Olive green	+ Olive green	++ Midnight blue
Citrobacter freundii	851	++ Green	-	+ Olive green	++ Olive green	+ Blue
Cronobacter sakazakii	1888	++ Green	+ Rouge	++ Olive green	++ Olive green	++ Grey
Enterobacter aerogenes	720	++ Green	+ Rouge	++ Olive green	++ Olive green	++ Grey
Enterobacter cloacae	760	++ Green	+ Rouge	++ Olive green	++ Olive green	++ Blue
Escherichia coli	402	+ Green	++ Rouge	++ Olive green	++ Olive green	+Black
Escherichia coli	199	+ Blue green	++ Rouge	++ Dark blue	++ Olive green	+ Black
Escherichia coli	481	++ Green	++ Rouge	++ Dark blue	++ Olive green	++ Black
Escherichia hermanii	1892	++ Green	++ Rouge	± Olive green	++ Olive green	+ Black
Klebsiella pneumoniae	411	++ Green	+ Rouge	++ Olive green	++ Olive green	++ Grey
Klebsiella pneumoniae	758	++ Green	+ Rouge	++ Olive green	++ Olive green	++ Grey
Pseudomonas aeruginosa	201	-	-	-	-	-
Pseudomonas aeruginosa	1119	-	-	-	-	-
Salmonella Abony	1919	-	-	-	-	-
Salmonella Dublin	627	-	-	-	-	-
Salmonella Enteritidis	723	-	-	-	-	-
Salmonella Typhimurium	722	-	-	-	-	-
Salmonella Typhimurium	853	-	-	-	-	-
Salmonella Virchow	703	-	-	-	-	-
Serratia marcescens	217	+ Green	Uncertain*	+ Olive green	Tr Olive green	-

Comment: Uncertain* means natural red pigmentation more prominent than rouge colour.

Table 22d. Evaluation of indoxyl β-galactosides in NA against several Gram-negative microorganisms for 40 hours at 37 °C.

Microorganisms	References	Commercially Available Substrates		Synthesised Substrates		
Gram-negative	**OCC no.**	**5-Br, 4-Cl 1a**	**6-F 1f**	**5-F 3a**	**5,6-F 3b**	**6-CF_3 3c**
Burkholderia cepacia	770	-	-	-	-	-
Citrobacter freundii	370	++ Blue green	++ Rouge	+ Olive green	++ Olive green	++ Midnight Blue
Citrobacter freundii	851	++ Green	++ Rouge	+ Olive green	++ Olive green	++ Midnight Blue
Cronobacter sakazakii	1888	++ Green	+ Rouge	++ Olive green	++ Olive green	++ Grey
Enterobacter aerogenes	720	++ Green	+ Rouge	++ Olive green	++ Olive green	++ Grey
Enterobacter cloacae	760	++ Green	+ Rouge	++ Olive green	++ Olive green	++ Blue
Escherichia coli	402	++ Green	++ Rouge	++ Olive green	++ Olive green	+ Black
Escherichia coli	199	++ Green	++ Rouge	++ Dark blue	++ Olive green	+ Black
Escherichia coli	481	++ Green	++ Rouge	++ Olive green	++ Olive green	++ Black
Escherichia hermanii	1892	++ Green	++ Rouge	++ Olive green	++ Olive green	+ Black
Klebsiella pneumoniae	411	++ Green	+ Rouge	++ Olive green	++ Olive green	++ Grey
Klebsiella pneumoniae	758	++ Green	+ Rouge	++ Olive green	++ Olive green	++ Grey
Pseudomonas aeruginosa	201	-	-	-	-	-
Pseudomonas aeruginosa	1119	-	-	-	-	-
Salmonella Abony	1919	-	-	-	-	-
Salmonella Dublin	627	-	-	-	-	-
Salmonella Enteritidis	723	-	-	-	-	-
Salmonella Typhimurium	722	-	-	-	-	-
Salmonella Typhimurium	853	-	-	-	-	-
Salmonella Virchow	703	-	-	-	-	-
Serratia marcescens	217	+ Green	Uncertain*	+ Brown	Tr Olive green	Tr Midnight blue

Table 23a. Evaluation of indoxyl β-galactosides in TSA against several Gram-positive microorganisms for 20 hours at 37 °C.

Microorganisms	**References**	**Commercially Available Substrates**		**Synthesised Substrates**		
Gram-positive	**OCC no.**	**5-Br, 4-Cl 1a**	**6-F 1f**	**5-F 3a**	**5,6-F 3b**	**6-CF_3 3c**
Bacillus cereus	754	-	-	-	-	-
Bacillus licheniformis	922	++ Blue green	+ Rouge	-	+ Olive green	-
Bacillus subtilis	214	-	-	-	-	-
Enterococcus faecalis	501	-	-	+ Olive green	+ Olive green	-
Enterococcus faecalis	640	+ Blue green	-	-	-	± Midnight blue
Enterococcus faecium	220	++ Blue green	+ Rouge	++ Olive green	++ Olive green	++ Midnight blue
Staphylococcus aureus	198	-	-	-	++ Grey	-
Staphylococcus aureus	638	-	-	++ Olive green	++ Olive green	-
Staphylococcus aureus v. oxford	100	-	-	++ Blue green	++ Olive green	-
Staphylococcus epidermis	919	-	-	+ Blue green	++ Grey	-
Staphylococcus haemolyticus	2223f	± Green	-	++ Blue green	++ Grey	± Grey
Staphylococcus saprophyticus	2079	++ Blue green	++ Rouge	++ Blue green	++ Grey	++ Midnight blue
Streptococcus agalactiae GBS	762	-	-	-	± Olive green	-
Streptococcus pneumoniae	1548	-	-	-	-	-
Streptococcus pyogenes	624	-	-	-	-	-
Streptococcus viridans	1683	-	-	-	-	-

Table 23b. Evaluation of indoxyl β-galactosides in TSA against several Gram-postive microorganisms for 40 hours at 37 °C.

Microorganisms	**References**	**Commercially Available Substrates**		**Synthesised Substrates**		
Gram-positive	**OCC no.**	**5-Br, 4-Cl 1a**	**6-F 1f**	**5-F 3a**	**5,6-F 3b**	**6-CF_3 3c**
Bacillus cereus	754	-	-	-	-	-
Bacillus licheniformis	922	++ Blue green	+ Rouge	-	++ Olive green	-
Bacillus subtilis	214	-	-	-	-	-
Enterococcus faecalis	501	-	-	+ Olive green	++Olive green	-
Enterococcus faecalis	640	+ Blue green	-	-	-	+ Midnight blue
Enterococcus faecium	220	++ Blue green	++ Rouge	++ Olive green	++ Olive green	++ Midnight blue
Staphylococcus aureus	198	-	-	-	++ Grey	-
Staphylococcus aureus	638	-	-	++ Olive green	++ OG	-
Staphylococcus aureus v. oxford	100	-	-	++ Blue green	++ OG	-
Staphylococcus epidermis	919	-	-	++ Blue green	++ Grey	-
Staphylococcus haemolyticus	2223f	++ Green	-	+ Blue green	++ Grey	+ Grey
Staphylococcus saprophyticus	2079	++ Blue green	++ Rouge	++ Blue green	++ Grey	++ Midnight blue
Streptococcus agalactiae GBS	762	-	-	-	+ Olive green	-
Streptococcus pneumoniae	1548	-	-	-	-	-
Streptococcus pyogenes	624	-	-	-	-	-
Streptococcus viridans	1683	-	-	-	-	-

Table 23c. Evaluation of indoxyl β-galactosides in TSA against several Gram-negative microorganisms for 20 hours at 37 °C.

Microorganisms	References	Commercially Available Substrates		Synthesised Substrates		
Gram-negative	**OCC no.**	**4-Cl, 5-Br 1a**	**6-F 1f**	**5-F 3a**	**5,6-F 3b**	**6-CF_3 3c**
Burkholderia cepacia	770	-	-	-	-	-
Citrobacter freundii	370	++ Green	++ Rouge	++ Olive green	++ Olive green	++ Midnight blue
Citrobacter freundii	851	++ Green	+ Rouge	++ Olive green	++ Olive green	++ Grey
Cronobacter sakazakii	1888	++ Green	++ Rouge	++ Olive green	++ Olive green	++ Grey
Enterobacter aerogenes	720	++ Green	++ Rouge	++ Olive green	++ Olive green	++ Blue
Enterobacter cloacae	760	++ Green	++ Rouge	++ Olive green	++ Olive green	++ Grey
Escherichia coli	402	++ Green	++ Rouge	++ Olive green	++ Olive green	++ Grey
Escherichia coli	199	++ Green	++ Rouge	++ Olive green	++ Olive green	++ Grey
Escherichia coli	481	++ Green	++ Rouge	++ Olive green	++ Olive green	++ Blue
Escherichia hermanii	1892	++ Green	++ Rouge	++ Olive green	+ Olive green	++ Grey
Klebsiella pneumoniae	411	++ Green	++ Rouge	++ Olive green	++ Olive green	++ Black
Klebsiella pneumoniae	758	++ Green	++ Rouge	++ Olive green	+ Grey	++ Black
Pseudomonas aeruginosa	201	-	-	-	-	-
Pseudomonas aeruginosa	1119	-	-	-	-	-
Salmonella Abony	1919	-	-	-	-	-
Salmonella Dublin	627	-	-	-	-	-
Salmonella Enteritidis	723	-	-	-	-	-
Salmonella Typhimurium	722	-	-	-	-	-
Salmonella Typhimurium	853	-	-	-	-	-
Salmonella Virchow	703	-	-	-	-	-
Serratia marcescens	217	+ Green	Uncertain*	Tr Olive green	Tr Olive green	Tr Grey

Table 23d. Evaluation of indoxyl β-galactosides in TSA against several Gram-negative microorganisms for 20 hours at 37 °C.

Microorganisms	**References**	**Commercially Available Substrates**		**Synthesised Substrates**		
Gram-negative	**OCC no.**	**5-Br, 4-Cl 1a**	**6-F 1f**	**5-F 3a**	**5,6-F 3b**	**6-CF_3 3c**
Burkholderia cepacia	770	-	-	-	-	-
Citrobacter freundii	370	++ Green	++ Rouge	++ Olive green	++ Olive green	++ Midnight blue
Citrobacter freundii	851	++ Green	++ Rouge	++ Olive green	++ Olive green	++ Grey
Cronobacter sakazakii	1888	++ Green	++ Rouge	++ Olive green	++ Olive green	++ Grey
Enterobacter aerogenes	720	++ Green	++ Rouge	++ Olive green	++ Olive green	++ Grey
Enterobacter cloacae	760	++ Green	++ Rouge	++ Olive green	++ Olive green	++ Midnight Blue
Escherichia coli	402	++ Green	++ Rouge	++ Olive green	++ Olive green	++ Grey
Escherichia coli	199	++ Green	++ Rouge	++ Olive green	++ Olive green	++ Grey
Escherichia coli	481	++ Green	++ Rouge	++ Olive green	++ Olive green	++ Blue
Escherichia hermanii	1892	++ Green	++ Rouge	++ Olive green	++ Olive green	++ Grey
Klebsiella pneumoniae	411	++ Green	++ Rouge	++ Grey	++ Olive green	++ Black
Klebsiella pneumoniae	758	++ Green	++ Rouge	++ Grey	++ Grey	++ Black
Pseudomonas aeruginosa	201	-	-	-	-	-
Pseudomonas aeruginosa	1119	-	-	-	-	-
Salmonella Abony	1919	-	-	-	-	-
Salmonella Dublin	627	-	-	-	-	-
Salmonella Enteritidis	723	-	-	-	-	-
Salmonella Typhimurium	722	-	-	-	-	-
Salmonella Typhimurium	853	-	-	-	-	-
Salmonella Virchow	703	-	-	-	-	-
Serratia marcescens	217	+ Green	Uncertain*	Tr Olive green	Tr Olive green	Tr Midnight blue

Table 24a. Evaluation of indoxyl β-glucosides in NA several Gram-positive microorganisms for 20 hours at 37 °C.

Microorganisms	References	Commercially Available Substrate	Synthesised Substrates		
Gram-positive	**OCC no.**	**5-Br, 4-Cl 2a**	**6-F 4a**	**5,6-F 4b**	**6-CF_3 4c**
Bacillus cereus	754	+ Green	-	± OG	++ Grey
Bacillus licheniformis	922	++ Blue-green	++ Olive green	++ Olive green	++ Midnight blue
Bacillus subtilis	214	++ Blue-green	++ Olive green	++ Olive green	++ Midnight blue
Enterococcus faecalis	501	++ Blue-green	++ Olive green	++ Olive green	++ Midnight blue
Enterococcus faecalis	640	++ Blue-green	++ Olive green	++ Olive green	++ Midnight blue
Enterococcus faecium	220	++ Blue-green	++ Olive green	++ Olive green	++ Midnight blue
Staphylococcus aureus	198	-	Tr Olive green	Tr Olive green	Tr Midnight blue
Staphylococcus aureus	638	-	-	-	-
Staphylococcus aureus v. oxford	100	-	+ Olive green	-	-
Staphylococcus epidermis	919	-	-	-	-
Staphylococcus haemolyticus	2223f	-	-	-	-
Staphylococcus saprophyticus	2079	-	-	-	-
Streptococcus agalactiae GBS	762	-	± Olive green	++ Olive green	-
Streptococcus pneumoniae	1548	-	-	-	-
Streptococcus pyogenes	624	+ Blue-green	± Olive green	+ Olive green	-
Streptococcus viridans	1683	+ Blue-green	± Olive green	+ Olive green	+ Midnight blue

Table 24b. Evaluation of indoxyl β-glucosides in NA several Gram-positive microorganisms for 40 hours at 37 °C.

Microorganisms	**References**	**Commercially Available Substrate**	**Synthesised Substrates**		
Gram-positive	**OCC no.**	**5-Br, 4-Cl 2a**	**6-F 4a**	**5,6-F 4b**	**6-CF_3 4c**
Bacillus cereus	754	+ Green	Tr Olive green	± Olive green	++ Grey
Bacillus licheniformis	922	++ Blue-green	++ Olive green	++ Olive green	++ Blue
Bacillus subtilis	214	++ Blue-green	++ Olive green	++ Olive green	++ Midnight blue
Enterococcus faecalis	501	++ Blue-green	++ Olive green	++ Olive green	++ Midnight blue
Enterococcus faecalis	640	++ Blue-green	++ Olive green	++ Olive green	++ Midnight blue
Enterococcus faecium	220	++ Blue-green	++ Olive green	++ Olive green	++ Midnight blue
Staphylococcus aureus	198	-	Tr Olive green	Tr Olive green	Tr Midnight blue
Staphylococcus aureus	638	-	-	-	-
Staphylococcus aureus v. oxford	100	-	+ Olive green	-	-
Staphylococcus epidermis	919	-	-	-	-
Staphylococcus haemolyticus	2223f	-	-	-	-
Staphylococcus saprophyticus	2079	-	-	-	-
Streptococcus agalactiae GBS	762	-	± Olive green	++ Olive green	-
Streptococcus pneumoniae	1548	-	-	-	-
Streptococcus pyogenes	624	++ Blue-green	+ Olive green	+ Olive green	-
Streptococcus viridans	1683	++ Blue-green	+ Olive green	+ Olive green	+ Midnight blue

Table 24c. Evaluation of indoxyl β-glucosides in NA several Gram-negative microorganisms for 20 hours at 37 °C.

Microorganisms	References	Commercially Available Substrates	Synthesised Substrates		
Gram-negative	**OCC no.**	**5-Br, 4-Cl 2a**	**6-F 4a**	**5,6-F 4b**	**6-CF_3 4c**
Burkholderia cepacia	770	Tr Blue-green	-	Tr Blue	Tr Grey
Citrobacter freundii	370	+ Green	++ Olive green	++ Olive green	++ Grey
Citrobacter freundii	851	± Green	++ Olive green	++ Olive green	++ Grey
Cronobacter sakazakii	1888	++ Green	++ Olive green	++ Olive green	++ Grey
Enterobacter aerogenes	720	++ Green	++ Olive green	++ Olive green	++ Grey
Enterobacter cloacae	760	++ Green	++ Olive green	++ Olive green	+ Grey
Escherichia coli	402	-	-	± Olive green	-
Escherichia coli	199	-	-	± Olive green	-
Escherichia coli	481	-	-	± Olive green	-
Escherichia hermanii	1892	-	++ Olive green	++ Olive green	++ Grey
Klebsiella pneumoniae	411	++ Green	++ Olive green	++ Olive green	++ Black
Klebsiella pneumoniae	758	++ Green	++ Olive green	++ Olive green	++ Black
Pseudomonas aeruginosa	201	-	-	-	-
Pseudomonas aeruginosa	1119	-	-	-	-
Salmonella Abony	1919	-	-	-	-
Salmonella Dublin	627	-	-	-	-
Salmonella Enteritidis	723	-	-	-	-
Salmonella Typhimurium	722	-	-	-	-
Salmonella Typhimurium	853	-	-	-	-
Salmonella Virchow	703	-	-	-	-
Serratia marcescens	217	+ Green	Tr Olive green	Tr Olive green	Tr Midnight blue

Table 24d. Evaluation of indoxyl β-glucosides in NA several Gram-negative microorganisms for 40 hours at 37 °C.

Microorganisms	References	Commercially Available Substrates	Synthesised Substrates		
Gram-negative	**OCC no.**	**5-Br, 4-Cl 2a**	**6-F 4a**	**5,6-F 4b**	**6-CF_3 4c**
Burkholderia cepacia	770	± Blue-green	Tr Olive green	± Olive green	+ Grey
Citrobacter freundii	370	++ Green	++ Olive green	± Olive green	++ Grey
Citrobacter freundii	851	+ Green	++ Olive green	++ Olive green	++ Grey
Cronobacter sakazakii	1888	++ Green	++ Olive green	++ Olive green	++ Grey
Enterobacter aerogenes	720	++ Green	++ Olive green	++ Olive green	++ Grey
Enterobacter cloacae	760	++ Green	++ Olive green	++ Olive green	+ Grey
Escherichia coli	402	-	+ Olive green	Olive green	-
Escherichia coli	199	-	+ Olive green	+ Olive green	-
Escherichia coli	481	-	+ Olive green	+ Olive green	-
Escherichia hermanii	1892	± Green	++ Olive green	++ Olive green	++ Grey
Klebsiella pneumoniae	411	++ Green	++ Olive green	++ Olive green	++ Grey
Klebsiella pneumoniae	758	++ Green	++ Olive green	++ Olive green	++ Grey
Pseudomonas aeruginosa	201	-	-	-	-
Pseudomonas aeruginosa	1119	-	-	-	-
Salmonella Abony	1919	-	-	-	-
Salmonella Dublin	627	-	-	-	-
Salmonella Enteritidis	723	-	-	-	-
Salmonella Typhimurium	722	-	-	-	-
Salmonella Typhimurium	853	-	-	-	-
Salmonella Virchow	703	-	-	-	-
Serratia marcescens	217	+ Green	Tr Olive green	Tr Olive green	Tr Midnight blue

Table 25a. Evaluation of indoxyl β-glucosides in TSA several Gram-positive microorganisms for 20 hours at 37 °C.

Microorganisms	**References**	**Commercially Available Substrate**	**Synthesised Substrates**		
Gram-positive	**OCC no.**	**5-Br, 4-Cl 2a**	**6-F 4a**	**5,6-F 4b**	**6-CF_3 4c**
Bacillus cereus	754	+ Green	-	± Olive green	± Grey
Bacillus licheniformis	922	++ Blue-green	++ Olive green	++ Olive green	++ Midnight blue
Bacillus subtilis	214	++ Blue-green	++ Olive green	++ Olive green	++ Midnight blue
Enterococcus faecalis	501	++ Blue-green	++ Olive green	++ Olive green	++ Midnight blue
Enterococcus faecalis	640	++ Blue-green	++ Olive green	++ Olive green	++ Midnight blue
Enterococcus faecium	220	++ Blue-green	++ Olive green	++ Olive green	++ Midnight blue
Staphylococcus aureus	198	-	-	+ Olive green	-
Staphylococcus aureus	638	-	-	-	-
Staphylococcus aureus v. oxford	100	-	+ Olive green	-	-
Staphylococcus epidermis	919	-	-	-	-
Staphylococcus haemolyticus	2223f	-	-	-	-
Staphylococcus saprophyticus	2079	-	-	-	-
Streptococcus agalactiae GBS	762	-	-	++ Olive green	-
Streptococcus pneumoniae	1548	-	-	-	-
Streptococcus pyogenes	624	± Blue-green	++ Olive green	+ Olive green	-
Streptococcus viridans	1683	+ Blue-green	++ Olive green	+ Olive green	+ Midnight blue

Table 25b. Evaluation of indoxyl β-glucosides in TSA several Gram-positive microorganisms for 40 hours at 37 °C.

Microorganisms	**References**	**Commercially Available Substrate**	**Synthesised Substrates**		
Gram-positive	**OCC no.**	**5-Br, 4-Cl 2c**	**6-F 4a**	**5,6-F 4b**	**6-CF_3 4c**
Bacillus cereus	754	+ Green	-	± Olive green	+ Grey
Bacillus licheniformis	922	++ Blue-green	++ Olive green	++ Olive green	++ Midnight blue
Bacillus subtilis	214	++ Blue-green	++ Olive green	++ Olive green	++ Midnight blue
Enterococcus faecalis	501	++ Blue-green	++ Olive green	++ Olive green	++ Midnight blue
Enterococcus faecalis	640	++ Blue-green	++ Olive green	++ Olive green	++ Midnight blue
Enterococcus faecium	220	++ Blue-green	++ Olive green	++ Olive green	++ Midnight blue
Staphylococcus aureus	198	-	-	++ Olive green	Tr Midnight blue
Staphylococcus aureus	638	-	-	-	-
Staphylococcus aureus v. oxford	100	-	+ Olive green	+ Olive green	-
Staphylococcus epidermis	919	-	-	-	-
Staphylococcus haemolyticus	2223f	-	-	++ Grey	-
Staphylococcus saprophyticus	2079	-	-	-	-
Streptococcus agalactiae GBS	762	Tr Blue-green	-	++ Olive green	Tr Midnight blue
Streptococcus pneumoniae	1548	-	-	-	-
Streptococcus pyogenes	624	++ Blue-green	++ Olive green	+ Olive green	Tr Midnight blue
Streptococcus viridans	1683	++ Blue-green	++ Olive green	+ Olive green	+ Midnight blue

Table 25c. Evaluation of indoxyl β-glucosides in TSA several Gram-negative microorganisms for 20 hours at 37 °C.

Microorganisms	References	Commercially Available Substrates	Synthesised Substrates		
Gram-negative	**OCC no.**	**5-Br, 4-Cl 2a**	**6-F 4a**	**5,6-F 4b**	**6-CF_3 4c**
Burkholderia cepacia	770	-	-	-	-
Citrobacter freundii	370	± Green	++ Olive green	++ Olive green	± Grey
Citrobacter freundii	851	-	++ Olive green	++ Olive green	± Grey
Cronobacter sakazakii	1888	++ Green	++ Olive green	++ Olive green	+ Grey
Enterobacter aerogenes	720	++ Green	++ Olive green	++ Olive green	++ Grey
Enterobacter cloacae	760	++ Green	++ Olive green	++ Olive green	± Grey
Escherichia coli	402	-	+ Olive green	± Olive green	-
Escherichia coli	199	-	+ Olive green	± Olive green	-
Escherichia coli	481	-	+ Olive green	± Olive green	-
Escherichia hermanii	1892	-	++ Olive green	++ Olive green	+ Grey
Klebsiella pneumoniae	411	++ Green	++ Olive green	++ Olive green	++ Grey
Klebsiella pneumoniae	758	++ Green	++ Olive green	++ Olive green	++ Grey
Pseudomonas aeruginosa	201	-	-	-	-
Pseudomonas aeruginosa	1119	-	-	-	-
Salmonella Abony	1919	-	-	-	-
Salmonella Dublin	627	-	-	-	-
Salmonella Enteritidis	723	-	-	-	-
Salmonella Typhimurium	722	-	-	-	-
Salmonella Typhimurium	853	-	-	-	-
Salmonella Virchow	703	-	-	-	-
Serratia marcescens	217	Tr Green	+ Olive green	Tr Olive green	Tr Midnight blue

Table 25d. Evaluation of indoxyl β-glucosides in TSA several Gram-negative microorganisms for 40 hours at 37 °C.

Microorganisms	References	Commercially Available Substrates	Synthesised Substrates		
Gram-negative	**OCC no.**	**5-Br, 4-Cl 2a**	**6-F 4a**	**5,6-F 4b**	**6-CF_3 4c**
Burkholderia cepacia	770	-	-	-	Tr Grey
Citrobacter freundii	370	± Green	++ Olive green	++ Olive green	+ Grey
Citrobacter freundii	851	-	++ Olive green	++ Olive green	+ Grey
Cronobacter sakazakii	1888	++ Green	++ Olive green	++ Brown	++ Brown
Enterobacter aerogenes	720	++ Green	++ Olive green	++ Olive green	++ Grey
Enterobacter cloacae	760	++ Green	++ Olive green	++ Olive green	+ Grey
Escherichia coli	402	-	+ Olive green	++ Brown	-
Escherichia coli	199	-	+ Olive green	++ Brown	-
Escherichia coli	481	-	+ Olive green	++ Brown	-
Escherichia hermanii	1892	-	++ Olive green	++ Olive green	++ Grey
Klebsiella pneumoniae	411	++ Green	++ Olive green	++ Olive green	++ Grey
Klebsiella pneumoniae	758	++ Green	++ Olive green	++ Olive green	++ Midnight blue Blue
Pseudomonas aeruginosa	201	-	-	-	-
Pseudomonas aeruginosa	1119	-	-	-	-
Salmonella Abony	1919	-	-	-	-
Salmonella Dublin	627	-	-	-	-
Salmonella Enteritidis	723	-	-	-	-
Salmonella Typhimurium	722	-	-	-	-
Salmonella Typhimurium	853	-	-	-	-
Salmonella Virchow	703	-	-	-	-
Serratia marcescens	217	+ Green	+ Olive green	Tr Olive green	Tr Midnight blue

4.4.3 The effect of prolong incubation of the chromogenic media

Incubating the media for up to 40 hours significantly improved the sensitivity of the chromogenic substrate. For example, no hydrolysis can be observed for substrates 5-F-β-D-gal **3a** and 6-F-β-D-gal **1f** in the presence of *Bacillus licheniformis* (OCC 922) when incubated for up to 20 hours. When the chromogenic media were incubated for up to 40 hours, colouration on the bacterial colonies can be observed (**Figure 43**). In this case, the two substrates exhibited slower hydrolysis when compared to other indoxyl β-galactosides (**Tables 22a-b**).

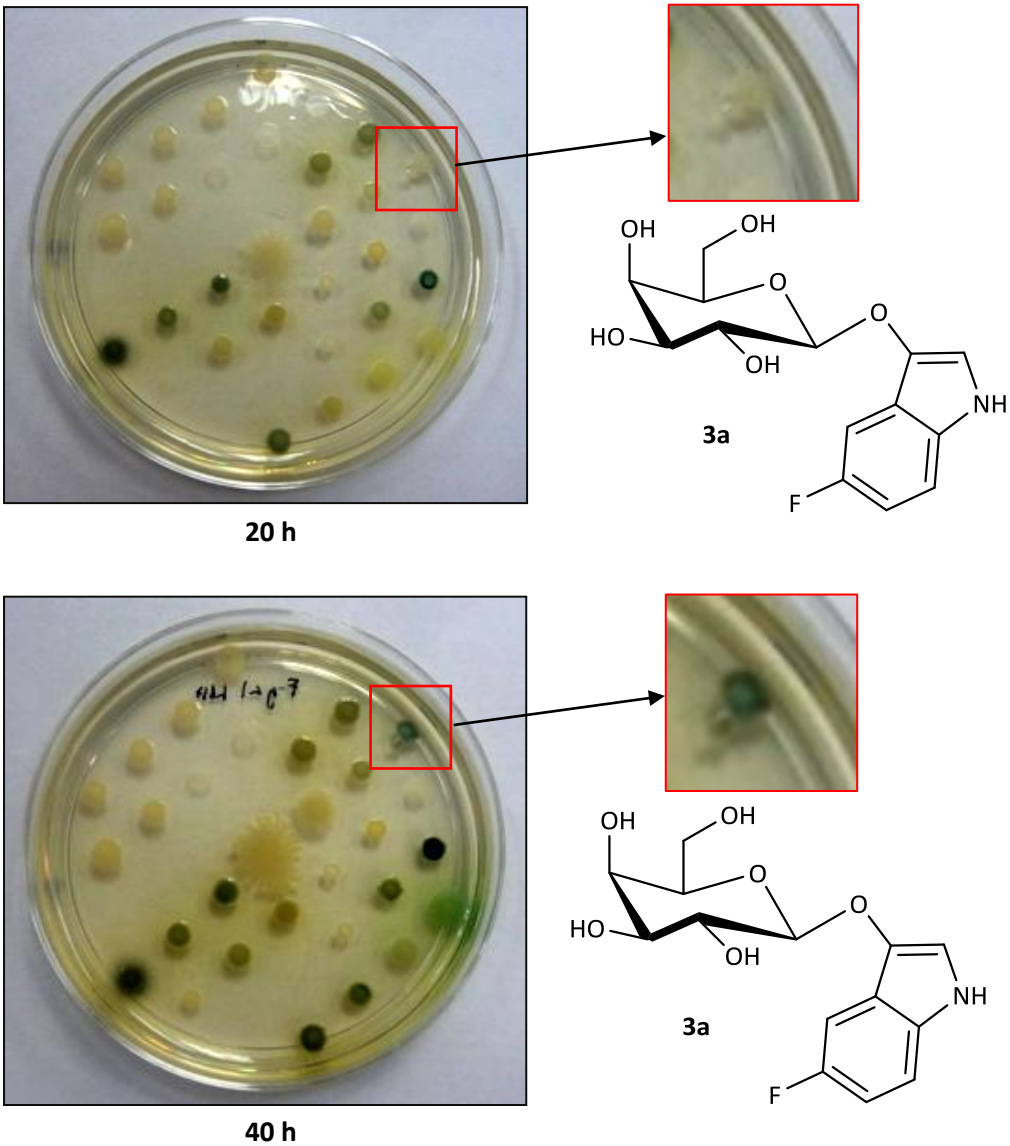

Figure 43. Hydrolysis of 5-fluoro-3-indolyl β-D-galactoside **3a** by *Bacillus licheniformis* (OCC 922) in NA for 20 and 40 hours.

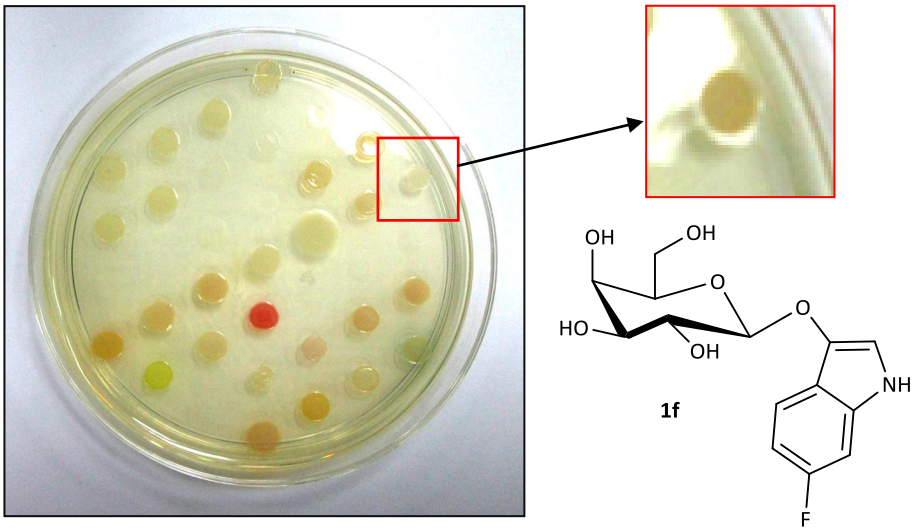

1f

20 h

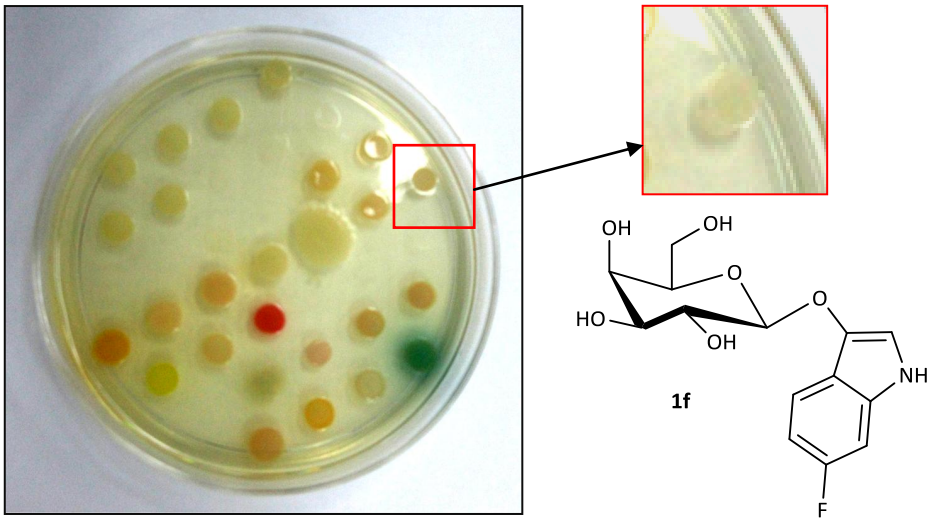

1f

40 h

Figure 43 (continued). Hydrolysis of 6-fluoro-3-indolyl β-D-galactoside **1f** by *Bacillus licheniformis* (OCC 922) in NA for 20 and 40 hours.

4.4.4 Differences in selectivities of indoxyl β-glycosides in agar media

Interestingly, substrates 5-F-β-D-gluc **4a** and 5,6-F-D-gluc 4**b** were hydrolysed by three strains of *E. coli* (OCC 402, 199 and 481) in TSA, whereas X-β-D-gluc **2a** was not. For *E. hermanii* (OCC 1892), all of the fluorinated indoxyl β-glucosides **4a**-**c** were hydrolysed in TSA (**Figure 44** and **Table 25c**). This can be explained by low level production of β-glucosidase enzyme in some *E. coli* strains.[134, 264, 265] This might imply that the mono- and di- fluoro

indoxyl β-D-glucosides **4a** and **4b**, and to an extent 6-(trifluoromethyl) indoxyl β-D-glucosides **4c**, were more sensitive substrates than the commercially available X-β-D-gluc due to better transport into the bacterial cells.

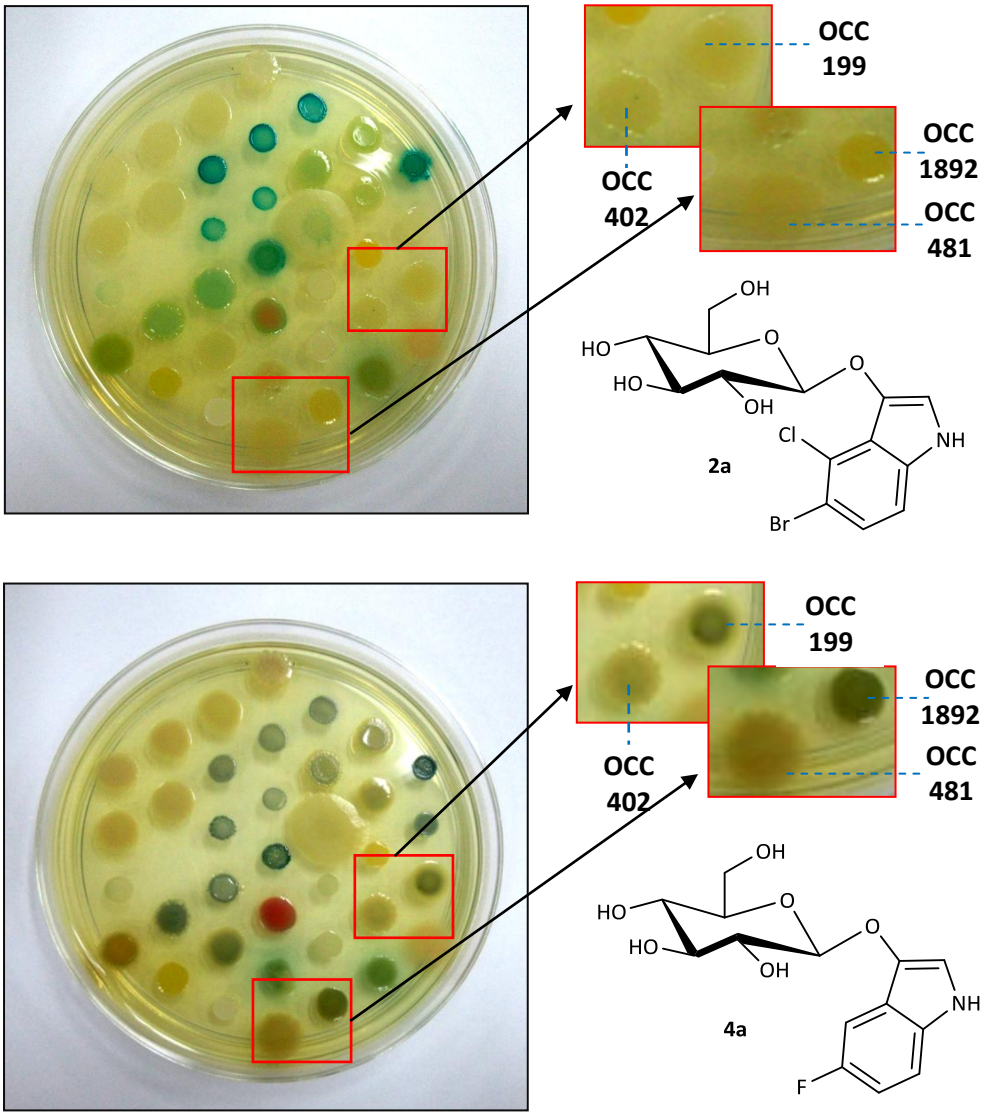

Figure 44. Comparison of indoxyl β-glucosides for the detection of *Escherichia* species in TSA for 40 hours. *E. coli* (OCC 402, 199 and 481) and *E. hermanii* (OCC 1892).

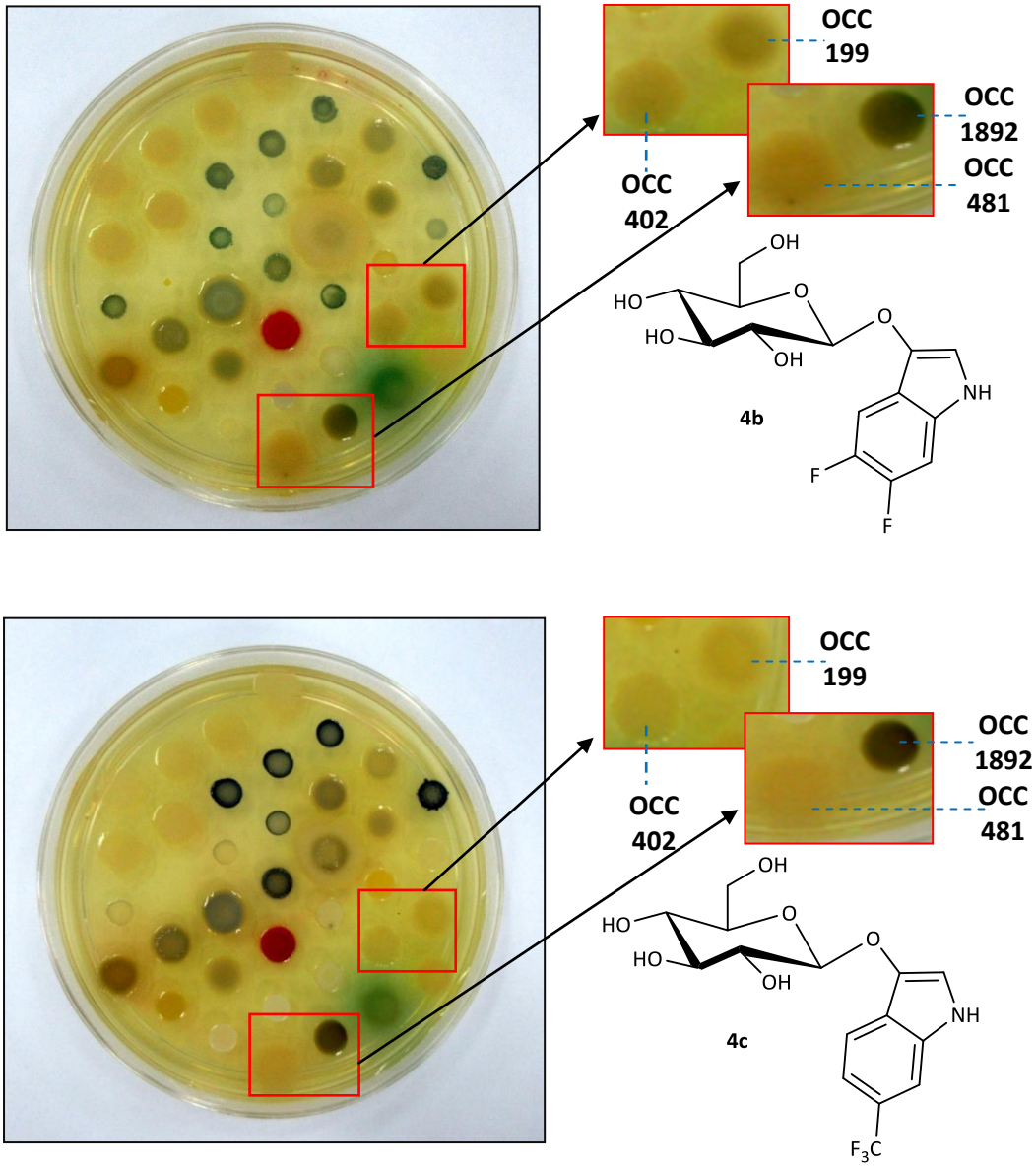

Figure 44 (continued). Comparison of indoxyl β-glucosides for the detection of *Escherichia* species in TSA for 40 hours. *E. coli* (OCC 402, 199 and 481) and *E. hermanii* (OCC 1892).

As shown in **Figure 45**, a number of *Staphylococcus* spp. (OCC 198, 638, 100, 919, 2223f and 2079) hydrolysed the mono- and di- fluoro indoxyl β-D-galactosides **3a** and **3b** in TSA. Substrate **3a** produced olive green and blue-green colours, whilst substrate **3b** produced olive green and grey colours. For substrates 6-CF_3-β-D-gal **3c** and X-β-D-gal **1a**, only *S. haemolyticus* (OCC 2223f) and *S. saprophyticus* (OCC 2079) were the only *Staphylococcus*

species that clearly hydrolysed the two substrates. *S. saprophyticus* was the only *Staphylococcus* species that was hydrolysed by substrate Rouge-β-D-gal **1f** (**Tables 23a-b**).

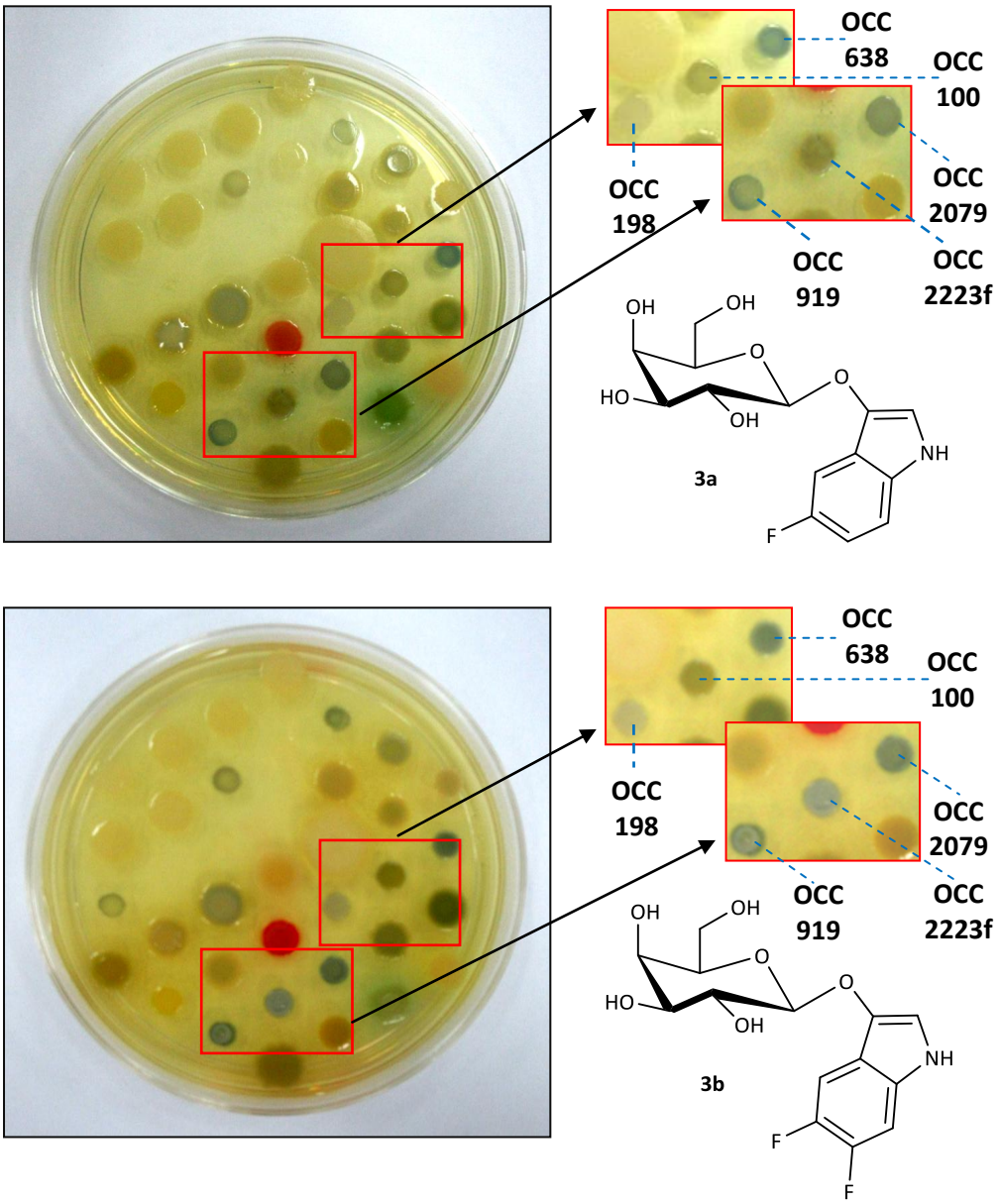

Figure 45. Comparison of indoxyl β-D-galactosides for the detection of *Staphylococcus* species in TSA for 40 hours. *S. aureus* (OCC 198 and 638); *S. aureus v oxford* (OCC 100); *S. epidermis* (OCC 919); *S. haemolylticus* (OCC 2223f); and, *S. saprophyticus* (OCC 2079).

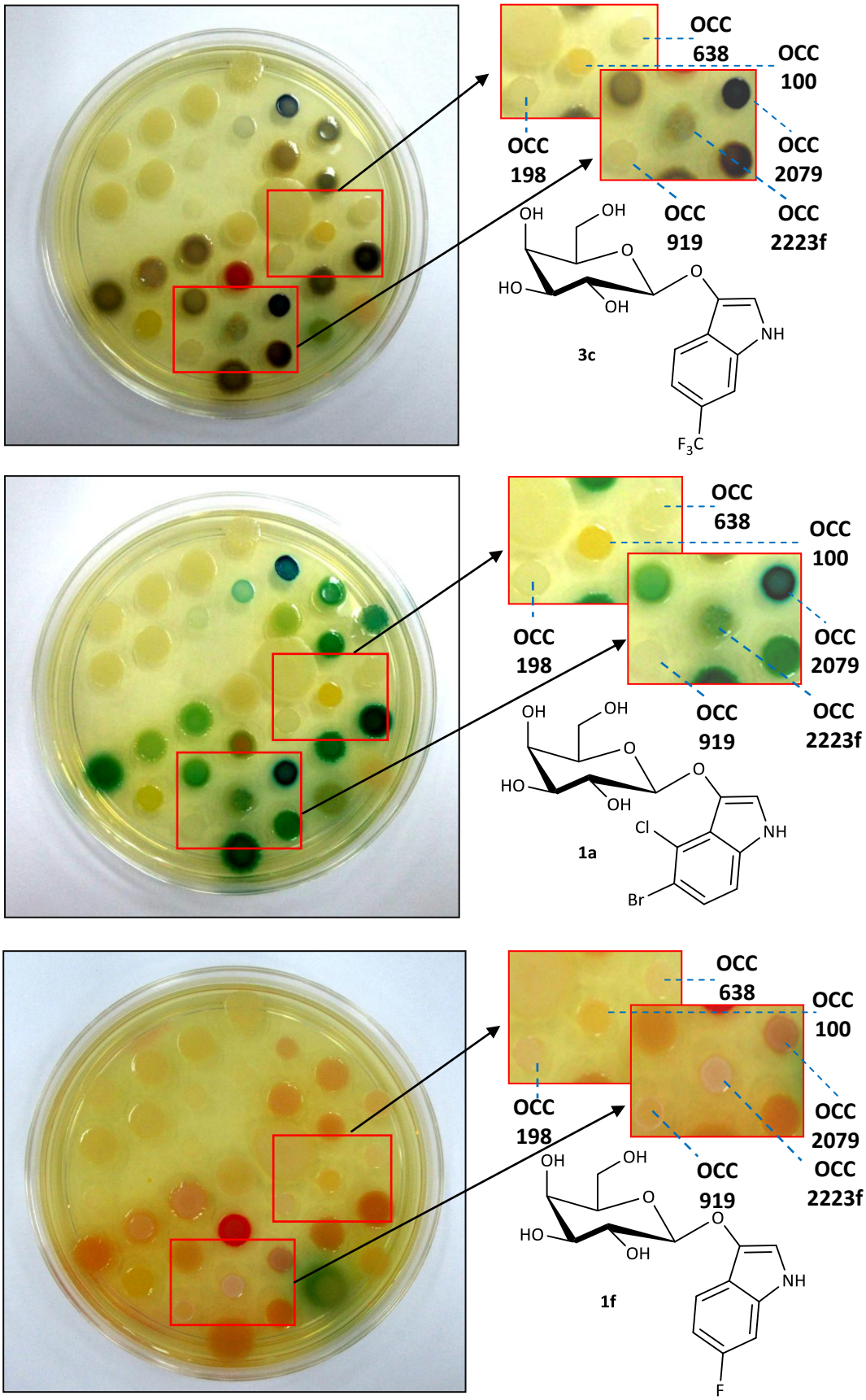

Figure 45 (cont). Comparison of indoxyl β-D-galactosides for the detection of *Staphylococcus* species in TSA for 40 hours. *S. aureus* (OCC 198, 638); *S. aureus v oxford* (OCC 100); *S. epidermis* (OCC 919); *S. haemolylticus* (OCC 2223f); and, *S. saprophyticus* (OCC 2079).

For bacteria that produce very bright natural pigments like *Serratia marcescens* (OCC 217) that possessed β-galactosidase and β-glucosidase enzymes, 5-bromo-4-chloro derivatives **1a** and **2a** were superior amongst the fluorinated β-D-galactosides in TSA and NA. For substrate **1f**, it was difficult to clearly visualise whether the substrate was hydrolysed or not by the bacterial strain, since the red pigmentation might overshadow the rouge dye. Under certain conditions when the microorganism did not produce the red pigment, a very weak colour of olive green was observed for substrate **3a**. In the absence of the red pigment, the fluorinated galactoside derivatives **3a-c** and **4a-c** would produce a stronger colouration on the microbial colonies (**Tables 22c-d**). Amongst the synthesised fluorinated substrates, 6-(trifluoromethyl) indoxyl β-galactoside **3c** provided very strong colouration that was easy to read on the agar plate. As a representative for the susbtrates used for the detection of *Serratia marcescens*, halogenated indoxyl β-galactosides in NA for 40 hours are provided in **Figure 46**.

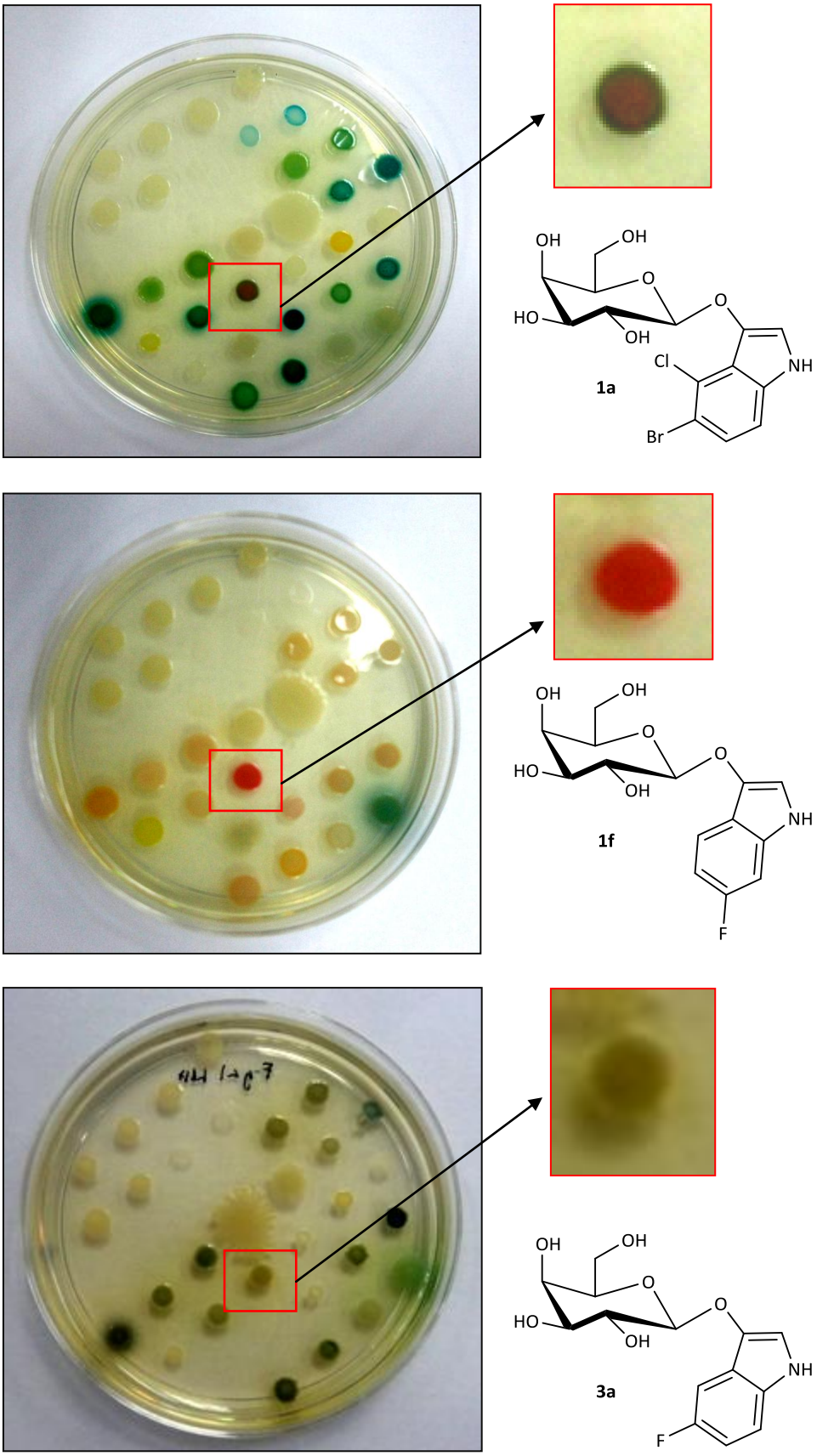

Figure 46. Detection of *Serratia marcescens* (OCC 217) using halogenated indoxyl β-galactosides in NA for 40 hours.

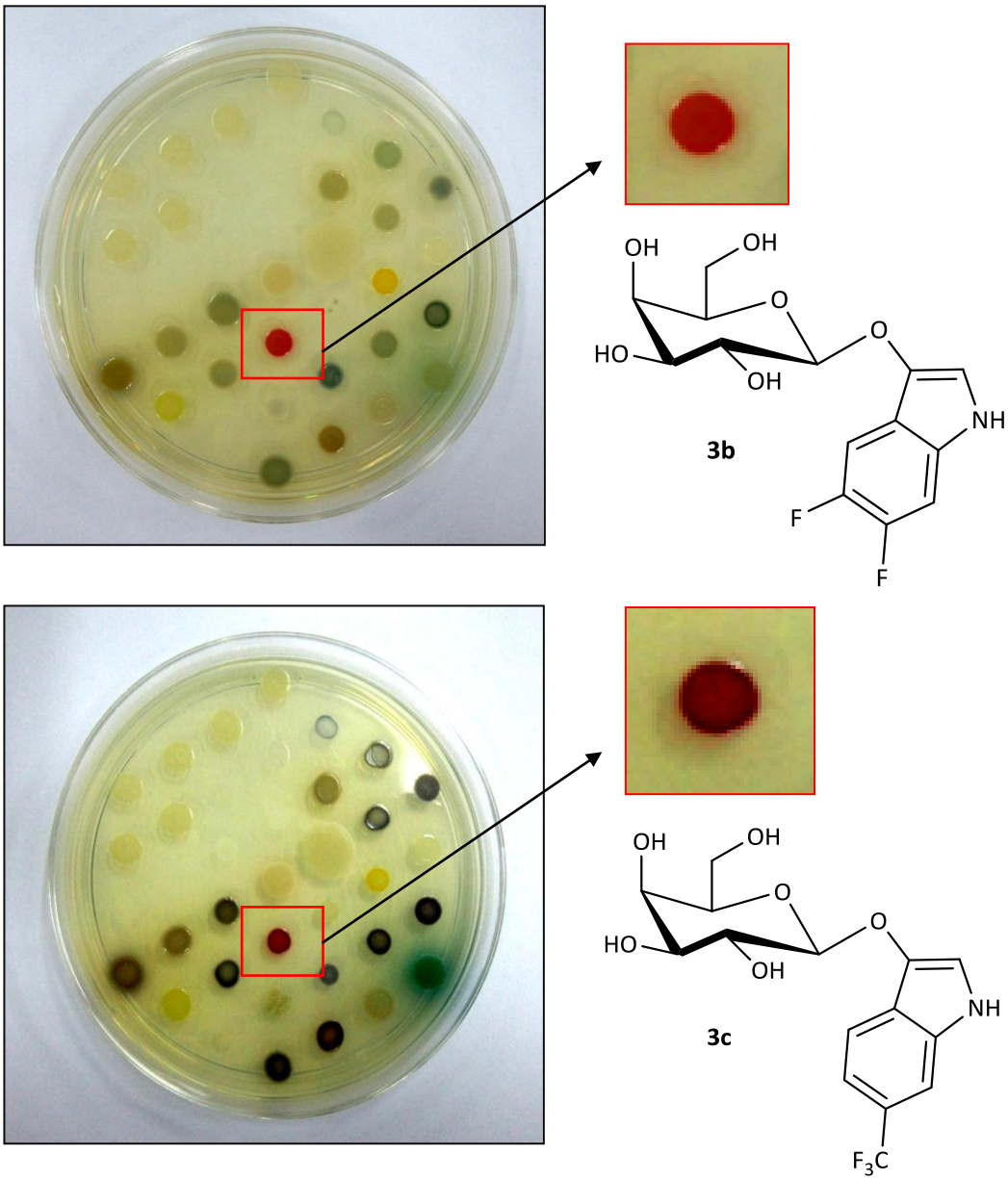

Figure 46 (continued). Detection of *Serratia marcescens* (OCC 217) using the halogenated indoxyl β-galactosides in NA for 40 hours. Note that substrate **3b** (top) produced traces of olive green colouration.

4.4.5 Differences on the colour of the dimersied fluorinated chromophore

Interestingly, two closely related substrates 5-F-β-D-gal **3a** and 6-F-β-D-gal **1f**, when hydrolysed, generated two contrasting colours of olive green and rouge colours, respectively. However, substrate **3a** shared the same colour of olive green with 5,6-F-β-D-gal **3b**. This implies that the position of the substituent has an effect on the maximum absorption of indigo, as shown in **Table 26**.

Table 26. Substituent effects at positions 5,5' and 6,6' on the longest wavelength absorption maxima (λ_{max}) of substituted indigo dyes.[135]

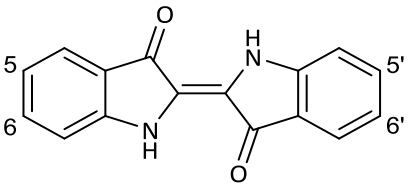

	Positions (λ_{max})	
Substituents	**5,5'**	**6,6'**
H	606	606
F	615	570
Cl	620	590
Br	620	590
I	610	590

Indigo dyes dissolved in 1,1,2,2-tetrachloroethane

The introduction of halogen substituents at positions 5,5' exerts a greater bathochromic shift than at position 6,6' of a dimerised substituted indigo. Therefore, 5,5-difluoro-substituted indigo of 5-F-β-D-gal **3a** has an absorption maximum (λ_{max}) at a longer wavelength than 6,6-difluoro-substituted indigo of 6-F-β-D-gal **1f**. Furthermore, it can be postulated that dimerised chromohpores of substrates **3a** and **3b** shared the same value of λ_{max}. This also applies to other glycosides linked to same indoxyls. Hence, the positions of substituents on the aromatic ring relative to either the NH or C=O group of a substituted indigo can be a determining factor on the colour differences.[135]

4.4.6 Evaluation of the bacterial hydrolysis of indoxyl glycosides

Differences in the hydrolysis of indoxyl β-D-glycosides by different bacterial species have been observed. One way to theoretically determine the rate of substrate uptake by bacteria is through comparison of calculated Log P values for the indoxyl β-galactosides. The values are presented in **Table 27**.

Table 27. Comparison of liphophilicity of indoxyl-β-D-galactoside derivatives.

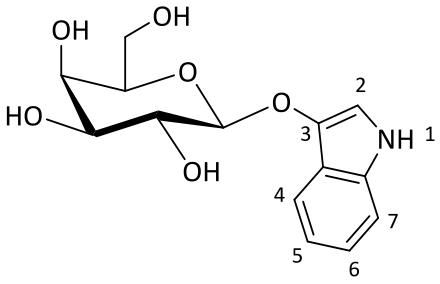

Indoxyl Subtrates	β-galactosides	Log P
X (4-Cl, 5-Br)	**1a**	0.73
Magenta (5-Br, 6-Cl)	**1c**	0.73
Midnight blue-gal (6-CF_3)*	**3c**	0.27
Blue (5-Br)	**1b**	0.17
Rose or Salmon (6-Cl)	**1d**	-0.10
Olive green (5, 6-F)*	**3a**	-0.34
Olive green (5-F)*	**3b**	-0.50
Rouge (6-F)	**1f**	-0.50
Green (*N*-Me)	**1i**	-0.42
Underivatised-gal (Y)	**1e**	-0.65

*Fluorinated indoxyl β-D-galactosides were synthesised within our laboratory.

Substrate 5-Br-4-Cl-β-D-gal **1a** is the most lipophilic, whereas the unsubstituted Y-β-D-galactoside **1e** was the least lipophilic. As illustrated in **Figure 47**, the theoretical of Log P values can be directly correlated with the initial rates of hydrolysis for each substrate, as previously reported by Davidson *et al*.[126] X-β-D-gal **1a** hydrolysed the fastest relative to other indoxyls derivatives, explaining why the chromogen is the 'gold standard' in diagnostic microbiology.

For the 6-trifluoromethyl indoxyl substrate **3c**, it can be hypothesised that the rate of hydrolysis would be much quicker than for the mono- and di- fluorinated substrates **3a** and **3b** based on different log P values -0.50 and -0.34, respectively.

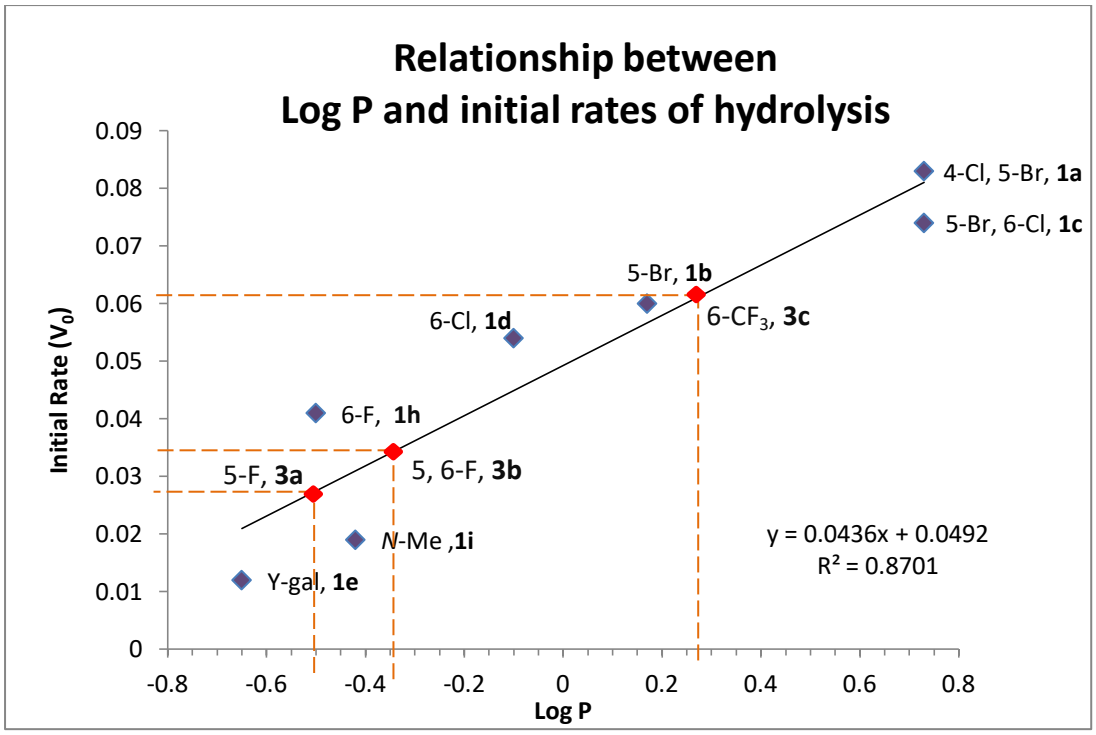

Figure 47. The correlation between Log P and initial rates of hydrolysis of the indoxyl derivatives by Davidson and co-workers[126] with modifications on the plotted graph.

Based on the empirical work by Davidson *et al.* the rate of hydrolysis was also dependent on the position of the halogen on the benzene ring of the indoxyl. As shown in **Figure 48**, the chlorine substitution at position 4 provided an indoxyl galactoside that was hydrolysed more rapidly than the corresponding derivatives with chlorine at position 6.

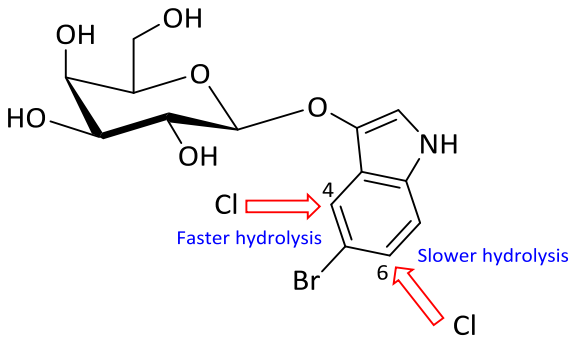

Figure 48. Halogen substitution at the aromatic ring of indoxyl related to the rate of hydrolysis.[126]

To probe this potential inter-relationship between log P values and rates of hydrolysis, further kinetic studies were performed with the fluorinated indoxyl glycosides.

4.4.7 Determination of the rate of hydrolysis of indoxyl β-glycosides

To ascertain the hierarchy for hydrolysis of the substrates, enzyme kinetic studies would be required. The Michaelis-Menten equation can be used to determine the enzyme-catalysed reaction rate, as shown in **Equation 1**.

$$v = \frac{V_{max}\,[S]}{K_M + [S]}$$

Equation 1. Michaelis-Menten equation for enzyme hydrolysis.

Where v is the reaction rate and S is the substrate concentration. The Michaelis-Menten constant (K_M) provides the concentration of substrate required for the catalysis to take place. A large K_M indicates a low affinity of the enzyme for a certain substrate, whereas a small K_M indicates high affinity of the enzyme for a certain substrate. The maximum rate of reaction (V_{max}) is achieved when a substrate reached saturation under defined experimental conditions. As shown in **Figure 49**, re-arranging the Michaelis-Menten equation provides a linear representation of the substrate-enzyme catalysis by a Lineweaver-Burk plot.[266]

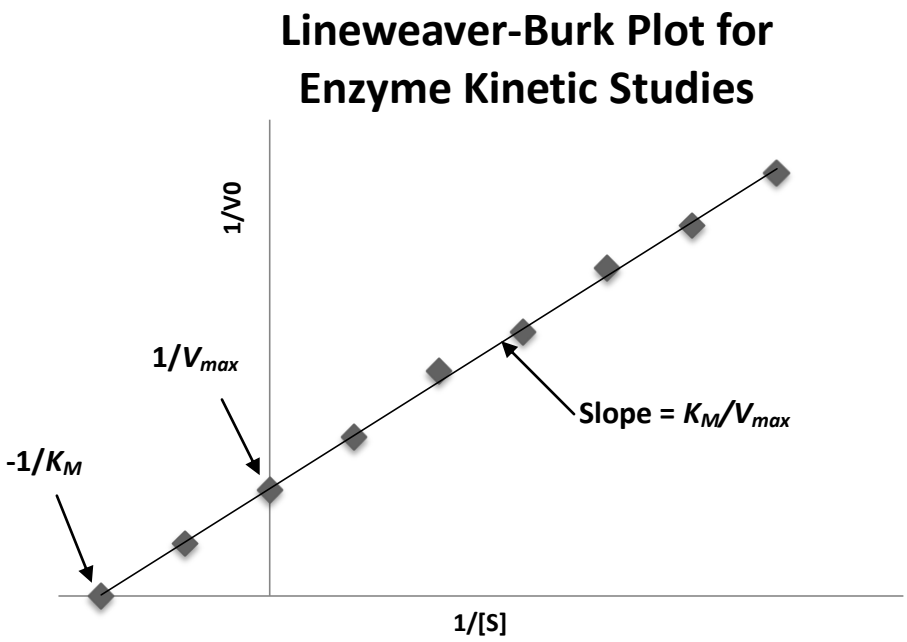

$$\frac{1}{V_0} = \frac{K_M}{V_{max}} \cdot \frac{1}{S} + \frac{1}{V_{max}}$$

$$y = mx + c$$

Figure 49. Lineweaver-Burk plot of enzyme kinetics.[266]

To probe this, kinetic studies have been initiated in our laboratory. The Michaelis-Menten constant, maximal velocity (V_{max}) and initial rate of velocity (V_0) were determined for the reaction of substrates 5-bromo-4-chloro-3-indolyl β-D-glucoside **2a** and 6-(trifluoromethyl)-3-indolyl β-D-glucoside **4c** (**Figure 50**) with β-glucosidase from almonds. Substrate **4c** was chosen for this study, since the 6-trifluormethyl indoxyl β-galactoside **3c** was the most lipophilic when compared to the synthesised mono- and di-fluoro β-galactoside **3a** and **3b** based on their Log P values. Note that the calculated Log P values of indoxyl β-galactosides were the same for their respective indoxyl β-D-glucosides.

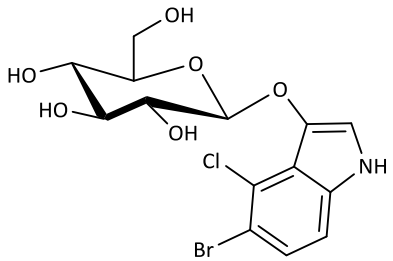

5-Bromo-4-chloro-3-indolyl β-D-glucoside
5-Br-4-Cl-β-D-gluc
2a

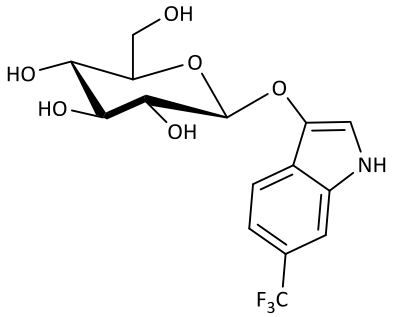

6-(trifluoromethyl)-3-indolyl β-D-glucoside
6-CF_3-β-D-gluc
4c

Figure 50. Enzyme kinetic studies of the two chromogenic substrates **3a** and **4c**.

High Performance Liquid Chromatography (HPLC) is quantitative technique that is used to separate compounds, which can be detected using ultra-violet absorption at a specific wavelength. The instrument is coupled with Evaporative Light Scattering Detector (ELSD) to detect non-absorbant organic compounds like sugar. In this study, of 5-bromo-4-chloro-3-indolyl β-D-glucoside **2a** and 6-(trifluoromethyl)-3-indolyl β-D-glucoside **4c** were analysed using HPLC. At different substrate concentrations, the solution reacted with a fixed amount of β-glucosidase enzyme solution at 37 °C. One milliltre of the reaction mixture was injected for every one minute, filtered and injected into the HPLC. The peak areas were converted into concentration using the calibration graphs of indoxyl glucosides **2a** and **4c**. The inverse of the intial rates and the substrate concentration were plotted to afford Lineweaver-Burk plots (**Figure 51**). The values of K_M, V_{max}, V_0 (**Table 28**) were determined from the intercept of this plot.

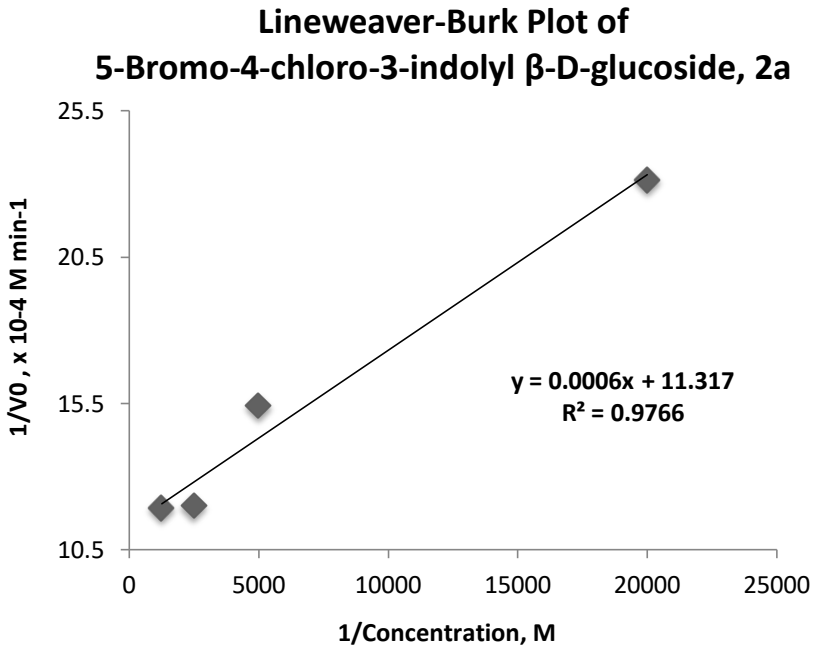

Figure 51. Lineweaver-Burk plot of substrate **2a**.

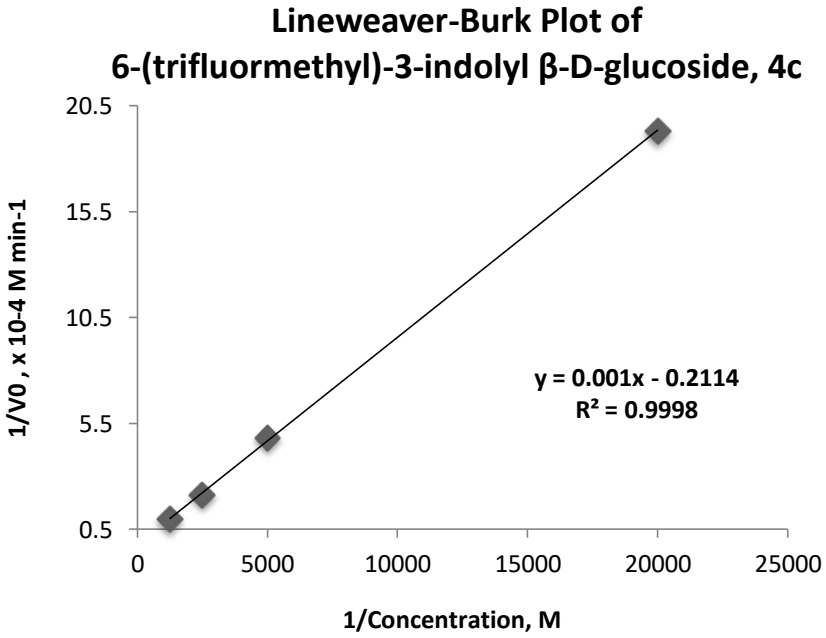

Figure 51 (continued). Lineweaver-Burk plot of substrate **4c**.

Table 28. Summary of the enzyme kinetic studies of substrates **2a** and **4c**.

Kinetic Studies	5-Br-4-Cl-β-D-gluc, 2a	6-CF_3-β-D-gluc, 4c
K_M (M)	5.30 x 10^{-5}	7.10 x 10^{-3}
V_{max} (M min^{-1})	0.08	3.05
V_0 (M min^{-1})	0.09	3.05

5-Bromo-4-chloro-3-indolyl β-D-glucoside **2a** exhibited a smaller K_M than substrate 6-(trifluoromethyl)-3-indolyl β-D-glucoside **4c**, indicating that substrate **2a** formed a stronger complex with the enzyme than substrate **4c**. A smaller K_M of the substrate **2a** would also mean that the rate of hydrolysis was much faster and quickly reached saturation.

On the other hand, increasing the concentration of substrate 6-(trifluoromethyl)-3-indolyl β-D-glucoside was needed to achieve V_{max}. However, the initial rate of velocity, V_0, of substrate **4c** was three times faster than **2a**, which was the opposite of what can be expected based on **Figure 51**.[126] Therefore, it can be concluded that Log P values alone are not sufficient to predict the hydrolysis kinetics, and further investigation is needed to ascertain the rate of hydrolysis of substrate **4c** relative to substrate **2a**. Furthermore, the position and size of the substrate affect the hydrolysis of the substrates, as discussed in **Section 4.5.6**.

4.5 Conclusion and Future Work

When the substrates were hydrolysed, different shades of colours relative to their respective chromogens were observed in solid media for the six fluorinated indoxyl β-glycosides, hence extending the scope utilities of these materials for the detection and identification of bacterial species. The colour of agar and bacterial colony might have influenced the colouration. Also, reaction between the solid media constituents and indigo might have occurred. Furthermore, prolong incubation of indoxyl glycosides enhanced the sensitivity of the chromogenic media.

For the chosen culture media, which were TSA and NA, the number of Gram-negative bacteria hydrolysed in both agars was the same. However, the number of Gram-positive bacteria that hydrolysed in TSA was greater than NA. Casein, as a main constituent of TSA, perhaps assisted with the hydrolysis of the substrates when tested against of *Staphylococcus* and *Enterococcus* species.

Substrates 5-fluoro-3-indolyl β-D-glucoside **4a** and 5,6-difluoro-3-indolyl β-D-glucoside **4b**, and to an extent 6-CF_3-3-indolyl β-D-glucoside **4c**, were hydrolysed by *Escherichia* spp. The fluorinated substrates were more readily hydrolysed by β-glucosidase enzyme in the bacteria, making the chromogens more sensitive than commercially available 5-bromo-4-chloro-3-indolyl β-D-glucoside **2a**. Furthermore, the 5-fluoro-3-indolyl β-D-galactoside **3a** and 5,6-difluoro-3-indolyl β-D-galactoside **3b** were mostly hydrolysed by *Staphylococcus* species in TSA, whereas only few *Staphylococci* hydrolysed the substrates 6-(trifluormoethyl)-3-indolyl β-galactoside **3c** and 5-bromo-4-chloro-3-indolyl β-D-galactoside **1a**.

For the fluorinated analogues 5-fluoro-3-indolyl β-D-galactoside **3a** and 6-fluoro-3-indolyl β-D-galactoside **1f** provided two contrasting colours when hydrolysed, but the former

produced the same colour as 5,6-difluoro-3-indolyl β-D-galactoside **3b**. The effect of the substituents on the aromatic ring can be attributed to its relationship to either the NH or C=O group of a dimerised chromophore. Further work is required to ascertain if this holds true. This can be achieved by comparisons of different analogues of mono- and di- fluoro derivatives at different positions at the aromatic ring using analytical instruments such as HPLC equipped with diode array or UV-Vis spectrophotometer. Aside from halogens as substituents, it would be interesting to study the effect of further electron-withdrawing groups like NO_2, as well as electron-donating groups such as benzyl, methyl and ethyl as substituents on the phenyl ring of the indoxyl, including their specificity, and rate of transport and hydrolysis.

The rate of hydrolysis of glycosides can be explained by the direct correlation between the lipophilicity via Log P and initial kinetic rates of reaction of the chromogen substrates. Amongst the indoxyl substrates, 5-bromo-4-chloro-3-indolyl β-D-galactoside **1a** was the most superior chromogenic substrate, as previously reported.[126] With the addition of the synthesised fluorinated derivatives, it can be postulated that the rate of hydrolysis was quicker for 6-trifluoromethyl substrates **3c** than that of mono- and di-fluoro indoxyls **1a** and **1b** based on the modified plotted graph in **Figure 30**. Therefore, the position and size of the substrate affect the hydrolysis of the substrates.

Based from the kinetic studies, 5-bromo-4-chloro-3-indolyl β-D-glucoside **2a** exhibited stronger affinity with β-glucosidase than 6-(trifluoromethyl)-3-indolyl β-D-glucoside **4c** based on the K_M values. This also indicated that substrate **2a** reached saturation quicker than **4c**. However, the rate of hydrolysis of compound **4c** was three time faster than **2a**. Therefore, further investigation is needed to establish the hydrolysis kinetics of **4c** relative to **2a**. Therefore, the steric and position of the substituents on the aromatic ring of the indoxyl influences the K_M, V_{max} and V_0.

Chapter 5 Conclusions and Future Works

5.1 Conclusions

5.1.1 Summary

The research presented in this work focussed on the synthesis and analysis of a series of fluorinated indoxyl β-glycosides as chromogenic substrates for the enhanced detection and presumptive identification of pathogenic bacteria. Indoxyl glycosides are widely exploited chromogenic probes in diagnostic microbiology. When the chromogens are hydrolysed by specific glycosidase enzymes, the substrates produced brightly coloured precipitates and are highly restricted within microbial colonies. The general principle on the incorporation of chromogenic substrates in the presence of bacteria is illustrated in **Figure 12** in **Chapter 1.**

To complement the existing range of commercially available indoxyl glycosides, the colours can be expanded by adding different substituents on the aromatic ring. This can be further extended by coupling an indoxyl-based substrate to a larger range of sugars to exploit the presence of a wider range of glycosidase enzymes in bacteria. The addition of two different chromogenic substrates in a polymicrobial media would be useful to differentiate different bacteria producing different glycosidase enzymes. This would allow better separation of the organisms in mixtures. For example, commercially available *Brilliance E. coli*/coliform is a differential agar that is used for the presumptive identification of *E. coli* and other coliforms from food and environmental samples. 5-Bromo-4-chloro-indoxyl-β-D-glucuronide is cleaved by β-D-glucuronidase, which the enzyme is almost exclusively present in *E. coli* strains. The second chromogenic substrate, 6-chloro-3-indolyl β-D-galactoside, is cleaved by most of the coliforms and *E. coli* strains, producing pink and purple/blue colonies, respectively. [267, 268] The medium also contains sodium lauryl sulfate, which acts as a selective agent, inhibiting the growth of Gram-positive bacteria. Wohlsen described the chromogenic agar as less laborious and time-consuming as compared to traditional method for the detection and enumeration of *E. coli* in sewage effluent samples. Out of 1171 colonies, 1157 (98.8%) were

confirmed as *E. coli* isolates; whilst 823 (out of 1034) were confirmed as non-*E.coli* colonies. The author reported that the results were confirmed within 24 hours without the need for further confirmation, as compared to 48 hours with the conventional method.[269]

Therefore, the research focussed on the synthesis and biological testing of six fluorinated indoxyl glycosides **3a-c** and **4a-c**. The β-glycosides were synthesised by following the synthetic route outlined for complimentary indoxy glycosides by Böttcher and co-workers. The substrates were tested for their chromogenic properties, and were evaluated and compared against commercially available indoxyl β-glycosides such as 5-bromo-4-chloro-3-indolyl β-D-galactoside **1a**, 5-bromo-4-chloro-3-indolyl β-D-glucoside **2a** and 6-fluoro-3-indolyl β-D-galactoside **1f,** as shown in **Figure 52**.

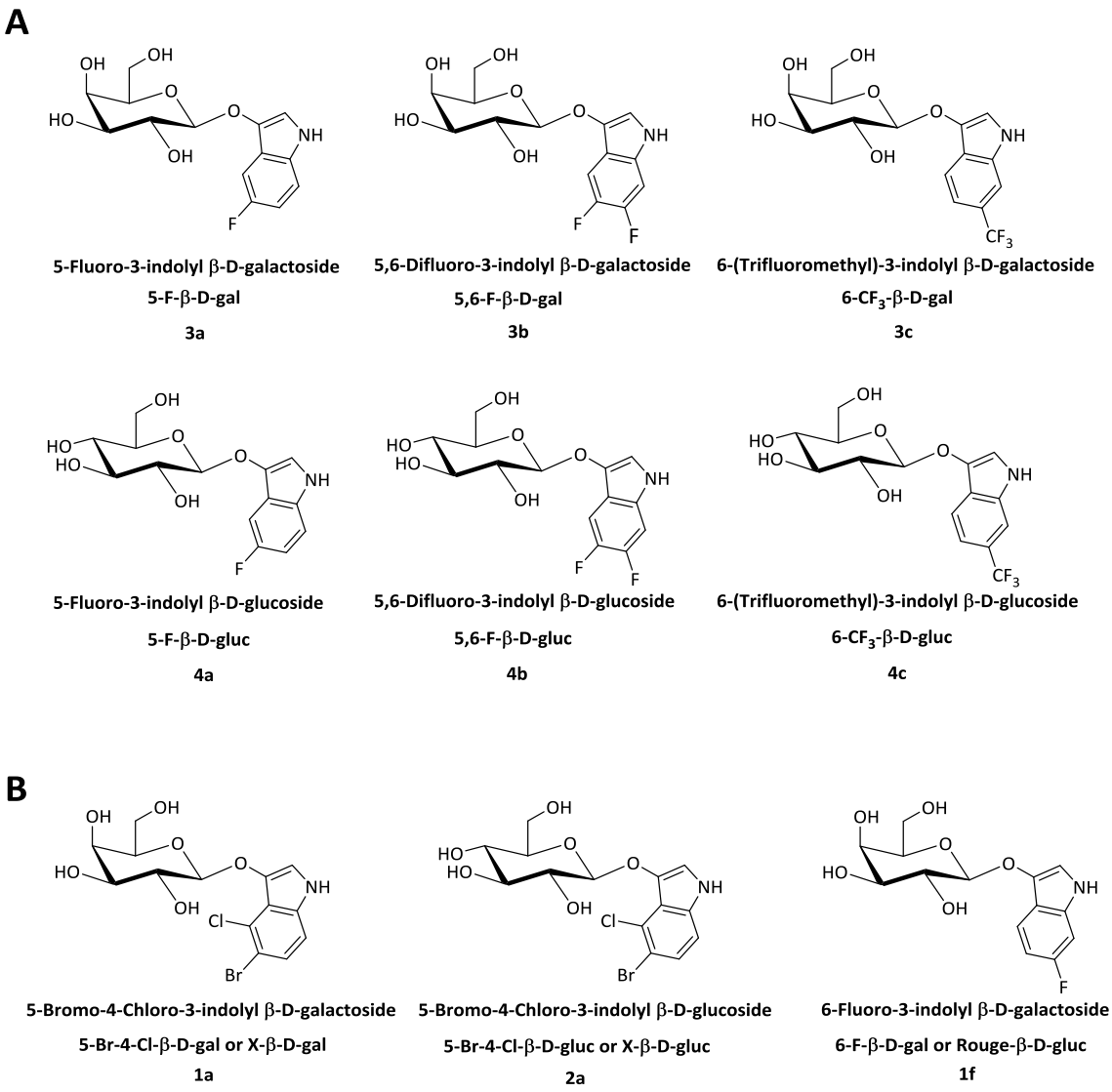

Figure 52. Fluorinated derivatives of indoxyl glycosides (Section **A**) and commercially available chromogenic substrates (Secton **B**) that have been utilised for the detection of bacteria.

5.1.2 Synthesis of indoxylic acid allyl ester and its fluorinated erivatives

Although indoxyl glycosides are effective chromogenic substrates, one of the major drawbacks is their challenging and low yielding synthesis. The conventional pathway for the synthesis of the indoxyl glycosides is via the Michael glycosidation route. The key precursor *N*-acetyl indoxyl is coupled with a glycosyl bromide using 1M NaOH in acetone. This method depends on keto-enol tautomerism, where the equilibrium exists between ketone and enol tautomers under basic condition (**Scheme 26**). However, the equilibrium greatly favours the ketone rather than the enol form; thus, allowing only a small proportion of indoxyl to readily couple with a glycosyl donor. Therefore, this approach provides low yields of acetylated indoxy glycosides or none at all.

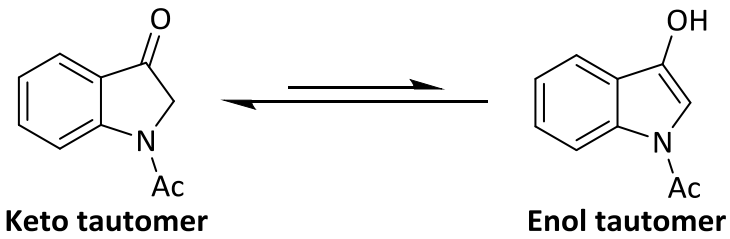

Scheme 26. Keto-enol tautomerism of indoxyl-based subtrates under basic conditions.

To optimise the synthetic route, this project followed the method developed by Böttcher and co-workers using phase-transfer catalysis.[128,158,222] As shown in **Scheme 27**, the indoxylic acid allyl esters and its fluorinated derivatives were prepared in good to excellent yields prior to glycosidation. The four-step synthesis mostly involves alkylaton and cyclisation towards the key precursors with overall yields varying from 20-30%.

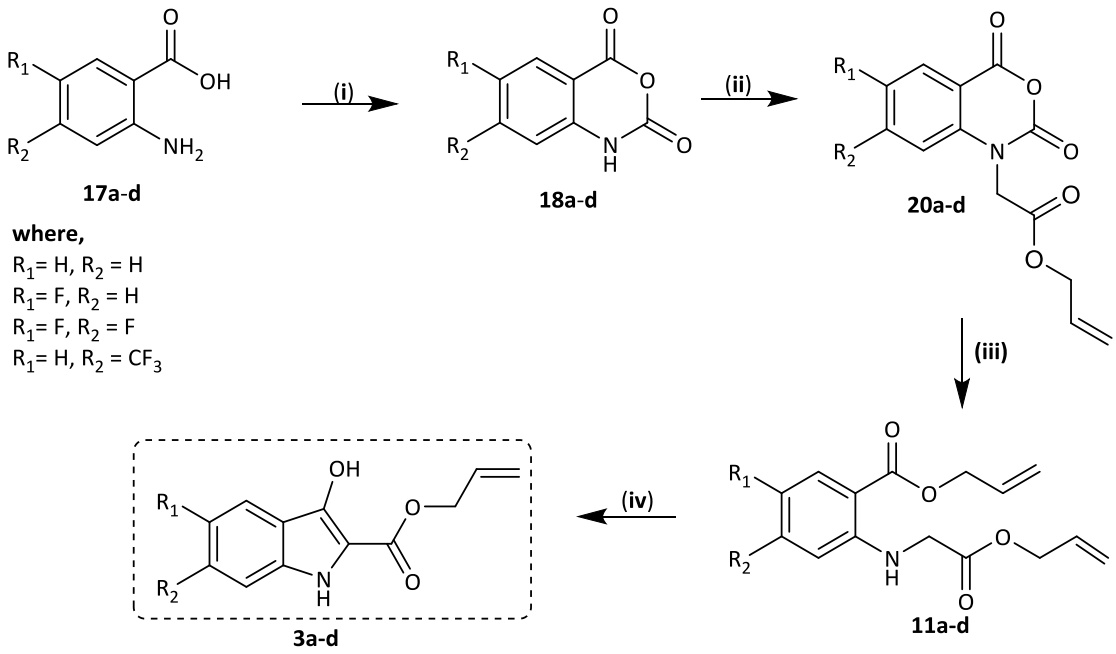

Scheme 27. The four-step synthesis of indoxylic acid allyl esters and its fluorinated derivatives. (**i**) MeCN, triphosgene, 45-50 °C, 3 h (75-92%); (**ii**) DMF sodium hydride, allyl bromoacetate rt, overnight (87-97%); (**iii**) allyl alcohol, NaH, rt, 1 h (49-86%); (**iv**) Et_2O, KO^tBu, reflux, 1 h (38-49%).

5.1.3 Synthesis of fluorinated indoxyl β-glycosides

Following the method by Böttcher *et al*.[128, 135, 158,] phase transfer catalysis was utilised to couple the fluorinated indoxylic acid allyl esters with the commonly known sugar donors acetobromogalactose and acetobromoglucose. Phase-transfer glycosidation follows the S_N2 style reaction with anchimeric assistance of the C-2 acetate in the carbohydrate ring to furnish 1,2-*trans* glycosides stereoselectively. As shown in **Scheme 28**, the biphasic method afforded the fluorinated per-*O*-acetyl indoxylic acid allyl ester β-glycosides **27a-c** and **28a-c** with high yields of 78-95%. Ideally, the yields of the fluorinated indoxyl β-galactoside were supposed to be higher than β-glucosides. The ability of the equatorial C-4 hydroxyl group to interact with the electronegative oxygen of the oxocarbenium ion during glycosylation was postulated to be responsible for the greater yield of β-galactosides.

The deprotection stage can be split into two steps. First, the allyl ester was removed by de-*O*-allylation followed by decarboxylation to afford the per-*O*-acetylated indoxyl derivatives **31a-c** and **32a-c** with moderate yields varying from 40-77%. Then, the acetylated glycosides were deprotected using sodim methoxide in methanol to furnish the final fluorinated indoxyl β-D-galactosides **3a-c** and β-D-glucosides **4a-c**. Ion-exchange resin was used to remove soium ion residues. Initial attempts to purify the crude products used normal phase flash chromatography using an isocratic system of 9:1 DCM:MeOH. Since the silica was acidic, early dimerisation of the substrate and sugar hydrolysis occurred affecting the yields of the products. The purification method was therefore optimised and automated reversed-phase flash chromotaography was the preferred way to purify and isolate compounds with yields varying from 19-90%. Finally, the overall yield for the glycosidation route of fluorinated indoxyl β-D-galactosides and β-D-glucosides varied from 7-21% and 21-58%, respectively.

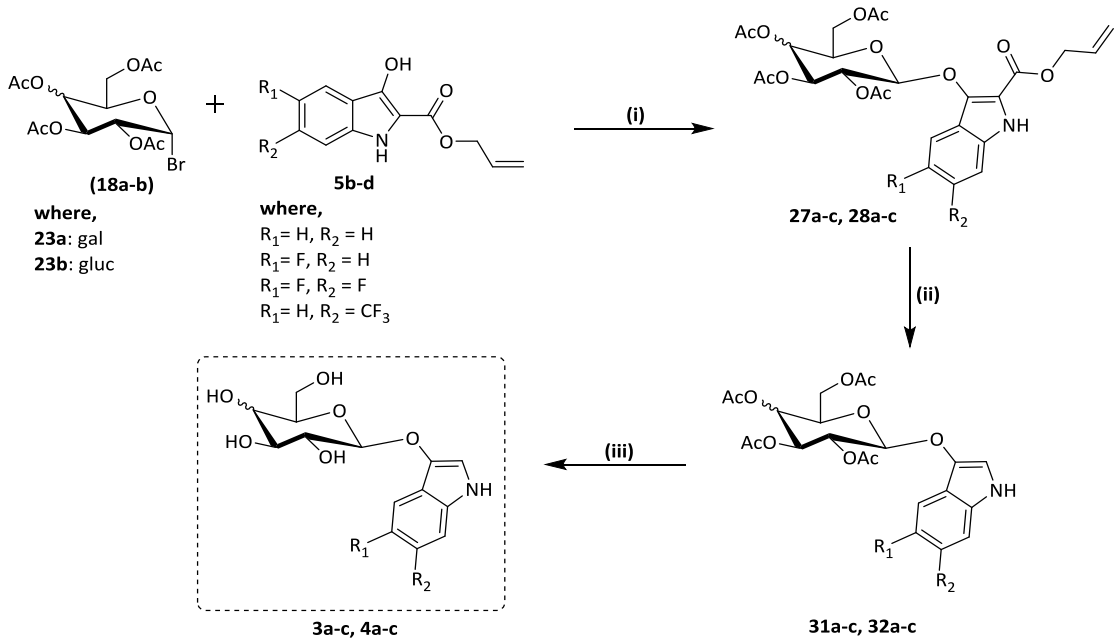

Scheme 28. Synthesis of the fluorinated indoxyl β-D-galactosides **3a-c** and β-D-glucosides **4a-c**. **(i)** TBAHS, 1M K_2CO_3, DCM, rt, 2 h (78-95%); **(ii)** THF, morpholine, $Pd(PPh_3)_4$, rt, overnight; Ac_2O, AgOAc, K_2CO_3, 90-110 °C reflux, 20 min to 1 h (40-77%). **(iii)** MeOH, cat. amount of NaOMe, Amberlite H^+ (19-90%).

5.1.4 Synthesis of indoxyl rhamnoside

Attempts to glycosidate the underivatised indoxylic acid allyl esters with rhamnoside failed via PTC. Since indoxyl rhamnoside was difficult to synthesise using the biphasic method, TMSOTf as promoter was investigated for glycosidation. The method used commercially available underivatised indoxylic acid methyl ester to glycosidate with L-rhamnosyl bromide generating a mixture of impure products. Separation of the mixtures was challenging even when automated normal-phase column chromatography was utilised for the purification.

It was decided to deacetylate the partially purified product and then using 0.1 M NaOH, decarboxylate using a silver-mediated reaction. Based on ^{1}H NMR spectroscopic anlaysis, the desired product was not successfully isolated. More study is therefore needed to optimise the synthetic route towards indoxyl rhamnoside.

The products synthesised in this project were chemically characterised by ^{1}H, ^{13}C and ^{19}F NMR, FT-IR and MS and the purity of the fluorinated indoxyl glycosides were analysed by HPLC. The stereochemical conformations of the glycosides were determined by ^{1}H, COSY, HSQC and HMBC spectra accompanied with structural elucidation using ^{13}C and DEPT spectra.

5.1.5 Chromogenic evaluation of the fluorinated indoxyl β-glycosides

As shown in **Figure 52** (**Section 5.1.1**), the fluorinated indoxyl β-glycosides were incorporated into the non-selective agars NA and TSA in the presence of several microorganisms, followed by incubation at 37 °C for 20 and 40 hours.

When the the β-D-glycosides were hydrolysed, the colours produced were normally dark olive green for substrates 5-fluoro-3-indolyl β-D-galactoside **3a**, 5,6-difluoro-3-indolyl β-D-galactoside **3b**, 5-fluoro-3-indolyl β-D-glucoside **4a**, 5,6-difluoro-3-indoly β-D-galactoside **4b**, and midnight blue for substrates 6-(trifluormethyl)-3-indolyl β-D-galactoside **3c** and 6-(trifluormethyl)-3-indolyl β-D-glucoside **4c**. However, a varying degree of different colouration with respect to their normal colour was observed. In general, the same number of Gram-negative bacteria hydrolysed the substrate in TSA and NA, especially for *Enterococcus* and *Staphylococcus* species. On the other hand, the number of Gram-positive bacteria that hydrolysed the substrates was higher on TSA than NA. For the detection of *Escherichia* species, synthesised fluorinated indoxyl β-glucosides **4a** and **4b**, and to an extent

4c, were more sensitive than commercially available 5-bromo-4-chloro-3-indolyl β-D-glucoside **2a** in TSA. For the detection of β-galactosidase enzyme in *Staphylococcus* spp. in TSA, synthesised substrates **3a** and **3b** were hydrolysed, whereas substrates **3c** and 5-bromo-4-chloro-3-indolyl β-D-galactoside **1a** were not hydrolysed.

For the synthesised fluorinated substrates, the UV absorptions of the synthesised substrates mono- and di-fluoro derivatives **3a**, **3b**, **4a** and **4b** were likely to be the same, since they share the same colour when hydrolysed. Substrates **3c** and **4c** would hydrolyse more rapidly than the mono and di-fluoro derivatives **3a**, **3b**, **4a** and **4b**. Based from the kinetic studies, 5-bromo-4-chloro-3-indolyl β-D-glucoside **2a** exhibited a stronger affinity to the β-glucosidase enzyme than 6-(trifluormethyl)-3-indolyl β-D-glucoside **4c**. Hence, substrate **2a** achieved saturation much quicker than **4c**. In addition, the hydrolysis of **2a** was three times faster compared to **4c**. Therefore, the effect of the substituents and their position on the aromatic ring influenced the UV absorption and rate of hydrolysis.

5.2 Future Work

5.2.1 Derivatisation of indoxyl-based substrates

To produce an array of different colours, more study is needed to expand the range of indoxyls, for example by adding different halogens and other electron-withdrawing substituents like NO_2 at various positions in the benzene ring. Therefore, it would also be interesting to investigate the effects of adding electron-donating substituents such as benzyl, methyl or ethyl either on their own or in a combination with electron withdrawing substituents on the benzene ring of the indoxyl.

The derivatisation can be further extended to thioindigo as the derivatives have shown interesting UV absorptions, which is provided in **Table 29**.[143] These indigo and thioindigo derivatives can be used to couple with commonly known sugars like galatose and glucose, and to an extent, to lesser known sugars such as rhamnose, expanding the library of existing chromogenic substrates.

Table 29. Absorption maximum of thioindigo dyes[a] at positions 5,5' and 6,6'.

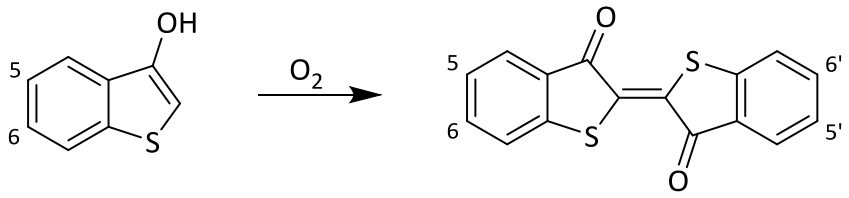

Thioindoxyl **Thioindigo**

	λ_{max} [143]	
Position	**5,5'**	**6,6'**
H	543	543
Cl	556	539
OEt	584	437
NO_2	513	567

[a]In dimethylformamide (DMF).

By following the synthetic route developed by Hansen and co-workers[270] commercially available thiosalicylic acid **39a** can be utilised as a starting material to prepare the unsubstituted methyl 3-hydroxybenzo[*b*]thiophene-2-carboxylate **39c** as a key precursor prior to glycosidation with a sugar, as shown in **Scheme 29**. The thiosalicylic acid **39a** was converted into a methyl ester and subsequently *S*-alkylated with methyl chloroacetate, diisopropylethylamine (DIPEA) and potassium iodide to produce **39b**. A Dieckmann type-ring closure reaction using 1,8-diazabicyclo(5.4.0)undec-7-ene (DBU) afforded thioindoxyl **39c**.

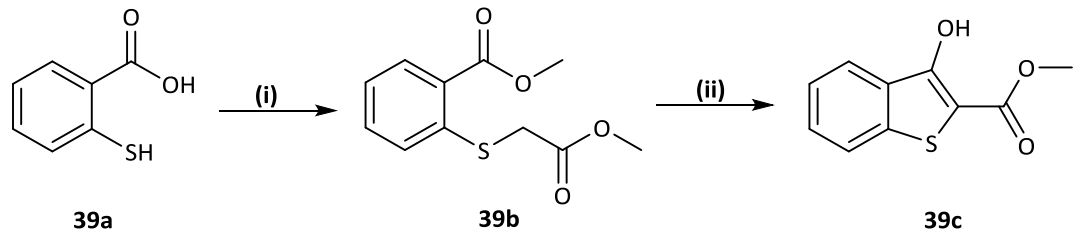

39a **39b** **39c**

Scheme 29. Synthesis of unsubstitued thioindoxyl as key intermeadiate prior to glycosidation with a glycosyl donor. **(i) a**. H_2SO_4, MeOH, reflux, **b**. methyl chloroacetate, DIPEA, KI, THF (73%); **(ii)** DBU, toluene, rt (98%).[270]

A slightly different route to substituted thiondoxyl key precursors **40a-e** can be obtained by treating commercially available 2-nitrobenzoic acids **41a-e** with methyl thioglycolate in the presence of lithium hydroxide as base, as shown in **Scheme 30**.[271]

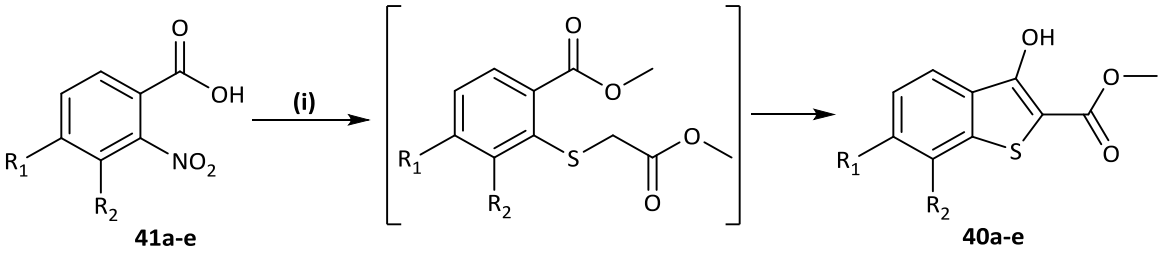

41a-e **40a-e**

R_1	R_2	Compounds	Yield (%)
H	H	**40a**	61
Cl	H	**40b**	75
H	Cl	**40c**	80
H	NO_2	**40d**	73
H	OCH_3	**40e**	50

Scheme 30. Synthesis of substitued thionindoxyl from *o*-nitrobenzoic acid. **(i) a**. H_2SO_4, MeOH, reflux, **b**. methyl thioglycolate, LiOH, DMF, rt.[271]

Under this condition, the nitro group was readily displaced by methyl thioglycolate anion (lithium salt) in DMF, and was subsequently followed by a based-catalysed cyclisation to furnish the substituted thioindoxyl methyl esters in significant yields. The products were purified using a recrystallisation method.[271]

5.2.2 Synthesis of indoxyl α-glycosides

Within our laboratory, phase-transfer glycosidation has proved to be successful to furnish 1,2-*trans* glycosides streoselectively. However, the biphasic route is not applicable to form 1,2-*cis* linkages. It would be useful to access these in order to prepare a further library of indoxyl glycosides that could be used to detect bacteria based on the presence of α-glycosidase.

As depicted in **Scheme 31A**, Boons and co-workers showed a novel glycosylation approach to control α-anomeric selectivity based on the anchimeric assistance of (1*S*)-phenyl-2-(phenylsulfanyl)ethyl moiety at C-2 of a glycosyl donor.[272] Following an S_N2 reaction, the oxocabenium ion was attacked intramolecularly by the phenylsulfanyl moiety of the C-2 auxiliary to form an intermediate sulfonium ion. Due to the steric and electronic effects only *trans*-decalin is formed as an intermediate. With the participation of the C-2 functionality, glycosidation of the equatorial sulfoxide donor affords 1,2-*cis* glycoside.

1,2-*cis* Glycosides are taxonomic markers for the detection of α-glycosidase enzymes in bacteria. For example, *E. coli* O157:H7 and *Salmonella* possess α-glucosidases. *E. coli* O157:H7 is a serotype bacterial species of *E. coli* and is associated with food-borne illnesses.[273] *Salmonella* are one the most common food-borne pathogens and are associated with food poisoning[274] and gastroenteritis.[275] Currently, there are a very few commercially available indoxyl α-glycosides such as 5-bromo-4-chloro-3-indolyl α-D-glucopyranoside and

6-chloro-3-indolyl α-D-glucospyranoside that are used for bacterial detection. Expanding the library of indoxyl α-glycosides would therefore be useful for the improved differentiation and selective isolation of bacterial species.

As shown in **Scheme 31B**, the glycosyl donor was prepared by treatment of (1*S*)-phenyl-2-(phenylsulfanyl)ethyl ester in $BF_3 \cdot OEt_2$, followed by treatment with $C(NH)CCl_3$ to form the α-anomeric trichloroacetimidate. Stereoselective glycosylation of the sulfoxide follows an S_N2 reaction upon treatment with TMSOTf in DCM to form the diasscharides. Removal of the (1*S*)-phenyl-2-(phenylsulfanyl)ethyl group can be achieved by treatment with $BF_3 \cdot OEt_2$ in acetic anhydride.[272] The method developed by Boons *et al.*[272] can be employed to glycosidate the modified sugar donor with indoxyl acid allyl (or methyl) ester to form 1,2-*cis* glycoside. Similar work developed by Turnbull and co-workers[276] has utilised thioglycosides as glycosyl donors *en route* to furnishing 1,2-*cis* glycosides.[276]

A

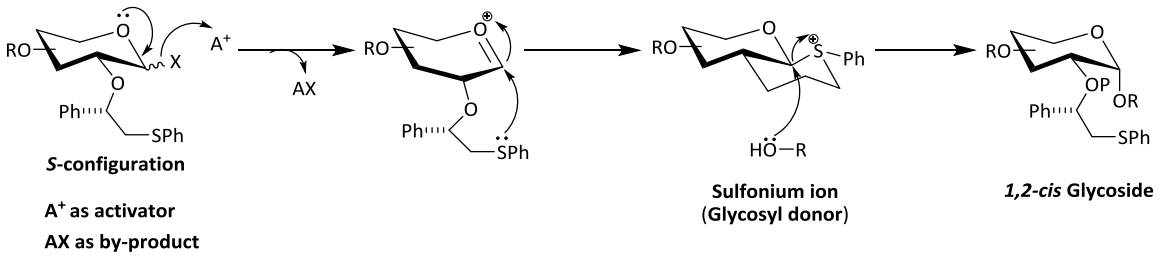

B

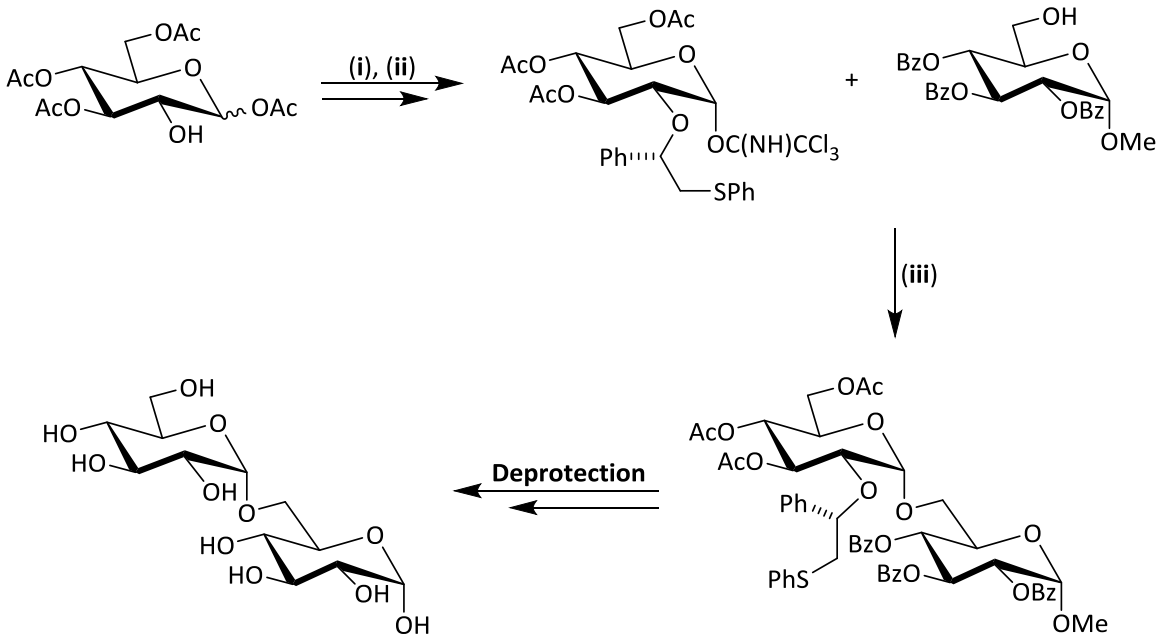

Scheme 31. **(A**) Neighbouring participation by C-2 functionality to form 1,2-*cis* glycosides. (**B**) Stereoselective glycosylation via S_N2 reaction. **(i)** (1*S*)-phenyl-2-(phenylsulfanyl)ethyl ester, $BF_3{\cdot}OEt_2$, CH_3COOH, molecular sieves (4Å), DCM, 0 °C, 30 min (71%). **(ii)** $H_2NNH_2{\cdot}HOAc$, DMF, rt, overnight (95%). **(iii)** TMSOTf, DCM, 2,6-di-*tert*-butyl-4-methylpyridine, molecular sieves (4Å), -78°C to rt, overnight.[272]

5.2.3 Combination of MALDI-TOF MS and chromogenic media for bacterial detection and identification

Over the last decade, the introduction of MALDI-TOF MS has been utilised to provide rapid and accurate identification of bacterial species.[277] This technique requires pure isolate and therefore requires inoculums to be taken from an isolation plate. Chromogenic media would therefore provide a good method of presumptively identifying organisms prior to identification by the MALDI-TOF MS.[278] The compatibility of MALDI-TOF MS with chromogenic media has proven useful for further detection and identification of bacteria in clinical samples.

For example, Joubrel and co-workers evaluated five different selective chromogenic media for the detection of Group B *Streptococcus* (GBS) screening in pregnant women. Detection and prelimanary identification GBS was facilitated in the culture media. The presence of GBS from vaginal swab samples, which was directly taken from the chromogenic media, was further identified and confirmed using MALDI-TOF MS. The authors explained the importance of correctly identifying and confirming the bacterium in question in the antenatal samples as closely related bacterial species, such as *Streptococcus porcinus, Streptococcus vestibularis, Streptococcus salivarius and Enterococcus faecalis,* were also present in the commensal flora having the same phenotypic aspect as GBS in order to avoid false positive results.[279]

Another example was the isolation *Clostridium difficile* in chromID C*. difficile* chromogenic agar from stool samples. Due to the high phenotypic similarities (morphology and and color change) of the pathogen to other closely related *Clostridium* species such as *C. hathewayi*, *C. tertium* and *C. disporicum*, MADLTI-TOF MS was incorporated to the study, improving the diagnostic accuracy of the the target organism. From the agar, the pathogen was analysed

by the instrument by direct transfer method. Bacterial identification was matched to an array of spectra in the mass spectrometry library program. Further confirmation of non-*Clostridium difficile* species can be identified by 16S rRNA gene sequencing.[280]

Finally, Charretier *et al.* have innovatively utilised mass spectrometry to detect a wide range of enzymes directly from pure colonies or positive blood cultures containing *Staphylococcus* strains. The authors demonstrated in-depth characterisation of *S. aureus,* which was the chosen model to exhibit the feasibility of the method*,* for rapid identification, resistance, virulence and type profiling. Since MALDI-TOF MS can quickly identify the pathogen within 60-80 minutes, this may accelerate the correct choice for a more targeted antibiotic prescribed to patients and would consequently reduced hospital expeditures.[281]Therefore, in an era of increasing reliance on technological advancement, chromogenic media should be used as a valuable adjunct to other POC diagnostic tools.

Chapter 6 Experimental

6.1 Equipments and materials

6.1.1 Chemical and reagents

All solvents, including anhydrous, were purchased from Fisher UK and Sigma Aldrich, unless otherwise stated. Chemicals and reagents were purchased from Alfa Aeser, Tokyo Chemical Industry Ltd and Fluka. All chemicals and reagents were used as received from the commercial suppliers.

6.1.2 Thin layer chromatography

Thin layer chromatography (TLC) was performed using aluminium backed silica gel 60 plates (Merck, Germany). The plates were visualised using ultraviolet light at 254 nm, and were subsequently treated with either of the following TLC stains: EtOH/H_2SO_4, (95:5 v/v), potassium permanganate ($KMNO_4$) or 2,4-dinitrophenylhydrazine (DNP) with subsequent heating.

6.1.3 Flash column chromatography

Flash column chromatography was used to separate the desired product from a mixture of unwanted materials such as starting materials and impurities. Purification was initially performed using silica gel (Sigma Aldrich) with 200-300 mesh, 40-63 µm particle size, pore size 60 Å, as an adsorbent. To protect the silica gel layer, low-iron sand (Fisher UK) with particle size 40-100 mesh was used for column chromatography.

For free indoxyl glycosides, the products were purified using the Reveleris X2® Flash Column Chromatography system. The deprotected products were purified using C18 reversed phase silica gel (ACROS Organics) with 17% C, ca. 0.8 mmol/g, 40-63 µ particle size and reveleris C18 column cartridges. The products were eluted on the silica using 70:30 acetonitrile and 0.1% (v/v) formic acid in water isocratically.

6.1.4 Melting range

The melting range for pure solid compounds was measured using Stuart Digital Melting Point 10 (SMP10) apparatus. The melting range is reported in degrees Celsius (°C).

6.2 Analytical Instrumentations

6.2.1 Nuclear Magnetic Resonance (NMR)

^{1}H and ^{13}C NMR spectra were obtained using Bruker Nanobay and/or Bruker DPX spectrometers (400 MHz for ^{1}H NMR and 100 MHz for ^{13}C NMR), where instruments run ICON NMR 4.2 under TOPSPIN 2.4 and ICON NMR 2.1 under TOPSPIN 1.3, respectively. The solvents used for NMR analysis were $CDCl_3$ (with TMS as internal standard, purchased from Sigma Aldrich), CD_3OD (Cambridge Isotope Laboratories) and DMSO-d_6 (Sigma Aldrich). Chemical shifts (δ) are reported in parts per million (ppm). All coupling constants (*J*) are quoted in Hz. The following splitting patterns are: "br. s" for broad singlet, "s" for singlet, "d" for doublet, "t" for triplet, "dd" for doublet of doublets, "dt" for doublet of triplets, "td" for triplet of doublets, "ddd" for doublet of doublet of doublets, "q" for quartet and "m" for multiplet.

6.2.2 Infrared (IR)

IR spectra were recorded using a Thermo Scientific iD5 ATR Diamond Nicolet™ iS5 spectrometer at 16 scans. The detector used was Deuterated Triglycine Sulfate (DTGS). The absorptions were reported as wavenumbers (cm^{-1}). The symbols "*s*", "*b*" and "*d"* are used to indicate stretching, bending and out-of-plane deformation vibrations. The band intensities are categorised as "w" for weak, "m" for medium, "s" for strong and "br" for broad.

6.2.3 Mass Spectrometry (MS)

The mass spectra were recorded using a Thermo Scientific LQ Orbitrap XL mass spectrometer. The resolution was set to scan 150-2000 m/z in positive ion mode at a resolution of 100K. A phthalate ion (214.089630) was used as a lock mass. Analysis was performed using Thermo Qual browser software. The samples were dissolved in either chloroform or methanol to give a concentration of approximately 1 mg mL^{-1}.

6.2.4 High-Performance Liquid Chromatography (HPLC)

The final indoxyl β-D-glycosides were analysed for their purity using an Agilent 1100 HPLC equipped with evaporative light scattering detector (ELSD). The column used for the separation was Prevail™ Carbohydrate ES HPLC column (Grace Davison Discovery Sciences), with dimensions of 53 mm x 7.0 mm. Free fluorinated indoxyl glycosides were eluted with 0.1% (v/v) formic acid in water (A) and acetonitrile (B). For five minutes, a solvent system of A = 0.1% (v/v) formic acid in water and B = MeCN was used with a flow rate of 1.5 mL/min. The derivatives were eluted with a gradient system of B = 5% for 2 minutes, increasing to 95% over 10 min, isocratic at 95% for 7 min, decreasing at 5% for 8 min and isocratic at 5% for 3 min. The gradient system method was used to detect any impurities such as hydrolysed sugar or dimerised chromophore. The wavelength used was according to the λ_{max} of each compound. The instrument was equipped with an ELSD that was used to detect non-UV absorbant compounds such as the hydrolysed sugars.

6.3 Microbiology

6.3.1 Microorganism Strain List

A list of microorganisms (including their origins) used in this programme is provided in **Tables 30a-b**.

Table 30a. A list of Gram-positive bacteria used in this project.

Microorganisms	OCC References	Culturre Collection References
Bacillus cereus	754	NCTC 2599, ATCC 14579
Bacillus licheniformis	922	NCTC 10341, ATCC 14580, CMCC 2620, NCIMB 9375 (651)
Bacillus subtilis	214	NCTC 10400, ATCC 6633
Enterococcus faecalis	501	NCTC 775, ATCC 19433
Enterococcus faecalis	640	NCTC 12697, ATCC 29212
Enterococcus faecium	220	ATCC 19434, NCTC 7171 (498)
Staphylococcus aureus	198	ATCC 25923
Staphylococcus aureus	638	ATCC 29213
Staphylococcus aureus v. oxford	100	NCTC 6571, ATCC 15305
Staphylococcus epidermis	919	ATCC 12228
Staphylococcus haemolyticus	2223f	Wildtype from Prince of Wales Hospital, Bridgend
Staphylococcus saprophyticus	2079	NCTC 7292, ATCC 15305
Streptococcus agalactiae GBS	762	NCTC 8181, ATCC 13813
Streptococcus pneumoniae	1548	ATCC 6305
Streptococcus pyogenes	624	ATCC 19615
Streptococcus viridans	1683	ATCC 1080

Abbreviations: American Type Culture Collection, ATCC; National Collection of Type Cultures, NCTC; National Collection of Industrial Food and Marine Bacteria, NCIMB.

Table 30b. A list of Gram-negative bacteria used in this project.

Microorganisms	OCC References	Culturre Collection References
Burkholderia cepacia	770	ATCC 25416, NCTC 10743 (1337)
Citrobacter freundii	370	NCTC 9750, ATCC 8090
Citrobacter freundii	851	Oxoid stock culture Unknown prepared from beads 28th September 2010
Cronobacter sakazakii	1888	NCTC 11467, ATCC 29544
Enterobacter aerogenes	720	NCTC 10006, ATCC 29544
Enterobacter cloacae	760	ATCC 13047 (954)
Escherichia coli	402	NCTC 9001, ATCC 8739
Escherichia coli	199	ATCC 25922
Escherichia coli	481	NCTC 12923, ATCC 8739
Escherichia hermanii	1892	NCTC 1219, ATCC 33650
Klebsiella pneumoniae	411	NCTC 11228, ATCC 29665
Klebsiella pneumoniae	758	NCTC 9633, ATCC 13883
Pseudomonas aeruginosa	201	NCTC 12903, ATCC 27853
Pseudomonas aeruginosa	1119	NCTC 9027
Salmonella Abony	1919	ATCC BAA-2162
Salmonella Dublin	627	OCC Reference 627
Salmonella Enteritidis	723	ATCC 13076, ATCC 25928
Salmonella Typhimurium	722	ATCC 13880, NCTC 10211 (1584)
Salmonella Typhimurium	853	CMCC 1792
Salmonella Virchow	703	NCTC 5742
Serratia marcescens	217	ATCC 13880, NCTC 10211 (1584)

6.4 Experimental methods and results of the precursor compounds prior to glycosidation

6.4.1 Synthesis of 1,2,3,4-tetra-O-acetyl-α,β-L-rhamnopyranose (33)

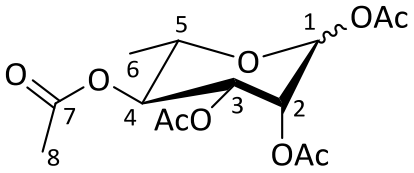

Under an argon atmosphere, the L-(+)-rhamnose monohydrate (5.04 g, 27.67 mmol) was dissolved in anhydrous DCM (30 mL), followed by the addition of anhydrous pyridine (20.0 mL, 247.28 mmol) and acetic anhydride (23.0 mL, 243.31 mmol). The reaction was left to stir for 1 hour, after which time the reaction deemed complete by TLC (1:1 PE 40-60:EA, R_f product **26** = 0.3). The reaction was quenched with ice-water (50 mL) and extracted with DCM (3 x 50 mL). The combined organic extracts were washed with 1M HCl (3 x 150 mL), water (2 x 150 mL), sat. NaCl (1 x 150 mL), water (2 x 150 mL), The collected organic extract was dried over $MgSO_4$, filtered and evaporated *in vacuo* to afford compound **33** as a colourless syrup in an α:β ratio of 3:1 (9.10 g, 28.24 mmol, 95% yield). The product was prepared before by Timmons and Jakeman.[204] **^{1}H NMR ($CDCl_3$, 400 MHz):** δ ppm = **α diastereomer**: 6.02 (1H, d, $^3J_{H\text{-}H}$ = 1.5 Hz, H-1), 5.31 (1H, dt, $^3J_{H\text{-}H}$ =6.5 Hz and 3.5 Hz, H-3), 5.25 (1H, dd, $^3J_{H\text{-}H}$ = 3.0 Hz and $^3J_{H\text{-}H}$ = 2.0 Hz H-2), 5.14 (1H, d, $^3J_{H\text{-}H}$ = 10.0 Hz, H-4), 3.94 (1H, dd, $^3J_{H\text{-}H}$ = 6.5 Hz and d, $^3J_{H\text{-}H}$ = 15.5 Hz, H-5), 2.17 (3H, s, H-8), 2.16 (3H, s, H-8), 2.07 (3H, s, H-8), 2.01 (3H, s, H-8) and 1.30 (3H, d, s, $^3J_{H\text{-}H}$ = 6.5 Hz, H-6). **β diasteoisomer:** 5.84 (1H, d, $^3J_{H\text{-}H}$ = 1.0 Hz, H-1), 5.48 (1H, br. s, H-2), 5.10-5.08 (1H, m, H-3, H-4), 3.67 (1H, d, $^3J_{H\text{-}H}$ = 6.0 Hz and $^3J_{H\text{-}H}$ = 12.0 Hz, H-5), 3.21 (3H, s, H-8), 2.21 (3H, s, H-8), 2.10 (3H, s, H-8), 2.07 (3H, s, H-8), 2.00 (3H, s, H-8) and 1.24 (3H, s, $^3J_{H\text{-}H}$ = 6.0 Hz, H-6). **^{13}C NMR ($CDCl_3$, 100 MHz):** δ ppm = **α diastereomer:** 170.10 (C-7), 169.95 (C-7), 169.83 (C-7), 169.39 (C-7), 90.65 (C-1), 70.48 (C-4), 68.78 (C-3), 68.73 (C-2) 68.65 (C-5), 20.92 (C-8), 20.80 (C-8), 20.77 (C-8) and

20.70 (C-8). **β diasteoisomer:** 170.31 (C-7), 169.92 (C-7), 169.95 (C-7), 168.50 (C-7), 90.33 (C-1), 71.51 (C-4), 70.72 (C-3), 70.26 (C-4), 68.73 (C-2), 68.53 (C-5), 20.92 (C-8), 20.80 (C-8), 20.75 (C-8) and 20.59 (C-8). **IR_{Vmax}:** cm^{-1} = 2886 (C-H, s, w), 1742 (C=O, s, m), 1368 (sp^3 C-H, s, m) and 1209 (C-O, s, s). **FTMS (ESI):** m/z calculated for $(M+H)^+$ $C_{14}H_{20}O_9Na$ requires 355.1000, found 355.1011.

6.4.2 2,3,4-tri-O-acetyl-α-rhamnopyranosyl bromide (34)

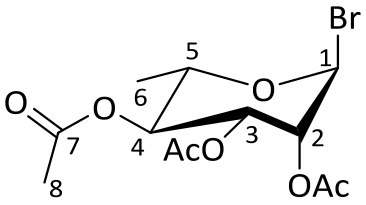

Under an argon atmosphere, the materials were dissolved in anhydrous DCM (30 mL): compound **33** (4.13 g, 12.81 mmol), HBr (33% in acetic acid) (17.0 mL, 294.15 mmol). The reaction was stirred for 45 min at rt. After this time, TLC analysis (1:1 PE 40-60:EA) indicated the formation of product (R_f = 0.54). The reaction was quenched with water (20 mL) and was extracted with DCM (3 x 20 mL). The combined organic extracts were washed with water (1 x 80 mL), sat. $NaHCO_3$ (1 x 80 mL) and water (1 x 80 mL). The collected organic extract was dried over $MgSO_4$, filtered and evaporated *in vacuo* to afford compound **34** as a pale yellow syrup with 87% (3.96 g, 12.30 mmol) yield. The product was prepared before by Timmons and Jakeman.[204] **^{1}H NMR ($CDCl_3$, 400 MHz):** δ ppm = 6.27 (1H, s, H-1), 5.67 (1H, dd, $^3J_{H-H}$ = 10.0 Hz and, $^3J_{H-H}$ = 3.5 Hz, H-3), 5.45 (1H, dd, $^3J_{H-H}$ = 3.5 Hz and $^3J_{H-H}$ = 1.0 Hz, H-2), 5.16 (1H, t, $^3J_{H-H}$ = 10.0 Hz, H-4), 4.16-4.08 (1H, m, H-5), 2.17 (C-8), 2.09 (C-8), 2.01 (C-8) and 1.29 (1H, d, $^3J_{H-H}$ = 6.0 Hz, H-6). **^{13}C NMR ($CDCl_3$, 100 MHz):** δ ppm = 169.90 (C-7), 169.81 (C-7), 169.67 (C-7), 83.71 (C-1), 72.46 (C-2), 71.12 (C-5), 70.32 (C-4), 67.94 (C-3), 20.80 (C-8), 20.76 (C-8), 20.62 (C-8) and 16.98 (C-6). **IR_{Vmax}:** cm^{-1} =2989 (C-H, s, w), 1742 (C=O, *s*, s), 1369 (sp^3 C-H, s, m) and 1207 (C-O, *s*, s).

6.4.3 Synthesis of allyl bromoacetate (19)

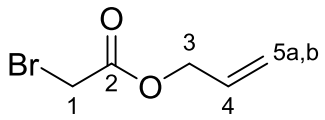

Under an argon atmosphere, the bromoacetyl bromide (29.00 mL, 143.68 mmol) was dissolved in anhydrous DCM (40 mL) at 0 °C whilst stirring. To the stirred solutions, K_3PO_4 (70.96 g, 334.29 mmol) was added portion-wise, followed by drop-wise addition of allyl alcohol (15.00 mL, 258.26 mmol). The reaction was left to stir for 0 °C for 45 minutes. After this time, the ice-bath was removed and the reaction was warmed to room temperature for 1 hour and 15 minutes. TLC analysis (9:1 PE 40-60:EA) indicated the formation of product (R_f = 0.64). The reaction was diluted with DCM (20 mL), and was subsequently quenched by adding distilled water. The aqueous phase was extracted with DCM (3x 75 mL) and the combined organic layer was washed with the following: 0.5 M HCl (1 x 75 mL) and distilled water (1 x 75 mL). The collected organic extract was dried over $MgSO_4$, filtered and dried *in vacuo* to give the key reagent **19** as a colourless yellow liquid product with 98% yield (38.61 g, 215.67 mmol). The product was prepared before by Bolsønes and co-workers.[161] **^{1}H NMR ($CDCl_3$, 400 MHz):** δ ppm = 5.93 (1H, ddd, $^3J_{H\text{-}H}$ = 16.5 Hz, $^3J_{H\text{-}H}$ = 11.0 Hz and $^3J_{H\text{-}H}$ = 5.5 Hz, H-4), 5.37 (1H, d, $^3J_{H\text{-}H}$ = 16.0 Hz, H-5a), 5.29 (1H, d, $^3J_{H\text{-}H}$ = 11.0 Hz, H-5b), 4.68 (2H, d, $^3J_{H\text{-}H}$ = 5.5 Hz, H-3) and 3.87 (1H, s, H-1). **^{13}C NMR ($CDCl_3$, 100 MHz):** δ ppm = 166.90 (C-2), 131.20 (C-4), 119.17 (C-5), 66.72 (C-3) and 25.72 (C-1). **IR_{Vmax}:** cm^{-1} = 3022 and 2952 (saturated C-H, *s*, w), 1732 (C=O, *s*, s) and 1275 (C-O, *s*, s).

6.4.4 General procedure: Formation of isatoic anhydride using pyridine and triphosgene

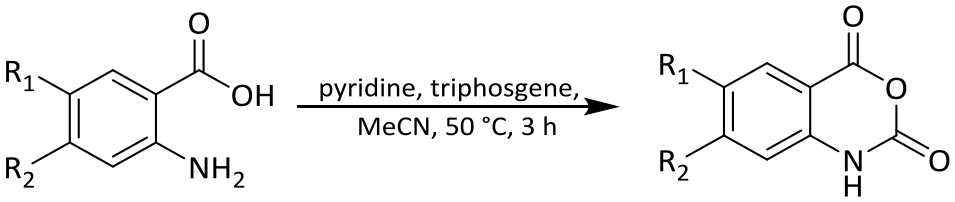

17a: R_1=H, R_2=H
17b: R_1=F, R_2=H
17c: R_1=F, R_2=F
17d: R_1=H, R_2=CF_3

18a: R_1=H, R_2=H
18b: R_1=F, R_2=H
18c: R_1=F, R_2=F
18d: R_1=H, R_2=CF_3

Using anhydrous solvents for the reaction, anthranilic acid (57.87-171.98 mmol, 1.00 mol equiv.) was dissolved in MeCN (20-35 mL) under an argon atmosphere. From separate syringes, a solution of triphosgene (3.00-3.30 mol equiv.) in DCM (10-20 mL) and pyridine (3.9-4.0 mol. equiv.) were added dropwise at the same time into the solution. The reaction was left to stir for approximately 3 hours at 45 °C. After this time, TLC analysis (9:1 DCM:MeOH) indicated the formation of product (R_f = 0.6-0.67). The reaction was quenched with the addition of water. The product was collected by suction filtration and was washed with water thoroughly and chilled DCM. The crude product was dried under high vacuum and was further dried in a freeze-dryer. Purification was not required at this stage.

6.4.4.1 Synthesis of 3,1-benzoxazine-2,4(1*H*)-dione (18a)

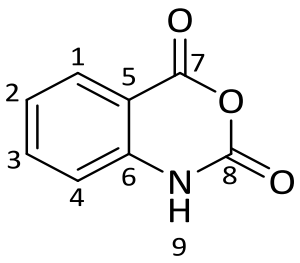

Compound **18a** was prepared according to **Section 6.4.4** general procedure using 2-aminobenzoic acid **17a** (10.16 g, 74.08 mmol), triphosgene (7.46g. 25.19 mmol), pyridine (11.60 mL, 143.42 mmol), MeCN (20 mL) and DCM (10 mL). R_f = 0.60 (9:1 DCM:MeOH). Yield: 84% (10.11 g, 34.02 mmol), white solid product. The product was prepared before by Huang *et al.*[159] **^{1}H NMR (DMSO-*d*$_6$, 400 MHz):** δ ppm = 11.72 (1H, s, H-9), 7.90 (1H, d, $^3J_{H\text{-}H}$ = 8.0 Hz, H-1), 7.72 (1H, t, $^3J_{H\text{-}H}$ = 7.0 Hz, H-3), 7.23 (1H, t, $^3J_{H\text{-}H}$ = 7.5 Hz, H-2) and 7.14 (1H, d, $^3J_{H\text{-}H}$ = 8.0 Hz, H-4). **^{13}C NMR (DMSO-*d*$_6$, 100 MHz):** δ ppm = 159.82 (C-7), 147.04, (C-8), 141.34 (C-6), 136.88 (C-3), 128.88 (C-1), 123.46 (C-4), 115.28 (C-2) and 110.19 (C-5). **IR $_{Vmax}$:** cm^{-1} = 3107.50 and 3070.00 (N-H, *s*, w), 3070.00 (Aromatic C-H, *s*, w), 1723.60 (C=O, *s*, m), 1614.23 and 1603.53 (Aromatic C=C, *s*, m,), 1511.96 (N-H, *b*, m), 1350.25 (C-O, *s*, s) and 747.63 (Aromatic, *d*, s). **FTMS (ESI):** m/z calculated for $(M+H)^+$ $C_8H_6O_3N$ requires 164.0353, found 164.0342.

6.4.4.2 Synthesis of 6-fluoro-2*H*-3,1-benzoxazine-2,4(1*H*)-dione (18b)

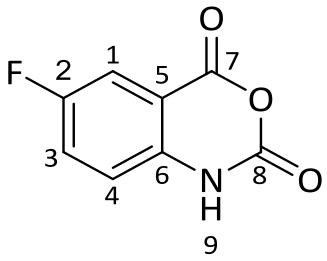

Compound **18b** was prepared according to **Section 6.4.4** general procedure using 2-amino-5-fluorobenzoic acid **17a** (26.08 g, 171.98 mmol), triphosgene (18.37 g, 62.04 mmol), pyridine (28 mL, 346.19 mmol), MeCN (60 mL) and DCM (20 mL). R_f = 0.62 (9:1 DCM:MeOH). Yield: 92% (28.71 g, 158.51 mmol), yellow solid product. The product was prepared before by Gupta and co-workers.[282] **^{1}H NMR (DMSO-*d*$_6$, 400 MHz):** δ ppm = 11.78 (1H, s, H-9), 7.67 (1H, dd, $^3J_{F\text{-}H}$ = 8.5 Hz and $^4J_{H\text{-}H}$ = 4.0 Hz, H-1), 7.62 (1H, dd, $^3J_{H\text{-}H}$ = 8.5 Hz and $^4J_{F\text{-}H}$ = 3.0 Hz, H-4) and 7.17 (1H, dd, $^3J_{F\text{-}H}$ = 9.0 Hz and $^4J_{H\text{-}H}$ = 4.0 Hz, H-3). **^{13}C NMR (DMSO-*d*$_6$, 100 MHz):** δ ppm = 159.14 (d, $^4J_{C\text{-}F}$ = 3.5 Hz, C-7), 157.28 (d, $^1J_{C\text{-}F}$ = 240.5 Hz, C-2), 146.74 (C-8), 138.06 (d, $^4J_{C\text{-}F}$ = 1.5 Hz, C-6), 124.73 (d, $^2J_{C\text{-}F}$= 24.5 Hz, C-1), 117.53 (d, $^3J_{C\text{-}F}$ = 9.0 Hz, C-4), 113.93 (d, $^2J_{C\text{-}F}$ 24.0 Hz, C-3) and 111.41 (d, $^3J_{C\text{-}F}$ = 9.0 Hz, C-5). **^{19}F NMR (DMSO-*d*$_6$, 376 MHz):** δ ppm = -118.81. **IR$_{Vmax}$:** cm^{-1} = 3185 and 3120 (N-H, w, w), 3082 (Aromatic C-H, *s*, w), 1758 (C=O, *s*, s), 1516, 1502 and 1488 (Aromatic C=C, *s*, w), 1426 (N-H, *b*, s), 1345 (C-O, *s*, s), 1040 (C-F, *s*, s), and 762 (Aromatic C-H, *d*, s). **FTMS (ESI):** m/z calculated for $(M+H)^+$ $C_8H_3{}^{19}FNO_3$ required 180.0102, found 180.0102.

6.4.4.3 Synthesis of 6,7-difluoro-2*H*-3,1-benzoxazine-2,4(1*H*)-dione (18c)

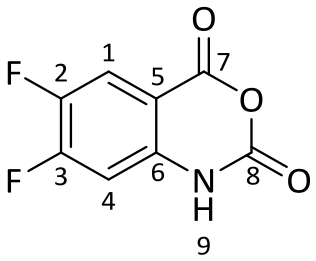

Compound **18c** was prepared according to **Section 6.4.4** general procedure using 2-amino-4,5-difluorobenzoic acid **17c** (10.02 g, 57.87 mmol), triphosgene (5.98 g, 20.19 g mol^{-1}), pyridine (9.50 mL, 117.45 mmol), MeCN (30 mL) and DCM (10 mL). R_f = 0.50 (9:1 DCM:MeOH). Yield: 77% (8.84 g, 44.39 mmol), purple-grey solid product. The product was prepared before by Verma *et al.*[283] **^{1}H NMR (DMSO-*d*$_6$, 400 MHz):** δ ppm = 11.89 (1H, s, H-9), 7.97 (1H, t, $^{3}J_{H\text{-}F}$ = 9.5 Hz, H-1) and 7.09 (1H, q, $^{3}J_{H\text{-}F}$ = 10.5 Hz and $^{4}J_{H\text{-}F}$ = 6.5 Hz, H-4). **^{13}C NMR** (**DMSO-*d*$_6$, 100 MHz**): δ ppm = 158.39 (d, $^{4}J_{C\text{-}F}$ = 3.0 Hz, C-7), 154.72 (dd, $^{1}J_{C\text{-}F}$ = 242.0 Hz and $^{2}J_{C\text{-}F}$ = 15.0 Hz, C-2), 146.69 (C-8), 145.76 (dd, $^{1}J_{C\text{-}F}$ = 244.0 Hz and $^{2}J_{C\text{-}F}$ = 13.0 Hz, C-3), 139.30 (dd, $^{3}J_{C\text{-}F}$ = 11.5 Hz and $^{4}J_{C\text{-}F}$ = 2.0 Hz, C-6), 117.22 (dd, $^{2}J_{C\text{-}F}$ = 20.0 Hz and $^{3}J_{C\text{-}F}$ = 2.0 Hz, C-1), 107.17 (dd, $^{3}J_{C\text{-}F}$ = 6.5 Hz and $^{4}J_{C\text{-}F}$ = 3.0 Hz, C-5), 104.23 (d, $^{2}J_{C\text{-}F}$ = 22.5 Hz, C-6) and 107.17 (d, $^{1}J_{C\text{-}F}$ = 7.0 Hz, C-4). **^{19}F NMR (DMSO-*d*$_6$, 376 MHz):** δ ppm = -124.06 and -143.16. **IR$_{vmax}$:** cm^{-1} = 3188.99 and 3124.06 (N-H, *s*, w), 3059 (Aromatic C-H s, w), 1759 (C=O *s*, s), 1639 and 1622 (Aromatic C=C, *s*, s), 1512 (N-H bending, *b*, s), 1335 (C-O, *s*, s), 1022 (C-F, *s*, s), and 750 (Aromatic C-H**,** *s*, **s**). **FTMS (ESI):** m/z calculated for $(M+H)^+$ $C_8H_2{}^{19}F_2NO_3$ required 198.0008, found 198.0008.

6.4.4.4 Synthesis of 7-(trifluoromethyl)-2*H*-3,1-benzoxazine-2,4(1*H*)-dione (18d)

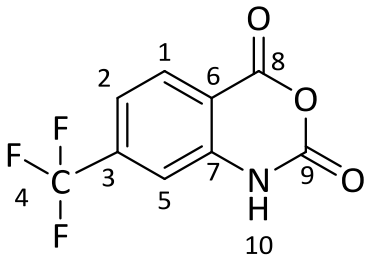

Compound **18d** was prepared according to **Section 6.4.4** general procedure using 2-amino-4-(trifluoromethyl)benzoic acid **17a** (25.01 g, 121.19 mmol), triphosgene (13.46 g, 45.45 mmol), pyridine (20 mL, 247.28 mmol), MeCN (35 mL) and DCM (18 mL). R_f = 0.68 (9:1 DCM:MeOH). Yield: 75% (21.03 g, 90.99 mmol), yellow solid product. The product was prepared before by Verma and co-workers.[283] **^{1}H NMR (DMSO-*d*$_6$, 400 MHz):** δ ppm = 11.98 (1H, s, H-10), 8.11 (d, $^3J_{H\text{-}H}$ = 8.0 Hz, H-1) 7.55 (1H, dd, $^3J_{H\text{-}H}$ = 8.0 Hz and $^4J_{H\text{-}F}$ = 1.0 Hz, H-2) and 7.39 (1H, s, H-5). **^{13}C NMR (DMSO-*d*$_6$, 100 MHz): δ ppm** = 159.02 (C-8), 146.66 (C-9), 141.77 (C-7), 134.96 (q, $^2J_{C\text{-}F}$ = 32.5 Hz, C-3), 130.47 (C-1), 123.01 (d, $^1J_{C\text{-}F}$ = 272.5 Hz, C-4), 119.36 (d, $^3J_{C\text{-}F}$ = 3.5 Hz, C-2), 113.97 (C-6) and 111.99 (d, $^3J_{C\text{-}F}$ = 3.5 Hz, C-5). **^{19}F NMR (DMSO-*d*$_6$, 376 MHz):** δ ppm = -62.46. **IR$_{Vmax}$:** cm^{-1} = 3191 and 3152 (N-H, *s*, w), 3046 (Aromatic C-H, s, w), 1771 (C=O, *s*, s), 1728 (N-H, *s*, s), 1634 and 1605 (Aromatic C=C, *s*, m), 1529 (N-H, *b*, s), 1315.81 (C-O, *s*, s), 1022 (C-F, *s*, s), and 749 (Aromatic C-H, *d*, s). **FTMS (ESI):** m/z calculated for $(M+H)^+$ $C_9H_5{}^{19}F_3NO_3$ required 232.0227, found 232.0216.

6.4.5 General procedure: *N*-alkylation of isatoic anhydride using sodium hydride

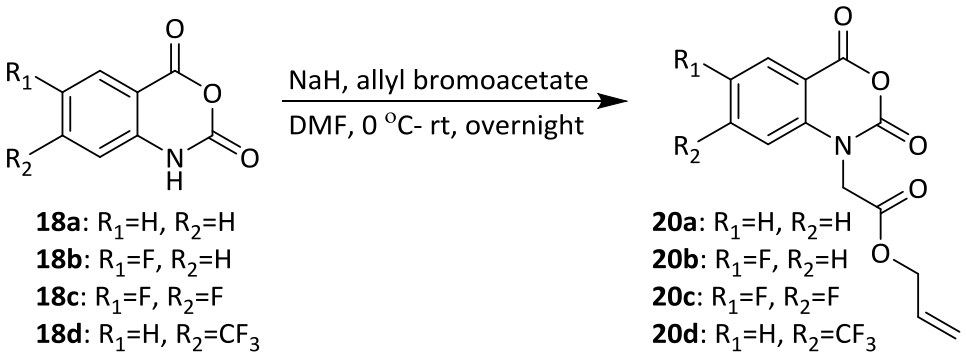

18a: R_1=H, R_2=H
18b: R_1=F, R_2=H
18c: R_1=F, R_2=F
18d: R_1=H, R_2=CF_3

20a: R_1=H, R_2=H
20b: R_1=F, R_2=H
20c: R_1=F, R_2=F
20d: R_1=H, R_2=CF_3

Under an argon atmosphere, isatoic anhydride (25.67-45.47 mmol, 1.00 mol equiv.) was dissolved in anhydrous DMF, and the solution was cooled in an ice bath. To the cooled solution, NaH (in 57-63% oil dispersion, 1.15 mol. equiv.) was added portionwise. The reaction was left to stir for 45 minutes. After this time, the ice bath was removed and the reaction mixture was warmed to room temperature. Then, allyl bromoacetate **19** (1.20 mol equiv.) was added to the mixture, and the reaction was left to stir overnight at room temperature. After the reaction was stirred overnight, TLC analysis (2:1 PE 40-60: EtOAc) indicated the formation of product (R_f = 0.52-0.83). After this time, water was added to quench the mixture. The crude product was collected via suction filtration and was washed thoroughly with water. Purification was not needed for this step.

6.4.5.1 Synthesis of allyl 2-(2,4-dioxo-2*H*-benzo[*d*][1,3]oxazin-1(4*H*)-yl)acetate (20a)

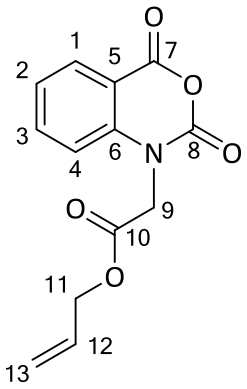

Compound **20a** was prepared according to **Section 6.4.5** general procedure using compound **18a** (9.07 g, 30.52 mmol), sodium hydride (1.81 g, 75.41 mmol) allyl bromoacetate **19** (8.30 mL, 69.63 mmol) and DMF (20 mL). R_f = 0.52 (2:1 PE 40-60:EA). Yield = 97% (14.03 g, 53.71 mmol), yellow solid product. **^{1}H NMR (DMSO-*d*$_6$, 100 MHz), 400 MHz):** δ ppm = 8.06 (1H, dd, $^3J_{H\text{-}H}$ = 8.0 Hz and $^4J_{H\text{-}H}$ = 1.5 Hz, H-1), 7.85 (1H, ddd, $^3J_{H\text{-}H}$ = 8.5 Hz and 7.5 Hz, $^4J_{H\text{-}H}$ = 1.5 Hz, H-3), 7.46 (1H, d, $^3J_{H\text{-}H}$ = 8.5 Hz, H-4), 7.38 (1H, d, $^3J_{H\text{-}H}$ = 7.5 and 7.5 Hz, H-2), 5.93 (1H, ddd, $^3J_{H\text{-}H}$ = 17.0 Hz, $^3J_{H\text{-}H}$ = 10.5 Hz and $^3J_{H\text{-}H}$ = 5.5 Hz, H-12), 5.33 (1H, dd, $^3J_{H\text{-}H}$ = 17.0 Hz and $^2J_{H\text{-}H}$ = 1.5 Hz, H-13a), 5.24 (1H, dd, $^3J_{H\text{-}H}$ =10.5 Hz and $^2J_{H\text{-}H}$ = 1.5 Hz, H-13b), 4.97 (2H, s, H-9), 4.68 (2H, dt, $^3J_{H\text{-}H}$ = 5.5 Hz and $^4J_{H\text{-}H}$ = 1.5 Hz, H-11). **^{13}C NMR (DMSO-*d*$_6$, 100 MHz), 100 MHz):** δ ppm = 167.25 (C-10), 158.30 (C-7), 147.73 (C-8), 141.20 (C-6), 137.42 (C-3), 131.95 (C-12), 129.73 (C-1), 124.17 (C-2), 118.14 (C-13), 114.71 (C-4), 111.14 (C-5), 65.62 (C-11), 46.66 (C-9). **IR$_{Vmax}$**: cm^{-1} = 3012 (Aromatic C-H, *s*, w), 2953, 2923 and 2853 (Saturated C-H, *s*, w), 1727 (C=O, *s*, s), 1606 (Tertiary amide, *s*, m), 1594 (C=C, *s*, m), 1374.55 (C-O, *s*, m), 870 and 854 (C=C, *d*, m), 751.34 (Aromatic C-H, *d*, s). **FTMS (ESI)**: m/z calculated for $(M+H)^+$ $C_{13}H_{12}NO_5$ required 262.0720, found 262.0710, and $(M+Na)^+$ $C_{13}H_{11}NO_5Na$ required 284.0540, found 284.0529.

6.4.5.2 Synthesis of allyl 2-(6-fluoro-2,4-dioxo-2*H*-benzo[*d*][1,3]oxazin-1(4*H*)-yl)acetate (20b)

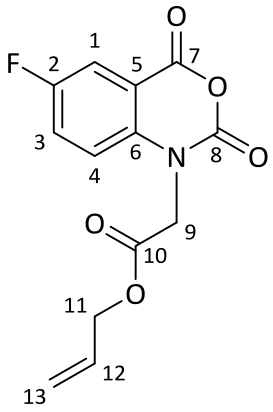

Compound **20b** was prepared according to **Section 6.4.5** general procedure using compound **18b** (25.67 g, 141.73 mmol), sodium hydride (5.21 g, 217.08 mmol) allyl bromoacetate **19** (20.00 mL, 167.57 mmol) and DMF (20 mL). R_f = 0.52 (2:1 PE 40-60:EA). Yield = 94% (37.10 g, 132.87 mmol), light yellow solid product. **^{1}H NMR (DMSO-d_6, 400 MHz):** δ ppm = 7.82 (1H, dd, $^3J_{H\text{-}F}$ = 8.0 Hz and $^4J_{H\text{-}H}$ = 3.0 Hz, H-1), 7.77 (dd, 1H, $^3J_{H\text{-}H}$ = 9.0 Hz and $^4J_{H\text{-}F}$ = 3.0 Hz, H-3), 7.54 (1H, dd, $^3J_{H\text{-}F}$ = 9.0 Hz and $^3J_{H\text{-}H}$ = 4.0 Hz, H-4), 5.92 (1H, ddd, $^3J_{H\text{-}H}$ = 17.0 Hz, $^3J_{H\text{-}H}$= 10.5 Hz, $^3J_{H\text{-}H}$ =5.5 Hz, H-12), 5.34 (1H, dd, $^3J_{H\text{-}H}$ = 17.0 Hz and $^2J_{H\text{-}H}$ = 1.5 Hz, H-13a), 5.24 (1H, dd, $^3J_{H\text{-}H}$ = 10.5 Hz and $^2J_{H\text{-}H}$ = 1.5 Hz, H-13b), 4.97 (2H, s, H-9) and 4.68 (2H, d, $^3J_{H\text{-}H}$ = 5.5 Hz, H-11). **^{13}C NMR (DMSO-d_6, 100 MHz):** δ ppm = 167.18 (C-10), 157.87 (d, $^1J_{C\text{-}F}$ = 242.0, C-2), 157.51 (d, $^4J_{C\text{-}F}$ = 3.0 Hz, C-7), 147.46 (C-8), 137.97 (d, $^4J_{C\text{-}F}$ = 2.0 Hz, C-6) 65.65 (C-9), 131.93 (C-12), 124.81 (d, $^2J_{C\text{-}F}$ = 24.0 Hz, C-1), 118.18 (C-13), 117.37 (d, $^3J_{C\text{-}F}$ = 8.0 Hz, C-4), 114.96 (d, $^2J_{C\text{-}F}$ = 24 Hz, C-3), 112.69 (d, $^3J_{C\text{-}F}$ = 8.5 Hz, C-5), 65.65 (C-11) and 45.99 (C-7). **^{19}F NMR (DMSO-d_6, 376 MHz):** δ ppm = -118.38. **IR$_{Vmax}$:** cm^{-1} = 3079 (Aromatic C-H, *s*, w), 2976.99, 2924 and 2853 (Saturated C-H, *s*, w), 1732 (C=O, *s*, s), 1626 (Tertiary amide, *s*, m), 1604 (C=C, *s*, m), 1341 (C-O, *s*, m), 1086 (C-F, *s*, m), 949 and 923 (C=C *d*, s), and 767 (Aromatic *d*, s). **FTMS (ESI):** m/z calculated for $(M+H)^+$ $C_{13}H_{11}{}^{19}FNO_5$ required 280.0627, found 280.0616 and $(M+Na)^+$ $C_{13}H_{10}O_5{}^{19}FNa$ required 302.0446, found 302.0434.

6.4.5.3 Synthesis of allyl 2-(6,7-difluoro-2,4-dioxo-2*H*-benzo[*d*][1,3]oxazin-1(4*H*)-yl)acetate (20c)

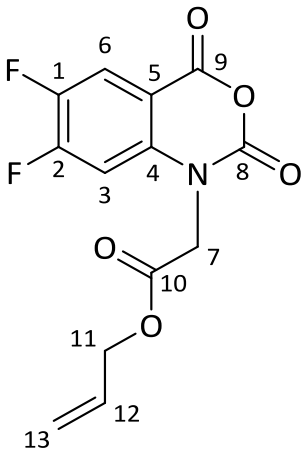

Compound **20c** was prepared according to **Section 6.4.5** general procedure using compound **18c** (7.51 g, 37.71 mmol), sodium hydride (1.14 g, 47.5 mmol), allyl bromoacetate **19** (5.54 mL, 46.42 mmol) and DMF (30 mL). R_f = 0.54 (2:1 PE 40-60:EA). Yield = 87% (9.76 g, 32.84 mmol), light grey solid product. **^{1}H NMR (DMSO-*d*$_6$, 400 MHz):** δ ppm = 8.11 (H, t, $^{3}J_{H\text{-}F}$ = 9.0 Hz, H-1), 7.82 (1H, dd, $^{3}J_{H\text{-}F}$ = 12.5 Hz and $^{4}J_{H\text{-}F}$ = 6.5 Hz, H-4), 5.93 (1H, ddd, $^{3}J_{H\text{-}H}$ = 16.0 Hz, $^{3}J_{H\text{-}H}$ = 10.5 Hz and $^{3}J_{H\text{-}H}$ = 4.5 Hz, H-12), 5.35 (1H, dd, $^{3}J_{H\text{-}H}$ = 16.0 Hz and $^{2}J_{H\text{-}H}$ = 1.5 Hz, H-13a), 5.25 (1H, dd, $^{2}J_{H\text{-}H}$ = 10.5 Hz and $^{4}J_{H\text{-}H}$ = 1.5 Hz, H-13b), 4.93 (2H, s, H-9) and 4.68 (1H, d, $^{3}J_{H\text{-}H}$ = 5.5 Hz, H-11). **^{13}C NMR (DMSO-*d*$_6$, 100 MHz):** δ ppm = 166.97 (C-10) 156.79 (d, $^{4}J_{C\text{-}F}$ = 1.0 Hz, C-7), 155.01 (dd, $^{1}J_{C\text{-}F}$ = 242.0 Hz and $^{2}J_{C\text{-}F}$ = 14.0 Hz, C-2), 147.32 (C8), 145.91 (dd, $^{1}J_{C\text{-}F}$ = 233.0 Hz and $^{2}J_{C\text{-}F}$ = 14.0 Hz, C-3), 139.48 (dd, $^{3}J_{C\text{-}F}$ = 9.5 Hz and $^{4}J_{C\text{-}F}$ = 1.5 Hz, C-6), 131.93 (C-12), 118.16 (C-13), 118.09 (dd, $^{2}J_{C\text{-}F}$ = 16.0 Hz and $^{3}J_{CF}$ = 2.0 Hz, C-1), 108.23 (dd, $^{3}J_{C\text{-}F}$ = 4.0 Hz and $^{4}J_{C\text{-}F}$ = 3.0 Hz, C-5), 105.26 (d, $^{2}J_{C\text{-}F}$ = 25.0 Hz, C-4), 65.70 (C-11) and 46.36 (C-8). **^{19}F NMR (DMSO-*d*$_6$, 376 MHz):** δ ppm = -123.11 and -142.50. **IR$_{Vmax}$:** cm^{-1} = 3069 (Aromatic C-H, *s*, w), 2954 2922 and 2852 (Saturated C-H, *s*, m), 1734 (C=O, *s*, s), 1651 (Tertiary amide, *s*, m), 1637 (C=C, *s*, m), 1384 (C-O, *s*, s), 1055 (C-F, s, m), 926 and 898 (C=C, *d*, s), and 752 (Aromatic C-H, *d*, s). **FTMS (ESI):** m/z calculated for $(M+H)^{+}$ $C_{13}H_{10}O_5N^{19}F_2$ required 298.0533, found 298.0522.

6.4.5.4 Synthesis of allyl 2-(2,4-dioxo-7-(trifluoromethyl)-2*H*-benzo[*d*][1,3]oxazin-1(4*H*)-yl)acetate (20d)

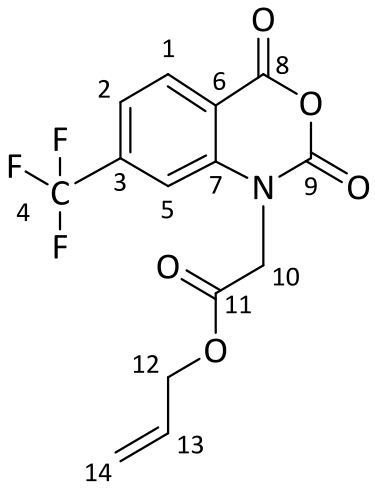

Compound **20** was prepared according to **Section 6.4.5** general procedure using compound **18d** (19.51 g, 45.47 mmol), sodium hydride (3.04 g, 126.67 mmol), allyl bromoacetate (**19**, 12.60 mL, 105.58 mmol) and DMF (40 mL). R_f = 0.83 (2:1 PE 40-60:EA). Yield = 97% (26.70 g, 81.10 mmol), yellow solid product. **^{1}H NMR (DMSO-d_6, 400 MHz):** δ ppm = 8.24 (1H, d, $^3J_{H\text{-}F}$ = 8.0 Hz, H-2), 7.87 (1H, s, H-1), 7.69 (1H, d, $^3J_{H\text{-}F}$ = 8.0 Hz, H-5), 5.92 (1H, ddd, $^3J_{H\text{-}H}$ = 17.0 Hz, $^3J_{H\text{-}H}$ = 10.5 Hz and $^3J_{H\text{-}H}$ = 5.0 Hz, H-13), 5.34 (1H, dd, $^3J_{H\text{-}H}$ = 17.0 Hz and $^2J_{H\text{-}H}$ = 1.5 Hz, H-14a), 5.24 (1H, dd, $^3J_{H\text{-}H}$ = 10.5 Hz and $^2J_{H\text{-}H}$ = 1.5 Hz, H-14b), 5.08 (1H, s, H-12) and 4.69 (2H, d, $^3J_{H\text{-}H}$ = 5.5 Hz, H-10). **^{13}C NMR (DMSO-d_6, 100 MHz):** δ ppm = 166.18 (C-11), 155.53 (C-8), 147.41 (C-7), 141.77 (C-9), 136.18 (q, $^2J_{C\text{-}F}$ = 32.5 Hz, C-3), 131.93 (C-13), 131.12 (C-1), 123.03 (d, $^1J_{C\text{-}F}$ = 272.0 Hz, C-4), 120.28 (d, $^3J_{C\text{-}F}$ = 3.5 Hz, C-2), 117.99 (C-14), 114.89 (C-6), 112.21 (d, $^3J_{C\text{-}F}$ = 4.5 Hz, C-5), 65.60 (C-12) and 46.08 (C-10). **^{19}F NMR (DMSO-d_6, 376 MHz)** δ ppm = -61.84. **IR_{Vmax}:** cm^{-1} = 3069 (Aromatic C-H, *s*, w), 2954, 2923 and 2853 (Saturated C-H, *s*, m), 1739 (C=O, *s*, s), 1651 (Tertiary amide, *s*, w), 1628 (C=C, *s*, m), 1304 (C-O, *s*, s), 1035 (C-F, *s*, m), 983 and 935 (C=C, *d*, m), and 871 (Aromatic C-H, *d,* s). **FTMS (ESI)**: m/z calculated for $(M+H)^+$ $C_{14}H_{10}{}^{19}F_3NO_5Na$ required 352.0414, found 352.0403.

6.4.6 General procedure: Formation of allyl *N*-[allyloxycarbonyl)methyl] anthranilate using sodium hydride

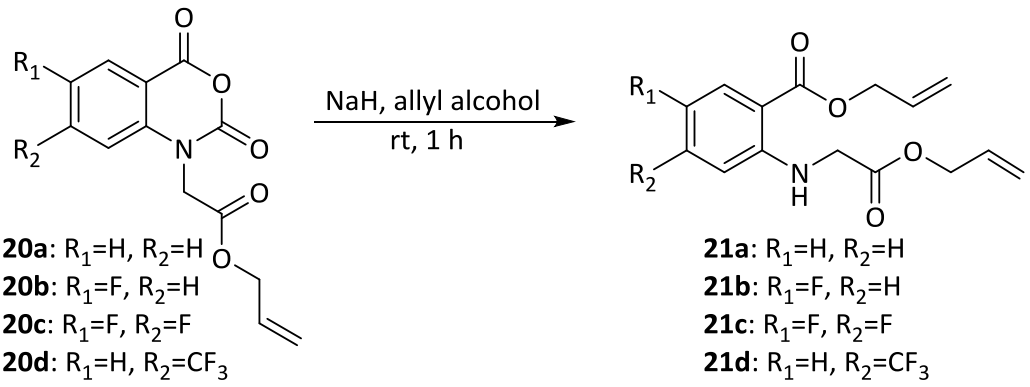

20a: R_1=H, R_2=H
20b: R_1=F, R_2=H
20c: R_1=F, R_2=F
20d: R_1=H, R_2=CF_3

21a: R_1=H, R_2=H
21b: R_1=F, R_2=H
21c: R_1=F, R_2=F
21d: R_1=H, R_2=CF_3

Under an argon atmosphere, NaH (0.3 mol. equiv.) was added portion-wise to a dissolved mixture of the *N*-[allyloxycarbonyl)methyl] isatoic anhydride (1.0 mol. equiv.) in allyl alcohol (25-90 mL). The reaction mixture was left to stir for approximately 2 hours at room temperature, after which time the reaction was deemed complete by TLC analysis (9:2 PE 40-60:EtOAc) (R_f = 0.40-0.75). The reaction mixture was quenched with distilled water. The aqueous phase was extracted with EtOAc three times. The filtrate was washed with water, followed by $NaHCO_3$ and once with water. The combined organic phase were dried with $MgSO_4$, filtered and concentrated *in vacuo*. The crude product was purified using flash column chromatography (9:2 PE 40-60:EtOAc).

6.4.6.1 Synthesis of allyl *N*-[allyloxycarbonyl)methyl]anthranilate (21a)

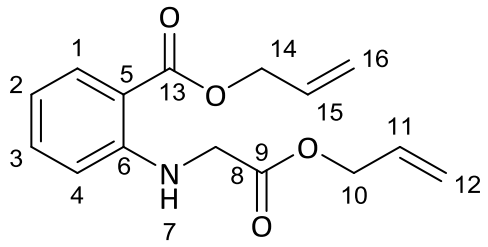

Compound **21a** was prepared according to **Section 6.4.6** general procedure using compound **20a** (12.52 g, 47.93 mmol), sodium hydride (0.43 g, 17.92 mmol) and allyl alcohol (25 mL). R_f = 0.54 (9:2 PE 40-60:EtOAc). Yield = 75% (9.86 g, 35.81 mmol), red-orange liquid product. **^{1}H NMR ($CDCl_3$, 400 MHz):** δ ppm = 8.21 (1H, s, H-7), 7.98 (1H, d, $^3J_{H\text{-}H}$ = 8.0 Hz and $^4J_{H\text{-}H}$ = 1.0 Hz, H-1), 7.37 (1H, ddt, $^2J_{H\text{-}H}$ = 7.0 Hz, $^2J_{H\text{-}H}$ = 7.0 Hz and $^3J_{H\text{-}H}$ = 1.0 Hz, H-3), 6.66 (1H, t, $^3J_{H\text{-}H}$ = 7.5 Hz, H-2), 6.54 (1H, d, $^3J_{H\text{-}H}$ = 8.5 Hz, H-4), 6.04 (1H, ddd, $^3J_{H\text{-}H}$ = 5.5 Hz, $^3J_{H\text{-}H}$ = 11.0 Hz and $^3J_{H\text{-}H}$ = 16.5 Hz, H-15), 5.92 (1H, ddd, $^3J_{H\text{-}H}$ = 5.5 Hz, 11.0 Hz and $^3J_{H\text{-}H}$ = 16.0 Hz, H-11), 5.40 (1H, dd, $^3J_{H\text{-}H}$ = 17.0 Hz and $^2J_{H\text{-}H}$ = 1.5 Hz, H-12a), 5.34 (1H, dd, $^3J_{H\text{-}H}$ = 17.0 Hz and $^2J_{H\text{-}H}$ = 1.0 Hz, H-16b), 5.28 (1H, dd, $^3J_{H\text{-}H}$ = 5.0 Hz and $^2J_{H\text{-}H}$ =1.0 Hz, H-12a), 5.25 (1H, dd, $^3J_{H\text{-}H}$ = 4.0 Hz and $^2J_{H\text{-}H}$ =1.0 Hz, H-12b), 4.79 (2H, d, $^3J_{H\text{-}H}$ = 5.5 Hz, H-14), 4.69 (2H, d, $^3J_{H\text{-}H}$ = 6.0 Hz, H-10) and 4.04 (1H, s, H-8). **^{13}C NMR ($CDCl_3$, 100 MHz):** δ ppm = 170.11 (C9), 167.95 (C-13), 149.99 (C-6), 134.69 (C-3), 132.47 (C-15), 131.80 (C-1), 131.63 (C-11), 118.89 (C-12), 117.99 (C-16), 115.67 (C-2), 111.15 (C-4), 110.92 (C-5), 65.90 (C-10), 65.03(C-14) and 44.97 (C-8). **IR_{Vmax}:** cm^{-1} = 3387 and 3351 (Secondary amide N-H, *s*, m), 3082 (Aromatic C-H, *s*, w), 2940, 2888 and 2845 (Saturated C-H, *s*, w), 1737 (C=O, *s*, s), 1679 (N-H *s*, s), 1649 (C=C, *s*, w), 1679 (Aromatic C=C, *s*, s), 1517 (N-H, *b*, s), 1224 (C-O, *s*, s), 989 and 972 (C=C, *d*, s), and 745 (Aromatic C-H, *d*, s). **FTMS (ESI):** m/z calculated for $(M+H)^+$ $C_{15}H_{18}NO_4$ required 275.2998 found 276.1230 and for $(M+Na)^+$ $C_{15}H_{17}NO_4Na$ required 298.2890, found 298.1050.

6.4.6.2 Synthesis of allyl 5-fluoro-*N*-[allyloxycarbonyl)methyl]anthranilate (21b)

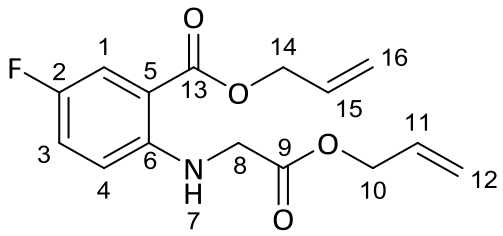

Compound **21b** was prepared according to **Section 6.4.6** general procedure using compound **20b** (25.61 g, 91.72 mmol), sodium hydride (0.80 g, 33.33 mmol) and allyl alcohol (75 mL). R_f = 0.57 (9:2 PE 40-60:EtOAc). Yield = 49% (18.84 g, 64.24 mmol), light yellow liquid product. **^{1}H NMR ($CDCl_3$, 400 MHz):** δ ppm = 8.02 (1H, s, H-7), 7.68 (1H, dd, $^3J_{H-F}$ = 9.5 Hz, $^4J_{H-H}$ = 2.0 Hz, H-1), 7.12 (1H, dd, $^3J_{H-F}$ = 9.0 Hz and $^4J_{H-H}$ = 3.0 Hz, H-3), 6.48 (1H, dd, $^3J_{H-F}$ = 9.0 Hz and $^4J_{H-H}$ = 4.0 Hz, H-4), 6.03 (1H, ddd, $^3J_{H-H}$ = 5.5 Hz, $^3J_{H-H}$ = 11.0 Hz and $^3J_{H-H}$ = 16.0 Hz, H-15) 5.93 (1H, ddd, $^3J_{H-H}$ = 5.5 Hz, $^3J_{H-H}$ = 10.5 Hz and $^3J_{H-H}$ = 16.0 Hz, H-11), 5.37 (1H, dd, $^3J_{H-H}$ = 6.5 Hz and $^2J_{H-H}$ = 1.5 Hz, H-16a), 5.36 (1H, dd, $^3J_{H-H}$ = 17.5 Hz and $^2J_{H-H}$ = 1.0 Hz, H-16b), 5.31 (1H, dd, $^3J_{H-H}$ = 6.5 Hz and $^2J_{H-H}$ = 1.5 Hz, H-12a), 5.26 (1H, dd, $^3J_{H-H}$ = 16.0 Hz and $^2J_{H-H}$ = 1.0 Hz, H-12b) 4.79 (2H, d, $^3J_{H-H}$ = 6.0 Hz, H-14), 4.69 (2H, d, $^3J_{H-H}$ = 6.0 Hz, H-10) and 4.02 (2H, $^3J_{H-H}$ = 5.5 Hz, H-8). **^{13}C NMR ($CDCl_3$, 100 MHz):** δ ppm = 170.03 (C-9), 167.09 (d, $^4J_{H-F}$ = 3.0 Hz, C-13), 116.56 (d, $^2J_{H-F}$ = 233.0 Hz, C-2), 146.82 (C-6), 132.16 (C-15), 131.60 (C-11), 122.21 (d, $^2J_{C-F}$ = 21.0 Hz, C-1), 118.96 (C-12), 118.39 (C-16), 117.18 (d, $^2J_{C-F}$ = 23.5 Hz, C-3), 112.66 (d, $^3J_{C-F}$ = 7.0 Hz, C-4), 111.01 (d, $^3J_{C-F}$ =6.5 Hz, C-5), 65.95 (C-10), 65.37 (C-14) and 45.30 (C-8). **^{19}F NMR ($CDCl_3$, 376 MHz):** δ ppm = -129.11. **IR_{Vmax}:** cm^{-1} = 3364 (Secondary amide N-H, *s*, b), 3087 (Aromatic C-H, *s*, w), 3020, 2989 and 2947 (Saturated C-H, s, w), 1746 (C=O, m, s), 1650 (C=C, *s*, w), 1588 (Aromatic C=C, *s*, m), 1519 (N-H *b*, s), 1178 (C-O, *s*, s), 1059 (C-F, *s*, m), 979 and 932 (C=C, *d,* s), 809 (Aromatic C-H, *d*, s). **FTMS (ESI):** m/z calculated for $(M+H)^+$ $C_{15}H_{17}{}^{19}FNO_4$ required 294.1147, found 294.1136, and $(M+Na)^+$ $C_{15}H_{16}{}^{19}FNO_4Na$ required 316.0967, found 316.0956.

6.4.6.3 Synthesis of allyl 4,5-di-fluoro-*N*-[allyloxycarbonyl)methyl]anthranilate (21c)

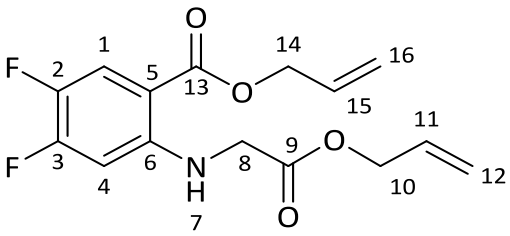

Compound **21c** was prepared according to **Section 6.4.6** general procedure using compound **20c** (7.53 g, 25.34 mmol), sodium hydride (0.21 g, 8.75 mmol) and allyl alcohol (45 mL). R_f = 0.40 (9:2 PE 40-60:EtOAc). Yield = 79% (6.20 g, 19.92 mmol), light yellow liquid product. **^{1}H NMR ($CDCl_3$, 400 MHz):** δ ppm = 8.21 (H-7), 7.79 (1H, dd, $^3J_{H\text{-}F}$ = 11.5 Hz and $^4J_{H\text{-}F}$ = 9.0 Hz, H-1), 6.30 (1H, dd, $^3J_{H\text{-}F}$ = 12.5 Hz and $^4J_{H\text{-}F}$ = 7.0 Hz, H-4), 6.03 (1H, ddd, $^3J_{H\text{-}H}$ = 5.5 Hz, $^3J_{H\text{-}H}$ = 11.0 Hz and $^3J_{H\text{-}H}$ = 16.0 Hz, H-15), 5.93 (1H, ddd, $^3J_{H\text{-}H}$ = 5.5 Hz, $^3J_{H\text{-}H}$ = 10.0 Hz and $^3J_{H\text{-}H}$ = 15.5 Hz, H-11), 5.40 (1H, dd $^3J_{H\text{-}H}$ = 15.5 Hz and $^2J_{H\text{-}H}$ = 1.0 Hz, H-16a), 5.35 (1H, dd, $^3J_{H\text{-}H}$ = 17.0 Hz and $^2J_{H\text{-}H}$ = 1.0 Hz, H-16b), 5.30 (1H, dd, $^3J_{H\text{-}H}$ = 4.5 Hz and $^2J_{H\text{-}H}$ = 1.0 Hz, H-12a), 5.28 (1H, dd, $^3J_{H\text{-}H}$ = 4.5 Hz and $^2J_{H\text{-}H}$ = 1.0 Hz, H-12b), 4.78 (2H, d, $^3J_{H\text{-}H}$ = 5.0 Hz, H-14), 4.70 (2H, d $^3J_{H\text{-}H}$ = 6.0 Hz, H-10) and 3.98 (2H, d, $^3J_{H\text{-}H}$ = 5.5 Hz, H-8). **^{13}C NMR ($CDCl_3$, 100 MHz):** δ ppm = 169.52 (C-9), 166.56 (d, $^4J_{C\text{-}F}$ = 2.0 Hz, C-13), 154.94 (dd, $^1J_{C\text{-}F}$ = 254.0 Hz and $^2J_{C\text{-}F}$ = 14.5 Hz, C-2), 148.05 (d, $^3J_{C\text{-}F}$ = 10.5 Hz, C-6), 141.33 (dd, $^1J_{C\text{-}F}$ = 236.5 Hz and $^2J_{C\text{-}F}$ = 13.5 Hz, C-3), 132.06 (C-15), 131.45 (C-10), 120.03 (dd, $^2J_{C\text{-}F}$ = 19.0 Hz and $^3J_{C\text{-}F}$ = 3.5 Hz, C-1), 119.17 (C-12), 118.55 (C-16), 106.23 (dd, $^3J_{C\text{-}F}$ = 4.5 Hz and $^4J_{C\text{-}F}$ = 2.5 Hz, C-5), 99.62 (d, $^2J_{C\text{-}F}$ = 22.0 Hz, C-4), 66.12 (C-10), 65.45 (C-14) and 45.19 (C-8) **^{19}F NMR ($CDCl_3$, 376 MHz):** δ ppm = -126.95 and -153.16. **IR_{Vmax}:** cm^{-1} = 3409 (Secondary amide N-H, *s*, s), 3058 (Aromatic C-H, *s*, w), 2950 (Saturated C-H, *s*, w), 1737 (C=O, *s*, m), 1637 (C=C, *s*, s), 1590 (Aromatic C=C, *s*, s), 1533 (N-H, *b*, s), 1300 (C-O, *s*, s), 1063 (C-F, *s*, m), 965 and 935 (C=C, *d*, s), and 779 (Aromatic C-H, *d*, s). **FTMS (ESI):** m/z calculated for $(M+H)^+$ $C_{15}H_{16}{}^{19}F_2NO_4$ required 312.1053, found 312.1042 and for $(M+Na)^+$ $C_{15}H_{15}{}^{19}F_2NO_4Na$ required 334.0872 found 334.0861.

6.4.6.4 Synthesis of 4-(trifluormethyl)-*N*-[allyloxycarbonyl)methyl] anthranilate (21d)

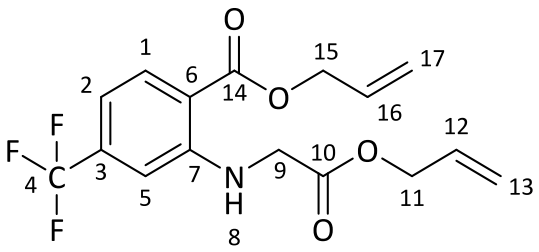

Compound **21d** was prepared according to **Section 6.4.6** general procedure using compound **20d** (25.94 g, 78.79 mmol), sodium hydride (0.62 g, 25.83), allyl alcohol (90 mL). R_f = 0.75 (9:2 PE 40-60:EtOAc).Yield = 86% (23.17 g, 71.67 mmol), yellow liquid product. **^{1}H NMR ($CDCl_3$, 400 MHz):** δ ppm = 8.38 (1H, s, H-8), 8.07 (1H, d $^3J_{H-H}$ = 8.5 Hz, H-2), 6.88 (1H, d, $^3J_{H-H}$ = 8.0 Hz, H-1), 6.74 (1H, s, H-5), 6.04 (1H, ddd, $^3J_{H-H}$ = 5.5 Hz, $^3J_{H-H}$ = 10.5 Hz and $^3J_{H-H}$ = 16.5 Hz, H-16), 5.94 (1H, ddd, $^3J_{H-H}$ = 5.5 Hz, $^3J_{H-H}$ =11.0 Hz and $^3J_{H-H}$ = 16.5 Hz, H-12), 5.41 (1H, dd, $^3J_{H-H}$ = 17.0 Hz and $^2J_{H-H}$ = 1.0 Hz, H-17a), 5.36 (1H, dd, $^3J_{H-H}$ = 17.5 Hz and $^2J_{H-H}$ = 1.0 Hz, H-17b), 5.29 (2H, t, $^3J_{H-H}$ = 9.0 Hz, H-13a and H-13b), 4.82 (2H, d, $^3J_{H-H}$ = 5.5 Hz, H-15), 4.71 (2H, $^3J_{H-H}$ = 6.0 Hz, H-11) and 4.07 (2H, $^3J_{H-H}$ = 5.0 Hz, H-9). **^{13}C NMR ($CDCl_3$, 100 MHz):** δ ppm = 169.53 (C-10), 167.95 (C-14), 149.76 (C-7), 135.92 (q, $^3J_{C-F}$ = 32.0 Hz, C-3), 132.60 (C-2), 132.05 (C-16), 131.45 (C-12), 123.53 (d, $^1J_{C-F}$ = 272.0 Hz, C-4), 119.16 (C-13), 118.56 (C-17), 113.47 (C-6), 111.82 (d, $^4J_{C-F}$ = 3.0 Hz, C-1), 107.96 (d, $^3J_{C-F}$ = 5.0 Hz, C-5), 66.14 (C-11), 65.55 (C-15) and 44.84 (C-9). **^{19}F NMR ($CDCl_3$, 376 MHz):** δ ppm = -63.83. **IR_{Vmax}:** cm^{-1} = 3345 (Secondary amide N-H, *s*, s), 3091 (Aromatic C-H, *s*, w), 2945 (Saturated C-H, *s*, w), 1747 (C=O, s, m), 1648 (C=C, *s*, s), 1622 (Aromatic C=C, *s*, s), 1582 (N-H, *b*, m), 1120 (C-O, *s*, s), 1087 (C-F, *s*, s), 986 and 933 (C=C, *d*, m), 853.59 (Aromatic, *d,* m). **FTMS (ESI):** m/z calculated for $(M+H)^+$ $C_{16}H_{17}{}^{19}F_3NO_4$ required 344.1115, found 344.1104.

6.4.7 General procedure: Formation of indoxylic acid allyl ester via Dieckmann condensation

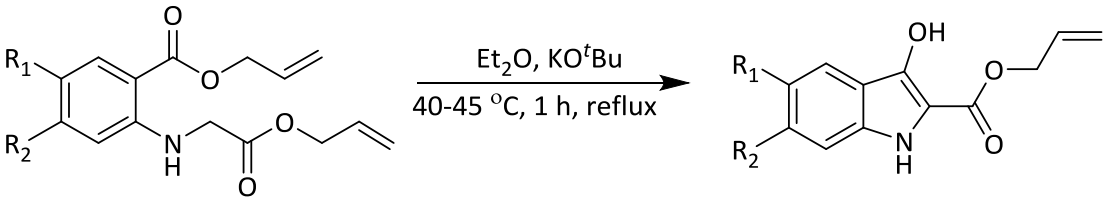

21a: R_1=H, R_2=H
21b: R_1=F, R_2=H
21c: R_1=F, R_2=F
21d: R_1=H, R_2=CF_3

5a: R_1=H, R_2=H
5b: R_1=F, R_2=H
5c: R_1=F, R_2=F
5d: R_1=H, R_2=CF_3

The reaction was carried under an argon atmosphere. The purified ally *N*-[allyloxycarbonyl)methyl] anthranilate (1.0 mol equiv.) was dissolved in anhydrous diethyl ether (40-250 mL). To the stirred solution, KO^{t}Bu (2.0 mol equiv.) was added portionwise. The reaction was heated to reflux (40-45 °C) for 2 hours. After this time, TLC analysis (4:1 PE 40-60:EtOAc) revealed the formation of product (R_f 0.57-0.71) The reaction was cooled to room temperature, and the solvent was removed *in vacuo*. The product was precipitated *via* the addition of 1 M HCl and was collected by vacuum filtration. The collected product was washed with water and 0.5 M HCl. The crude product was partially purified using flash column chromatography.

6.4.7.1 Synthesis of allyl 3-hydroxy-5-methyl-1*H*-indole-2-carboxylate (5a)

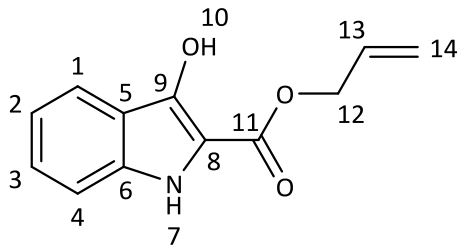

Compound **5a** was prepared according to **Section 6.4.7** using compound **21a** (8.98 g, 32.62 mmol), KO^{t}Bu (9.48 g, 84.48 mmol) and diethyl ether (40 mL). R_f = 0.52 (3:1 PE 40-60:EtOAc). Yield = 49% (3.40 g, 34.16 mmol), yellow solid product. **^{1}H NMR (DMSO-*d*$_6$, 400 MHz):** δ ppm = 10.82 (1H, s, H-10), 9.36 (1H, s, H-7), 7.71 (1H, d, $^2J_{H\text{-}H}$ = 8.0 Hz, H-1), 7.29 (1H, d, $^2J_{H\text{-}H}$ = 8.0 Hz, H-4), 7.22 (td, $^3J_{H\text{-}H}$ = 6.5 Hz and $^3J_{H\text{-}H}$ = 8.5 Hz and $^4J_{H\text{-}H}$ = 1.0 Hz, H-3), 6.96 (t, $^3J_{H\text{-}H}$ = 7.5 Hz, H-2), 6.05 (1H, ddd, $^3J_{H\text{-}H}$ = 17.0 Hz, $^3J_{H\text{-}H}$ = 10.5 Hz and $^3J_{H\text{-}H}$ = 5.0 Hz, H-13), 5.44 (1H, dd, $^3J_{H\text{-}H}$ = 17.0 Hz and $^2J_{H\text{-}H}$ = 1.5 Hz, H-14a), 5.26 (dd, $^3J_{H\text{-}H}$ = 10.5 Hz and $^2J_{H\text{-}H}$ =1.5 Hz, H-14b) and 4.80 (1H, d, $^3J_{H\text{-}H}$ = 5.0 Hz, H-12). **^{13}C NMR (DMSO-*d*$_6$, 100 MHz):** δ ppm = 161.24 (C-11), 143.36 (C-6), 134.98 (C-5), 133.08 (C-13), 125.76 (C-3), 119.82 (C-1), 118.30 (C-2), 118.22 (C-8), 117.33 (C-14), 112.31 (C-4), 108.88 (C-9) and 63.86 (C-12). **IR$_{Vmax}$:** cm^{-1} = 3432 (Secondary amide N-H, *s*, m), 3334 (O-H, *s*, br), 3082 (Aromatic C-H, *s*, w), 2974 and 2945 (Saturated C-H, *s*, w), 1682 (C=O, *s*, m), 1582 (C=C, *s*, m), 1548 (Aromatic C=C, *s*, m), 1507 (N-H, *b*, s), 1231 (C-O, *s*, s), 974.82 and 965 (C=C, *d*, s), and 736 (aromatic C-H, *d,* s). **FTMS (ESI):** m/z calculated for $(M+Na)^+$ $C_{12}H_9NO_3Na$ required 238.0458, found 238.0475.

6.4.7.2 Synthesis of 5-fluoro-allyl 3-hydroxy-1*H*-indole-2-carboxylate (5a)

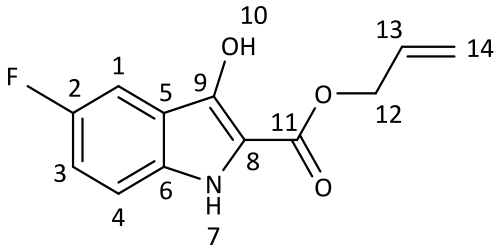

Compound **5b** was prepared according to **Section 6.4.7** general procedure using compound **21b** (9.78 g, 33.35 mmol), KO^{t}Bu (5.79 g, 51.60 mmol) and diethyl ether (250 mL). R_f = 0.57 (3:1 PE 40-60:EtOAc). Yield = 69% (9.55 g, 40.60 mmol), yellow solid product. **^{1}H NMR (DMSO-*d*$_6$, 400 MHz):** δ ppm = 10.94 (1H, s, H-10), 9.44 (H-7), 7.45 (1H, dd, $^3J_{H\text{-}F}$ = 9.5 Hz and $^4J_{H\text{-}H}$ = 2.0 Hz, H-1), 7.30 (1H, dd, $^3J_{H\text{-}H}$ = 9.0 Hz and $^4J_{F\text{-}H}$ = 4.0 Hz, H-4), 7.10 (1H, td, $^3J_{H\text{-}F}$ = 9.0 Hz and $^4J_{H\text{-}H}$ = 2.5 Hz, H-3), 6.04 (1H, ddt, $^3J_{H\text{-}H}$ = 17.0 Hz, $^3J_{H\text{-}H}$ = 10.5 Hz and $^3J_{H\text{-}H}$ = 5.0 Hz, H-13), 5.44 (1H, dd, $^3J_{H\text{-}H}$ = 17.5 Hz and $^2J_{H\text{-}H}$ = 1.5 Hz, H-14a), 5.26 (1H, dd, $^3J_{H\text{-}H}$ = 11.0 Hz and $^2J_{H\text{-}H}$ = 1.5 Hz, H-14b) and 4.80 (2H, d, $^3J_{H\text{-}H}$ = 5.0 Hz, H-12). **^{13}C NMR (DMSO-*d*$_6$, 100 MHz):** δ ppm = 160.95 (C-11), 155.96 (d, $^1J_{C\text{-}F}$ = 233.5 Hz, C-2), 142.90 (d, $^4J_{C\text{-}F}$ = 5.5 Hz, C-6), 132.98 (C-13), 131.66 (C-8), 117.79 (C-5), 117.37 (C-14), 114.73 (d, $^2J_{C\text{-}F}$ = 26.0 Hz, C-3), 113.82 (d, $^3J_{C\text{-}F}$ = 9.5 Hz, C-4), 110.80 (C-9), 103.84 (d, $^2J_{C\text{-}F}$ = 24.0 Hz, C-1) and 63.98 (C-12). **^{19}F NMR (DMSO-*d*$_6$, 376 MHz):** δ ppm = -124.71. **IR$_{Vmax}$:** cm^{-1} = 3482 (Secondary amide N-H, *s*, m), 3337 (O-H, *s*, br), 3075 (Aromatic C-H, *s*, w), 3016, 2970 and 2947 (Saturated C-H, *s*, m), 1739 (C=O, *s*, s), 1588 (C=C, *s*, m), 1549 (Aromatic C=C, *s*, m), 1514 (N-H, *b*, s), 1366 (C-O, *s*, s), 1090 (C-F, *s*, m), 981 and 957 (C=C, *d*, s), and 762 (Aromatic C-H, *d*, s). **FTMS (ESI):** m/z calculated for $(M+Na)^+$ $C_{12}H_8{}^{19}FNO_3Na$ required 256.0391, found 256.0380 and for $(M+Na)^{2+}$ $C_{12}H_9{}^{19}FNO_3Na$ required 257.0469 found 257.0459.

6.4.7.3 Synthesis of allyl 3-hydroxy-5,6-dimethyl-1H-indole-2-carboxylate (5c)

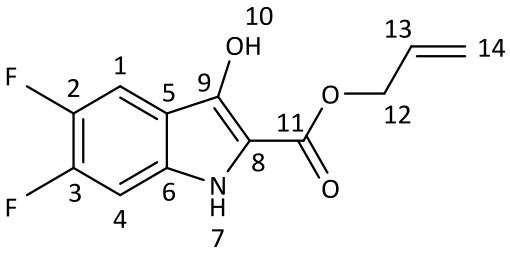

Compound **5c** was prepared according to **Section 6.4.7** general procedure using compound **21c** (18.17 g, 58.37 mmol), KO^{t}Bu (15.37 g, 136.96 mmol) and diethyl ether (120 mL). R_f = 0.57 (3:1 PE 40-60:EtOAc). Yield = 38% (5.60 g, 22.12 mmol), yellow solid product. **^{1}H NMR (DMSO-*d*$_6$, 400 MHz):** δ ppm = 11.04 (H-10), 9.63 (H-7), 7.68 (1 H, dd, $^3J_{H\text{-}F}$ = 11.0 and Hz and $^4J_{H\text{-}F}$ = 8.0 Hz, H-1), 7.20 (1H, dd, $^3J_{H\text{-}F}$ = 11.0 Hz and $^4J_{H\text{-}F}$ = 7.0 Hz, H-4), 6.03 (1H, ddd, $^3J_{H\text{-}H}$ = 5.0 Hz, $^3J_{H\text{-}H}$ = 10.0 Hz and $^3J_{H\text{-}H}$ = 15.5 Hz, H-13), 5.43 (1H, dd, $^3J_{H\text{-}H}$ = 17.0 Hz and $^2J_{H\text{-}H}$ 2.0 Hz, H-14a), 5.25 (1H, dd, $^3J_{H\text{-}H}$ = 10.5 Hz and $^2J_{H\text{-}H}$ = 1.5 Hz, H-14b) and 4.78 (2H, d, $^3J_{H\text{-}H}$ = 5.0 Hz, H-12). **^{13}C NMR (DMSO-*d*$_6$, 100 MHz):** δ ppm = 160.58 (C-11), 148.99 (dd, $^1J_{C\text{-}F}$ = 244.0 Hz and $^2J_{C\text{-}F}$ = 16.5 Hz, C-3), 144.75 (dd, $^1J_{C\text{-}F}$ = 237.5 Hz and $^2J_{C\text{-}F}$ = 16.5 Hz, C-2), 143.09 (dd, $^3J_{C\text{-}F}$ = 5.0 Hz and $^4J_{C\text{-}F}$ = 2.0 Hz, C-6), 133.02 (C-13), 130.27 (d, $^3J_{C\text{-}F}$ = 11.0 Hz, C-5), 117.39 (C-14), 113.41 (d, $^4J_{C\text{-}F}$ = 7.5 Hz, C-9), 110.65 (d, $^5J_{C\text{-}F}$ = 4.0 Hz, C-8), 106.34 (d, $^2J_{C\text{-}F}$ = 19.0 Hz, C-1), 99.74 (d, $^2J_{C\text{-}F}$ = 21.0 Hz, C-4) and 63.97 (C-12). **^{19}F NMR (DMSO-*d*$_6$, 376 MHz):** δ ppm = -138.51 and -147.95. **IR$_{Vmax}$:** cm^{-1} = 3452 (Secondary amide N-H, *s*, m), 3312 (O-H, *s*, br), 3016 (Aromatic C-H, *s*, w), 2970, and 2947 (Saturated C-H, *s*, m), 1739 (C=O, *s*, s), 1626 (C=C, *s*, s), 1554 (Aromatic C=C, *s*, m), 1475 (N-H, *b*, s), 1366 (C-O, *s*, s), 1089 (C-F, *s*, m), 992 and 943 (C=C, *d*, s), and 768.36 (Aromatic C-H, *d*, s). **FTMS (ESI)**: m/z calculated for $(M+H)^+$ $C_{12}H_8{}^{19}F_2NO_3$ required 252.0477, found 252.0478.

6.4.7.4 Synthesis of allyl 3-hydroxy-6-(trifluoromethyl)-1*H*-indole-2-carboxylate (5d)

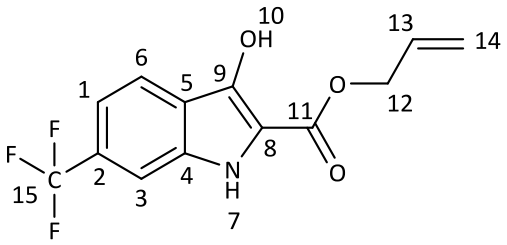

Compound **5d** was prepared according to **Section 6.4.7** general procedure using compound **21d** (20.12 g, 58.61 mmol), Ko^{t}Bu (13.93 g, 124.13) and diethyl ether (50 mL). R_f = 0.71 (3:1 PE 40-60:EtOAc). Yield = 49% (7.42 g, 26.02 mmol), yellow solid product. **^{1}H NMR (DMSO-*d*$_6$, 400 MHz):** δ ppm = 11.33 (H-11), 9.77 (H-8), 7.95 (1H, d, $^3J_{H\text{-}H}$ = 8.5 Hz, H-1), 7.61 (1H, s, H-5), 7.23 (1H, dd, $^3J_{H\text{-}H}$ = 8.5 Hz and $^4J_{H\text{-}H}$ = 1.5 Hz, H-2), 6.05 ppm (1H, ddd, $^3J_{H\text{-}H}$ = 17.0 Hz, $^3J_{H\text{-}H}$ = 10.5 Hz and $^3J_{H\text{-}H}$ = 5.0 Hz, H-13) 5.45 (1H, dd, $^3J_{H\text{-}H}$ = 17.0 Hz and $^2J_{H\text{-}H}$ = 1.5 Hz, H-14a), 5.27 (1H, dd, $^3J_{H\text{-}H}$ = 10.5 Hz and $^2J_{H\text{-}H}$ = 1.5 Hz, H-14b) and 4.82 (2H, d, $^3J_{H\text{-}H}$ = 5.0 Hz, H-12). **^{13}C NMR (DMSO-*d*$_6$, 100 MHz):** δ ppm = 160.78 (C-12), 142.44 (C-7), 135.15 (C-14), 132.87 (C-6), 125.50 (q, $^2J_{C\text{-}F}$ = 32.0 Hz, C-3), 124.86 (d, $^1J_{C\text{-}F}$ = 272.0 Hz, C-4), 121.34 (C-1), 120.51 (C-9), 117.55 (C-15), 114.13 (d, $^3J_{C\text{-}F}$ = 3.0 Hz, C-2), 111.75 (C-10), 109.68 (d, $^3J_{C\text{-}F}$ = 4.5 Hz, C-5) and 64.23 (C-13). **^{19}F NMR (DMSO-*d*$_6$, 376 MHz):** δ ppm **=** -59.96. **IR$_{Vmax}$:** cm^{-1} = 3455 (Secondary amide N-H, *s*, m), 3321 (O-H, *s*, b), 3455 (Aromatic C-H, *s*, w), 3016, 2970 and 2947 (Saturated C-H, *s*, m), 1739 (C=O, *s*, s), 1595 (C=C, *s*, m), 1520 (Aromatic C=C, *s*, m), 1479 (N-H, *b*, s), 1365 (C-O, *s*, s), 1051 (C-F, *s*, m), 959 and 878 (C=C, *d,* s), and 770.90 (aromatic C-H, *d*, s). **FTMS (ESI):** m/z calculated for (M+H$^+$) $C_{13}H_9{}^{19}F_3NO_3$ required 284.0540, found 284.0540.

6.5 Experimental methods and results of the glycosidated and deprotected compounds

6.5.1 General Procedure: Phase-transfer catalysis *O*-glycosylation

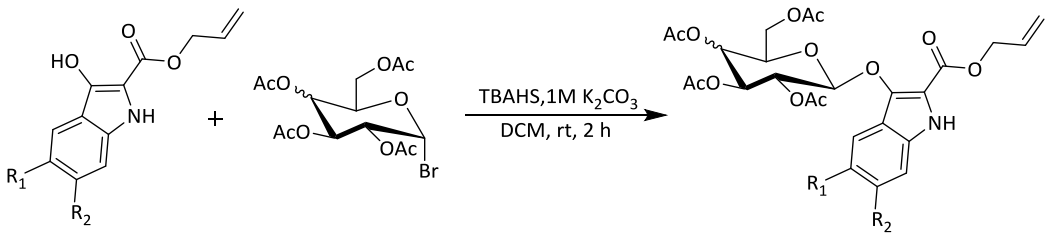

5b: R_1=F, R_2=H
5c: R_1=F, R_2=F
5d: R_1=H, R_2=CF_3

23a: Acetobromogalactose
23b: Acetobromoglucose

27a & 28a: R_1=F, R_2=H
27b & 28b: R_1=F, R_2=F
27c & 28c: R_1=H, R_2=CF_3

Under an argon atmosphere, the fluorinated indoxylic acid allyl esters were dissolved in anhydrous DCM: acetobromogalactose or acetobromoglucose (1.0 mol equiv), indoxylic cid allyl acceptor (1.0 mol equiv) and TBAHS (1.0-1.5 mol equiv). Then, 1M K_2CO_3 was added to the mixture. The reaction was left to stir at rt until TLC analysis (2:1 and 1:1 PE 40-60:EtOAc) indicated complete consumption of the glycosyl donor and revealed the formation of product (R_f 0.21-0.61). The reaction mixture was quenched with distilled water. The aqueous phase was extracted with DCM three times. The combined organic phase were dried with Na_2SO_4, filtered and concentrated *in vacuo*. The crude product was purified with flash column chromatography.

6.5.1.1 Synthesis of (5-fluoro-indox-3-ylic acid allyl ester)-2,3,4,6-tetra-*O*-acetyl-β-D-galactopyranoside (27a)

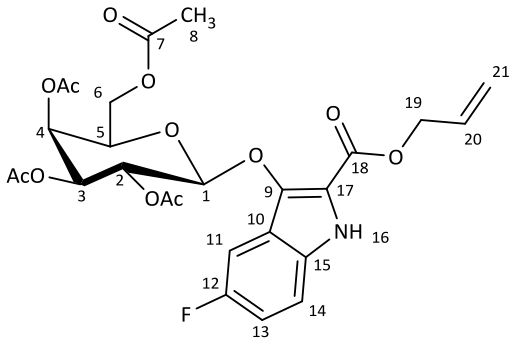

Compound **27a** was prepared according to **Section 6.5.1** general procedure using compound **5b** (1.51 g, 6.42 mmol), acetobromogalactose **23a** (2.70 g, 6.57 mmol) and TBAHS (2.24 g, 6.59 mmol), DCM (20 mL) and 1M K_2CO_3 (20 mL). R_f = 0.21 (2:1 PE 40-60:EtOAc). Yield = 95% (3.45 g, 6.10 mmol), yellow solid product. mp 91-92 °C. **^{1}H NMR ($CDCl_3$, 400 MHz):** δ ppm = 8.61 (1H, s, H-16), 7.49 (1H, dd, $^3J_{H\text{-}F}$ = 9.5 Hz and $^4J_{H\text{-}H}$ = 2.0 Hz, H-11), 7.27 (1H, dd, $^4J_{H\text{-}F}$ = 9.0 Hz and $^3J_{H\text{-}H}$ = 4.5 Hz, H-14), 7.09 (1H, td, $^3J_{F\text{-}H}$ = 9.0 Hz and $^4J_{H\text{-}H}$ = 2.5 Hz, H-13), 6.03 (1H, ddt, $^3J_{H\text{-}H}$ = 16.0 Hz, $^3J_{H\text{-}H}$ = 11.0 Hz and $^3J_{H\text{-}H}$ = 5.0 Hz, H-20), 5.58 (1H, dd, $^3J_{H\text{-}H}$ = 10.5 Hz and $^3J_{H\text{-}H}$ = 8.0 Hz, H-2), 5.45 (1H, d, $^3J_{H\text{-}H}$ = 2.5 Hz, H-4), 5.42 (1H, dd, $^3J_{H\text{-}H}$ = 16.0 Hz and $^2J_{H\text{-}H}$ = 2.5 Hz, H-21a), 5.32 (1H, dd, $^3J_{H\text{-}H}$ = 10.5 Hz and $^2J_{H\text{-}H}$ = 1.0 Hz, H-21b), 5.12 (1H, d, $^3J_{H\text{-}H}$ = 8.0 Hz, H-1), 5.11 (1H, dd, $^3J_{H\text{-}H}$ = 10.5 Hz and $^3J_{H\text{-}H}$ = 3.5 Hz, H-3), 4.84 (2H, ddd, $^3J_{H\text{-}H}$ = 6.0 Hz, $^4J_{H\text{-}H}$ = 5.5 Hz and $^4J_{H\text{-}H}$ = 1.0 Hz, H-19), 4.21-4.11 (2H, m, H-6a and H-6b), 3.97 (1H, t, $^3J_{H\text{-}H}$ = 6.5 Hz, H-5), 2.22 (3H, s, H-8), 2.13 (3H, s, H-8), 2.02 (3H, s, H-8) and 1.96 (3H, s, H-8). **^{13}C NMR ($CDCl_3$, 100 MHz):** δ ppm = 170.53 (C-7), 170.33 (C-7), 170.15 (C-7), 169.77 (C-7), 159.80 (C-18), 157.86 (d, $^1J_{C\text{-}F}$ = 239.0 Hz, C-12), 140.85 (d, $^4J_{C\text{-}F}$ = 5.5 Hz, C-15), 131.99 (C-17), 130.41 (C-20), 121.30 (d, $^3J_{C\text{-}F}$ = 12.0 Hz, C-10), 118.94 (C-21), 116.68 (C-9), 115.70 (d, $^2J_{C\text{-}F}$ = 27.0 Hz, C-13), 113.07 (d, $^3J_{C\text{-}F}$ = 9.0 Hz, C-14), 105.24 (d, $^2J_{C\text{-}F}$ = 25.5 Hz, C-11), 102. 83 (C-1), 71.18 (C-5), 70.95 (C-3), 68.83 (C-2), 67.14 (C-4), 65.50, (C-19), 61.66 (C-6), 20.98 (C-8), 20.72 (C-8), 20.60 (C-8) and 20.44 (C-8).**^{19}F NMR ($CDCl_3$, 376 MHz):** δ ppm = -121.01. **IR_{Vmax}:** cm^{-1} = 3352 (Secondary amide N-H, *s*, br), 2970 (Aromatic C-H, *s*, w) 1742 (C=O, *s*, s), 1552 (C=C, *s*,

m), 1213 (C-O, *s*, s), 1036 (C-F, *s*, s), and 951 and 913 (C=C, *d*, s). **FTMS (ESI):** m/z calculated for $(M+Na)^+$ $C_{26}H_{28}{}^{19}FNO_{12}Na$ required 588.1499, found 588.1488.

6.5.1.2 Synthesis of (5-fluoro-indox-3-ylic acid allyl ester)-2,3,4,6-tetra-*O*-acetyl-β-D-glucopyranoside 28a

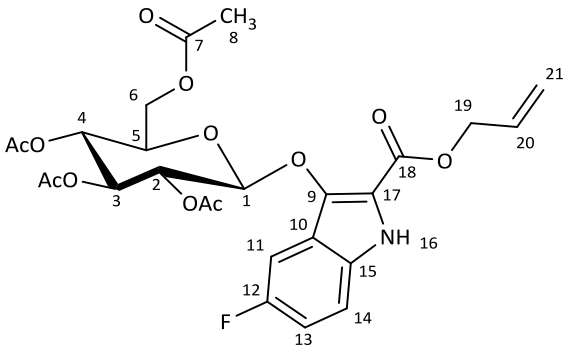

Compound **28a** was prepared according to **Section 6.5.1** general procedure using compound **5b** (2.00 g, 8.50 mmol), acetobromoglucose **23b** (3.57 g, 8.68 mmol) and TBAHS (2.92 g, 8.60 mmol). R_f = 0.21 (2:1 PE 40-60:EtOAc). Yield = 78% (3.74 g, 6.61 mmol), yellow solid product. mp 72-73 °C. **^{1}H NMR ($CDCl_3$, 400 MHz):** δ ppm = 8.61 (1H, s, H-16), 7.46 (1H, dd, $^3J_{H-F}$ = 9.5 Hz and $^4J_{H-H}$ = 2.0 Hz, H-11), 7.27 (1H, dd, $^4J_{H-F}$ = 9.0 Hz and $^3J_{H-H}$ = 4.0 Hz, H-14), 7.08 (1H, td, $^3J_{H-F}$ = 9.0 Hz and $^4J_{H-H}$ = 2.5 Hz, H-13), 6.03 (1H, ddt, $^3J_{H-H}$ = 16.0 Hz, $^3J_{H-H}$ = 10.5 Hz and $^3J_{H-H}$ = 5.5 Hz, H-20), 5.42 (1H, dd, $^3J_{H-H}$ = 17.0 Hz and $^2J_{H-H}$ = 1.5 Hz, H-21a), 5.72 (1H, dd, $^3J_{H-H}$ = 9.5 Hz and $^2J_{H-H}$ = 2.0 Hz, H-21b), 5.33-5.27 (2H, m, H-2 and H-3), 5.18 (1H, dd, $^3J_{H-H}$ = 8.0 Hz and $^3J_{H-H}$ = 2.0 Hz, H-4), 5.17 (1H, d, $^3J_{H-H}$ = 8.0 Hz, H-1) 4.83 (2H, ddt, $^3J_{H-H}$ = 7.0 Hz, $^4J_{H-H}$ = 6.0 Hz and $^4J_{H-H}$ = 1.5 Hz H-19), 4.25 (1H, dd, $^3J_{H-H}$ = 12.0 Hz and $^3J_{H-H}$ = 5.5 Hz, H-6a), 4.12 (1H, dd, $^3J_{H-H}$ = 12.0 Hz and $^3J_{H-H}$ = 2.50 Hz, H-6b), 3.77 (1H, ddd, $^3J_{H-H}$ = 10.0 Hz, $^3J_{H-H}$ = 5.0 Hz and $^3J_{H-H}$ = 2.0 Hz, H-5), 2.11 (3H, s, H-8), 2.04 (1H, s, H-8), 2.04 (3H, s, H-8) and 2.02 (3H, s, H-8). **^{13}C NMR ($CDCl_3$, 100 MHz):** δ ppm = 170.72 (C-7), 170.27 (C-7), 169.64 (C-7), 169.46 (C-7), 159.83 (C-18), 157.88 (d, $^1J_{C-F}$ = 239.5 Hz, C-12), 140.55 (d, $^4J_{C-F}$ = 5.0 Hz, (C-15), 131.94 (C-17), 130.39 (C-20), 121.34 (d, $^3J_{C-F}$ = 11.0 Hz, C-10), 118.99 (C-21), 116.71 (C-9), 115.72 (d, $^2J_{C-F}$ = 27.0 Hz, C-13), 113.07 (d, $^3J_{C-F}$ = 8.5 Hz, C-14), 105.15 (d, $^2J_{C-F}$ = 27.5 Hz, C-11),

102.22 (C-1), 72.81 (C-3), 72.00 (C-5), 71.39 (C-2), 68.44 (C-4), 65.53, (C-19), 62.08 (C-6), 20.85 (C-8), 20.64 (C-8), 20.61 (C-8) and 20.48 (C-8). **^{19}F NMR ($CDCl_3$ 376 MHz):** δ ppm = -121.97. **IR_{Vmax}**: cm^{-1} = 3341 (Secondary amide N-H, *s*, br), 2852 (Aromatic C-H, *s*, w) 1745 (C=O, *s*, s), 1552 (C=C, *s*, m), 1213 (C-O, *s*, s), 1033 (C-F, *s*, s), 988 and 908 (C=C, *d*, s). **FTMS (ESI):** m/z calculated for $(M+Na)^+$ $C_{26}H_{28}{}^{19}FNO_{12}Na$ required 588.1499, found, 588.1488.

6.5.1.3 Synthesis of (5,6-difluoro-indox-3-ylic acid allyl ester)-2,3,4,6-tetra-*O*-acetyl-β-D-galactopyranoside (27b)

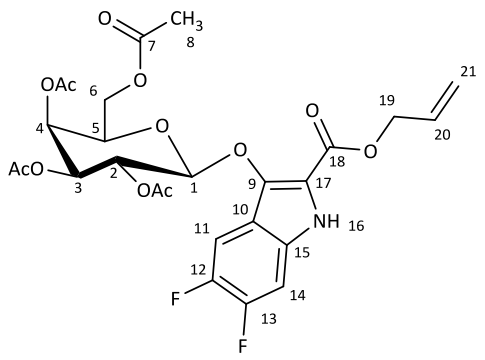

Compound **27b** was prepared according to **Section 6.5.1** general procdure using compound **5c** (1.04 g, 4.11 mmol), acetobromogalactose **23a** (1.17 g, 2.85 mmol) and TBAHS (1.42 g, 4.18 mmol). R_f = 0.61 (1:1 PE 40-60:EtOAc). Yield = 85% (2.05 g, 3.51 mmol), yellow solid product. mp 93-94 °C. **^{1}H NMR ($CDCl_3$, 400 MHz):** δ ppm = 8.68 (1H, s, H-16), 7.61 (1H, dd, $^3J_{H\text{-}F}$ = 10.5 Hz and Hz, $^4J_{H\text{-}F}$ = 8.0 Hz, H-11), 7.11 (1H, dd, $^3J_{H\text{-}F}$ = 10.0 Hz and $^4J_{H\text{-}H}$ = 6.5 Hz, H-14), 6.03 (1H, ddt, $^3J_{H\text{-}H}$ = 16.0 Hz, $^3J_{H\text{-}H}$ = 10.0 Hz and $^3J_{H\text{-}H}$ = 6.0 Hz, H-20), 5.57 (1H, dd, $^3J_{H\text{-}H}$ = 10.5 Hz and $^3J_{H\text{-}H}$ = 8.0 Hz, H-2), 5.45 (1H, d, $^3J_{H\text{-}H}$ = 3.5 Hz, H-4), 5.42 (1H, dd, $^3J_{H\text{-}H}$ = 17.0 Hz and $^2J_{H\text{-}H}$ = 1.5 Hz, H-21a), 5.32 (1H, dd, $^3J_{H\text{-}H}$ = 10.5 Hz and $^2J_{H\text{-}H}$ = 1.0 Hz, H-21b), 5.10 (1H, d, $^3J_{H\text{-}H}$ = 8.0 Hz, H-1), 5.11 (1H, dd, $^3J_{H\text{-}H}$ = 10.5 Hz and $^3J_{H\text{-}H}$ = 3.5 Hz, H-3), 4.83 (2H, t, $^3J_{H\text{-}H}$ = 6.0 Hz, H-19), 4.17 (1H, d, $^3J_{H\text{-}H}$ = 6.0 Hz, H-6a and H-6b), 3.96 (1H, t, $^3J_{H\text{-}H}$ = 6.5 Hz, H-5), 2.23 (3H, s, H-8), 2.13 (3H, s, H-8), 2.02 (3H, s, H-8) and 1.97 (3H, s, H-8). **^{13}C NMR ($CDCl_3$, 100 MHz):** δ ppm = 170.50 (C-7), 170.32 (C-7), 170.16 (C-7), 169.84 (C-7), 159.41 (C-18), 144.23 (dd, $^1J_{C\text{-}F}$ =

246.5 Hz and $^{2}J_{C\text{-}F}$ = 16.0 Hz, C-12), 144.23 (dd, $^{1}J_{C\text{-}F}$ = 239.5 Hz and $^{2}J_{C\text{-}F}$ = 19.0 Hz, C-13), 140.99 (dd, $^{4}J_{C\text{-}F}$ = 5.0 Hz and $^{5}J_{C\text{-}F}$ = 2.0 Hz, C-9), 131.90 (C-20), 129.10 (d, $^{3}J_{C\text{-}F}$, = 11.5 Hz, C-15), 119.09 (C-21), 116.70 (d, $^{3}J_{C\text{-}F}$, = 8.0 Hz, C-10), 116.21 (d, $^{5}J_{C\text{-}F}$, = 4.0 Hz, C-17), 107.42 (d, $^{2}J_{C\text{-}F}$, = 20.5 Hz, C-11), 102.87 (C-1), 99.53 (d, $^{3}J_{C\text{-}F}$ = 24.5 Hz, C-14), 71.18 (C-5), 70.84 (C-3), 68.71 (C-2), 67.07 (C-4), 65.54 (C-19), 61.61 (C-6), 20.99 (C-8), 20.71 (C-8), 20.60 (C-8) and 20.45 (C-8).**^{19}F NMR ($CDCl_3$, 376 MHz):** δ ppm = -135.98 and -144.17. **IR_{Vmax}:** cm^{-1} = 3341 (Secondary amide N-H, *s*, br), 2970 (Aromatic C-H, *s*, w) 1745 (C=O, *s*, s), 1557 (C=C, *s*, m), 1214 (C-O, *s*, s), 1036 (C-F, *s*, s), 915 and 833 (C=C, *d*, s). **FTMS (ESI):** m/z calculated for $(M+Na)^{+}$ $C_{26}H_{27}{}^{19}F_2NO_{12}Na$ required 606.1405, found 606.1394.

6.5.1.4 Synthesis of (5,6-difluoro-indox-3-ylic acid allyl ester)-2,3,4,6-tetra-*O*-acetyl-β-D-glucopyranoside (28b)

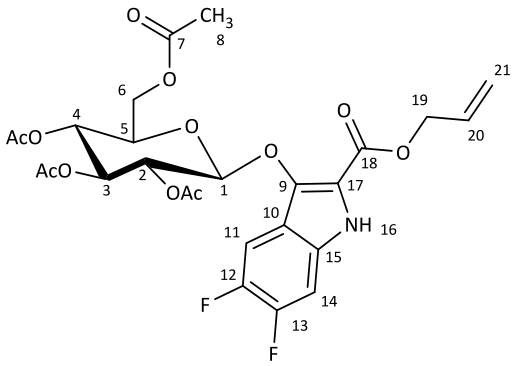

Compound **28b** was prepared according to **Section 6.5.1** general procedure using compound **5c** (1.04 g, 4.10 mmol), acetobromoglucose **23b** (1.70 g, 4.13 mmol) and TBAHS (1.50 g, 4.41 mmol). R_f = 0.57 (1:1 PE 40-60:EtOAc). Yield = 86% (2.06 g, 3.53 mmol), yellow solid product. mp 76-77 °C. **^{1}H NMR ($CDCl_3$, 400 MHz):** δ ppm = 8.72 (1H, s, H-16), 7.58 (1H, dd, $^{3}J_{H\text{-}F}$ = 10.5 Hz and Hz, $^{4}J_{H\text{-}F}$ = 8.0 Hz, H-11), 7.10 (1H, dd, $^{3}J_{H\text{-}F}$ = 10.0 Hz and $^{4}J_{H\text{-}H}$ = 6.5 Hz, H-14), 6.03 (1H, ddt, $^{3}J_{H\text{-}H}$ = 16.5 Hz, $^{3}J_{H\text{-}H}$ = 10.5 Hz and $^{3}J_{H\text{-}H}$ = 7.0 Hz, H-20), 5.44-5.28 (4H, m, H-2 and H-3, H-21a and H-21b), 5.16 (1H, dd, $^{3}J_{H\text{-}H}$ = 9.0 Hz, H-4), 5.15 (1H, d, $^{3}J_{H\text{-}H}$ = 8.0 Hz, H-1), 4.83 (2H, t, $^{4}J_{H\text{-}H}$ = 6.0 Hz, H-19), 4.25 (1H, dd, $^{2}J_{H\text{-}H}$ = 12.0 Hz and $^{3}J_{H\text{-}H}$ = 5.5 Hz, H-6a), 4.12 (1H, dd,

$^{2}J_{H\text{-}H}$ = 12.0 Hz and $^{3}J_{H\text{-}H}$ = 2.0 Hz, H-6b), 3.76 (1H, ddd, $^{3}J_{H\text{-}H}$ = 10.0 Hz, $^{3}J_{H\text{-}H}$ = 5.5 Hz and $^{3}J_{H\text{-}H}$ = 2.0 Hz, H-5), 2.12 (3H, s, H-8), 2.04 (1H, s, H-8), 2.04 (3H, s, H-8) and 2.03 (3H, s, H-8). **^{13}C NMR ($CDCl_3$, 100 MHz):** δ ppm = 170.66 (C-7), 170.26 (C-7), 170.16 (C-7), 169.67 (C-7), 159.48 (C-18), 151.05 (dd, $^{1}J_{C\text{-}F}$ = 249.0 Hz and $^{2}J_{C\text{-}F}$ = 19.0 Hz, C-12), 147.11 (dd, $^{1}J_{C\text{-}F}$ = 240.5 Hz and $^{2}J_{C\text{-}F}$ = 16.0 Hz, C-13), 140.67 (dd, $^{4}J_{C\text{-}F}$ = 5.0 Hz and $^{5}J_{C\text{-}F}$ = 2.0 Hz, C-9), 131.88 (C-20), 129.13 (d, $^{3}J_{C\text{-}F}$ = 10.5 Hz, C-15), 119.11 (C-21), 116.85 (d, $^{3}J_{C\text{-}F}$ = 7.0 Hz, C-10), 116.46 (d, $^{5}J_{C\text{-}F}$ = 4.0 Hz, C-17), 107.35 (d, $^{2}J_{C\text{-}F}$ =17.0 Hz, C-11), 102.24 (C-1), 99.57 (d, $^{3}J_{C\text{-}F}$ = 23.0 Hz, C-14), 72.72 (C-3), 72.04 (C-5), 71.32 (C-2), 68.38 (C-4), 65.57 (C-19), 62.01 (C-6), 20.85 (C-8), 20.63 (C-8), 20.60 (C-8) and 20.48 (C-8). **^{19}F NMR ($CDCl_3$, 376 MHz):** δ ppm = -135.82 and -144.93. **IR_{Vmax}:** cm^{-1} = 3340 (Secondary amide N-H, *s*, br), 2945 (Aromatic C-H, *s*, w) 1745 (C=O, *s*, s), 1558 (C=C, *s*, m), 1216 (C-O, *s*, s), 1038 (C-F, *s*, s), 982 and 913 (C=C, *d*, s). **FTMS (ESI):** m/z calculated for $(M+Na)^{+}$ $C_{26}H_{27}{}^{19}F_2NO_{12}Na$ required 606.1394, found 606.1394.

6.5.1.5 Synthesis of [6-(trifluoromethyl)-indox-3-ylic acid allyl ester]-2,3,4,6-tetra-*O*-acetyl-β-D-galactopyranoside (27c)

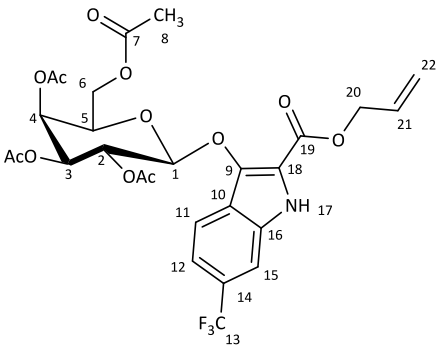

Compound **27c** was prepared according to **Section 6.5.1** general procedure using compound **5d** (1.06 g, 3.72 mmol), acetobromogalactose **23a** (1.62 g, 3.94 mmol) and TBAHS (1.35 g, 3.98 mmol). R_f = 0.29 (2:1 PE 40-60:EtOAc). Yield = 89% (2.02 g 3.28 mmol), yellow solid product. mp 94-95 °C. **^{1}H NMR ($CDCl_3$, 400 MHz):** δ ppm = 8.93 (1H, s, H-17), 7.91 (1H, d, $^{5}J_{H\text{-}H}$ = 8.5 Hz, H-11), 7.64 (1H, s, H-15), 7.33 (1H, d, $^{4}J_{H\text{-}H}$ = 8.5 Hz, H-12), 6.05 (1H, ddd, $^{3}J_{H\text{-}H}$ =

16.0 Hz, $^{3}J_{H\text{-}H}$ = 10.5 Hz and $^{3}J_{H\text{-}H}$ = 5.0 Hz, H-21), 5.60 (1H, dd, $^{3}J_{H\text{-}H}$ = 10.5 Hz and $^{3}J_{H\text{-}H}$ = 8.0 Hz, H-2), 5.47-5.42 (2H, m, H-4 and H-22a), 5.34 (1H, dd, $^{3}J_{H\text{-}H}$ = 10.0 Hz, H-22a), 5.13 (1H, d, $^{3}J_{H\text{-}H}$ = 8.5 Hz, H-1), 5.13 (1H, dd, $^{3}J_{H\text{-}H}$ = 8.5 Hz and $^{3}J_{H\text{-}H}$ = 5.5 Hz, H-3), 4.88-4.87 (2H, m, H-20), 4.18 (1H, d, $^{3}J_{H\text{-}H}$ = 11.5 Hz and $^{3}J_{H\text{-}H}$ = 7.0 Hz H-6a), 4.10 (1H, dd, $^{3}J_{H\text{-}H}$ = 11.5 Hz and $^{3}J_{H\text{-}H}$ = 6.5 Hz, H-6b), 3.93 (1H, t, $^{3}J_{H\text{-}H}$ = 7.0 Hz, H-5), 2.23 (C-8), 2.15 (C-8), 2.03 (C-8) and 1.87 (C-8). **^{13}C NMR ($CDCl_3$, 100 MHz):** δ ppm = 170.36 (C-7), 170.32 (C-7), 170.18, (C-7), 169.87 (C-7), 159.63 (C-19), 140.37 (C-9), 132. 27 (C-16), 131.76 (C-21), 128.65 (q, $^{2}J_{C\text{-}F}$ = 31.0 Hz, C-14), 124.49 (d, $^{1}J_{C\text{-}F}$ = 270.0 Hz, C-13), 123.66 (C-10), 121.88 (C-11), 119.20 (C-22), 117.46 (C-18), 116.94 (d, $^{3}J_{C\text{-}F}$ = 2.5 Hz, C-12), 109.62 (d, $^{3}J_{C\text{-}F}$ = 4.0 Hz, C-15), 102.95 (C-1), 71.04 (C-5), 70.83 (C-3), 68.80 (C-2), 66.98 (C-4), 65.77 (C-20), 61.30 (C-6), 20.98 (C-8), 20.72 (C-8), 20.61 (C-8), and 20.48 (C-8). **^{19}F NMR ($CDCl_3$, 376 MHz):** δ ppm = -61.67. **IR_{Vmax}: cm^{-1}** = 3326 (Secondary amide N-H, *s*, br), 2950 (Aromatic C-H, *s*, w) 1747 (C=O, *s*, s), 1553 (C=C, *s*, w), 1214 (C-O, *s*, s), 1038 (C-F, *s*, s), 983 and 913 (C=C, *d*, s). **FTMS (ESI):** m/z calculated for $(M+Na)^{+}$ $C_{27}H_{28}{}^{19}F_3NO_{12}Na$ required 638.1456, found 638.1456.

6.5.1.6 Synthesis of [6-(trifluoromethyl)-indox-3-ylic acid allyl ester]-2,3,4,6-tetra-*O*-acetyl-β-D-glucopyranoside (28c)

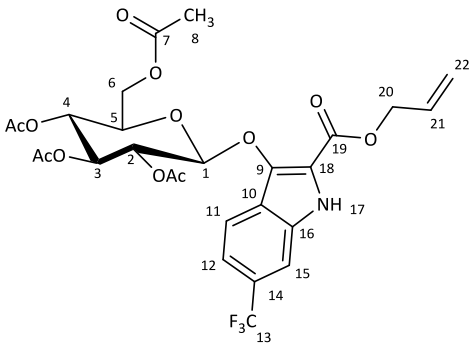

Compound **28c** was prepared according to **Section 6.5.1** general procedure using compound **5d** (1.11 g, 4.30 mmol), acetobromoglucose **23b** (1.71 g, 4.16 mmol) and TBAHS (1.48 g, 4.36 mmol). R_f = 0.30 (2:1 PE 40-60:EtOAc). Yield = 90% (2.17 g, 3.51 mmol), yellow solid

product. mp 144-145 °C. **^{1}H NMR ($CDCl_3$, 400 MHz):** δ ppm = 8.90 (1H, s, H-17), 7.89 (1H, d, $^{3}J_{H-H}$ = 8.5 Hz, H-11), 7.64 (1H, s, H-15), 7.33 (1H, d, $^{3}J_{H-H}$ = 8.5 Hz, H-12), 6.05 (1H, ddd, $^{3}J_{H-H}$ = 16.5 Hz, $^{3}J_{H-H}$ = 10.0 Hz and $^{3}J_{H-H}$ = 6.0 Hz, H-21), 5.46-5.29 (4H, m, H-2, H-3, H-22a and H-22b), 5.19 (1H, d, $^{3}J_{H-H}$ = 8.0 Hz, H-1), 5.19 (1H, t, $^{3}J_{H-H}$ = 9.5 Hz, H-4), 4.87 (1H, d, $^{3}J_{H-H}$ = 5.5 Hz and $^{3}J_{H-H}$ = 1.0 Hz, H-20), 4.28 (1H, dd, $^{2}J_{H-H}$ =12.5 Hz and $^{3}J_{H-H}$ = 5.5 Hz, H-6a), 4.05 (1H, dd, $^{3}J_{H-H}$ = 12.0 Hz and $^{3}J_{H-H}$ = 2.0 Hz, H-6b), 3.73 (1H, ddd, $^{3}J_{H-H}$ = 10.0 Hz, $^{3}J_{H-H}$ = 5.6 Hz and $^{3}J_{H-H}$ = 2.5 Hz, H-5), 2.12 (C-8), 2.05 (C-8), 2.04 (C-8) and 1.93 (C-8). **^{13}C NMR ($CDCl_3$, 100 MHz):** δ ppm = 170.51 (C-7), 170.28 (C-7), 169.70 (C-7), 169.47 (C-7), 159.64 (C-19), 140.13 (C-9), 132.27 (C-16), 131.73 (C-21), 128.19 (q, $^{2}J_{C-F}$ = 32.0 Hz, C-14), 124.48 (d, $^{1}J_{C-F}$ = 273.0 Hz, C-13), 123.59 (C-10), 121.75 (C-11), 119.26 (C-22), 117.55 (C-18), 117.01 (C-12), 109.63 (d, $^{3}J_{C-F}$ = 4.0 Hz, C-15), 102.33 (C-1), 72.70 (C-3), 71.96 (C-5), 71.36 (C-2), 68.48 (C-4), 65.80 (C-20), 61.98 (C-6), 20.86 (C-8), 20.64 (C-8), 20.60 (C-8) and 20.52 (C-8). **^{19}F NMR ($CDCl_3$, 376 MHz):** δ ppm = -61.67. **IR_{Vmax}:** cm^{-1} = 3276 (Secondary amide N-H, *s*, br), 2955 (Aromatic C-H, *s*, w) 1727 (C=O, *s*, s), 1552 (C=C, *s*, s), 1207 (C-O, *s*, s), 1029 (C-F, *s*, s), 971 and 941 (C=C, *d*, s). **FTMS (ESI):** m/z calculated for $(M+Na)^{+}$ $C_{27}H_{28}{}^{19}F_3NO_{12}Na$ required 638.1456, found 638.1456.

6.5.2 General Procedure: De-*O*-allylation and decarboxylation of allyl ester

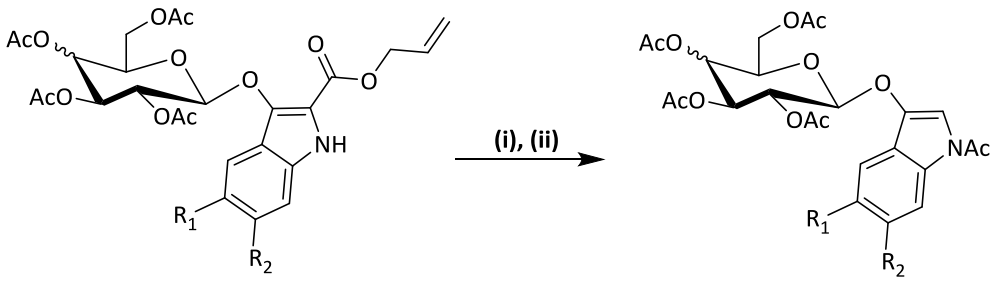

27a & 28a: R_1=F, R_2=H
27b & 28b: R_1=F, R_2=F
27c & 28c: R_1=H, R_2=CF_3

31a & 32a: R_1=F, R_2=H
31b & 32b: R_1=F, R_2=F
31c & 32c: R_1=H, R_2=CF_3

(i): Pd(PPh3)4, morpholine, THF, rt, overnight; **(ii):** AgOAc, K_2CO_3, Ac_2O, 90-100 °C, 30-60 min.

The reaction was conducted under an argon atmosphere and with exclusion of light. The following materials were dissolved in anhydrous THF: per-*O*-acetyl indoxylic acid allyl ester glycoside (1.0 mol equiv) and morpholine (10.0 mol equiv), $Pd(PPh_3)_4$ (10.0 mol equiv). The reaction mixture was stirred overnight. After leaving the reaction overnight, the solvent was removed *in vacuo*. The residue together with AgOAc (3 mol equiv) and K_2CO_3 (7 mol equiv) were dissolved in Ac_2O (mL). The reaction mixture was heated at 90-100 °C under reflux for 30-60 min. After cooling the reaction to rt, the reaction was diluted with DCM, followed by vacuum filtration under Celite® pad with washing of DCM. The filtrate was washed with water twice, followed by saturated $NaHCO_3$ and once with water. The collected organic extract was dried with Na_2SO_4, filtered and concentrated *in vacuo*. The crude product was purified with flash column chromatography.

6.5.2.1 Synthesis of *N*-acetyl-5-fluoro-3-indolyl-2,3,4,6-tetra-*O*-acetyl-β-D-galactopyranoside (31a)

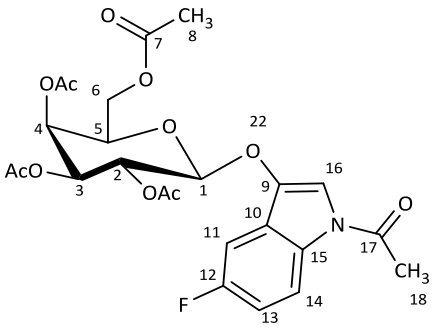

Compound **31** was prepared according to **Section 6.5.2** general procedure using compound **27a** (3.41 g, 6.03 mmol), morpholine (5 mL, 60.30 mmol), Pd(PPh3)4 (0.70 g, 0.60 mmol), THF (15 mL), AgOAc (3.02 g, 18.09 mmol), K_2CO_3 (8.47 g, 61.28 mmol), Ac2O (20 mL). R_f = 0.50 (2:1 PE 40-60:EtOAc). Yield = 40% (3.17 g, 6.06 mmol), yellow solid product. mp 168-169 °C. The product was prepared before by Parshotam *et al.*[127] **^{1}H NMR ($CDCl_3$ 400 MHz):** δ ppm = 8.35 (1H, br. s, H-16), 7.19 (1H, $^4J_{H\text{-}F}$ = 9.0 Hz and $^3J_{H\text{-}H}$ = 2.5 Hz, H-14), 7.16 (1H, dd, $^3J_{H\text{-}F}$ = 8.0 and Hz, $^4J_{H\text{-}H}$ = 2.5 Hz, H-11), 7.27 (1H, td, $^3J_{H\text{-}F}$ = 8.0 Hz and $^4J_{H\text{-}F}$ = 2.5 Hz, H-13), 5.54 (1H, dd, $^3J_{H\text{-}H}$ = 10.6 Hz and $^3J_{H\text{-}H}$ = 8.0 Hz, H-2), 5.48 (1H, d, $^3J_{H\text{-}H}$ = 2.5 Hz, H-4), 5.13 (1H, dd, $^3J_{H\text{-}H}$ = 10.5 Hz and $^3J_{H\text{-}H}$ = 3.5 Hz, H-3), 4.98 (1H, d, $^3J_{H\text{-}H}$ = 8.0 Hz, H-1), 4.24 (2H, d, $^3J_{H\text{-}H}$ = 6.5 Hz, H-6a and H-6b), 4.13-4.06 (1H, m, H-5), 2.59 (3H, s, H-18), 2.21 (3H, s, H-8), 2.14 (3H, s, H-8), 2.08 (3H, s, H-8) and 2.03 (3H, s, H-8). **^{13}C NMR ($CDCl_3$, 100 MHz):** δ ppm = 170.36 (C-7), 170.17 (C-7), 170.09 (C-7), 169.34 (C-7), 167.90 (C-17), 159.60 (d, $^1J_{C\text{-}F}$ = 240.0 Hz, C-12), 141.23 (d, $^4J_{C\text{-}F}$ = 4.0 Hz, C-15), 129.98 (C-9), 125.01 (d, $^3J_{C\text{-}F}$ = 10.0 Hz, C-20), 117.91 (C-16), 114.35 (d, $^2J_{C\text{-}F}$ = 20.5 Hz, C-13), 111.02 (C-14), 103.55 (d, $^2J_{C\text{-}F}$ = 23.0 Hz, C-11), 101.51 (C-1), 71.64 (C-5), 70.60 (C-3), 68.49, (C-2), 66.99 (C-4), 61.83 (C-6) 23.71 (C-18), 20.78 (C-8), 20.67 (C-8), 20.67 (C-8) and 20.57 (C-8). **^{19}F NMR ($CDCl_3$, 376 MHz):** δ ppm = -118.26. **IR_{Vmax}:** cm^{-1} = 2970 (C-H, s, w) 1744 (C=O, s, s), 1581 (C=C, s, w), 1216 (C-O, s, s), 1056 (C-F, s, s), 945 and 902 (C=C, d, w). **FTMS (ESI):** m/z calculated for $(M+Na)^+$ $C_{22}H_{23}{}^{19}FNO_{10}$ required

480.1301, found 480.1311 and for $(M+Na)^+$ $C_{24}H_{26}{}^{19}FNO_{11}Na$ required 546.1382, found 546.1382.

6.5.2.2 Synthesis of *N*-acetyl-5-fluoro-3-indolyl-2,3,4,6-tetra-*O*-acetyl-β-D-glucopyranoside (32a)

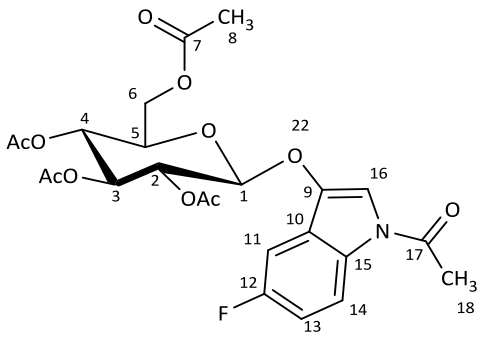

Compound **32a** was prepared according to **Section 6.5.2** general procedure using compound **28a** (3.62 g, 5.68 mmol), morpholine (6 mL, 68.60 mmol), $Pd(PPh_3)_4$ (0.74 g, 0.64 mmol), THF (15 mL), AgOAc (3.31 g, 19.83 mmol), K_2CO_3 (8.97 g, 64.90 mmol), Ac_2O (mL). R_f = 0.36 (2:1 PE 40-60:EtOAc). Yield = 57% (3.36 g, 6.42 mmol), yellow solid product. mp 152-153 °C. **^{1}H NMR ($CDCl_3$, 400 MHz):** δ ppm = 8.35 (1H, br. s, H-16), 7.19 (1H, $^4J_{H-F}$ = 9.0 Hz and $^3J_{H-H}$ = 2.5 Hz, H-14), 7.14 (1H, dd, $^3J_{H-F}$ = 8.0 Hz and $^4J_{H-H}$ = 2.5 Hz, H-11), 7.27 (1H, td, $^3J_{H-F}$ = 8.0 Hz and $^4J_{H-H}$ = 2.5 Hz, H-13), 5.34-5.28 (2H, m, H-1 and H-3), 5.18 (1H, tt, $^3J_{H-H}$ = 9.0 Hz and $^3J_{H-H}$ = 3.0 Hz, H-4), 5.01 (1H, dd, $^3J_{H-H}$ = 8.5 Hz and $^3J_{H-H}$ = 6.5 Hz, H-2), 4.30 (1H, dd, $^2J_{H-H}$ = 12.0 Hz and $^3J_{H-H}$ = 2.0 Hz, H-6a), 4.23 (1H, dd, $^2J_{H-H}$ = 12.5 Hz and $^3J_{H-H}$ = 5.0 Hz, H-6b), 3.89 (1H, ddd, $^3J_{H-H}$ = 2.0 Hz, $^3J_{H-H}$ = 4.5 Hz and $^3J_{H-H}$ = 7.0 Hz, H-5), 2.59 (3H, s, H-18), 2.13 (3H, s, H-8), 2.09 (3H, s, H-8), 2.06 (3H, s, H-8) and 2.06 (3H, s, H-8). **^{13}C NMR ($CDCl_3$, 100 MHz):** δ ppm = 170.52 (C-7), 170.18 (C-7), 169.38 (C-7), 169.22 (C-7), 167.97 (C-16), 159.56 (d, $^1J_{C-F}$ = 239.5 Hz, C-12), 140.86 (d, $^4J_{C-F}$ = 4.5 Hz, C-15), 129.92 (C-9), 125.0 (d, $^4J_{C-F}$ = 10 Hz, C-10), 117.95 (C-16), 114.08 (d, $^2J_{C-F}$ = 29.5 Hz, C-13), 11.61 (C-12) 103.53 (d, $^2J_{C-F}$ = 24.0 Hz, C-11), 100.82 (C-1), 72.47 (C-3), 71.01 (C-5), 68.19 (C-4), 61.94 (C-6), 23.68 (C-18)20.68 (C-8), 20.67 (C-8), 20.59

(C-8) and 20.57 (C-8). **^{19}F NMR ($CDCl_3$, 376 MHz)** δ ppm = -118.14. **IR_{Vmax}:** cm^{-1} **=** 2970 (C-H, *s*, w) 1744 (C=O, *s*, s), 1580 (C=C, *s*, w), 1213 (C-O, *s*, s), 1032 (C-F, *s*, s), 944 and 910 (C=C, *d*, w). **FTMS (ESI):** m/z calculated for $(M+H)^+$ $C_{22}H_{23}{}^{19}FNO_{10}$ required 480.1305, found 480.1311.

6.5.2.3 Synthesis of *N*-acetyl-5,6-difluoro-3-indolyl-2,3,4,6-tetra-*O*-acetyl-β-D-galactopyranoside (31b)

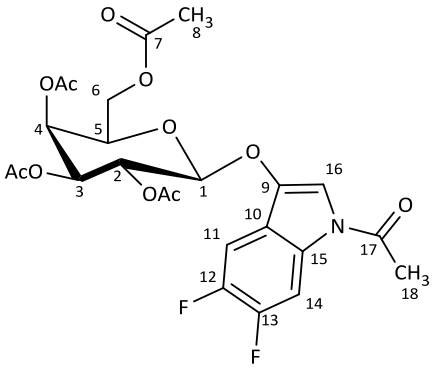

Compound **31b** was prepared according to **Section 6.5.2** general procedure using compound **27b** (2.19 g, 4.04 mmol), morpholine (4 mL, 45.73 mmol), $Pd(PPh_3)_4$ (0.49 g, 0.42 mmol), THF (20 mL), AgOAc (1.92 g, 11.50 mmol), K_2CO_3 (3.82 g, 27.64 mmol), Ac_2O (20 mL). R_f = 0.82 (1:1 PE 40-60:EtOAc). Yield = 61% (1.23 g, 2.27 mmol), yellow solid product. mp 83-84 °C. The product was prepared before by Parshotam and co-workers.[127] **^{1}H NMR ($CDCl_3$, 400 MHz):** δ ppm = 8.29 (1H, br. s, H-16), 7.24 (1H, dd, $^4J_{H-F}$ = 8.5 and Hz, H-11), 7.14 (1H, br. s, H-14), 5.53 (1H, dd, $^3J_{H-H}$ = 10.5 Hz and $^3J_{H-H}$ = 8.0 Hz, H-2), 5.49 (1H, d, $^3J_{H-H}$ = 3.5 Hz, H-4), 5.13 (1H, dd, $^3J_{H-H}$ = 10.5 Hz and $^3J_{H-H}$ = 3.5 Hz, H-3), 4.97 (1H, d, $^3J_{H-H}$ = 8.0 Hz, H-1), 4.23 (2H, d, $^3J_{H-H}$ = 6.0 Hz, H-6a and H-6b), 4.08 (1H, t, $^3J_{H-H}$ = 6.5 Hz, H-5), 2.58 (3H, s, H-18), 2.21 (3H, s, H-8), 2.13 (3H, s, H-8), 2.08 (3H, s, H-8) and 2.03 (3H, s, H-8). **^{13}C NMR ($CDCl_3$, 100 MHz):** δ ppm = 170.36 (C-7), 170.15 (C-7), 170.09 (C-7), 169.34 (C-7), 167.95 (C-17), 150.31 (dd, $^1J_{C-F}$ = 161.0 Hz and $^2J_{C-F}$ = 17.0 Hz, C-12), 147.86 (dd, $^1J_{C-F}$ = 161.0 Hz and $^2J_{C-F}$ = 13.0 Hz, C-12), 140.24 (d, $^4J_{C-F}$ = 4.5 Hz, C-9), 128.63 (d, $^3J_{C-F}$ = 8.5 Hz, C-15), 119.67 (d, $^3J_{C-F}$ = 8.0 Hz, C-15), 110.24 (d, $^3J_{C-F}$ = 3.5 Hz, C-11), 105.05 (d, $^3J_{C-F}$ = 20.5 Hz, C-14), 101.47 (C-1), 71.65 (C-5),

70.53 (C-3), 68.41 (C-2), 66.93 (C-4), 61.82 (C-6), 23.55 (C-8), 20.78 (C-8), 20.68 (C-8), 20.66 (C-8) and 20.58 (C-8). **^{19}F NMR ($CDCl_3$, 376 MHz):** δ ppm = -135.98 and -144.17. **IR_{Vmax}:** cm^{-1} = 2970 (C-H, *s*, w) 1743 (C=O, *s*, s), 1610 (C=C, *s*, w), 1212 (C-O, *s*, s), 1037 (C-F, *s*, s), 984 and 905 (C=C, *d*, w). **FTMS (ESI):** m/z calculated for $(M+Na)^+$ $C_{24}H_{25}{}^{19}F_2NO_{11}Na$ required 564.1288, found 564.1288.

6.5.2.4 Synthesis of *N*-acetyl-5,6-difluoro-3-indolyl-2,3,4,6-tetra-*O*-acetyl-β-D-glucopyranoside (32b)

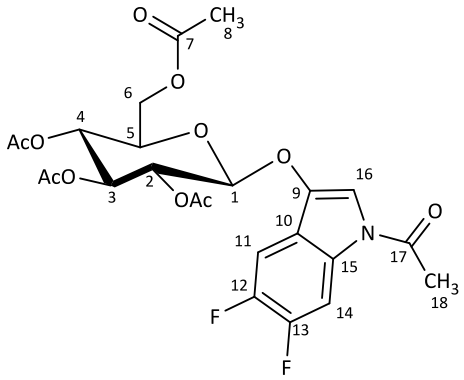

Compound **32b** was prepared according to **Section 6.5.2** general procedure using compound **32b** (2.02 g, 3.73 mmol), morpholine (3 mL, 34.30 mmol), $Pd(PPh_3)_4$ (0.40 g, 0.35 mmol), THF (20 mL), AgOAc (1.77 g, 10.60 mmol), K_2CO_3 (4.90 g, 35.45 mmol), Ac_2O (20 mL). R_f = 0.81 (1:1 PE 40-60: EtOAc). Yield = 42% (1.53 g, 2.83 mmol), yellow solid product. mp 93-94 °C. **^{1}H NMR ($CDCl_3$, 400 MHz):** δ ppm = 8.29 (1H, br. s, H-16), 7.24 (1H, dd, $^4J_{H\text{-}F}$ = 8.5 Hz, H-11), 7.14 (1H, br. s, H-14), 5.31 (2H, d, $^3J_{H\text{-}H}$ = Hz, H-1 and H-3), 5.19 (1H, d, $^3J_{H\text{-}H}$ = 9.0 Hz, H-2), 5.01 (1H, dd, $^3J_{H\text{-}H}$ =6.0 Hz, H-4), 4.30 (1H, dd, $^2J_{H\text{-}H}$ = 12.0 Hz, H-6a), 4.23 (1H, dd, $^2J_{H\text{-}H}$ = 12.5 Hz and $^3J_{H\text{-}H}$ = 5.0 Hz, H-6b), 3.88 (1H, m, H-5), 2.59 (3H, s, H-18), 2.13 (3H, s, H-8), 2.09 (3H, s, H-8), 2.07 (3H, s, H-8), and 2.06 (3H, s, H-8). **^{13}C NMR ($CDCl_3$, 100 MHz):** δ ppm = 170.52 (C-7), 170.21 (C-7), 169.41 (C-7), 169.25 (C-7), 168.05 (C-17), 150.09 (dd, $^1J_{C\text{-}F}$ = 146.0 Hz and $^2J_{C\text{-}F}$ = 15.0 Hz, C-12), 147.85 (dd, $^1J_{C\text{-}F}$ = 160.0 Hz and $^2J_{C\text{-}F}$ = 16.5 Hz, C-12),

140.58 (C-9), 128.63 (d, $^{3}J_{C\text{-}F}$ = 11.5 Hz, C-15), 119.70 (d, $^{3}J_{C\text{-}F}$ = 8.0 Hz, C-15), 110.91 (d, $^{3}J_{C\text{-}F}$ = 3.5 Hz, C-11), 105.05 (d, $^{3}J_{C\text{-}F}$ = 18.0 Hz, C-14), 100.80 (C-1), 72.50 (C-3), 72.38 (C-5), 70.96 (C-1), 68.12 (C-2), 61.90 (C-6), 23.56 (C-18), 20.71 (C-8), 20.69 (C-8), 20.61 (C-8) and 20.61 (C-8). **^{19}F NMR ($CDCl_3$, 376 MHz):** δ ppm = -137.54 and -140.92. **IR_{Vmax}:** cm^{-1} **=** 2969 (C-H, *s*, w) 1747 (C=O, *s*, s), 1607 (C=C, *s*, w), 1208 (C-O, *s*, s), 1030 (C-F, *s*, s), 982 and 905 (C=C, *d*, w). **FTMS (ESI):** m/z calculated for $(M+Na)^{+}$ $C_{24}H_{25}{}^{19}F_2NO_{11}Na$ required 564.1288, found 564.1288.

6.5.2.5 Synthesis of *N*-acetyl-6-(trifluoromethyl)-3-indolyl-2,3,4,6-tetra-*O*-acetyl-β-D-galactopyranoside (31c)

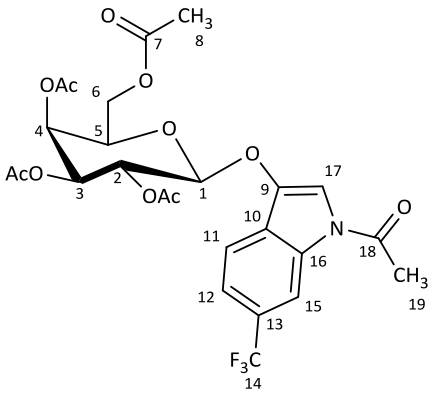

Compound **31c** was prepared according to **Section 6.5.2** general procedure using compound **27c** (2.08 g, 3.38 mmol), morpholine (3 mL, 34.30 mmol), $Pd(PPh_3)_4$, (0.41 g, 0.35 mmol), THF (15 mL), AgOAc (1.43 g, 8.57 mmol), K_2CO_3 (2.74 g, 19.82 mmol), Ac_2O (15 mL). R_f = 0.46 (1:1 PE 40-60: EtOAc). Yield = 77% (1.25 g, 2.18 mmol), off-white solid product. mp 174-175 °C. **^{1}H NMR ($CDCl_3$, 400 MHz):** δ ppm = 8.71 (1H, br. s, H-17), 7.60 (1H, d, $^{3}J_{H\text{-}H}$ = 8.0 Hz, H-11), 7.53 (1H, d, $^{3}J_{H\text{-}H}$ = 8.0 Hz, H-12), 7.28 (1H, s, H-15), 5.56 (1H, dd, $^{3}J_{H\text{-}H}$ = 10.5 Hz and $^{3}J_{H\text{-}H}$ = 8.0 Hz, H-2), 5.50 (1H, d, $^{3}J_{H\text{-}H}$ = 2.5 Hz, H-4), 5.14 (1H, dd, $^{3}J_{H\text{-}H}$ = 10.5 Hz and $^{3}J_{H\text{-}H}$ = 3.0 Hz, H-3), 5.01 (1H, d, $^{3}J_{H\text{-}H}$ = 8.0 Hz, H-1), 4.25 (1H, d, $^{3}J_{H\text{-}H}$ = 3.0 Hz, H-6a), 4.23 (1H, d, $^{3}J_{H\text{-}H}$ = 1.5 Hz, H-6b), 4.09 (1H, t, $^{3}J_{H\text{-}H}$ = 6.5 Hz, H-5), 2.63 (3H, s, H-19), 2.21 (3H, s, H-8), 2.13

(3H, s, H-8) 2.07 (3H, s, H-8) 2.04 (3H, s, H-8). **^{13}C NMR ($CDCl_3$, 100 MHz):** δ ppm = 170.31 (C-7), 170.13 (C-7), 170.06 (C-7), 169.36 (C-7), 168.05 (C-18), 141.01 (C-9), 132.59 (C-16), 128.38 (d, $^2J_{C\text{-}F}$ = 30.5 Hz, C-13), 126.07 (C-10), 124.48 (d, $^1J_{C\text{-}F}$ = 273.0 Hz, C-12), 123.12 (C-12), 120.47 (d, $^3J_{C\text{-}F}$ = 4.0 Hz, C-12), 118.22 (C-11), 114.12 (C-17), 111.53 (C-15), 101.50 (C-1), 71.66 (C-5), 70.51 (C-3), 68.42 (C-2), 66.92 (C-4), 61.76 (C-6), 23.85 (C-19), 20.75 (C-7), 20.67(C-7), 20.64 (C-7) and 20.56 (C-7). **^{19}F NMR ($CDCl_3$, 376 MHz):** δ ppm = -61.20. **IR_{Vmax}:** cm^{-1} = 2977 (C-H, s, w) 1742 (C=O, s, s), 1572 (C=C, *s*, w), 1220 (C-O, *s*, s), 1045 (C-F, *s*, s), 941 and 901 (C=C, *d*, m). **FTMS (ESI):** m/z calculated for $(M+Na)^+$ $C_{25}H_{26}{}^{19}F_3NO_{11}Na$ required 596.1350, found 596.1350.

6.5.2.6 Synthesis of *N*-acetyl-6-(trifluoromethyl)-3-indolyl-2,3,4,6-tetra-*O*-acetyl-β-D-glucopyranoside (32c)

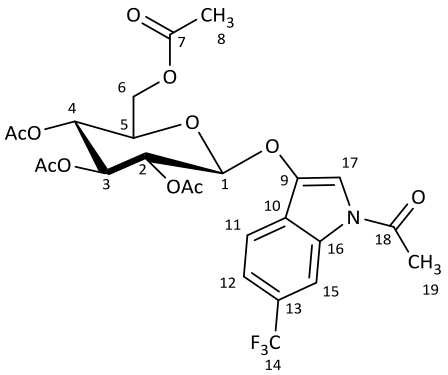

Compound **32c** was prepared according to **Section 6.5.2** general procedure compound **28c** (2.08 g, mmol), morpholine (3 mL, mmol), $Pd(PPh3)_4$ (0.41 g, mmol), THF (15 mL), AgOAc (1.70 g, 10.19 mmol), K_2CO_3 (3.28 g, 23.73 mmol), Ac_2O (15 mL). R_f = 0.43 (1:1 PE 40-60: EtOAc). Yield = 72% (1.93 g, 3.37 mmol), off-white solid product. mp 177-178 °C. **^{1}H NMR ($CDCl_3$, 400 MHz):** δ ppm = 8.64 (1H, br. s, H-17), 7.52 (1H, d, $^3J_{H\text{-}H}$ = 8.0 Hz, H-11), 7.45 (1H, d, $^3J_{H\text{-}H}$ = 8.0 Hz, H-12), 7.23 (1H, s, C-15), 5.26 (1H, d, $^3J_{H\text{-}H}$ = 3.0 Hz, H-3) 5.25 (1H, d, $^3J_{H\text{-}H}$ = 7.5 Hz, H-1), 5.12 (1H, m, H-4), 4.97 (1H, d, 7.0 Hz, H-2), 4.23 (1H, dd, $^2J_{H\text{-}H}$ = 12.0 Hz and

$^{3}J_{H\text{-}H}$ = 2.0 Hz, H-6a), 4.17 (1H, dd, $^{2}J_{H\text{-}H}$ = 12.5 Hz and $^{3}J_{H\text{-}H}$ = 4.5 Hz, H-6b), 3.81 (1H, ddd, $^{3}J_{H\text{-}H}$ = 10.0 Hz, $^{3}J_{H\text{-}H}$ = 4.5 Hz and $^{3}J_{H\text{-}H}$ = 2.5 Hz, H-5), 2.57 (3H, s, H-19), 2.05 (3H, s, H-8), 2.00 (3H, s, H-8), 1.99 (3H, s, H-8) and 1.99 (3H, s, H-8). **^{13}C NMR ($CDCl_3$, 100 MHz):** δ ppm = 169.46 (C-7), 169.16 (C-7), 168.38 (C-7), 169.23 (C-7), 167/14 (C-18), 139.65 (C-9), 131.57 (C-16), 127.31 (d, $^{2}J_{C\text{-}F}$ = 32.0 Hz, C-13), 125.34 (C-10), 123.47 (d, $^{1}J_{C\text{-}F}$ = 270.0 Hz, C-12), 122.11 (C-11), 119.46 (d, $^{3}J_{C\text{-}F}$ = 4.0 Hz, C-12), 117.21 (C-11), 113.20 (C-17), 111.20 (C-15), 99.83 (C-1), 71.55 (C-3), 71.38 (C-5), 69.99 (C-2), 67.15 (C-4), 60.86 (C-6), 22.83 (C-19), 19.89 (C-7), 19.65 (C-7), 19.59 (C-7) and 20.56 (C-7). **^{19}F NMR ($CDCl_3$, 376 MHz):** δ ppm = -61.20. **IR_{Vmax}:** cm^{-1} = 2969 (C-H, *s*, w) 1742 (C=O, *s*, s), 1575 (C=C, *s*, w), 1217 (C-O, *s*, s), 1043 (C-F, *s*, s), 991 and 941 (C=C, *d*, m). **FTMS (ESI): m/z** calculated for $(M+Na)^{+}$ $C_{25}H_{26}{}^{19}F_3NO_{11}Na$ required 596.1350, found 596.1350.

6.5.3 General Procedure: Zemplén de-*O*-acetylation of per-*O*-acetyl indoxyl glycosides

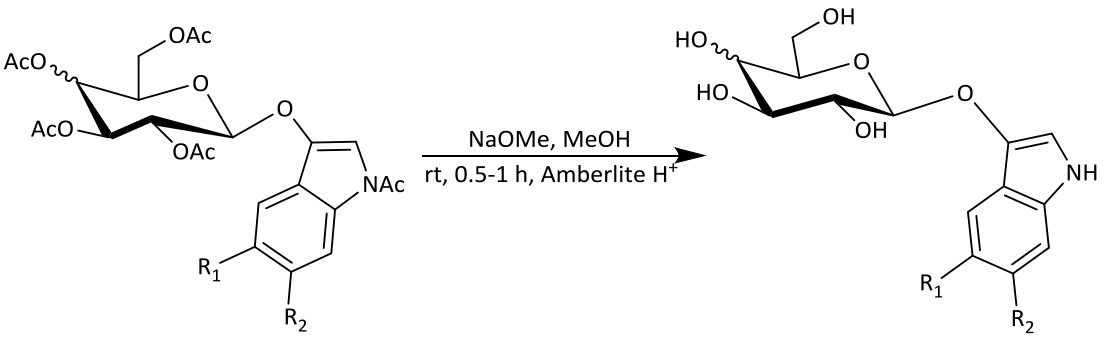

31a & 32a: R_1=F, R_2=H
31b & 32b: R_1=F, R_2=F
31c & 32c: R_1=H, R_2=CF_3

3a & 4a: R_1=F, R_2=H
3b & 4b: R_1=F, R_2=F
3c & 4c: R_1=H, R_2=CF_3

Under an argon atmosphere, the acetylated indoxyl glcyosides (1.0 equiv mol) was dissolved in anhydrous methanol with a catalytic amount of NaOMe. The reaction was stirred at rt until TLC indicated complete deprotection (9:1 DCM:MeOH) with R_f products between 0.07-0.17. The solution was neutralised with Amberilite IR 120 (H^+), the resin was filtered off via vacuum filtration. The solvent was removed *in vacuo*. The crude products were either purified using normal phase flash column chromatography (9:1 DCM:MeoH) or using reversed-phase automated flash column chromatography (70:30, 0.1% v/v formic acid in H_2O:MeCN).

6.5.3.1 Synthesis of 5-fluoro-3-indolyl β-D-galactopyranoside (3a)

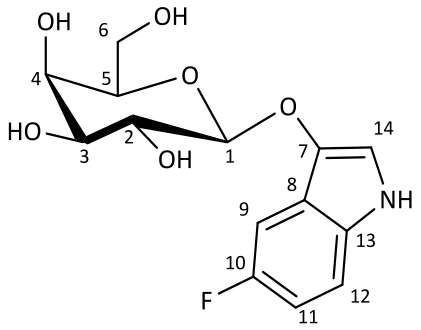

Compound **3a** was prepared according to **Section 6.5.3** general procedure using compound **31a** (1.51 g, 2.88 mmol), catalytic NaOMe (0.50 g, 9.25 mmol), MeOH (8 mL). R_f = 0.10 (9:1 DCM: MeOH). Yield = 19% (0.17 g, 0.54 mmol), solid product. mp 226-227 °C. The product was prepared before by Parshotam *et al.*[127] **^{1}H NMR (MeOD, 400 MHz):** δ ppm = 7.37 (1H, dd, $^{3}J_{H\text{-}F}$ = 10.0 Hz and Hz, $^{4}J_{H\text{-}H}$ = 2.0 Hz, H-9), 7.23 (1H, dd, $^{4}J_{H\text{-}F}$ = 9.0 Hz and Hz, $^{2}J_{H\text{-}H}$ = 4.0 Hz, H-12), 7.16 (1H, s, H-14), 6.85 (1H, td, $^{3}J_{H\text{-}F}$ = 9.0 Hz and $^{4}J_{H\text{-}H}$ = 2.5 Hz, H-11), 4.64 (1H, d, $^{3}J_{H\text{-}H}$ = 8.0 Hz, H-1), 3.90 (1H, d, $^{3}J_{H\text{-}H}$ = 3.0 Hz), 3.84 (1H, dd, $^{3}J_{H\text{-}H}$ = 8.0 Hz, H-2), 3.81 (2H, t, $^{2}J_{H\text{-}H}$ = 5.5 Hz, H-6a and H-6b), 3.61-5.33 (2H, m, H-3 and H-5). **^{13}C NMR (MeOD, 100 MHz):** δ ppm = 158.67 (d, $^{1}J_{C\text{-}F}$ = 230.0 Hz, C-10), 139.21 (d, $^{4}J_{C\text{-}F}$ = 4.5 Hz, C-13), 131.84 (C-7), 121.52 (d, $^{3}J_{C\text{-}F}$ = 10.0 Hz, C-8), 114.73 (C-14), 113.21 (d, $^{3}J_{C\text{-}F}$ = 9.5 Hz, C-12), 111.03 (d, $^{2}J_{C\text{-}F}$ = 27.0 Hz, C-11), 106.64 (C-1), 103.24 (d, $^{2}J_{C\text{-}F}$ = 26.0 Hz), 76.98 (C-3), 74.93 (C-5), 72.51 (C-2), 70.26 (C-4) and 62.46 (C-6). **^{19}F NMR (MeOD, 376 MHz):** δ ppm = -128.02. **IR_{Vmax}:** cm^{-1} = 3457 (Secondary amide N-H, *s*, w), 3250 (O-H, *s*, br) 2922 (C-H, *s*, w), 1558 (C=C, *s*, m), 1333 (C-O, *s*, s), 1010 (C-F, *s*, s), 939 (C=C, *d*, w). **FTMS (ESI):** m/z calculated for $(M+Na)^{+}$ $C_{14}H_{16}{}^{19}FNO_6Na$ required 336.0854, found, 336.0854.

6.5.3.2 Synthesis of 5-fluoro-3-indolyl β-D-glucopyranoside (4a)

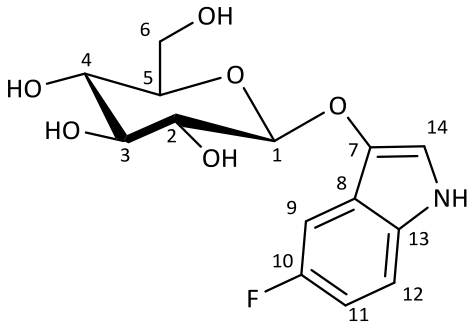

Compound **4a** was prepared according to **Section 6.5.3** general procedure using compound **32a** (1.37 g, 2.61 mmol), catalytic NaOMe (0.52 g, 10.54 mmol), MeOH (13 mL). R_f = 0.17 (9:1 DCM: MeOH). Yield = 48% (0.53 g, mmol), off-white solid product. mp 195-196 °C. **^{1}H NMR (MeOD, 400 MHz):** δ ppm = 7.37 (1H, dd, $^3J_{H\text{-}F}$ = 9.5 Hz and Hz, $^4J_{H\text{-}H}$ = 2.5 Hz, H-9), 7.23 (1H, dd, $^4J_{H\text{-}F}$ = 9.0 and Hz, $^2J_{H\text{-}H}$ = 4.0 Hz, H-12), 7.17 (1H, s, H-14) 6.85 (1H, td, $^3J_{H\text{-}F}$ = 9.0 Hz and $^4J_{H\text{-}H}$ = 2.5 Hz, H-11), 4.68 (1H, d, $^3J_{H\text{-}H}$ = 7.5 Hz, H-1), 3.92 (1H, d, $^2J_{H\text{-}H}$ = 12.0 Hz and $^3J_{H\text{-}H}$ = 5.0 Hz, H-6a), 3.73 (1H, d, $^2J_{H\text{-}H}$ = 12.0 Hz and $^3J_{H\text{-}H}$ = 2.0 Hz, H-6b), 3.52-3.34 (4H, m, H-2, H-3, H-4 and H-5). **^{13}C NMR (MeOD, 100 MHz):** δ ppm = 158.69 (d, $^1J_{C\text{-}F}$ = 233.0 Hz, C-10), 139.11 (d, $^4J_{C\text{-}F}$ = 5.0 Hz,C-13), 131.84 (C-7), 121.47 (d, $^3J_{C\text{-}F}$ = 9.0 Hz, C-8), 114.70 (C-14), 113.24 (d, $^3J_{C\text{-}F}$ = 9.5 Hz, C-12), 111.08 (d, $^2J_{C\text{-}F}$ = 27.0 Hz, C-11), 105.98 (C-1), 103.20 (d, $^2J_{C\text{-}F}$ = 25.0 Hz), 78.21 (C-5), 78.02 (C-3), 75.06 (C-2), 71.55 (C-4) and 62.66 (C-6). **^{19}F NMR (MeOD, 376 MHz):** δ ppm = -127.92. **IR$_{Vmax}$:** cm^{-1} = 3468 (Secondary amide N-H, *s*, w), 3362 (O-H, *s*, br) 2900 (C-H, *s*, w), 1558 (C=C, *s*, m), 1336 (C-O, *s*, s), 1077 (C-F, *s*, s), 934 (C=C, *d*, w). **FTMS (ESI):** m/z calculated for $(M+Na)^+$ $C_{14}H_{16}{}^{19}FNO_6Na$ required 336.0854, found, 336.0854.

6.5.3.3 Synthesis of 5,6-difluoro-3-indolyl β-D-galactopyranoside (3b)

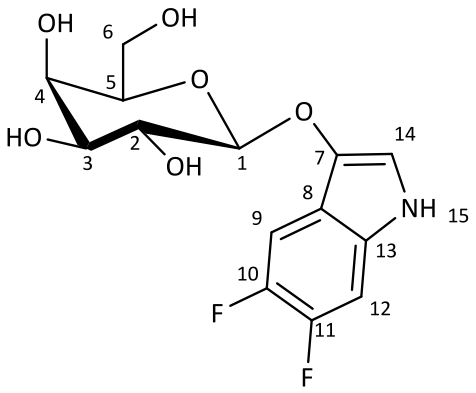

Compound **3b** was prepared according to **Section 6.5.3** general procedure using compound **31b** (1.20 g, 2.22 mmol), catalytic NaOMe (0.18 g, 3.33 mmol) MeOH (24 mL) R_f = 0.10 (9:1 DCM:MeOH). Yield = 66% (0.48 g, 1.46 mmol), off-white solid product. The product was prepared before by Parshotam and co-workers.[127] **^{1}H NMR (MeOD, 400 MHz):** δ ppm = 7.41 (1H, dd, $^{3}J_{H\text{-}F}$ = 11.0 Hz and $^{4}J_{H\text{-}H}$ = 8.0 Hz, H-9), 7.04 (1H, s, H-14), 7.02 (1H, dd, $^{3}J_{H\text{-}F}$ = 11.0 and Hz, $^{4}J_{H\text{-}H}$ = 6.5 Hz, H-12), 4.51 (1H, dd, $^{3}J_{H\text{-}H}$ = 8.0 Hz, H-1), 3.79 (1H, d, $^{3}J_{H\text{-}H}$ = 3.0 Hz, H-4), 3.74-3.68 (3H, m, H-2 and H-6), 3.5 (1H, t, $^{3}J_{H\text{-}H}$ = 6.5 Hz, H-3), 3.45 (1H, dd, $^{3}J_{H\text{-}H}$ = 10.0 Hz and $^{3}J_{H\text{-}H}$ = 3.0 Hz, H-5). **^{13}C NMR (MeOD, 100 MHz):** δ ppm = 149.38 (dd, $^{1}J_{C\text{-}F}$ = 221.0 Hz and $^{2}J_{C\text{-}F}$ = 13.5 Hz, C-9), 147.04 (dd, d, $^{1}J_{C\text{-}F}$ = 218.0 Hz and d, $^{2}J_{C\text{-}F}$ = 16.0 Hz, C-12), 139.25 (C-13), 130.11 (d, $^{4}J_{C\text{-}F}$ = 14.0 Hz, C-7), 116.83 (d, $^{3}J_{C\text{-}F}$ = 8.5 Hz, C-8), 114.20 (d, $^{4}J_{C\text{-}F}$ = 3.5 Hz, C-14), 106.66 (C-1), 105.22 (d, $^{2}J_{C\text{-}F}$ = 17.5 Hz, C-9), 99.93 (d, $^{2}J_{C\text{-}F}$ = 23.5 Hz, C-12), 77.03 (C-3), 74.90 (C-5), 72.46 (C-2), 70.26 (C-4) and 62.49 (C-6). **^{19}F NMR (MeOD, 376 MHz)**: δ ppm = -147.31 and -151.46. **IR_{Vmax}:** cm^{-1} = 3458 (Secondary amide, *s*, w), 3250 (O-H, *s*, br), 2921 (C-H, *s*, w) 1557 (C=C, *s*, w), 1333 (C-O, *s*, s), 1010 (C-F, *s*, s), 939 (C=C, *d*, w). **FTMS (ESI):** m/z calculated for $(M+Na)^{+}$ $C_{14}H_{15}{}^{19}F_2NO_6Na$ required 354.0760, found 354.0760.

6.5.3.4 Synthesis of 5,6-difluoro-3-indolyl β-D-glucoside (4b)

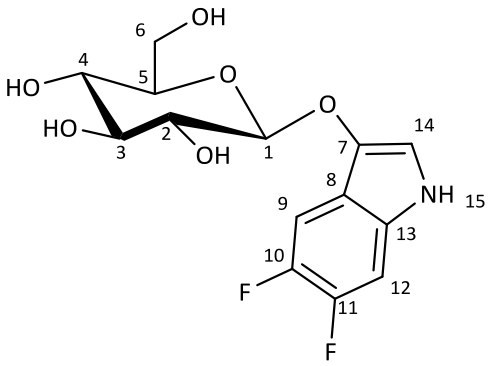

Compound **4b** was prepared according to **Section 6.5.3** general procedure using compound **32b** (1.31 g, 2.42 mmol), catalytic NaOMe (0.61 g, 11.29 mmol), MeOH (10 mL). R_f = 0.09 (9:1 DCM:MeOH). Yield = 45% (0.85 g, mmol), off-white solid product. mp 146-147 °C. **^{1}H NMR (MeOD, 400 MHz):** δ ppm = 7.51 (1H, dd, $^3J_{H\text{-}F}$ = 11.0 Hz and $^4J_{H\text{-}H}$ = 8.0 Hz, H-9), 7.15 (1H, s, H-14), 7.13 (1H, dd, $^3J_{H\text{-}F}$ = 11.0 and Hz, $^4J_{H\text{-}H}$ = 7.0 Hz, H-12), 4.66 (1H, dd, $^3J_{H\text{-}H}$ = 7.5 Hz, H-1), 3.92 (1H, d, $^2J_{H\text{-}H}$ = 12.0 Hz and $^3J_{H\text{-}H}$ = 2.0 Hz, H-6a), 3.73 (1H, d, $^3J_{H\text{-}H}$ = 12.0 Hz and $^3J_{H\text{-}H}$ = 5.5 Hz, H-6b), 3.51-3.36 (4H, m, H-2, H-3, H-4 and H-5). **^{13}C NMR (MeOD, 100 MHz):** δ ppm = 149.42 (dd, $^1J_{C\text{-}F}$ = 218.0 Hz and $^2J_{C\text{-}F}$ = 15.5 Hz, C-9), 147.07 (dd, d, $^1J_{C\text{-}F}$ = 214.5 Hz and d, $^2J_{C\text{-}F}$ = 14.5 Hz, C-12), 139.15 (C-13), 130.12 (d, $^4J_{C\text{-}F}$ = 12.0 Hz, C-7), 116.78 (d, $^3J_{C\text{-}F}$ = 9.5 Hz, C-8), 114.20 (d, $^4J_{C\text{-}F}$ = 3.5 Hz, C-14), 106.02 (C-1), 105.18 (d, d, $^2J_{C\text{-}F}$ = 19.0 Hz, C-9), 99.96 (d, $^2J_{C\text{-}F}$ = 24.0 Hz, C-12), 78.24 (C-5), 78.00 (C-3), 75.03 (C-2), 71.55 (C-4) and 62.66 (C-6). **^{19}F NMR ($CDCl_3$, 376 MHz):** δ ppm = -147.22 and -151.35. **IR_{Vmax}: cm^{-1}** = 3572 (OH, *s*, br), 3350 (Secondary amide, s, w), 2939 (C-H, *s*, w) 1600 (C=C, *s*, m), 1339 (C-O, *s*, s), 1048 (C-F, *s*, s), 932 and 907 (C=C, *d*, w). **FTMS (ESI):** m/z calculated for $(M+Na)^+$ $C_{14}H_{15}{}^{19}F_2NO_6Na$ required 354.0760, found 354.0760.

6.5.3.5 Synthesis of 6-(trifluoromethyl)-3-indolyl β-D-galactopyranoside (3c)

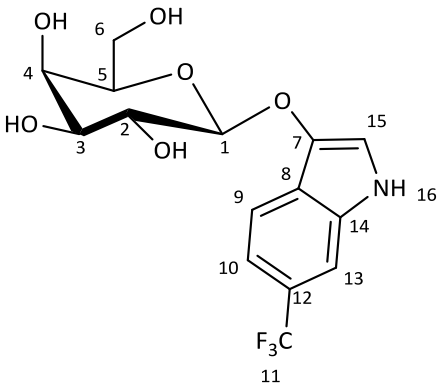

Compound **3c** was prepared according to **Section 6.5.3** general procedure using compound **31c** (1.10 g, 1.92 mmol), catalytic NaOMe, MeOH (15 mL). R_f = 0.07 (9:1 DCM:MeOH). Yield = 31% (0.21 g, 0.58 mmol), off-white solid product. mp 174-175 °C. **^{1}H NMR (MeOD, 400 MHz):** δ ppm = 7.85 (1H, d, $^{3}J_{H\text{-}H}$ = 8.5 Hz, H-9), 7.60 (1H, s, H-13), 7.30 (1H, s, H-15), 7.22 (1H, d, $^{3}J_{H\text{-}H}$ = 8.5 Hz, H-10), 4.69 (1H, d, $^{3}J_{H\text{-}H}$ = 8.0 Hz, H-1), 3.91-3.77 (4H, m, H-3, H-4, H-6a and H-6b), 3.62 (1H, t, $^{3}J_{H\text{-}H}$ = 5.0 Hz, H-3), 3.58 (1H, dd, $^{3}J_{H\text{-}H}$ = 9.5 Hz and $^{3}J_{H\text{-}H}$ = 3.5 Hz, H-5). **^{13}C NMR (MeOD, 100 MHz):** δ ppm = 139.11 (C-7), 133.83 (C-14), 126.91 (d, $^{1}J_{C\text{-}F}$ = 267.0 Hz, C-11), 124.70 (q, $^{2}J_{C\text{-}F}$ = 34.5 Hz, C-12), 123.60 (C-8), 119.50 (C-9), 115.76 (d, $^{3}J_{C\text{-}F}$ = 3.5 Hz, C-10), 115.59 (C-15), 109.83 (d, $^{3}J_{C\text{-}F}$ = 5.0 Hz, C-13), 106.47 (C-1), 77.09 (C-3), 74.93 (C-5), 72.48 (C-2), 70.30 (C-4) and 62.53 (C-6). **^{19}F NMR ($CDCl_3$, 376 MHz):** δ ppm = -62.01. **IR_{Vmax}:** cm^{-1} = 3550 (Secondary amide, *s*, w), 3382 (O-H, *s*, br), 2950 (C-H, *s*, w) 1559 (C=C, *s*, m), 1337 (C-O, *s*, s), 1074 (C-F, *s*, s), 914 (C=C, *d*, w). **FTMS (ESI):** m/z calculated for $(M+Na)^+$ $C_{15}H_{16}{}^{19}F_3NO_6Na$ required 386.0822, found 386.0822.

6.5.3.6 Synthesis of 6-(trifluoromethyl)-3-indolyl β-D-glucopyranoside (4c)

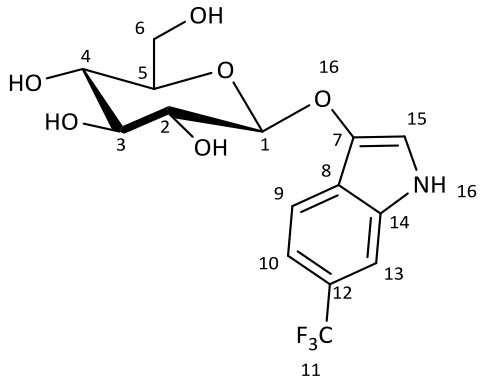

Compound **4c** was prepared according to **Section 6.5.3** general procedure using compound **32c** (1.40 g, 2.44 mmol), catalytic NaOMe, MeOH (10 mL). R_f = 0.06 (9:1 DCM:MeOH). Yield = 90% (0.79 g, 2.17 mmol), off-white solid product. mp 196-197 °C. **^{1}H NMR (MeOD, 400 MHz):** δ ppm = 7.85 (1H, d, $^3J_{H-H}$ = 8.5 Hz, H-9), 7.61 (1H, s, H-13), 7.31 (1H, s, H-15), 7.23 (1H, d, $^3J_{H-H}$ = 8.5 Hz, H-10), 4.73 (1H, d, $^3J_{H-H}$ = 7.5 Hz, H-1), 3.94 (1H, dd, $^3J_{H-H}$ = 12.5 Hz and $^3J_{H-H}$ = 1.5 Hz, H-6a), 3.73 (1H, dd, $^3J_{H-H}$ =12.0 Hz and $^3J_{H-H}$ =5.0 Hz, H-6b), 3.54-3.40 (H-2, H-3, H-4 and H-5). **^{13}C NMR (MeOD, 100 MHz):** δ ppm = 139.00 (C-7), 133.83 (C-14), 126.89 (d, $^1J_{C-F}$ = 270.5 Hz, C-11), 124.73 (q, $^2J_{C-F}$ = 30.5 Hz, C-12), 123.56 (C-8), 119.47 (C-9), 115.80 (q, $^3J_{C-F}$ = 3.0 Hz, C-10), 115.59 (C-15), 109.85 (q, $^3J_{C-F}$ = 5.0 Hz, C-13), 105.83 (C-1), 78.28 (C-5), 78.03 (C-3), 75.06 (C-2), 71.55 (C-4) and 62.67 (C-6). **^{19}F NMR ($CDCl_3$, 376 MHz) δ ppm** = -62.02. **IR_{Vmax}:** cm^{-1} = 3489 (Secondary amide, *s*, w), 3277 (O-H, *s*, br), 2950 (C-H, *s*, w) 1554 (C=C, *s*, m), 1335 (C-O, *s*, s), 1020 (C-F, *s*, s), 916 (C=C, *d*, w). **FTMS (ESI):** m/z calculated for $(M+Na)^+$ $C_{15}H_{16}{}^{19}F_3NO_6Na$ required 386.0822, found 386.0822.

6.5.4 General Prodedure: Preparation of chromogenic media

The glycosidic derivatives were incorporated into the non-selective, general purpose agar media, NA (Oxoid CM0003, **Table 31**) and TSA (Oxoid CM00131, **Table 32**), and organisms were multi-point inoculated on the surface of the plates. Both media are rich in nutrients and support the growth of all the organisms that were tested. The media were sterilised by autoclaving at 121 °C for 15 min. The substrates were aseptically added to NA and TSA to give a final concentration range of 100 mg L^{-1}. The bacterial strain were inoculated from plate stock culture into Nutrient Broth (Oxoid BO0210E) and grown overnight at 37 °C. Cultures were then diluted in 0.85% saline (Oxoid EB0209E) to an approximate concentration of 1.5 x 10^7 CFU mL^{-1} (by optical density) and multi-point inoculated onto the surface to the NA and TSA plates. The inoculated plates were incubated at 37 °C and were examined for up to 20 and 40 hours. The colours of colonies were noted. Control plates without chromogens were inoculated for each set to ensure all the microogsnisms grew the media base.

Table 31. Contents of Nutrient agar (CM0003)

Component	g L^{-1}
'Lab-Lemco' powder	1.0
Yeast extract	2.0
Peptone	5.0
Sodium chloride	5.0
Agar	15.0
pH 7.4 ± 0.2 @ 25 °C	

Table 32. Contents of Tryptone Soya Agar (CM0131).

Component	g L^{-1}
Pancreatic digest casein	15.0
Enzymatic digest soya bean	5.0
Sodium chloride	5.0
Agar	15.0
pH 7.43 ± 0.2 @ 25 °C	

6.5.4.1 Inoculator well template with references to the bacteria utilised in this project.

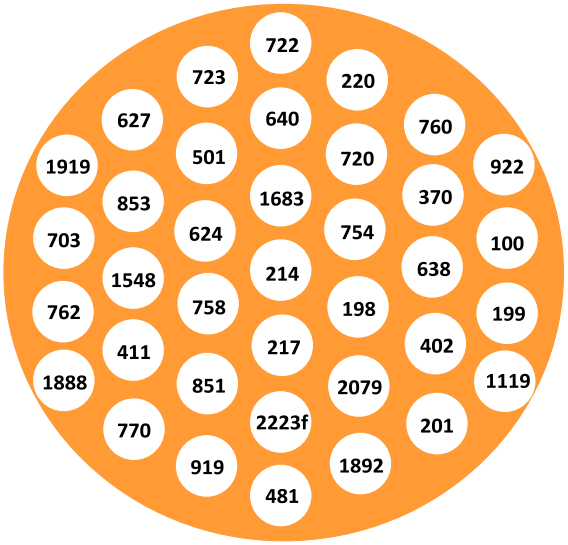

Gram-positive	OCC no.	Gram-negative	OCC no.
Bacillus cereus	754	*Burkholderia cepacia*	770
Bacillus licheniformis	922	*Citrobacter freundii*	370
Bacillus subtilis	214	*Citrobacter freundii*	851
Enterococcus faecalis	501	*Cronobacter sakazakii*	1888
Enterococcus faecalis	640	*Enterobacter aerogenes*	720
Enterococcus faecium	220	*Enterobacter cloacae*	760
Staphylococcus aureus	198	*Escherichia coli*	402
Staphylococcus aureus	638	*Escherichia coli*	199
Staphylococcus aureus v. oxford	100	*Escherichia coli*	481
Staphylococcus epidermis	919	*Escherichia hermanii*	1892
Staphylococcus haemolyticus	2223f	*Klebsiella pneumoniae*	411
Staphylococcus saprophyticus	2079	*Klebsiella pneumoniae*	758
Streptococcus agalactiae GBS	762	*Pseudomonas aeruginosa*	201
Streptococcus pneumoniae	1548	*Pseudomonas aeruginosa*	1119
Streptococcus pyogenes	624	*Salmonella* Abony	1919
Streptococcus viridans	1683	*Salmonella* Dublin	627
		Salmonella Enteritidis	723
		Salmonella Typhimurium	722
		Salmonella Typhimurium	853
		Salmonella Virchow	703
		Serratia marcescens	217

6.5.4.2 Bacterial testing on solid culture media

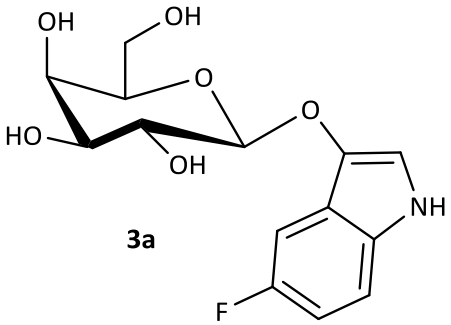

3a

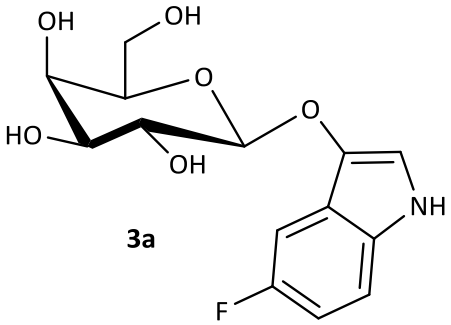

3a

Figure 53a. Substrate **3a** in NA for 20 (top) and 40 (bottom) hours.

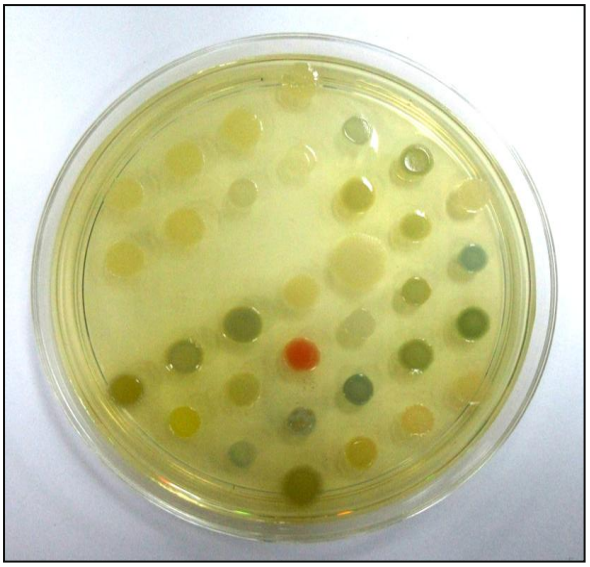

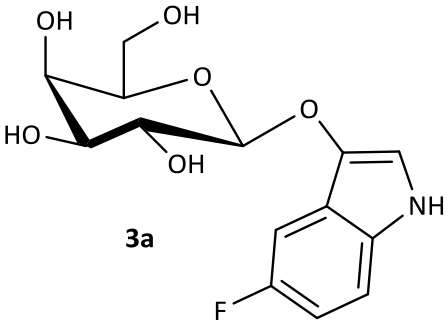

3a

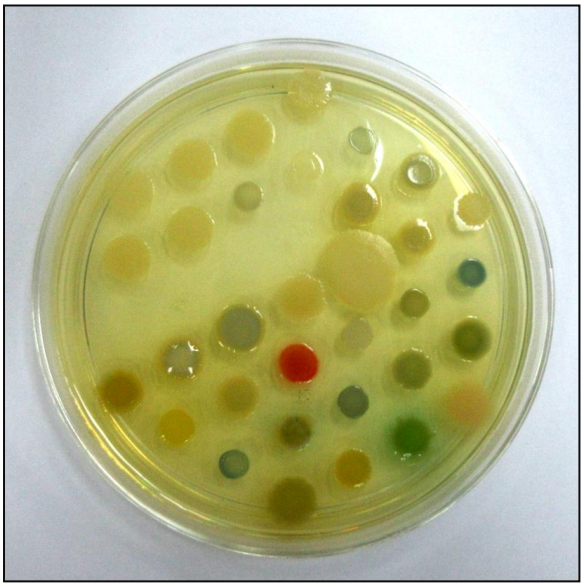

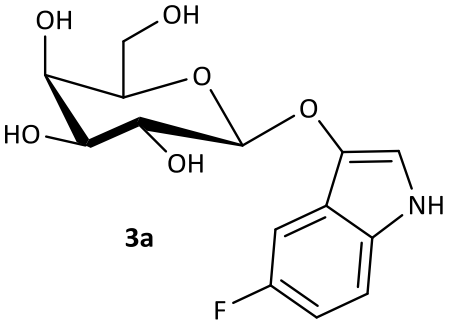

3a

Figure 53b. Substrate **3a** in TSA for 20 (top) and 40 (bottom) hours.

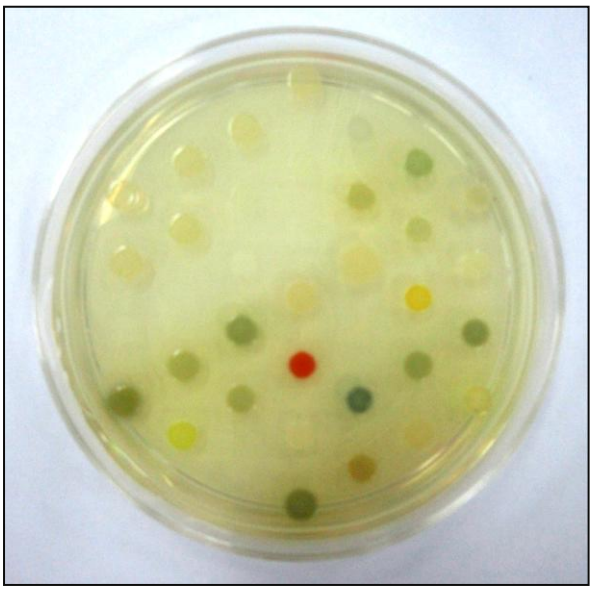

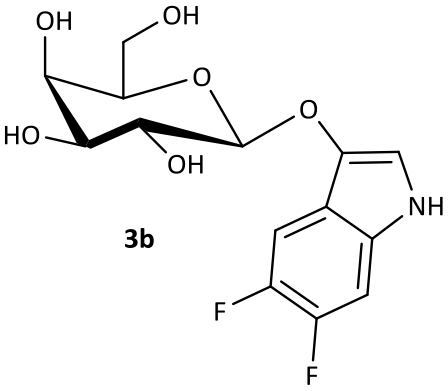

3b

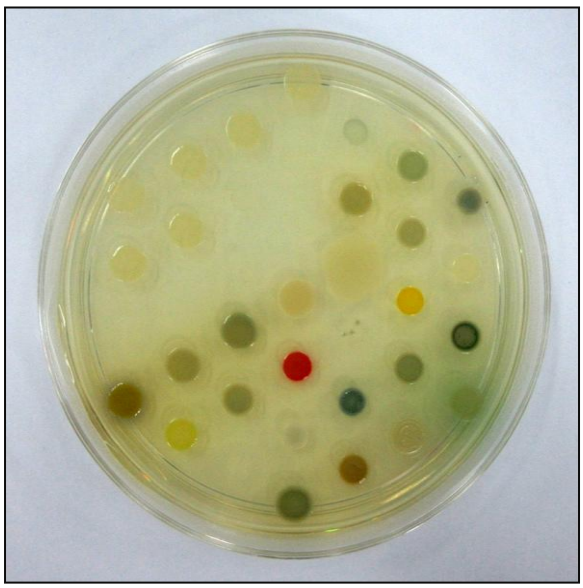

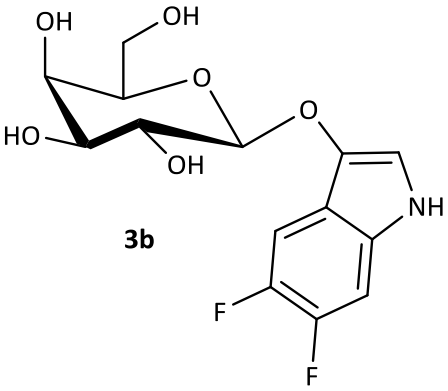

3b

Figure 54a. Substrate **3b** in NA for 20 (top) and 40 (bottom) hours.

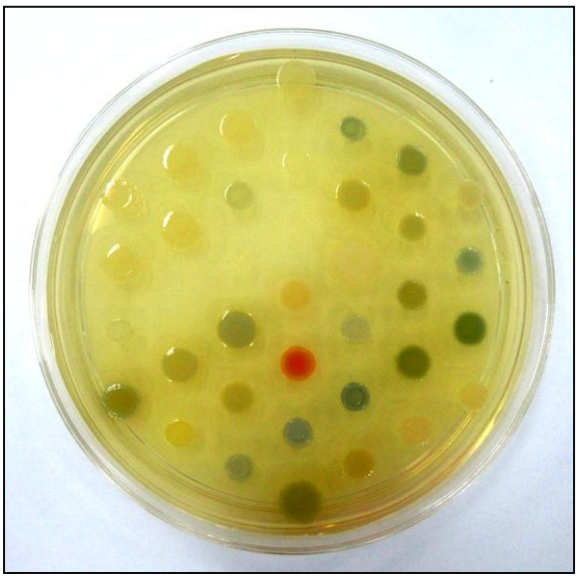

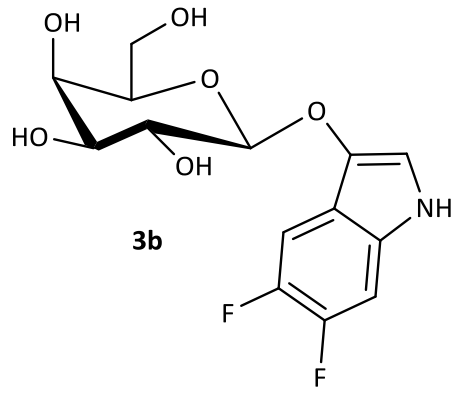

3b

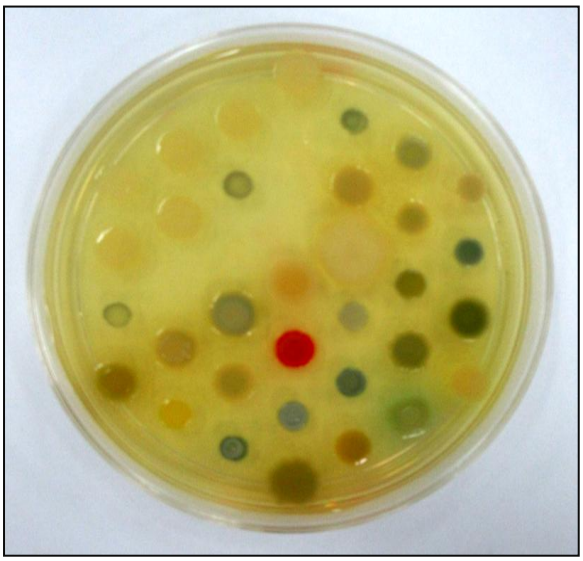

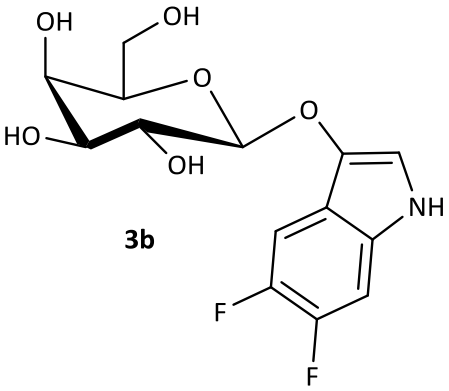

3b

Figure 54b. Substrate **3b** in TSA for 20 (top) and 40 (bottom) hours.

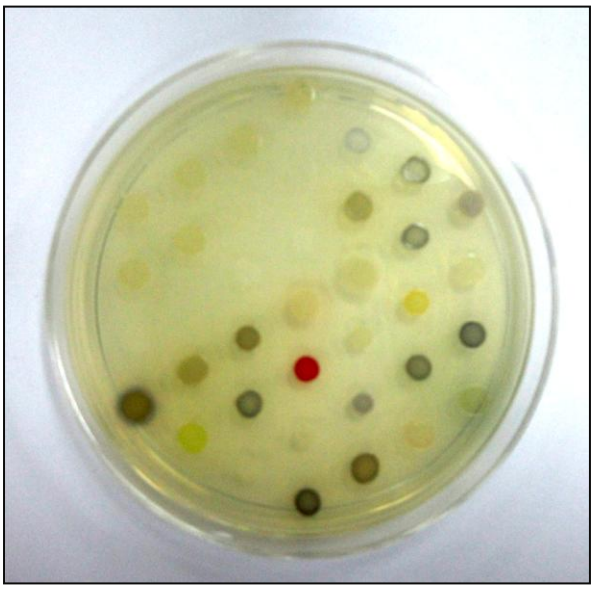

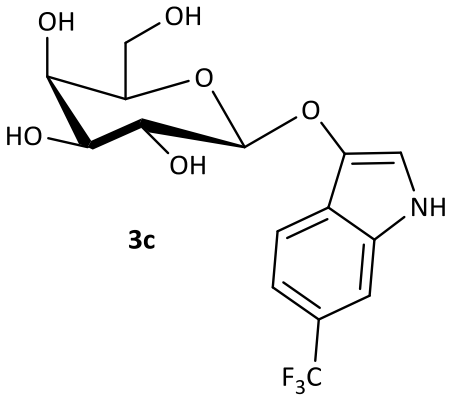

3c

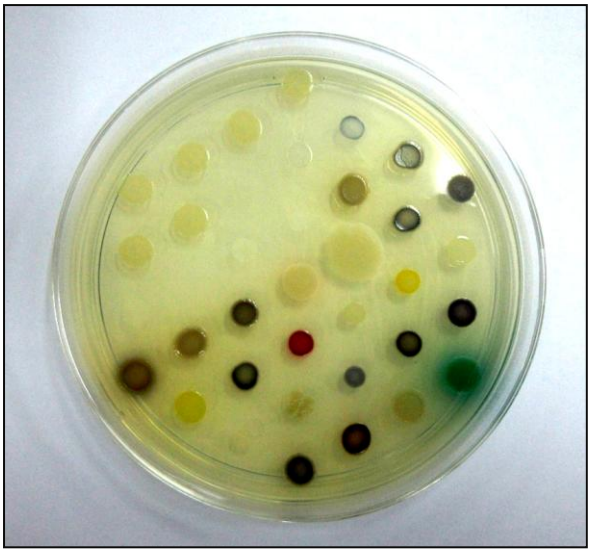

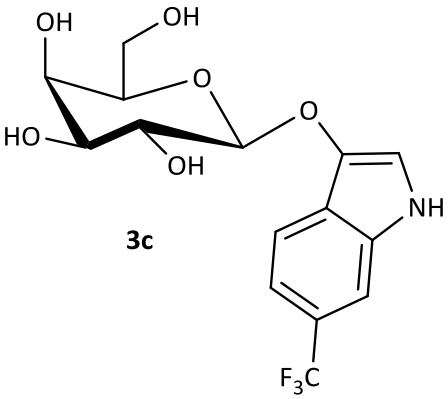

3c

Figure 55a. Substrate **3c** in NA for 20 (top) and 40 (bottom) hours.

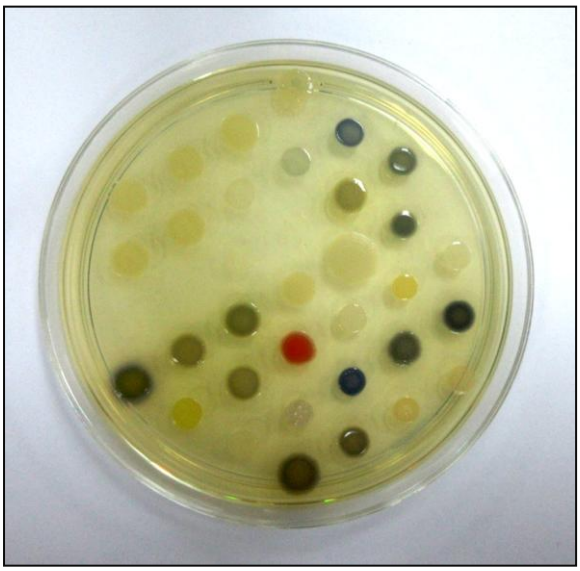

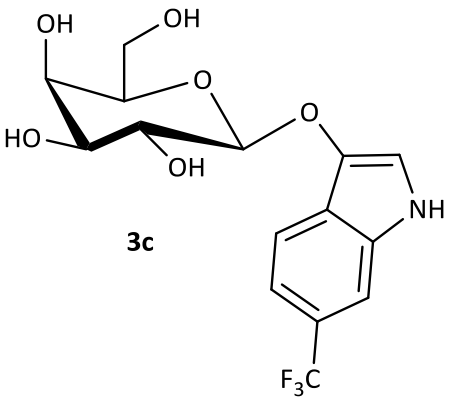

3c

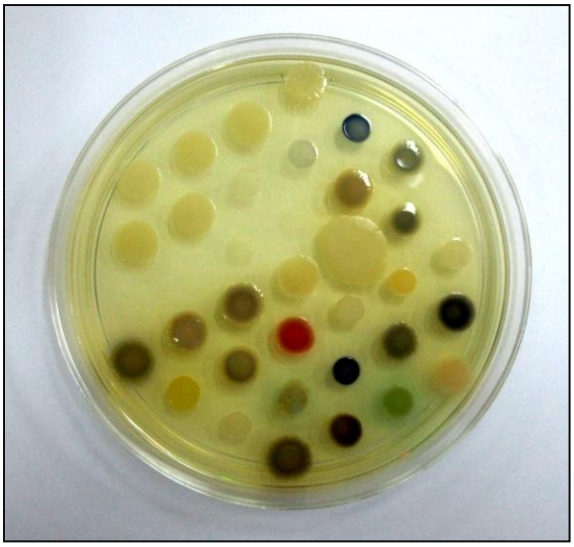

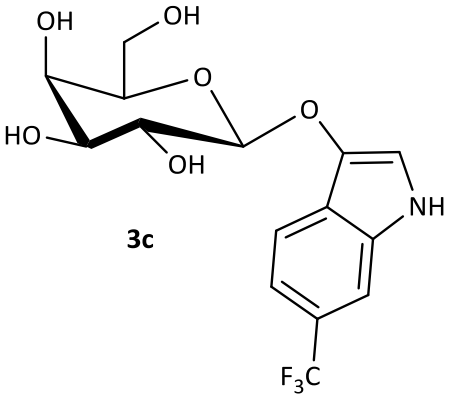

3c

Figure 55b. Substrate **3c** in TSA for 20 (top) and 40 (bottom) hours.

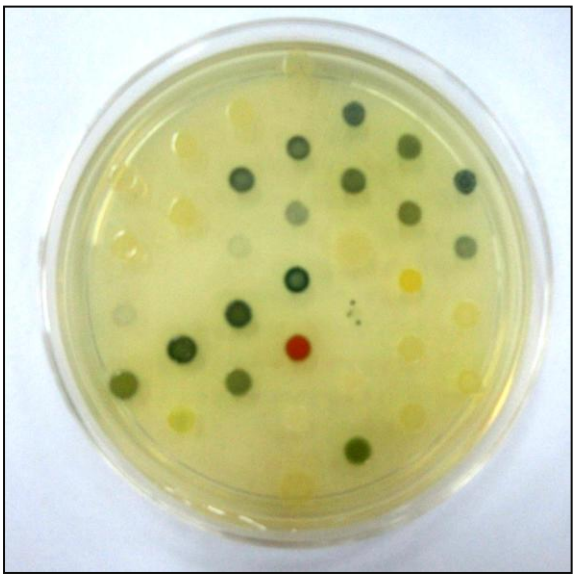

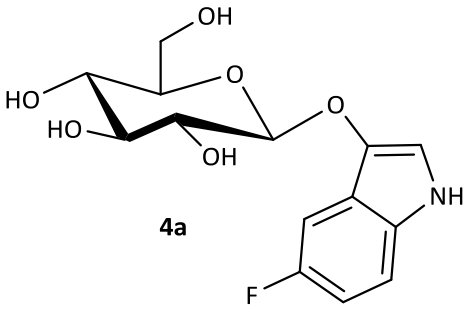

4a

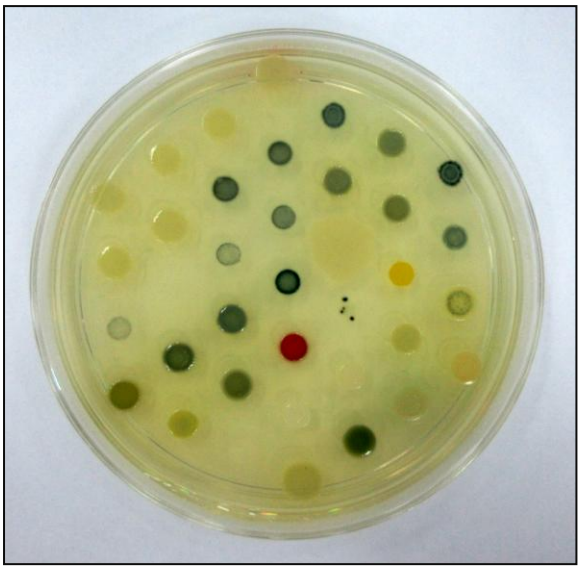

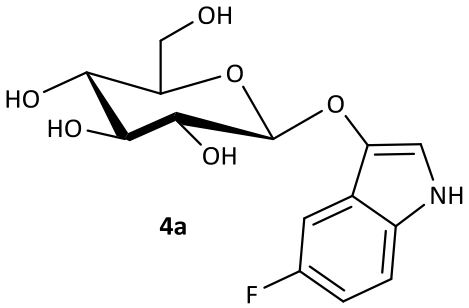

4a

Figure 56a. Substrate **4a** in NA for 20 (top) and 40 (bottom) hours.

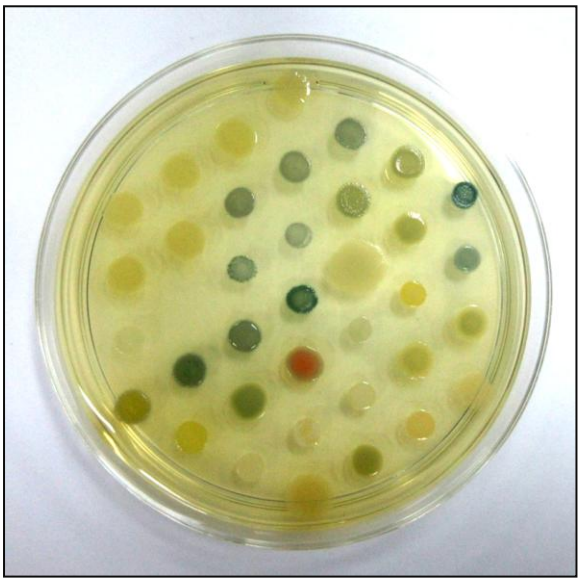

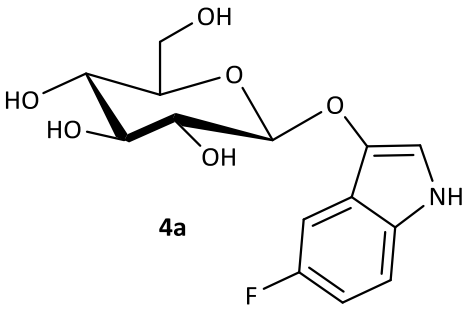

4a

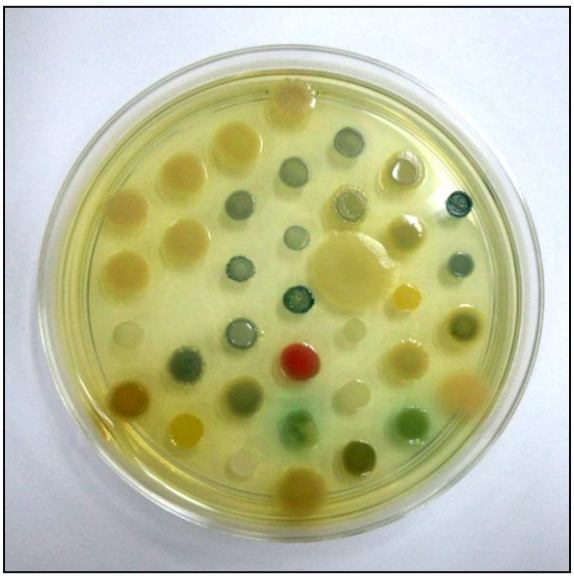

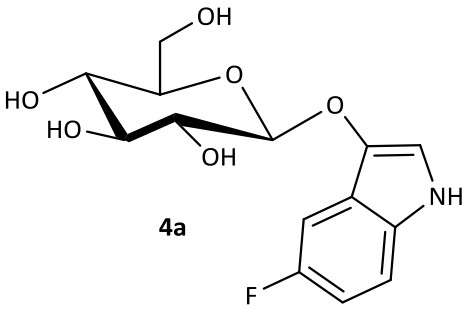

4a

Figure 56b. Substrate **4a** in TSA for 20 (top) and 40 (bottom) hours.

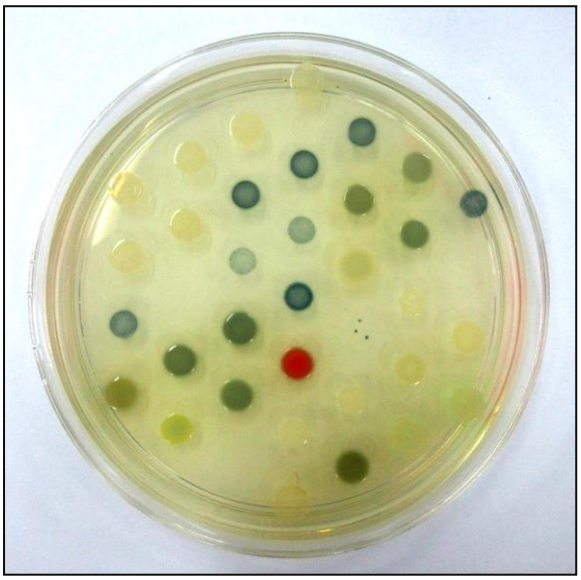

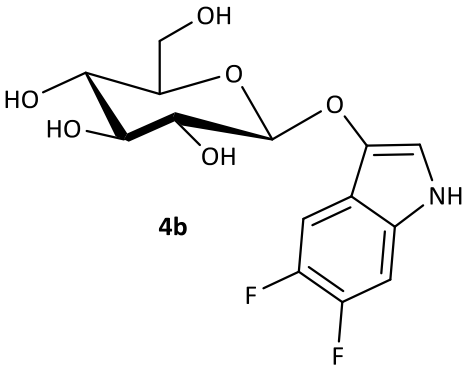

4b

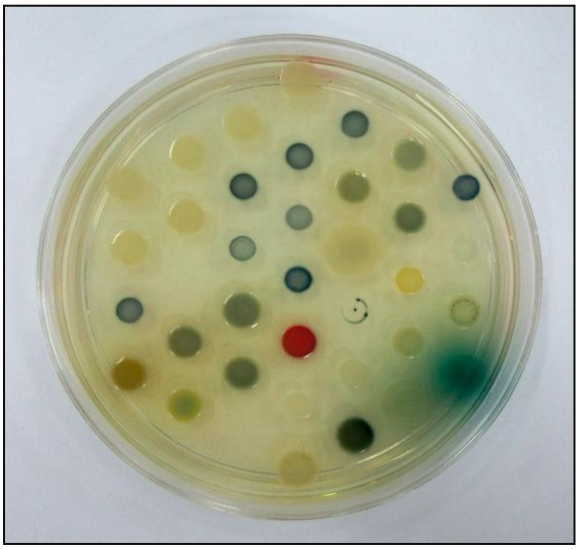

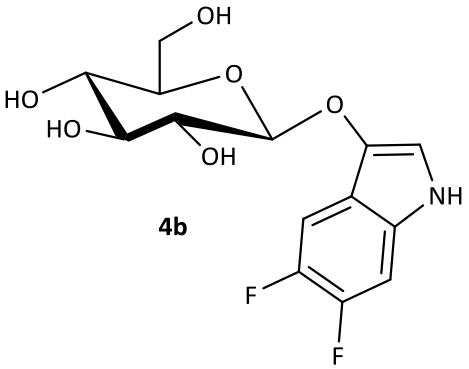

4b

Figure 57a. Substrate **4b** in NA for 20 (top) and 40 (bottom) hours.

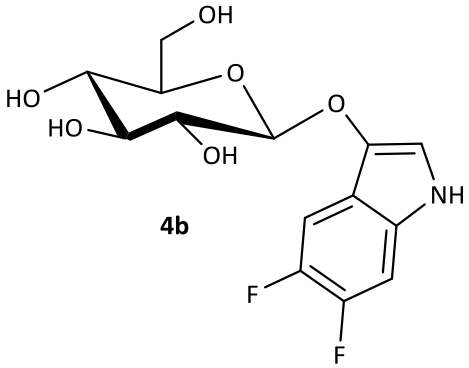

4b

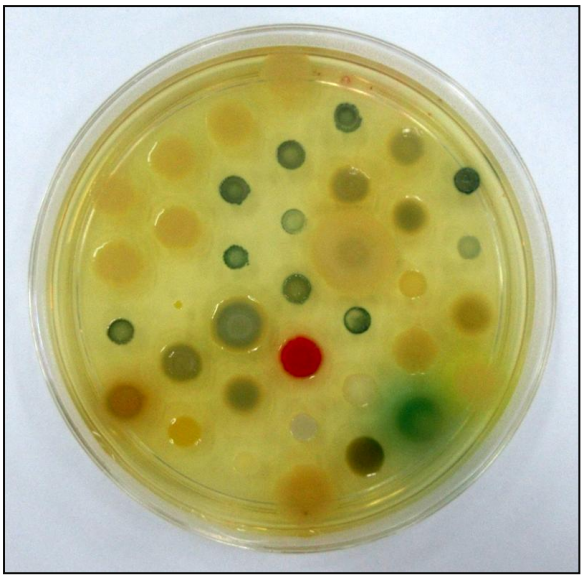

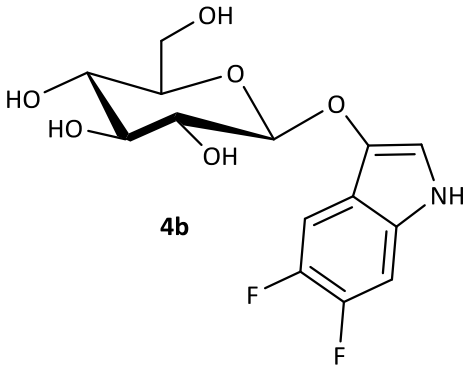

4b

Figure 57b. Substrate **4b** in TSA for 20 (top) and 40 (bottom) hours.

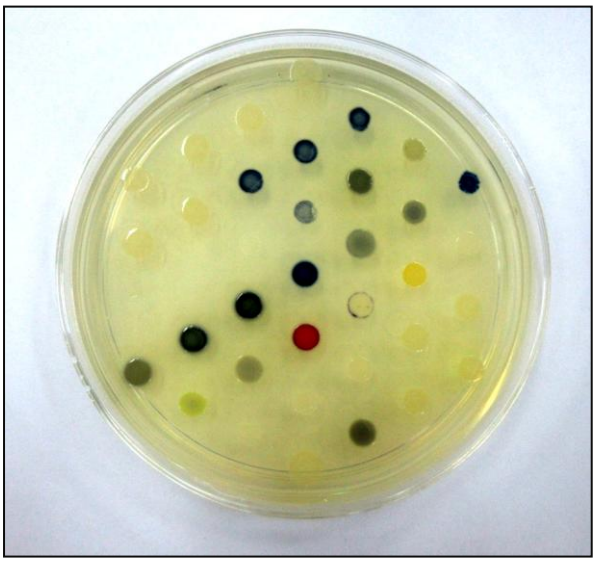

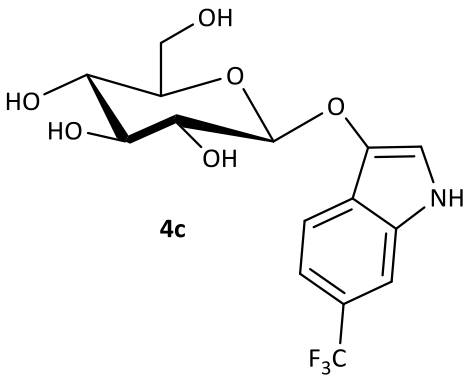

4c

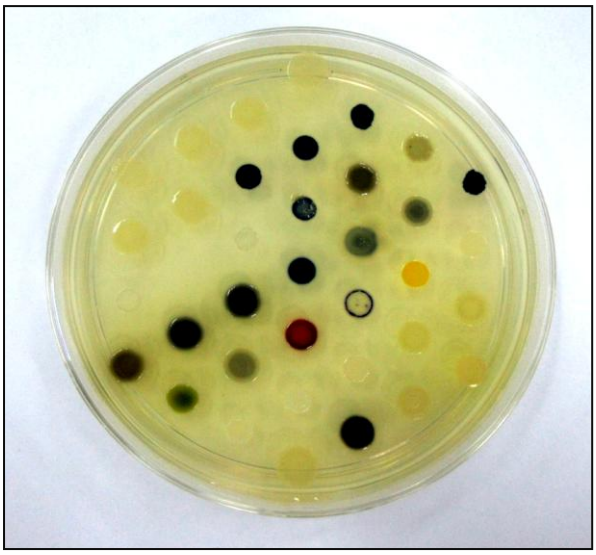

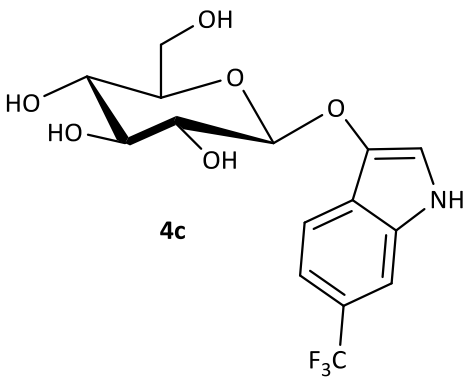

4c

Figure 58a. Substrate **4c** in NA for 20 (top) and 40 (bottom) hours.

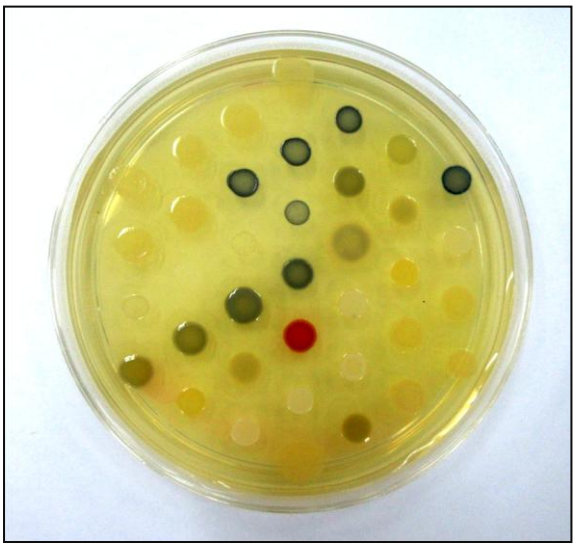

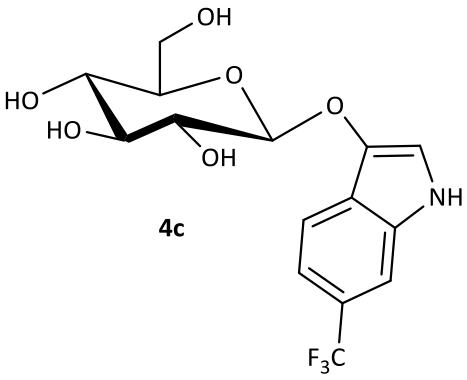

4c

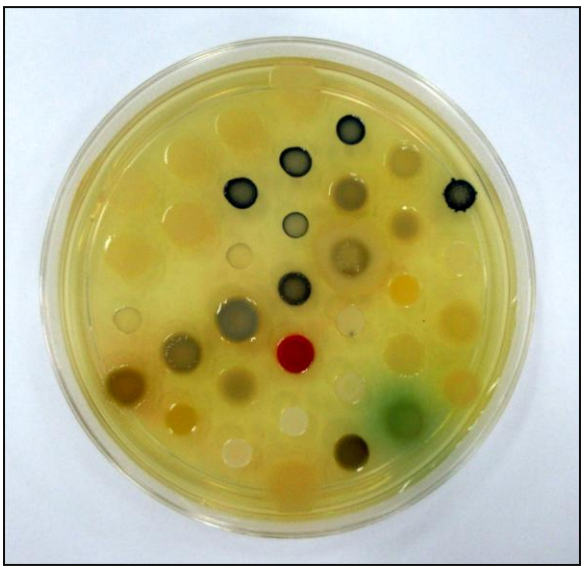

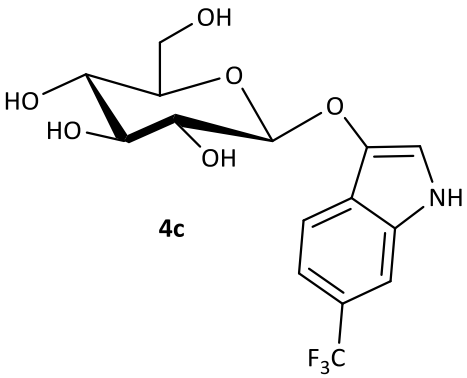

4c

Figure 58b. Substrate **4c** in TSA for 20 (top) and 40 (bottom) hours.

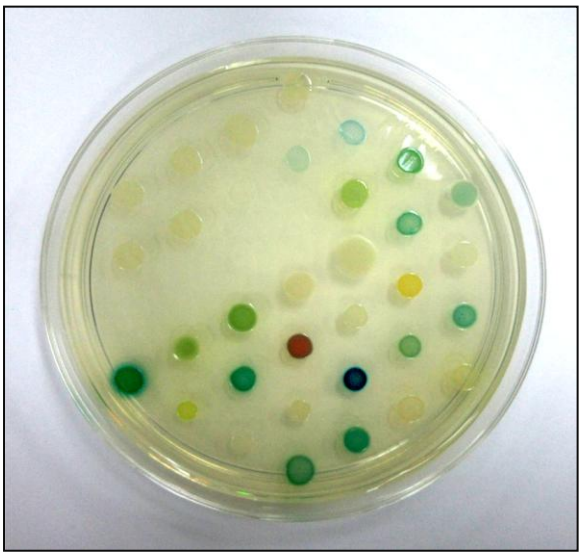

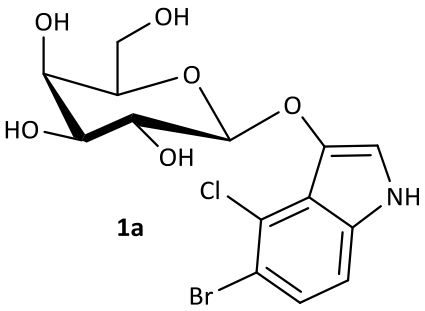

1a

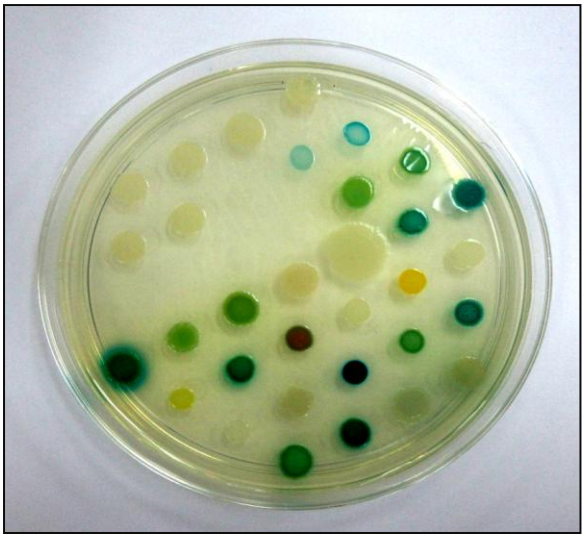

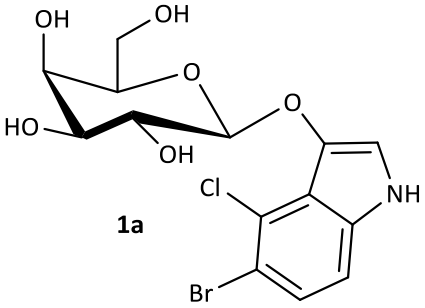

1a

Figure 59a. Substrate **1a** in NA for 20 (top) and 40 (bottom) hours.

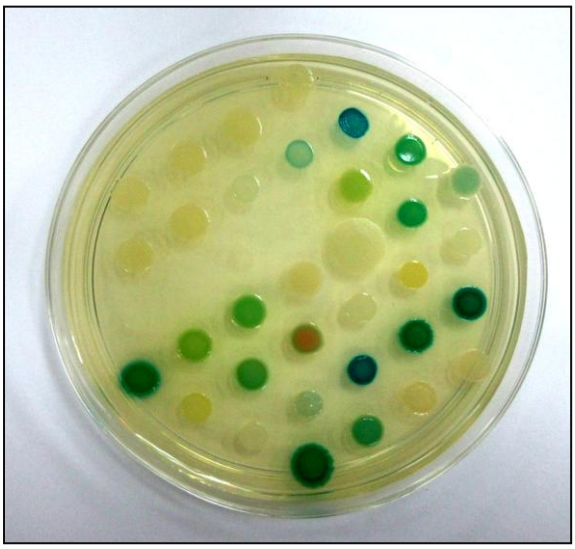

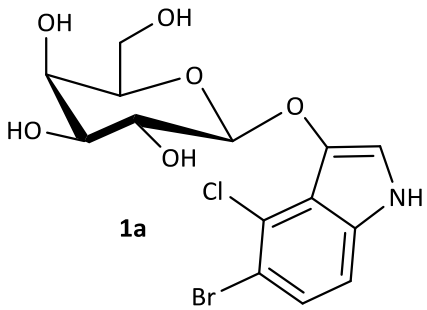

1a

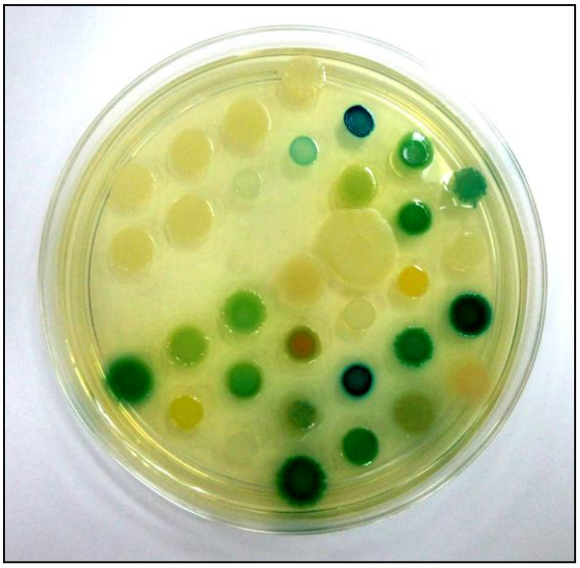

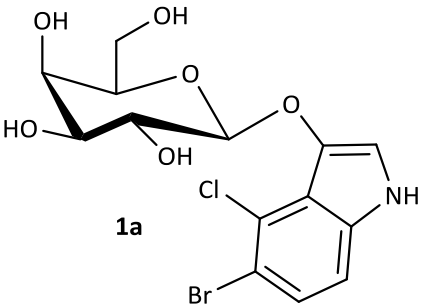

1a

Figure 59b. Substrate **1a** in TSA for 20 (top) and 40 (bottom) hours.

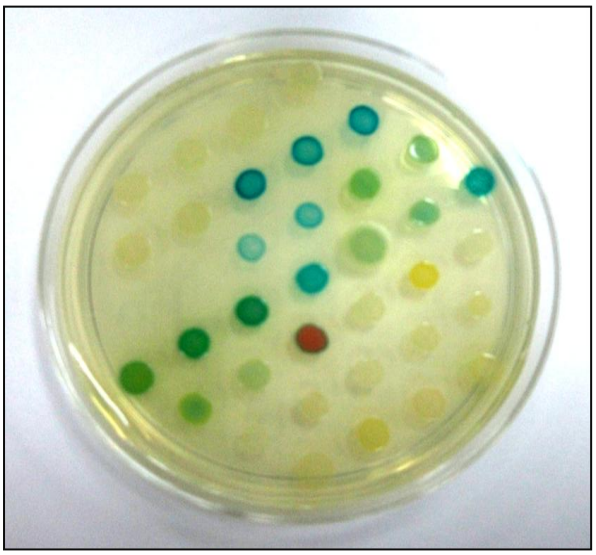

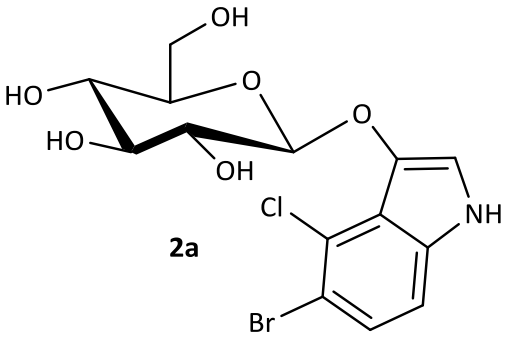

2a

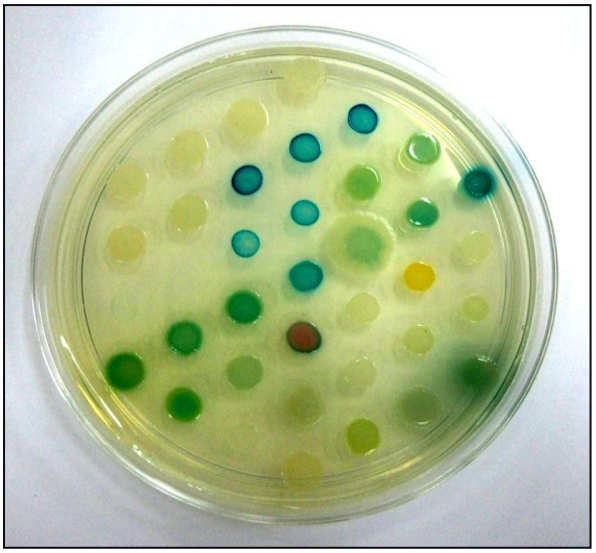

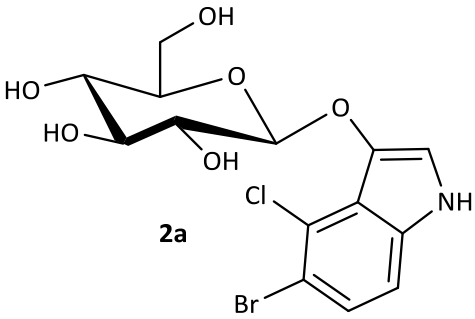

2a

Figure 60a. Substrate **2a** in NA for 20 (top) and 40 (bottom) hours.

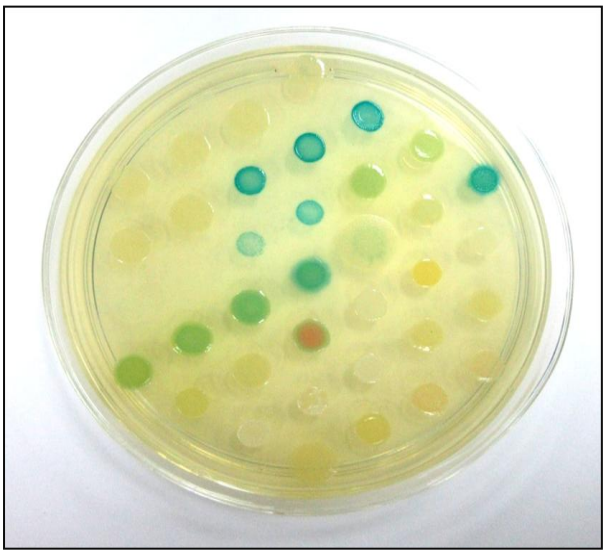

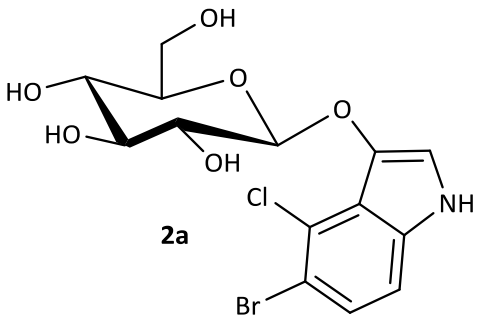

2a

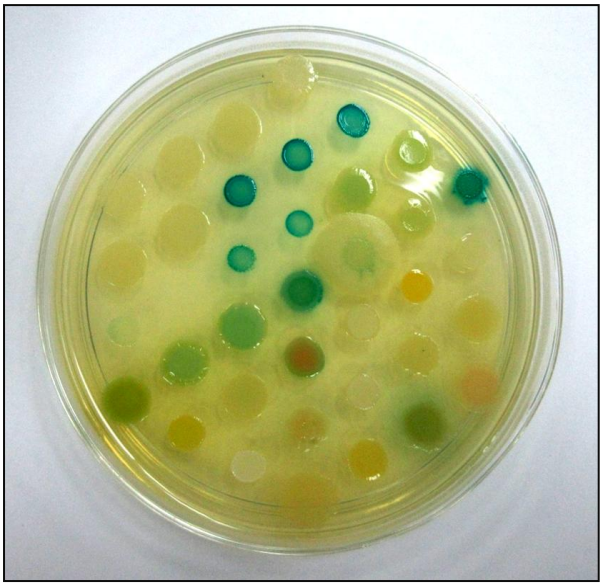

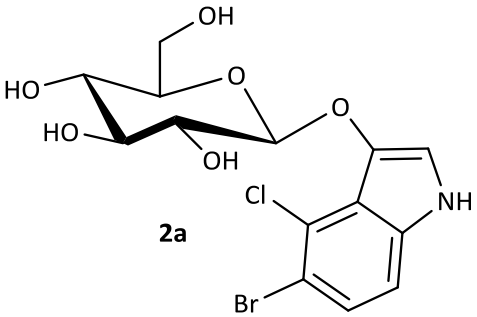

2a

Figure 60b. Substrate **2a** in TSA for 20 (top) and 40 (bottom) hours.

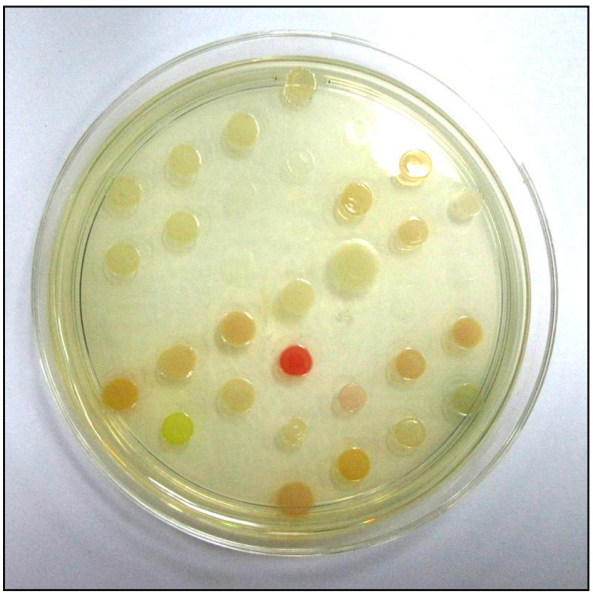

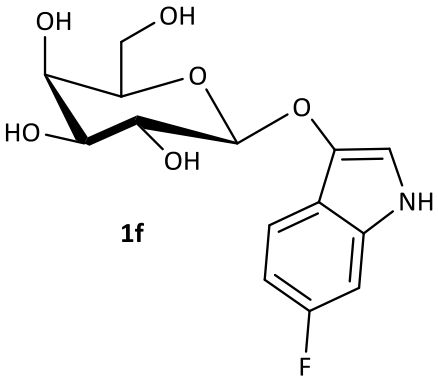

1f

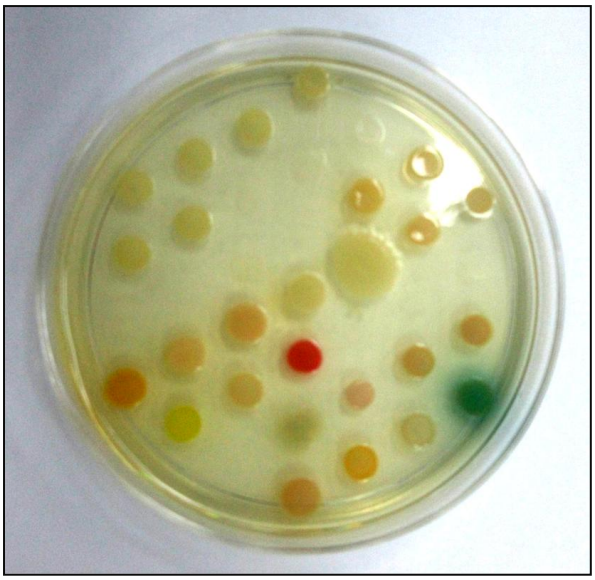

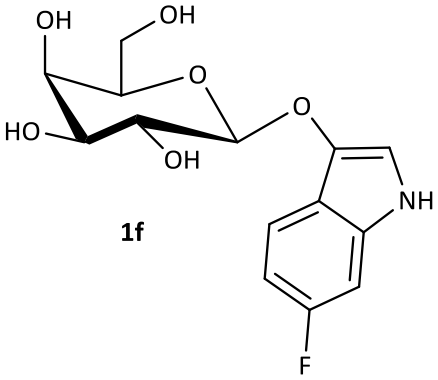

1f

Figure 61a. Substrate **1f** in NA for 20 (top) and 40 (bottom) hours.

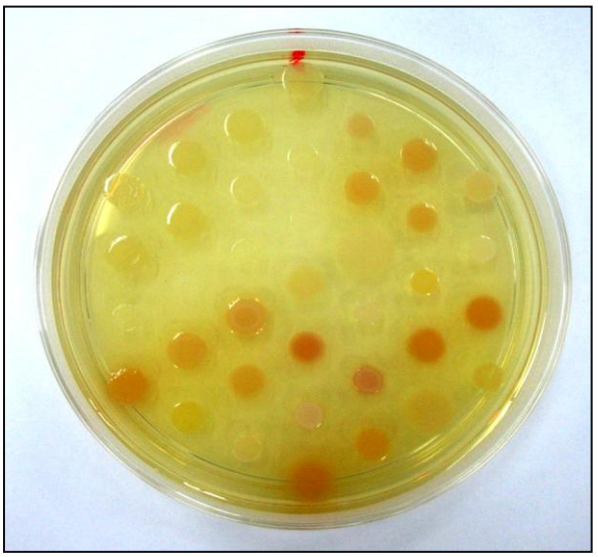

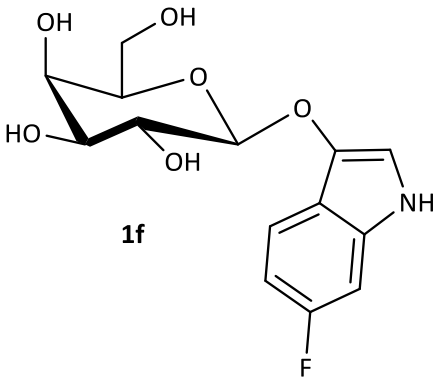

1f

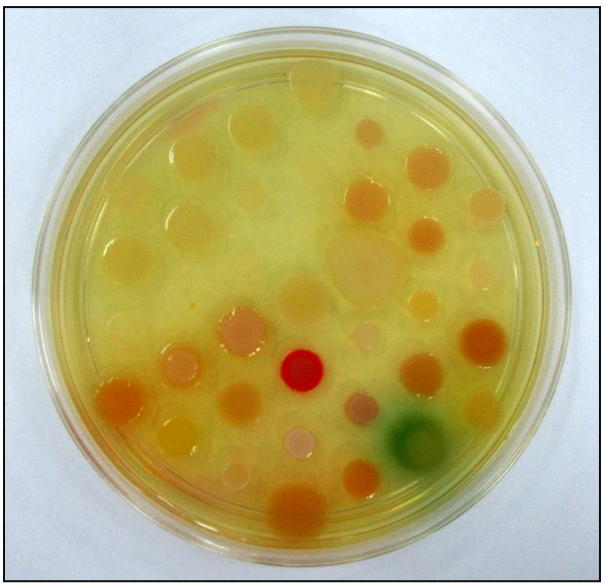

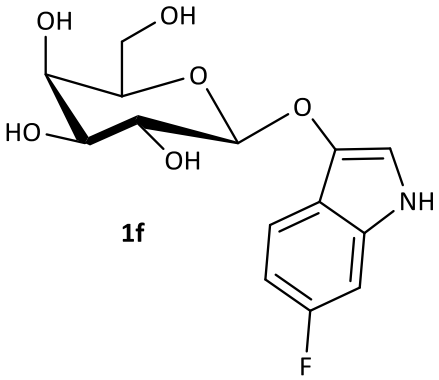

1f

Figure 61b. Substrate **1f** in TSA for 20 (top) and 40 (bottom) hours.

6.5.5 General Procedure: Enzyme kinetics assay

The substrates 5-bromo-4-chloro-3-indolyl β-D-glucoside **2a** and 6-(trifluormethyl)-3-indolyl β-D-glucoside **4c** were dissolved in Dulbecco's Phophate-Buffered Saline (pH 7.2) at four different concentrations (0.5, 2.0, 4.0 and 8.0 x 10^{-4} M). The β-glucosidase enzyme (96 U) was dissolved in PBS (1 mL). The reaction was warmed at 37 °C and 600 µL of the enzyme solution was added to the reaction. The reaction mixture was sub-sampled (1 mL) for every 1 minute, filtered and injected into the HPLC (Agilent 1100). The column used for the assay was Prevail™ Carbohydrate ES HPLC column (Grace Davison Discovery Sciences) with dimensions of 53 mm x 7.0 mm. The substrates were eluted using an isocratic mobile phase system: 0.3% (v/v) trifluoroacetic acid in H_2O:MeCN (70:30) with a flow rate of 1.5 mL/min. The injection volume was 25 µL. The peak areas were measured at wavelengths (λ_{max}) 292 and 282 nm for substrates **2a** and **4c**, respectively. The concentrations of the substrates were determined from the calibration curves (**Figure 62**).

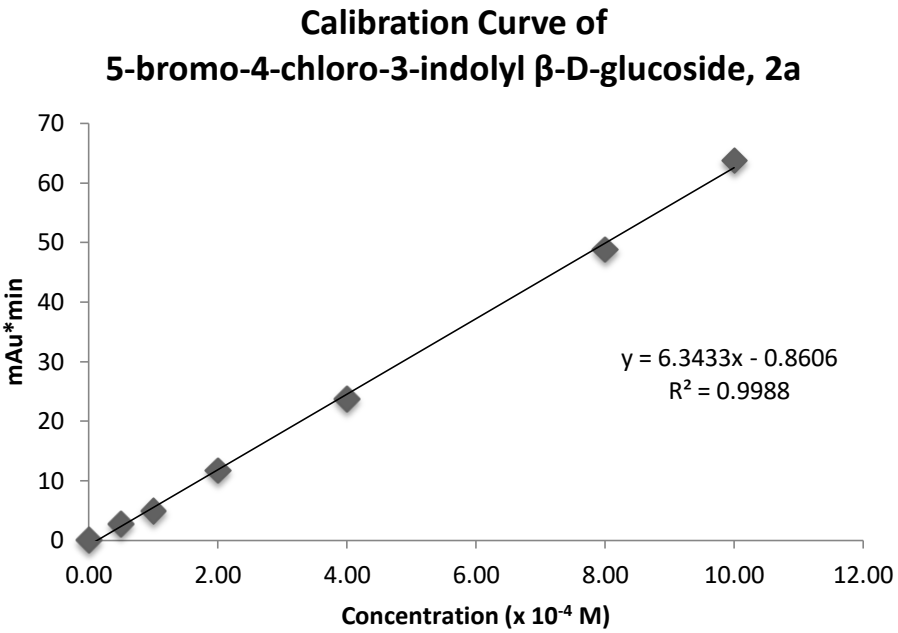

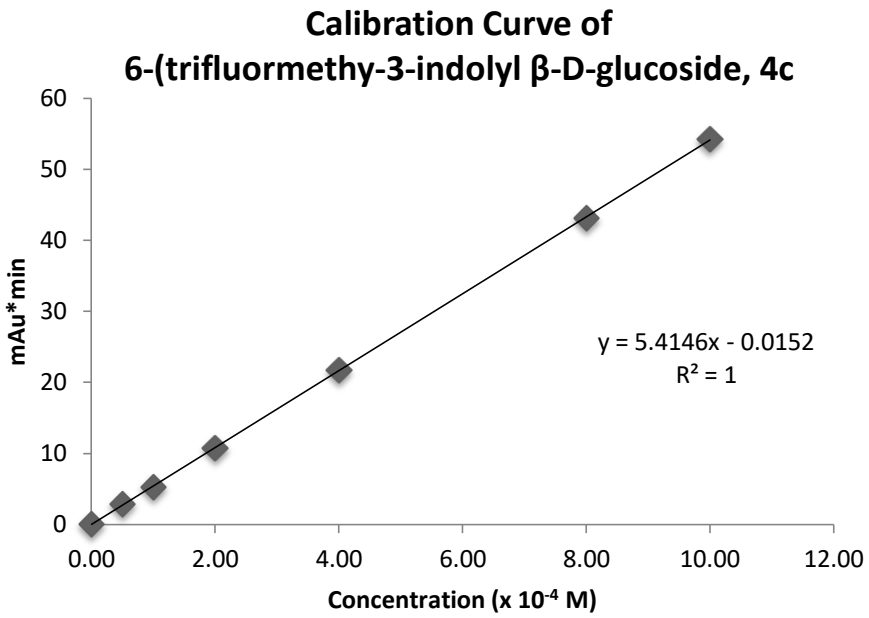

Figure 62. Calibration curves of compounds **2a** and **4c**.

Chapter 7 References

1. Arakawa, Y., Epidemiology of drug-resistance and clinical microbiologists in the 21st century. *The Japanese Journal of Clinical Pathology* **2000**, 1-8.

2. Ferri, M.; Ranucci, E.; Romagnoli, P.; Giaccone, V., Antimicrobial resistance: A global emerging threat to public health systems. *Critical Reviews in Food Science and Nutrition* **2017,** *57* (13), 2857-2876.

3. Health Europa, Medical technologies in the fight against antimicrobial resistance. Health Europa: **2018**; Vol. 2019.

4. Coudron, L.; McDonnell, M. B.; Munro, I.; McCluskey, D. K.; Johnston, I. D.; Tan, C. K. L.; Tracey, M. C., Fully integrated digital microfluidics platform for automated immunoassay; A versatile tool for rapid, specific detection of a wide range of pathogens. *Biosensors and Bioelectronics* **2019,** *128*, 52-60.

5. De Plano, L. M.; Fazio, E.; Rizzo, M. G.; Franco, D.; Carnazza, S.; Trusso, S.; Neri, F.; Guglielmino, S. P. P., Phage-based assay for rapid detection of bacterial pathogens in blood by Raman spectroscopy. *Journal of Immunological Methods* **2019,** *465*, 45-52.

6. Bağcıoğlu, M.; Fricker, M.; Johler, S.; Ehling-Schulz, M., Detection and Identification of *Bacillus cereus*, *Bacillus cytotoxicus*, *Bacillus thuringiensis*, *Bacillus mycoides* and *Bacillus weihenstephanensis* via Machine Learning Based FTIR Spectroscopy. *Frontiers in Microbiology* **2019,** *10* (902).

7. Sharaha, U.; Rodriguez-Diaz, E.; Sagi, O.; Riesenberg, K.; Lapidot, I.; Segal, Y.; Bigio, I. J.; Huleihel, M.; Salman, A., Detection of Extended-Spectrum β-Lactamase-Producing Escherichia coli Using Infrared Microscopy and Machine-Learning Algorithms. *Analytical Chemistry* **2019,** *91* (3), 2525-2530.

8. Percival, S. L.; Finnegan, S.; Donelli, G.; Vuotto, C.; Rimmer, S.; Lipsky, B. A., Antiseptics for treating infected wounds: efficacy on biofilms and effect of pH. *Critical Reviews in Microbiology* **2016,** *42* (2), 293-309.

9. Dang, Q.; Liu, K.; Liu, C.; Xu, T.; Yan, J.; Yan, F.; Cha, D.; Zhang, Q.; Cao, Y., Preparation, characterization, and evaluation of 3,6-*O*-*N*-acetylethylenediamine modified chitosan as potential antimicrobial wound dressing material. *Carbohydrate Polymers* **2018,** *180*, 1-12.

10. Hook, E. R.; Owen, O. J.; Bellis, C. A.; Holder, J. A.; O'Sullivan, D. J.; Barbour, M. E., Development of a novel antimicrobial-releasing glass ionomer cement functionalized with chlorhexidine hexametaphosphate nanoparticles. *Journal of Nanobiotechnology* **2014,** *12* (1), 3.

11. ter Boo, G.-J. A.; Grijpma, D. W.; Moriarty, T. F.; Richards, R. G.; Eglin, D., Antimicrobial delivery systems for local infection prophylaxis in orthopedic and trauma surgery. *Biomaterials* **2015,** *52*, 113-125.

12. Inzana, J. A.; Trombetta, R. P.; Schwarz, E. M.; Kates, S. L.; Awad, H. A., 3D printed bioceramics for dual antibiotic delivery to treat implant-associated bone infection. *European Cells and Materials* **2015,** *30*, 232-247.

13. Mills, D. K.; Jammalamadaka, U.; Tappa, K.; Weisman, J., Studies on the cytocompatibility, mechanical and antimicrobial properties of 3D printed poly(methyl methacrylate) beads. *Bioactive Materials* **2018,** *3* (2), 157-166.

14. Gustafson, R. H.; Bowen, R. E., Antibiotic use in animal agriculture. *Journal of Applied Microbiology* **1997,** *83* (5), 531-541.

15. Capita, R.; Alonso-Calleja, C., Antibiotic-resistant bacteria: a challenge for the food industry. *Critical Reviews in Food Science and Nutrition* **2013,** *53* (1), 11-48.

16. O'Neill, J., Antimicrobial Resistance: Tackling a crisis for the health and wealth of nations. *Review on Antimicrobial Resistance* **2014,** *1* (1), 1-16.

17. European Academies Science Advisory Council (EASAC) *Tackling antibacterial resistance in Europe*; The Royal Society: London, **2007**.

18. Varadi, L.; Luo, J. L.; Hibbs, D. E.; Perry, J. D.; Anderson, R. J.; Orenga, S.; Groundwater, P. W., Methods for the detection and identification of pathogenic bacteria: past, present, and future. *Chemical Society Reviews* **2017,** *46* (16), 4818-4832.

19. O'Neill, J., Tackling drug-resistant infections globally: final report and recommendations. *Review on Antimicrobial Resistance* **2016**, 1-79.

20. European Centre for Disease Prevention and Control (ECDC) and European Medicines Agency (EMEA) *ECDC/EMEA Joint Technical Report - The bacterial challenge: time to react*; European Centre for Disease Prevention and Control (ECDC) and European Medicines Agency (EMEA): Stockholm, Sweden, 2009.

21. World Health Organization (WHO) *The evolving threat of antimicrobial resistance: options for action*; World Health Organization: Geneva, Switzerland, **2012**.

22. O'Neill, J., Infection prevention, control and surveilance: limiting the development and spread of drug resistance. *Review on Antimicrobial Resistance* **2016**, 1-30.

23. Madigan, M., Matinko, J., Bender, K., Buckley, D. and Stahl, D., *Brock Biology of Microorganisms*. 14th ed.; Pearson Education Limited: Edinburgh, 2015.

24. Brett, J. A.; Johnson, S. A.; Cameron, D. R. M.; Lane, C. R.; Easton, M.; van Diemen, A.; Sutton, B.; Bull, A. L.; Richards, M. J.; Worth, L. J., Carbapenemase-producing *Enterobacteriaceae* in Australian hospitals: outcome of point-prevalence screening in high-risk wards. *Journal of Hospital Infection* **2019,** *101* (2), 163-166.

25. Díaz-Agero Pérez, C.; López-Fresneña, N.; Rincon Carlavilla, A. L.; Hernandez Garcia, M.; Ruiz-Garbajosa, P.; Aranaz-Andrés, J. M.; Maechler, F.; Gastmeier, P.; Bonten, M. J. M.; Canton, R., Local prevalence of extended-spectrum beta-lactamase (ESBL) producing *Enterobacteriaceae* intestinal carriers at admission and co-expression of ESBL and OXA-48 carbapenemase in *Klebsiella pneumoniae*: a prevalence survey in a Spanish University Hospital. *British Medical Journal Open* **2019,** *9* (3).

26. Salge, T. O.; Vera, A.; Antons, D.; Cimiotti, J. P., Fighting MRSA Infections in Hospital Care: How Organizational Factors Matter. *Health Services Research* **2017,** *52* (3), 959-983.

27. Kampmeier, S.; Kossow, A.; Clausen, L. M.; Knaack, D.; Ertmer, C.; Gottschalk, A.; Freise, H.; Mellmann, A., Hospital acquired vancomycin resistant enterococci in surgical intensive care patients – a prospective longitudinal study. *Antimicrobial Resistance & Infection Control* **2018,** *7* (1), 103.

28. Public Health England (PHE) *English Surveillance Programme for Antimicrobial Utilisation and Resistance (EUSPAR)*; Public Health England: England, **2017**.

29. British Broadcasting Coorporation (BBC), Antibiotic resistance plan to fight 'urgent' global threat. British Broadcasting Coorporation: **2019**.

30. Public Health England (PHE) *English Surveillance Programme for Antimicrobial Utilisation and Resistance (ESPAUR)*; Public Health England England, **2018**.

31. World Health Organization (WHO), WHO published list of bacteria for which new antibiotics are urgently needed. World Health Organization: Geneva, Switzerland, **2017**.

32. Ventola, C. L., The Antibiotic Resistance Crisis: Part 1: Causes and Threats. *Pharmacy and Therapeutics* **2015,** *40* (4), 277-283.

33. Andrei, S.; Valeanu, L.; Chirvasuta, R.; Stefan, M.-G., New FDA approved antibacterial drugs: 2015-2017. *Discoveried Journals* **2018**, 10.

34. Centers for Disease Control and Prevention (CDC) *Antibiotic resistance threats in the United States*; Centers for Disease Control and Prevention: USA, **2013**.

35. Renwick, M. J.; Simpkin, V.; Mossialos, E. *Targeting innovation in antibiotic drug discovery and development. The need for a One Health – One Europe – One World Framework*; The Netherlands, **2016**.

36. Megget, K., Novartis exit from antibiotics a setback for race against resistance. *Chemistry World.* 2018.

37. O'Neill, J., Tackling a global health crisis: initial steps. *Review on Antimicrobial Resistance* **2015**, 1-20.

38. Bowater, L., *The Microbes Fight Back: Antibiotic Resistance*. The Royal Society of Chemistry: 2017; p 289.

39. European Centre for Disease Prevention and Control (ECDC) Key messages for primary care prescribers. https://antibiotic.ecdc.europa.eu/en/get-informedkey-messages/key-messages-primary-care-prescribers (accessed 16 August 2019).

40. National Institute for Health and Care Excellence (NICE), Summary of antimicrobial prescribing guidance – managing common infections National Institute for Health and Care Excellence: **2019**.

41. Klein, E. Y.; Van Boeckel, T. P.; Martinez, E. M.; Pant, S.; Gandra, S.; Levin, S. A.; Goossens, H.; Laxminarayan, R., Global increase and geographic convergence in antibiotic consumption between 2000 and 2015. *Proceedings of the National Academy of Sciences* **2018,** *115* (15), 3463-3470.

42. Delepierre, A.; Gayot, A.; Carpentier, A., Update on counterfeit antibiotics worldwide; public health risks. *Médecine et Maladies Infectieuses* **2012,** *42* (6), 247-255.

43. Kelesidis, T.; Falagas, M. E., Substandard/Counterfeit Antimicrobial Drugs. *Clinical Microbiology Reviews* **2015,** *28* (2), 443.

44. Ayukekbong, J. A.; Ntemgwa, M.; Atabe, A. N., The threat of antimicrobial resistance in developing countries: causes and control strategies. *Antimicrobial Resistance & Infection Control* **2017,** *6* (1), 47.

45. Laxminarayan, R.; Chaudhury, R. R., Antibiotic Resistance in India: Drivers and Opportunities for Action. *PLOS Medicine* **2016,** *13* (3).

46. Diggikar, R., Pharmacies violating norms face FDA music. Times of India: India, **2015**.

47. Canton, N., 64% of antibiotics sold in India unapproved: UK study. Times of India: **2018**.

48. Van Boeckel, T. P.; Brower, C.; Gilbert, M.; Grenfell, B. T.; Levin, S. A.; Robinson, T. P.; Teillant, A.; Laxminarayan, R., Global trends in antimicrobial use in food animals. *Proceedings of the National Academy of Sciences* **2015,** *112* (18), 5649.

49. Grace, D., Review of evidence on antimicrobial resistance and animal agriculture in developing countries. Department of International Development: **2015**.

50. National Health Sevice (NHS) Antibiotic use in farm animals 'threatens human health'. https://www.nhs.uk/news/medication/antibiotic-use-in-farm-animals-threatens-human-health/ (accessed 31 August 2019).

51. O'Neill, J., Antimicrobials in agriculture and environment: reducing unnecessary use and waste. *Review on Antimicrobial Resistance* **2015**, 1-38.

52. Liu, Y.-Y.; Wang, Y.; Walsh, T. R.; Yi, L.-X.; Zhang, R.; Spencer, J.; Doi, Y.; Tian, G.; Dong, B.; Huang, X.; Yu, L.-F.; Gu, D.; Ren, H.; Chen, X.; Lv, L.; He, D.; Zhou, H.; Liang, Z.; Liu, J.-H.; Shen, J., Emergence of plasmid-mediated colistin resistance mechanism MCR-1 in animals and human beings in China: a microbiological and molecular biological study. *The Lancet Infectious Diseases* **2016,** *16* (2), 161-168.

53. Walsh, T. R.; Wu, Y., China bans colistin as a feed additive for animals. *The Lancet Infectious Diseases* **2016,** *16* (10), 1102-1103.

54. Veterinary Medicines Directorate (VMD) *UK Veterinary Antibiotic Resistance and Sales Surveillance Report*; Surrey, **2018**.

55. European Food Safety Authority (EFSA) and European Centre for Disease Prevention Control (ECDPC) *The European Union summary report on antimicrobial resistance in zoonotic and indicator bacteria from humans, animals and food in 2015*; 1831-4732; 2017.

56. Varadi, L.; Gray, M.; Groundwater, P. W.; Hall, A. J.; James, A. L.; Orenga, S.; Perry, J. D.; Anderson, R. J., Synthesis and evaluation of fluorogenic 2-amino-1,8-naphthyridine derivatives for the detection of bacteria. *Organic & Biomolecular Chemistry* **2012,** *10* (13), 2578-2589.

57. Nwokoro, E.; Leach, R.; Årdal, C.; Baraldi, E.; Ryan, K.; Plahte, J., An assessment of the future impact of alternative technologies on antibiotics markets. *Journal of Pharmaceutical Policy and Practice* **2016,** *9* (1), 34.

58. O'Neill, J., Rapid diagnostics: stopping unnecessary use of antibiotics. *Review on Antimicrobial Resistance* **2015**, 1-34.

59. Bruslin, L. Microbiology. http://library.open.oregonstate.edu/microbiology/chapter/bacteria-cell-walls/. (accessed 29 June 2018).

60. Wiley, J. M., Sherwood, L. M. and Woolverton, C. J., *Prescott's Microbiology*. 9th ed.; McGraw International Edition: New York, 2014.

61. Graham, L. P., *An Introduction to Medicinal Chemistry*. Oxford University Press: Oxford, **2005**.

62. Tommassen, J., Assembly of outer-membrane proteins in bacteria and mitochondria. *Microbiology* **2010,** *156* (9), 2587-2596.

63. Hutchins, M. The Synthesis and Microbiological Analysis of Nadifloxacin Glycosides. Thesis, University of Reading, **2016**.

64. Nikaido, H., Molecular Basis of Bacterial Outer Membrane Permeability Revisited. *Microbiology and Molecular Biology Reviews* **2003,** *67* (4), 593-656.

65. Koebnik, R.; Locher, K. P.; Van Gelder, P., Structure and function of bacterial outer membrane proteins: barrels in a nutshell. *Molecular Microbiology* **2000,** *37* (2), 239-253.

66. Ge, B.; Meng, J., Advanced Technologies for Pathogen and Toxin Detection in Foods: Current Applications and Future Directions. *Journal of the Association for Laboratory Automation* **2009,** *14* (4), 235-241.

67. Feng, P., Rapid methods for the detection of foodborne pathogens: current and next-generation technologies. In *Food Microbiology: Fundamentals and Frontiers, Third Edition*, American Society of Microbiology: 2007; pp 911-934.

68. Stevens, K. A.; Jaykus, L.-A., Bacterial Separation and Concentration from Complex Sample Matrices: A Review. *Critical Reviews in Microbiology* **2004,** *30* (1), 7-24.

69. Zadik, P. M.; Chapman, P. A.; Siddons, C. A., Use of tellurite for the selection of verocytotoxigenic *Escherichia coli* O157. *Journal of Medical Microbiology* **1993,** *39* (2), 155-158.

70. Walter, E. G.; Taylor, D. E., Plasmid-mediated resistance to tellurite: Expressed and cryptic. *Plasmid* **1992,** *27* (1), 52-64.

71. Tomás, J. M.; Kay, W. W., Tellurite susceptibility and non-plasmid-mediated resistance in *Escherichia coli*. *Antimicrobial agents and chemotherapy* **1986,** *30* (1), 127-131.

72. Chasteen, T. G.; Fuentes, D. E.; Tantaleán, J. C.; Vásquez, C. C., Tellurite: history, oxidative stress, and molecular mechanisms of resistance. *Federation of European Microbiological Societies Microbiology Reviews* **2009,** *33* (4), 820-832.

73. Gracias, K. S.; McKillip, J. L., A review of conventional detection and enumeration methods for pathogenic bacteria in food. *Canadian Journal of Microbiology* **2004,** *50* (11), 883-890.

74. Rohde, A.; Hammerl, J. A.; Boone, I.; Jansen, W.; Fohler, S.; Klein, G.; Dieckmann, R.; Al Dahouk, S., Overview of validated alternative methods for the detection of foodborne bacterial pathogens. *Trends in Food Science & Technology* **2017,** *62*, 113-118.

75. Jasson, V.; Jacxsens, L.; Luning, P.; Rajkovic, A.; Uyttendaele, M., Alternative microbial methods: An overview and selection criteria. *Food Microbiology* **2010,** *27* (6), 710-730.

76. Doyle, M. P.; Buchanan, R. L., *Food microbiology: fundamentals and frontiers*. American Society for Microbiology Press: 2012.

77. Pulido, M. R.; García-Quintanilla, M.; Martín-Peña, R.; Cisneros, J. M.; McConnell, M. J., Progress on the development of rapid methods for antimicrobial susceptibility testing. *Journal of Antimicrobial Chemotherapy* **2013,** *68* (12), 2710-2717.

78. MacVane, S. H.; Nolte, F. S., Benefits of Adding a Rapid PCR-Based Blood Culture Identification Panel to an Established Antimicrobial Stewardship Program. *Journal of Clinical Microbiology* **2016,** *54* (10), 2455-2463.

79. Emonet, S.; Shah, H. N.; Cherkaoui, A.; Schrenzel, J., Application and use of various mass spectrometry methods in clinical microbiology. *Clinical Microbiology and Infection* **2010,** *16* (11), 1604-1613.

80. Angeletti, S., Matrix assisted laser desorption time of flight mass spectrometry (MALDI-TOF MS) in clinical microbiology. *Journal of Microbiological Methods* **2017,** *138*, 20-29.

81. de Boer, E.; Beumer, R. R., Methodology for detection and typing of foodborne microorganisms. *International Journal of Food Microbiology* **1999,** *50* (1–2), 119-130.

82. Amodio, E.; Dino, C., Use of ATP bioluminescence for assessing the cleanliness of hospital surfaces: A review of the published literature (1990–2012). *Journal of Infection and Public Health* **2014,** *7* (2), 92-98.

83. Harrigan, W. F., *Laboratory methods in food microbiology*. Gulf Professional Publishing: 1998.

84. Patchett, R. A.; Back, J. P.; Pinder, A. C.; Kroll, R. G., Enumeration of bacteria in pure cultures and in foods using a commercial flow cytometer. *Food Microbiology* **1991,** *8* (2), 119-125.

85. Bottari, B.; Ercolini, D.; Gatti, M.; Neviani, E., Application of FISH technology for microbiological analysis: current state and prospects. *Applied Microbiology and Biotechnology* **2006,** *73* (3), 485-494.

86. Wagner, M.; Horn, M.; Daims, H., Fluorescence in situ hybridisation for the identification and characterisation of prokaryotes. *Current Opinion in Microbiology* **2003,** *6* (3), 302-309.

87. Adawi, A.; Bisignano, C.; Genovese, T.; Filocamo, A.; Khouri-Assi, C.; Neville, A.; Feuerstein, G. Z.; Cuzzocrea, S.; Neville, L. F., *In vitro* and *in vivo* properties of a fully human IgG1 monoclonal antibody that combats multi-drug resistant *Pseudomonas aeruginosa*. *International Journal of Molecular Medicine* **2012,** *30* (3), 455-464.

88. Gan, S. D.; Patel, K. R., Enzyme Immunoassay and Enzyme-Linked Immunosorbent Assay. *Journal of Investigative Dermatology* **2013,** *133* (9), 1-3.

89. Yang, L.; Bashir, R., Electrical/electrochemical impedance for rapid detection of foodborne pathogenic bacteria. *Biotechnology Advances* **2008,** *26* (2), 135-150.

90. Dupont, J.; Dumont, F.; Menanteau, C.; Pommepuy, M., Calibration of the impedance method for rapid quantitative estimation of Escherichia coli in live marine bivalve molluscs. *Journal of Applied Microbiology* **2004,** *96* (4), 894-902.

91. Besant, J. D.; Sargent, E. H.; Kelley, S. O., Rapid electrochemical phenotypic profiling of antibiotic-resistant bacteria. *Lab on a Chip* **2015,** *15* (13), 2799-2807.

92. Reis, N. M.; Pivetal, J.; Loo-Zazueta, A. L.; Barros, J. M. S.; Edwards, A. D., Lab on a stick: multi-analyte cellular assays in a microfluidic dipstick. *Lab on a Chip* **2016,** *16* (15), 2891-2899.

93. Carbonnelle, E.; Mesquita, C.; Bille, E.; Day, N.; Dauphin, B.; Beretti, J.-L.; Ferroni, A.; Gutmann, L.; Nassif, X., MALDI-TOF mass spectrometry tools for bacterial identification in clinical microbiology laboratory. *Clinical Biochemistry* **2011,** *44* (1), 104-109.

94. Burckhardt, I.; Zimmermann, S., Using matrix-assisted laser desorption ionization-time of flight mass spectrometry to detect carbapenem resistance within 1 to 2.5 hours. *Journal of Clinical Microbiology* **2011,** *49* (9), 3321-3324.

95. López-Campos, G.; Martínez-Suárez, J.; Aguado-Urda, M.; López-Alonso, V., Detection, Identification, and Analysis of Foodborne Pathogens. In *Microarray Detection and Characterization of Bacterial Foodborne Pathogens*, Springer US: 2012; pp 13-32.

96. Naravaneni, R.; Jamil, K., Rapid detection of food-borne pathogens by using molecular techniques. *Journal of Medical Microbiology* **2005,** *54* (1), 51-54.

97. McConnell, M. J.; Pérez-Ordóñez, A.; Pérez-Romero, P.; Valencia, R.; Lepe, J. A.; Vázquez-Barba, I.; Pachón, J., Quantitative Real-Time PCR for Detection of *Acinetobacter baumannii* Colonization in the Hospital Environment. *Journal of Clinical Microbiology* **2012,** *50* (4), 1412-1414.

98. Clarke, P. H., Hydrogen sulphide production by bacteria. *Microbiology* **1953,** *8* (3), 397-407.

99. Küster, E.; Williams, S., Production of hydrogen sulfide by streptomycetes and methods for its detection. *Applied Environmental Microbiology* **1964,** *12* (1), 46-52.

100. Bang, W.-G.; Lang, S.; Sahm, H.; Wagner, F., Production L-tryptophan by *Escherichia coli* cells. *Biotechnology and Bioengineering* **1983,** *25* (4), 999-1011.

101. Darkoh, C.; Chappell, C.; Gonzales, C.; Okhuysen, P., A rapid and specific method for the detection of indole in complex biological samples. *Applied and Environmental Microbiology* **2015,** *81* (23), 8093-8097.

102. Facklam, R.; Pigott, N.; Franklin, R.; Elliott, J., Evaluation of three disk tests for identification of *Enterococci*, *Leuconostocs*, and *Pediococci*. *Journal of Clinical Microbiology* **1995,** *33* (4), 885-887.

103. Bennett, A.; MacPhee, S.; Betts, R.; Post, D., Use of pyrrolidonyl peptidase to distinguish *Citrobacter* from *Salmonella*. *Letters in Applied Microbiology* **1999,** *28* (3), 175-178.

104. King, S.; Metzger, W. I., A new plating medium for the isolation of enteric pathogens: II. Comparison of Hektoen enteric agar with SS and EMB agar. *Appl. Environ. Microbiol.* **1968,** *16* (4), 579-581.

105. Gaillot, O.; Di Camillo, P.; Berche, P.; Courcol, R.; Savage, C., Comparison of CHROMagar *Salmonella* medium and Hektoen Enteric agar for isolation of *Salmonellae* from stool samples. *Journal of Clinical Microbiology* **1999,** *37* (3), 762-765.

106. Perez, J.; Cavalli, P.; Roure, C.; Renac, R.; Gille, Y.; Freydiere, A., Comparison of four chromogenic media and Hektoen agar for detection and presumptive identification of *Salmonella* strains in human stools. *Journal of Clinical Microbiology* **2003,** *41* (3), 1130-1134.

107. Perry, J.; Freydiere, A., The application of chromogenic media in clinical microbiology. *Journal of Applied Microbiology* **2007,** *103* (6), 2046-2055.

108. Burke, H. M.; Gunnlaugsson, T.; Scanlan, E. M., Recent advances in the development of synthetic chemical probes for glycosidase enzymes. *Chemical Communications* **2015,** *51* (53), 10576-10588.

109. Orenga, S.; James, A. L.; Manafi, M.; Perry, J. D.; Pincus, D. H., Enzymatic substrates in microbiology. *Journal of Microbiological Methods* **2009,** *79* (2), 139-155.

110. Kiernan, J. A., Indigogenic substrates for detection and localization of enzymes. *Biotechnic & Histochemistry* **2007,** *82* (2), 73-103.

111. Bovill, R.; Druggan, P., The use of chromogenic enzyme substrates in microbial identification. In *Culture*, 2005.

112. Lederberg, J., The β-D-Galactosidase of *Escherichia coli*, Strain K-12. *Journal of Bacteriology* **1950,** *60* (4), 381-392.

113. Barber, M.; Kuper, S., Identification of Staphylococcus pyogenes by the phosphatase reaction. *The Journal of pathology and bacteriology* **1951,** *63* (1), 65-68.

114. Bennett, A. R.; MacPhee, S.; Betts, R.; Post, D., Use of pyrrolidonyl peptidase to distinguish *Citrobacter* from *Salmonella*. *Letters in Applied Microbiology* **1999,** *28* (3), 175-178.

115. Lindell, S. S.; Quinn, P., Use of bile-esculin agar for rapid differentiation of Enterobacteriaceae. *Journal of clinical microbiology* **1975,** *1* (5), 440-443.

116. James, A. L.; Perry, J. D.; Ford, M.; Armstrong, L.; Gould, F. K., Cyclohexenoesculetin-β-D-glucoside: a new substrate for the detection of bacterial β-D-glucosidase. *Journal of Applied Microbiology* **1997,** *82* (4), 532-536.

117. James, A. L.; Perry, J. D.; Ford, M.; Armstrong, L.; Gould, F. K., Evaluation of cyclohexenoesculetin-β-D-galactoside and 8-hydroxyquinoline-β-D-galactoside as substrates for the detection of beta-galactosidase. *Applied and Environmental Microbiology* **1996,** *62* (10), 3868-3870.

118. Manafi, M.; Kneifel, W.; Bascomb, S., Fluorogenic and chromogenic substrates used in bacterial diagnostics. *Microbiological Reviews* **1991,** *55* (3), 335-348.

119. Manafi, M., New developments in chromogenic and fluorogenic culture media. *International Journal of Food Microbiology* **2000,** *60* (2), 205-218.

120. Chilvers, K. F.; Perry, J. D.; James, A. L.; Reed, R. H., Synthesis and evaluation of novel fluorogenic substrates for the detection of bacterial β-galactosidase. *Journal of Applied Microbiology* **2001,** *91* (6), 1118-1130.

121. Váradi, L.; Hibbs, D. E.; Orenga, S.; Babolat, M.; Perry, J. D.; Groundwater, P. W., β-Alanyl aminopeptidase-activated fluorogenic probes for the rapid identification of Pseudomonas aeruginosa in clinical samples. *RSC Advances* **2016,** *6* (64), 58884-58889.

122. Plovins, A.; Alvarez, A. M.; Ibañez, M.; Molina, M.; Nombela, C., Use of fluorescein-di-β-D-galactopyranoside (FDG) and C12-FDG as substrates for beta-galactosidase detection by flow cytometry in animal, bacterial, and yeast cells. *Applied and Environmental Microbiology* **1994,** *60* (12), 4638-4641.

123. James, A. L.; Perry, J. D.; Chilvers, K.; Robson, I. S.; Armstrong, L.; Orr, K. E., Alizarin-β-D-galactoside: a new substrate for the detection of bacterial β-galactosidase. *Letters in Applied Microbiology* **2000,** *30* (4), 336-340.

124. Thermo Fisher Scientific Oxoid Brilliance™ Candida Agar CM1002. http://www.oxoid.com/UK/blue/prod_detail/prod_detail.asp?pr=CM1002&cat=&c=UK&lang=EN (accessed 08 August 2018).

125. Thermo Fisher Scientific Oxoid Brilliance™ *E. C*oli /Coliform Selective Agar CM1046. http://www.oxoid.com/UK/blue/prod_detail/prod_detail.asp?pr=CM1046&cat=&c=UK&lang=EN (accessed 08 August 2018).

126. Davidson, G. The development of chromogenic substrates for microbial detection. Thesis, University of Reading, 2011.

127. Parshotam, J. Design, synthesis and analysis of novel chromogens for improved bacterial detection. Thesis, University of Reading, 2014.

128. Böttcher, S.; Hederos, M.; Champion, E.; Dékány, G.; Thiem, J., Novel Efficient Routes to Indoxyl Glycosides for Monitoring Glycosidase Activities. *Organic Letters* **2013,** *15* (14), 3766-3769.

129. Wilson, D. M.; Ajl, S., Metabolism of L-rhamnose by Escherichia coli: II. The Phosphorylation of L-Rhamnulose. *Journal of Bacteriology* **1957,** *73* (3), 415-420.

130. Boronat, A.; Aguilar, J., Metabolism of L-fucose and L-rhamnose in *Escherichia coli*: differences in induction of propanediol oxidoreductase. *Journal of Bacteriology* **1981,** *147* (1), 181-185.

131. Baldomà, L.; Aguilar, J., Metabolism of L-fucose and L-rhamnose in *Escherichia coli*: aerobic-anaerobic regulation of L-lactaldehyde dissimilation. *Journal of bacteriology* **1988,** *170* (1), 416-421.

132. Saleh, N.; Awada, S.; Awwad, R.; Jibai, S.; Arfoul, C.; Zaiter, L.; Dib, W.; Salameh, P., Evaluation of antibiotic prescription in the Lebanese community: a pilot study. *Infection Ecology & Epidemiology* **2015,** *5*, 10.3402/iee.v5.27094.

133. Koivistoinen, O. M.; Hilditch, S.; Voutilainen, S. P.; Boer, H.; Penttilä, M.; Richard, P., Identification in the yeast *Pichiastipitis* of the first L-rhamnose-1-dehydrogenase gene. *Federation of European Biochemical Societies* **2008,** *275* (10), 2482-2488.

134. Perry, J. D.; Morris, K. A.; James, A. L.; Oliver, M.; Gould, F. K., Evaluation of novel chromogenic substrates for the detection of bacterial β-glucosidase. *Journal of Applied Microbiology* **2007,** *102* (2), 410-415.

135. Gordon, P. F.; Gregory, P., *Organic Chemistry in Colour*. Springer Berlin Heidelberg: 1983.

136. Christie, R. M., Why is indigo blue? *Biotechnic & Histochemistry* **2007,** *82* (2), 51-56.

137. Głowacki, E. D.; Voss, G.; Leonat, L.; Irimia-Vladu, M.; Bauer, S.; Sariciftci, N. S., Indigo and Tyrian Purple – From Ancient Natural Dyes to Modern Organic Semiconductors. *Israel Journal of Chemistry* **2012,** *52* (6), 540-551.

138. Lavinda, O.; Mironova, I.; Karimi, S.; Pozzi, F.; Samson, J.; Ajiki, H.; Massa, L.; Ramig, K., Singular thermochromic effects in dyeings with indigo, 6-bromoindigo, and 6,6'-dibromoindigo. *Dyes and Pigments* **2013,** *96* (2), 581-589.

139. Christian, G. D.; Dasgupta, P.; Schug, K., *Analytical Chemistry*. 7th ed.; Wiley Global Education: 2013.

140. Süsse, P., Steins, M. and Kupcik, V. , Indigo: Crystal structure refinement based on synchrotron data. In *Zeitschrift für Kristallographie*, 1988; Vol. 184, p 269.

141. Kettner, F.; Hüter, L.; Schäfer, J.; Röder, K.; Purgahn, U.; Krautscheid, H., Selective crystallization of indigo B by a modified sublimation method and its redetermined structure. *Acta Crystallographica* **2011,** *67* (Pt 11), o2867-o2867.

142. Konarev, D. V.; Khasanov, S. S.; Kuzmin, A. V.; Shestakov, A. F.; Otsuka, A.; Yamochi, H.; Saito, G.; Lyubovskaya, R. N., *cis*-Conformation of indigo in the coordination complex (indigo-O,O)(Cp*CrIICl). *Dalton Transactions* **2016,** *45* (43), 17095-17099.

143. Zollinger, H., *Color chemistry: syntheses, properties, and applications of organic dyes and pigments*. John Wiley & Sons: 2003.

144. Christie, R., *Colour Chemistry*. Royal Society of Chemistry: 2014.

145. Chadha, N.; Silakari, O., Indoles as therapeutics of interest in medicinal chemistry: Bird's eye view. *European Journal of Medicinal Chemistry* **2017,** *134*, 159-184.

146. Anderson, F. B.; Leaback, D. H., Substrates for the histochemical localization of some glycosidases. *Tetrahedron* **1961,** *12* (4), 236-239.

147. Choi, S.-J.; Lee, J.-E.; Jeong, S.-Y.; Im, I.; Lee, S.-D.; Lee, E.-J.; Lee, S. K.; Kwon, S.-M.; Ahn, S.-G.; Yoon, J.-H.; Han, S.-Y.; Kim, J.-I.; Kim, Y.-C., 5,5'-Substituted Indirubin-3'-oxime Derivatives as Potent Cyclin-Dependent Kinase Inhibitors with Anticancer Activity. *Journal of Medicinal Chemistry* **2010,** *53* (9), 3696-3706.

148. Gandy, M. N.; Byrne, L. T.; Stubbs, K. A., A simple and robust preparation of *N*-acetylindoxyls: precursors for indigogenic substrates. *Organic & Biomolecular Chemistry* **2015,** *13* (3), 905-908.

149. Guyen, B.; Schultes, C. M.; Hazel, P.; Mann, J.; Neidle, S., Synthesis and evaluation of analogues of 10H-indolo[3,2-*b*]quinoline as G-quadruplex stabilising ligands and potential inhibitors of the enzyme telomerase. *Organic & Biomolecular Chemistry* **2004,** *2* (7), 981-988.

150. Horwitz, J. P.; Chua, J.; Curby, R. J.; Tomson, A. J.; Da Rooge, M. A.; Fisher, B. E.; Mauricio, J.; Klundt, I., Substrates for Cytochemical Demonstration of Enzyme Activity. I. Some Substituted 3-Indolyl-β-D-glycopyranosides 1a. *Journal of Medicinal Chemistry* **1964,** *7* (4), 574-575.

151. McNab, H., *Heterocyclic Chemistry* 5th ed.; Wiley-Blackwell: 2011.

152. Rodríguez-Domínguez, J. C.; Balbuzano-Deus, A.; López-López, M. A.; Rodríguez-Domínguez, J. C.; Kirsch, G., An improved synthesis of 1-acetyl-1*H*-indol-3-yl acetates. *Journal of Heterocyclic Chemistry* **2009,** *44* (1), 273-275.

153. Sugasawa, T.; Adachi, M.; Sasakura, K.; Kitagawa, A., Aminohaloborane in organic synthesis. 2. Simple synthesis of indoles and 1-acyl-3-indolinones using specific *ortho*, α-chloroacetylation of anilines. *The Journal of Organic Chemistry* **1979,** *44* (4), 578-586.

154. Sugasawa, T.; Toyoda, T.; Adachi, M.; Sasakura, K., Aminohaloborane in organic synthesis. 1. Specific ortho substitution reaction of anilines. *Journal of the American Chemical Society* **1978,** *100* (15), 4842-4852.

155. Wei, X.; Wu, Q.; Zhang, J.; Zhang, Y.; Guo, W.; Chen, M.; Gu, Q.; Cai, Z.; Lu, M., Synthesis of precipitating chromogenic/fluorogenic β-glucosidase/β-galactosidase substrates by a new method and their application in the visual detection of foodborne pathogenic bacteria. *Chemical Communications* **2017,** *53* (1), 103-106.

156. Clayden, J.; Greeves, N.; Warren, S., *Organic Chemistry*. 1st ed.; Oxford University Press: 2001.

157. Klein, D. R., *Organic Chemistry As a Second Language: Second Semester Topics*. 3th ed.; Wiley: 2012.

158. Böttcher, S.; Thiem, J., Indoxylic Acid Esters as Convenient Intermediates Towards Indoxyl Glycosides. *European Journal of Organic Chemistry* **2014,** *2014* (3), 564-574.

159. Huang, J.-M.; Chen, H.; Chen, R.-Y., An unusual addition and ring-closure reaction of 1-(2-bromoethyl)-2, 3-dihydro-3-propyl-1, 3, 2-benzo-diazaphosphorin-4 (1*H*)-one 2-oxide with carbon disulfide for a new and convenient synthesis of the fused phosphorus heterocyclic compound. *Synthetic Communications* **2002,** *32* (14), 2215-2225.

160. Dolbier, W. R., *Guide to fluorine NMR for organic chemists*. John Wiley & Sons: 2016.

161. Bolsønes, M.; Bonge-Hansen, H. T.; Bonge-Hansen, T., Intramolecular Cyclopropanation of Bromodiazoacetates. *Synlett* **2014,** *25* (02), 221-224.

162. Malamas, M. S.; Millen, J., Quinazolineacetic acids and related analogs as aldose reductase inhibitors. *Journal of Medicinal Chemistry* **1991,** *34* (4), 1492-1503.

163. Bös, M.; Jenck, F.; Martin, J.; Moreau, J.; Mutel, V.; Sleight, A.; Widmer, U., Synthesis, pharmacology and therapeutic potential of 10-methoxypyrazino [1, 2-α] indoles, partial agonists at the 5HT2C receptor. *European Journal of Medicinal Chemistry* **1997,** *32* (3), 253-261.

164. Dropinski, J. F.; Akiyama, T.; Einstein, M.; Habulihaz, B.; Doebber, T.; Berger, J. P.; Meinke, P. T.; Shi, G. Q., Synthesis and biological activities of novel aryl indole-2-carboxylic acid analogs as PPARγ partial agonists. *Bioorganic & Medicinal Chemistry Letters* **2005,** *15* (22), 5035-5038.

165. Brito-Arias, M., *O*-glycoside Formation. In *Synthesis and Characterization of Glycosides*, 1st ed.; Springer: 2016; pp 81-168.

166. Horta, J. E., Simple Microwave-Assisted Claisen and Dieckmann Condensation Experiments for the Undergraduate Organic Chemistry Laboratory. *Journal of Chemical Education* **2011,** *88* (7), 1014-1015.

167. Renaudet, O.; Dasgupta, G.; Bettahi, I.; Shi, A.; Nesburn, A. B.; Dumy, P.; BenMohamed, L., Linear and branched glyco-lipopeptide vaccines follow distinct cross-presentation pathways and generate different magnitudes of antitumor immunity. *PLOS One* **2010,** *5* (6).

168. Newsom-Davis, T. E.; Wang, D.; Steinman, L.; Chen, P. F. T.; Wang, L.-X.; Simon, A. K.; Screaton, G. R., Enhanced immune recognition of cryptic glycan markers in human tumors. *Cancer Research* **2009,** *69* (5), 2018-2025.

169. Arita, H.; Sugita, K.; Nomura, A.; Sato, K.; Kawanami, J. i., Studies on antiviral glycosides. Synthesis and biological evaluation of various phenyl glycosides. *Carbohydrate Research* **1978,** *62* (1), 143-154.

170. Srivastav, N. C.; Shakya, N.; Mak, M.; Agrawal, B.; Tyrrell, D. L.; Kumar, R., Antiviral Activity of Various 1-(2′-Deoxy-β-d-lyxofuranosyl), 1-(2′-Fluoro-β-d-xylofuranosyl), 1-(3′-Fluoro-β-d-arabinofuranosyl), and 2′-Fluoro-2′,3′-didehydro-2′,3′-dideoxyribose Pyrimidine Nucleoside Analogues against Duck Hepatitis B Virus (DHBV) and Human Hepatitis B Virus (HBV) Replication. *Journal of Medicinal Chemistry* **2010,** *53* (19), 7156-7166.

171. Tromans, R. A.; Carter, T. S.; Chabanne, L.; Crump, M. P.; Li, H.; Matlock, J. V.; Orchard, M. G.; Davis, A. P., A biomimetic receptor for glucose. *Nature Chemistry* **2019,** *11* (1), 52-56.

172. Hartree, A. S.; Renwick, A., Molecular structures of glycoprotein hormones and functions of their carbohydrate components. *Biochemical Journal* **1992,** *287* (Pt 3), 665.

173. Davidson, M. B., Effect of growth hormone on carbohydrate and lipid metabolism. *Endocrine Reviews* **1987,** *8* (2), 115-131.

174. Sharon, N.; Lis, H., Carbohydrates in cell recognition. *Scientific American* **1993,** *268* (1), 82-89.

175. Bucior, I.; Burger, M. M., Carbohydrate–carbohydrate interactions in cell recognition. *Current Opinion in Structural Biology* **2004,** *14* (5), 631-637.

176. Disney, M. D.; Seeberger, P. H., The use of carbohydrate microarrays to study carbohydrate-cell interactions and to detect pathogens. *Chemistry & Biology* **2004,** *11* (12), 1701-1707.

177. Perillo, N.; Marcus, M. E.; Baum, L. G., Galectins: versatile modulators of cell adhesion, cell proliferation, and cell death. *Journal of Molecular Medicine* **1998,** *76* (6), 402-412.

178. Ferreira, S. S.; Passos, C. P.; Madureira, P.; Vilanova, M.; Coimbra, M. A., Structure–function relationships of immunostimulatory polysaccharides: A review. *Carbohydrate Polymers* **2015,** *132*, 378-396.

179. Howse, G. L.; Bovill, R. A.; Stephens, P. J.; Osborn, H. M. I., Synthesis and antibacterial profiles of targeted triclosan derivatives. *European Journal of Medicinal Chemistry* **2019,** *162*, 51-58.

180. Boons, G. J., *Carbohydrate Chemistry*. Springer: 1998.

181. The Royal Society of Chemistry (RSC), Chemistry for Biologists: Carbohydrates.

182. Demchenko, A. V., *Handbook of chemical glycosylation: advances in stereoselectivity and therapeutic relevance*. John Wiley & Sons: 2008.

183. Downey, A. M.; Hocek, M., Strategies toward protecting group-free glycosylation through selective activation of the anomeric center. *Beilstein Journal of Organic Chemistry* **2017,** *13*, 1239-1279.

184. Williams, R. J.; Paul, C. E.; Nitz, M., Protecting-group-free *O*-glysosidation using *p*-toluenesulfonohydrazide and glycosyl chloride donors. *Carbohydrate Research* **2014,** *386*, 73-77.

185. Butterworth, L. A.; Perry, J. D.; Davies, G.; Burton, M.; Reed, R. H.; Gould, F. K., Evaluation of novel β-ribosidase substrates for the differentiation of Gram-negative bacteria. *Journal of Applied Microbiology* **2004,** *96* (1), 170-176.

186. Khamsi, J.; Ashmus, R. A.; Schocker, N. S.; Michael, K., A high-yielding synthesis of allyl glycosides from peracetylated glycosyl donors. *Carbohydrate Research* **2012,** *357*, 147-150.

187. Böttcher, S.; Thiem, J., Facile preparation of indoxyl-and nitrophenyl glycosides of lactosamine and isolactosamine. *RSC Advances* **2014,** *4* (21), 10856-10861.

188. Jacobsson, M.; Malmberg, J.; Ellervik, U., Aromatic O-glycosylation. *Carbohydrate Research* **2006,** *341* (10), 1266-1281.

189. Singh, Y.; Demchenko, A. V., Koenigs–Knorr Glycosylation Reaction Catalyzed by Trimethylsilyl Trifluoromethanesulfonate. *Chemistry – A European Journal* **2019,** *25* (6), 1461-1465.

190. Cellier, M.; Fazackerley, E.; James, A. L.; Orenga, S.; Perry, J. D.; Turnbull, G.; Stanforth, S. P., Synthesis of 2-arylbenzothiazole derivatives and their application in bacterial detection. *Bioorganic & Medicinal Chemistry* **2014,** *22* (4), 1250-1261.

191. Valerio, S.; Iadonisi, A.; Adinolfi, M.; Ravidà, A., Novel Approaches for the Synthesis and Activation of Thio- and Selenoglycoside Donors. *The Journal of Organic Chemistry* **2007,** *72* (16), 6097-6106.

192. Xiong, D.-C.; Zhang, L.-H.; Ye, X.-S., Bromodimethylsulfonium Bromide-Silver Triflate: A New Powerful Promoter System for the Activation of Thioglycosides. *Advanced Synthesis & Catalysis* **2008,** *350* (11-12), 1696-1700.

193. Smith, R.; Müller-Bunz, H.; Zhu, X., Investigation of α-Thioglycoside Donors: Reactivity Studies toward Configuration-Controlled Orthogonal Activation in One-Pot Systems. *Organic Letters* **2016,** *18* (15), 3578-3581.

194. Wei, G.; Gu, G.; Du, Y., Silver Triflate. A Mild Alternative Catalyst for Glycosylation Conditions Using Trichloroacetimidates as Glycosyl Donors. *Journal of Carbohydrate Chemistry* **2003,** *22* (6), 385-393.

195. Li, Y.; Mo, H.; Lian, G.; Yu, B., Revisit of the phenol O-glycosylation with glycosyl imidates, BF3·OEt2 is a better catalyst than TMSOTf. *Carbohydrate Research* **2012,** *363*, 14-22.

196. Larsen, K.; Olsen, C. E.; Motawia, M. S., Acid-catalysed rearrangement of glycosyl trichloroacetimidates: a novel route to glycosylamines. *Carbohydrate Research* **2008,** *343* (2), 383-387.

197. Codée, J. D. C.; Ali, A.; Overkleeft, H. S.; van der Marel, G. A., Novel protecting groups in carbohydrate chemistry. *Comptes Rendus Chimie* **2011,** *14* (2), 178-193.

198. Guo, J.; Ye, X.-S., Protecting groups in carbohydrate chemistry: Influence on stereoselectivity of glycosylations. *Molecules* **2010,** *15* (10), 7235-7265.

199. Lee, E.; Bruzzi, A.; O'Brien, E.; O'Colla, P. S., Selective acetylation of D-mannose and D-xylose. *Carbohydrate Research* **1979,** *71* (1), 331-334.

200. Thorsheim, K.; Siegbahn, A.; Johnsson, R. E.; Stålbrand, H.; Manner, S.; Widmalm, G.; Ellervik, U., Chemistry of xylopyranosides. *Carbohydrate Research* **2015,** *418*, 65-88.

201. Tsuruta, T.; Koyama, T.; Yasutake, M.; Hatano, K.; Matsuoka, K., Synthesis of chiral dopants based on carbohydrates. *Carbohydrate Research* **2014,** *393*, 15-22.

202. Herde, Z. D.; John, P. D.; Alvarez-Fonseca, D.; Satyavolu, J.; Burns, C. T., Stereoselective acetylation of hemicellulosic C5-sugars. *Carbohydrate Research* **2017,** *443-444*, 1-14.

203. Timmons, S. C.; Jakeman, D. L., Stereoselective Chemical Synthesis of Sugar Nucleotides via Direct Displacement of Acylated Glycosyl Bromides. *Organic Letters* **2007,** *9* (7), 1227-1230.

204. Timmons, S. C.; Jakeman, D. L., Stereospecific synthesis of sugar-1-phosphates and their conversion to sugar nucleotides. *Carbohydrate Research* **2008,** *343* (5), 865-874.

205. Huo, Z.; Ding, D.; Zhang, Y.; Lei, N.; Gu, G.; Gao, J.; Guo, Z.; Cai, F., Carbohydrate O-benzylation through trialkylsilane-mediated reductive etherification. *Journal of Carbohydrate Chemistry* **2018,** *37* (6), 327-346.

206. Santra, A.; Ghosh, T.; Misra, A. K., Removal of benzylidene acetal and benzyl ether in carbohydrate derivatives using triethylsilane and Pd/C. *Beilstein Journal of Organic Chemistry* **2013,** *9* (1), 74-78.

207. Mydock, L. K.; Demchenko, A. V., Mechanism of chemical *O*-glycosylation: from early studies to recent discoveries. *Organic & Biomolecular Chemistry* **2010,** *8* (3), 497-510.

208. Anderson, F.; Leaback, D., Substrates for the histochemical localization of some glycosidases. *Tetrahedron* **1961,** *12* (4), 236-239.

209. Kaneko, S.; Kitaoka, M.; Kuno, A.; Hayashi, K., Syntheses of 4-methylumbelliferyl-β-D-xylobioside and 5-bromo-3-indolyl-β-D-xylobioside for sensitive detection of xylanase activity on agar plates. *Bioscience, Biotechnology, and Biochemistry* **2000,** *64* (4), 741-745.

210. Kunz, H.; Waldmann, H., The allyl group as mildly and selectively removable carboxy-protecting group for the synthesis of labile *O*-glycopeptides. *Angewandte Chemie International Edition in English* **1984,** *23* (1), 71-72.

211. Vogel, C.; Murphy, P., *Carbohydrate Chemistry: Proven Synthetic Methods*. CRC Press: 2017.

212. Cornella, J.; Sanchez, C.; Banawa, D.; Larrosa, I., Silver-catalysed protodecarboxylation of ortho-substituted benzoic acids. *Chemical Communications* **2009,** (46), 7176-7178.

213. Thatcher, G. R. J., Anomeric and Associated Stereoelectronic Effects. In *The Anomeric Effect and Associated Stereoelectronic Effects*, American Chemical Society: 1993; Vol. 539, pp 6-25.

214. Lemieux, R. U.; Kullnig, R. K.; Bernstein, H. J.; Schneider, W. G., Configurational Effects on the Proton Magnetic Resonance Spectra of Six-membered Ring Compounds *Journal of the American Chemical Society* **1958,** *80* (22), 6098-6105.

215. Davis, B. G.; Fairbanks, A. J., *Carbohydrate Chemistry*. Oxford University Press: 2002.

216. Das, R.; Mukhopadhyay, B., Chemical *O*-Glycosylations: An Overview. *ChemistryOpen* **2016,** *5* (5), 401-433.

217. Miljković, M.; Yeagley, D.; Deslongchamps, P.; Dory, Y. L., Experimental and theoretical evidence of through-space electrostatic stabilization of the incipient oxocarbenium ion by an axially oriented electronegative substituent during glycopyranoside acetolysis. *The Journal of Organic Chemistry* **1997,** *62* (22), 7597-7604.

218. Haasnoot, C. A. G.; de Leeuw, F. A. A. M.; Altona, C., The relationship between proton-proton NMR coupling constants and substituent electronegativities—I: An empirical generalization of the Karplus equation. *Tetrahedron* **1980,** *36* (19), 2783-2792.

219. Coxon, B., Developments in the Karplus equation as they relate to the NMR coupling constants of carbohydrates. *Advances in Carbohydrate Chemistry and Biochemistry* **2009,** *62*, 17-82.

220. Trost, B. M., New rules of selectivity: allylic alkylations catalyzed by palladium. *Accounts of Chemical Research* **1980,** *13* (11), 385-393.

221. Kocienski, P. J., *Protecting groups*. 3rd edition ed.; Thieme Stuttgart: 2005.

222. Böttcher, S. T., J., Indoxyl glycosides - Challenges and developments. *Trends in Carbohydrate Research* **2014,** (6), 1-10.

223. Jandera, P., Liquid Chromatography| Normal Phase. In *Reference Module in Chemistry, Molecular Sciences and Chemical Engineering*, Elsevier: 2013.

224. Matés, J. M.; Pérez-Gómez, C., Polysaccharides | Liquid Chromatography. In *Encyclopedia of Separation Science*, Wilson, I. D., Ed. Academic Press: Oxford, 2000; pp 3929-3937.

225. Liu, X.; Cheng, J.; Lu, X.; Wang, R., Surface acidity of quartz: understanding the crystallographic control. *Physical Chemistry Chemical Physics* **2014,** *16* (48), 26909-26916.

226. Demetzos, C.; Skaltsounis, A.-L.; Tillequin, F. o.; Koch, M., Phase-transfer-catalyzed synthesis of flavonoid glycosides. *Planta Medica* **1990,** *56* (06), 535-535.

227. Roy, R., Phase transfer catalysis in carbohydrate chemistry. In *Handbook of Phase Transfer Catalysis*, Sasson, Y.; Neumann, R., Eds. Springer Netherlands: Dordrecht, 1997; pp 244-275.

228. Bottone, E. J., *Bacillus cereus*, a Volatile Human Pathogen. *Clinical Microbiology Reviews* **2010,** *23* (2), 382-398.

229. Peng, H.; Ford, V.; Frampton, E. W.; Restaino, L.; Shelef, L. A.; Spitz, H., Isolation and enumeration of Bacillus cereus from foods on a novel chromogenic plating medium. *Food Microbiology* **2001,** *18* (3), 231-238.

230. Fernández-No, I. C.; Guarddon, M.; Böhme, K.; Cepeda, A.; Calo-Mata, P.; Barros-Velázquez, J., Detection and quantification of spoilage and pathogenic *Bacillus cereus*, *Bacillus subtilis* and *Bacillus licheniformis* by real-time PCR. *Food Microbiology* **2011,** *28* (3), 605-610.

231. Chen, Z.; Meng, T.; Li, Z.; Liu, P.; Wang, Y.; He, N.; Liang, D., Characterization of a β-glucosidase from B*acillus licheniformis* and its effect on bioflocculant degradation. *AMB Express* **2017,** *7* (1), 197-197.

232. Drobniewski, F. A., *Bacillus cereus* and related species. *Clinical Microbiology Reviews* **1993,** *6* (4), 324-338.

233. Setlow, B.; Cabrera-Martinez, R.-M.; Setlow, P., Mechanism of the hydrolysis of 4-methylumbelliferyl-β-D-glucoside by germinating and outgrowing spores of *Bacillus* species. *Journal of Applied Microbiology* **2004,** *96* (6), 1245-1255.

234. Miranda, J.; Franco, C.; Vázquez, B.; Fente, C.; Barros-Velázquez, J.; Cepeda, A., Evaluation of Chromocult® *Enterococci* agar for the isolation and selective enumeration of *Enterococcus* spp. in broilers. *Letters in Applied Microbiology* **2005,** *41* (2), 153-156.

235. Domig, K. J.; Mayer, H. K.; Kneifel, W., Methods used for the isolation, enumeration, characterisation and identification of Enterococcus spp.: 1. Media for isolation and enumeration. *International Journal of Food Microbiology* **2003,** *88* (2), 147-164.

236. Ledeboer, N. A.; Das, K.; Eveland, M.; Roger-Dalbert, C.; Mailler, S.; Chatellier, S.; Dunne, W. M., Evaluation of a novel chromogenic agar medium for isolation and differentiation of Vancomycin-resistant *Enterococcus faecium* and *Enterococcus faecalis* isolates. *Journal of Clinical Microbiology* **2007,** *45* (5), 1556-1560.

237. Archer, G. L., *Staphylococcus aureus*: a well-armed pathogen. *Reviews of Infectious Diseases* **1998,** *26* (5), 1179-1181.

238. Perry, J. D.; Rennison, C.; Butterworth, L. A.; Hopley, A. L. J.; Gould, F. K., Evaluation of *S. aureus* ID, a new chromogenic agar medium for detection of *Staphylococcus aureus*. *Journal of Clinical Microbiology* **2003,** *41* (12), 5695-5698.

239. Kearns, A. M.; Ganner, M.; Holmes, A., The '*Oxford Staphylococcus*': a note of caution. *Journal of Antimicrobial Chemotherapy* **2006,** *58* (2), 480-481.

240. Otto, M., *Staphylococcus epidermidis*-the 'accidental' pathogen. *Nature Reviews Microbiology* **2009,** *7* (8), 555-567.

241. Kloos, W.; Wolfshohl, J., Identification of Staphylococcus species with the API STAPH-IDENT system. *Journal of Clinical Microbiology* **1982,** *16* (3), 509-516.

242. Kloos, W. E.; Bannerman, T. L., Update on clinical significance of coagulase-negative staphylococci. *Clinical Microbiology Reviews* **1994,** *7* (1), 117-140.

243. Perry, J. D.; Oliver, M.; Nicholson, A.; Wright, J.; Gould, F. K., Evaluation of a new chromogenic agar medium for isolation and identification of Group B *Streptococci*. *Letters in Applied Microbiology* **2006,** *43* (6), 615-618.

244. James, A.; Perry, J.; Ford, M.; Armstrong, L.; Gould, F., Note: Cyclohexenoesculetin-β-D-glucoside: a new substrate for the detection of bacterial β-D-glucosidase. *Journal of Applied Microbiology* **1997,** *82* (4), 532-536.

245. Kadioglu, A.; Andrew, P. W., The innate immune response to pneumococcal lung infection: the untold story. *Trends in Immunology* **2004,** *25* (3), 143-149.

246. Terra, V. S.; Homer, K. A.; Rao, S. G.; Andrew, P. W.; Yesilkaya, H., Characterization of novel β-galactosidase activity that contributes to glycoprotein degradation and virulence in *Streptococcus pneumoniae*. *Infection and Immunity* **2010,** *78* (1), 348-357.

247. Cunningham, M. W., Pathogenesis of Group A *Streptococcal* infections. *Clinical Microbiology Reviews* **2000,** *13* (3), 470-511.

248. Doern, C. D.; Burnham, C.-A. D., It's not easy being green: the *viridans* Group *Streptococci*, with a gocus on pediatric clinical manifestations. *Journal of Clinical Microbiology* **2010,** *48* (11), 3829-3835.

249. Edberg, S.; Trepeta, R.; Kontnick, C.; Torres, A., Measurement of active constitutive beta-D-glucosidase (esculinase) in the presence of sodium desoxycholate. *Journal of Clinical Microbiology* **1985,** *21* (3), 363-365.

250. Coenye, T.; Vandamme, P.; Govan, J. R. W.; LiPuma, J. J., Taxonomy and Identification of the *Burkholderia cepacia* Complex. *Journal of Clinical Microbiology* **2001,** *39* (10), 3427-3436.

251. Vandamme, P.; Mahenthiralingam, E.; Holmes, B.; Coenye, T.; Hoste, B.; De Vos, P.; Henry, D.; Speert, D. P., Identification and Population Structure of *Burkholderia stabilis* sp. nov. (formerly *Burkholderia cepacia* Genomovar IV). *Journal of Clinical Microbiology* **2000,** *38* (3), 1042-1047.

252. Wright, R. M.; Moore, J. E.; Shaw, A.; Dunbar, K.; Dodd, M.; Webb, K.; Redmond, A. O. B.; Crowe, M.; Murphy, P. G.; Peacock, S.; Elborn, J. S., Improved cultural detection of *Burkholderia cepacia* from sputum in patients with cystic fibrosis. *Journal of Clinical Pathology* **2001,** *54* (10), 803-805.

253. Ranjan, K. P.; Ranjan, N., Citrobacter: An emerging health care associated urinary pathogen. *Urology annals* **2013,** *5* (4), 313-314.

254. Hunter, C. J.; Petrosyan, M.; Ford, H. R.; Prasadarao, N. V., *Enterobacter sakazakii*: an emerging pathogen in infants and neonates. *Surgical Infections* **2008,** *9* (5), 533-539.

255. Oh, S.-W.; Kang, D.-H., Fluorogenic Selective and Differential Medium for Isolation of *Enterobacter sakazakii*. *Applied and Environmental Microbiology* **2004,** *70* (9), 5692-5694.

256. Davin-Regli, A.; Monnet, D.; Saux, P.; Bosi, C.; Charrel, R.; Barthelemy, A.; Bollet, C., Molecular epidemiology of *Enterobacter aerogenes* acquisition: one-year prospective study in two intensive care units. *Journal of Clinical Microbiology* **1996,** *34* (6), 1474-1480.

257. Krzymińska, S.; Koczura, R.; Mokracka, J.; Puton, T.; Kaznowski, A., Isolates of the Enterobacter cloacae complex induce apoptosis of human intestinal epithelial cells. *Microbial Pathogenesis* **2010,** *49* (3), 83-89.

258. Allocati, N.; Masulli, M.; Alexeyev, M. F.; Di Ilio, C., *Escherichia coli* in Europe: an overview. *International Journal of Environmental Research and Public Health* **2013,** *10* (12), 6235-6254.

259. Tong, Y. Q.; Xin, B.; Sun, S. Q., Pyelonephritis Caused Solely by *Escherichia hermanii*. *Journal of Microbiology* **2014,** *7* (5), e18138-e18138.

260. Chung, P. Y., The emerging problems of *Klebsiella pneumoniae* infections: carbapenem-resistance and biofilm formation. *FEMS Microbiology Letters* **2016,** *363* (20).

261. Bassetti, M.; Vena, A.; Croxatto, A.; Righi, E.; Guery, B., How to manage *Pseudomonas aeruginosa* infections. *Drugs in Context* **2018,** *7*, 1-18.

262. Eng, S.-K.; Pusparajah, P.; Ab Mutalib, N.-S.; Ser, H.-L.; Chan, K.-G.; Lee, L.-H., *Salmonella*: A review on pathogenesis, epidemiology and antibiotic resistance. *Frontiers in Life Science* **2015,** *8* (3), 284-293.

263. Leng, P.; Huang, W. L.; He, T.; Wang, Y. Z.; Zhang, H. N., Outbreak of *Serratia marcescens* postoperative infection traced to barbers and razors. *Journal of Hospital Infection* **2015,** *89* (1), 46-50.

264. Edberg, S. C.; Pittman, S.; Singer, J. M., Esculin hydrolysis by *Enterobacteriaceae*. *Journal of Clinical Microbiology* **1977,** *6* (2), 111-116.

265. Burton, M.; Perry, J. D.; Stanforth, S. P.; Turner, H. J., The synthesis of novel chromogenic enzyme substrates for detection of bacterial glycosidases and their applications in diagnostic microbiology. *Bioorganic & Medicinal Chemistry* **2018,** *26* (17), 4841-4849.

266. Berg, J. M.; Tymoczko, J. L.; Stryer, L., *Biochemistry*. 6th ed.; W. H. Freeman and Company: 2007.

267. Kilian, M.; Bülo, P., Rapid diagnosis of *Enterobacteriaceae. Acta Pathologica Microbiologica Scandinavica Section B Microbiology* **1976,** *84B* (5), 245-251.

268. Kilian, M.; Bülow, P., Rapid identification of *Enterobacteriaceae*. *Acta Pathologica Microbiologica Scandinavica Section B Microbiology* **1979,** *87B* (1-6), 271-276.

269. Wohlsen, T. D., Comparative evaluation of chromogenic agar CM1046 and mFC agar for detection of *E. coli* and thermotolerant coliform bacteria from water samples. *Letters in Applied Microbiology* **2011,** *53* (2), 155-160.

270. Hansen, F. K.; Khankischpur, M.; Tolaymat, I.; Mesaros, R.; Dannhardt, G.; Geffken, D., Efficient synthesis and 5-LOX/COX-inhibitory activity of some 3-hydroxybenzo[b]thiophene-2-carboxylic acid derivatives. *Bioorganic & Medicinal Chemistry Letters* **2012,** *22* (15), 5031-5034.

271. Beck, J. R., Synthesis of methyl 3-hydroxybenzo[*b*]thiophene-2-carboxylate esters by nitro displacement. *The Journal of Organic Chemistry* **1973,** *38* (23), 4086-4087.

272. Kim, J.-H.; Yang, H.; Park, J.; Boons, G.-J., A general strategy for stereoselective glycosylations. *Journal of the American Chemical Society* **2005,** *127* (34), 12090-12097.

273. Rangel, J. M.; Sparling, P. H.; Crowe, C.; Griffin, P. M.; Swerdlow, D. L., Epidemiology of *Escherichia coli* O157:H7 outbreaks, United States, 1982-2002. *Emerging Infectious Diseases* **2005,** *11* (4), 603-609.

274. Dang-Xuan, S.; Nguyen-Viet, H.; Pham-Duc, P.; Grace, D.; Unger, F.; Nguyen-Hai, N.; Nguyen-Tien, T.; Makita, K., Simulating Cross-Contamination of Cooked Pork with *Salmonella* enterica from Raw Pork through Home Kitchen Preparation in Vietnam. *International Journal of Environmental Research and Public Health* **2018,** *15* (10), 2324.

275. Simon, R.; Levine, M. M., Glycoconjugate vaccine strategies for protection against invasive *Salmonella* infections. *Human Vaccines & Immunotherapeutics* **2012,** *8* (4), 494-498.

276. Fascione, M. A.; Adshead, S. J.; Stalford, S. A.; Kilner, C. A.; Leach, A. G.; Turnbull, W. B., Stereoselective glycosylation using oxathiane glycosyl donors. *Chemical Communications* **2009,** (39), 5841-5843.

277. van Belkum, A.; Chatellier, S.; Girard, V.; Pincus, D.; Deol, P.; Dunne, W. M., Progress in proteomics for clinical microbiology: MALDI-TOF MS for microbial species identification and more. *Expert Review of Proteomics* **2015,** *12* (6), 595-605.

278. Perry, J. D., A decade of development of chromogenic culture media for clinical microbiology in an era of molecular diagnostics. *Clinical Microbiology Reviews* **2017,** *30* (2), 449-479.

279. Joubrel, C.; Gendron, N.; Dmytruk, N.; Touak, G.; Verlaguet, M.; Poyart, C.; Réglier-Poupet, H., Comparative evaluation of 5 different selective media for Group B *Streptococcus* screening in pregnant women. *Diagnostic Microbiology and Infectious Disease* **2014,** *80* (4), 282-284.

280. Chen, J. H. K.; Cheng, V. C. C.; Wong, O.-Y.; Wong, S. C. Y.; So, S. Y. C.; Yam, W.-C.; Yuen, K.-Y., The importance of matrix-assisted laser desorption ionization–time of flight mass spectrometry for correct identification of Clostridium difficile isolated from chromID C. difficile chromogenic agar. *Journal of Microbiology, Immunology and Infection* **2017,** *50* (5), 723-726.

281. Charretier, Y.; Dauwalder, O.; Franceschi, C.; Degout-Charmette, E.; Zambardi, G.; Cecchini, T.; Bardet, C.; Lacoux, X.; Dufour, P.; Veron, L., Rapid bacterial identification, resistance, virulence and type profiling using selected reaction monitoring mass spectrometry. *Scientific Reports* **2015,** *5*, 13944.

282. Gupta, N.; Pons, V.; Noël, R.; Buisson, D.-A.; Michau, A.; Johannes, L.; Gillet, D.; Barbier, J.; Cintrat, J.-C., (*S*)-*N*-Methyldihydroquinazolinones are the Active Enantiomers of Retro-2 Derived Compounds against Toxins. *ACS Medicinal Chemistry Letters* **2014,** *5* (1), 94-97.

283. Verma, C.; Sharma, S.; Pathak, A., A phosgene and peroxide-free one-pot tandem synthesis of isatoic anhydrides involving anthranilic acid, Boc anhydride, and 2-chloro-N-methyl pyridinium iodide. *Tetrahedron Letters* **2013,** *54* (50), 6897-6899.